

Inflammatory Diseases in Mice Lacking Interleukin-1 Receptor Antagonist

Joanna Shepherd

A thesis submitted for the degree of Doctor of Philosophy
April 2002

Division of Genomic Medicine
University of Sheffield



IMAGING SERVICES NORTH

Boston Spa, Wetherby

West Yorkshire, LS23 7BQ

www.bl.uk

BEST COPY AVAILABLE.

VARIABLE PRINT QUALITY



IMAGING SERVICES NORTH

Boston Spa, Wetherby
West Yorkshire, LS23 7BQ
www.bl.uk

**TEXT BOUND CLOSE TO
THE SPINE IN THE
ORIGINAL THESIS**

Summary

Mice lacking the functional gene for the anti-inflammatory protein IL-1ra (*Il1rn*) were generated. This thesis is an investigation of the inflammatory phenotypes which spontaneously arise in *Il1rn*^{-/-} mice. Three inflammatory diseases have been found in *Il1rn*^{-/-} mice; an arteritis of the aorta and major arteries, a rheumatoid arthritis (RA)-like disease, and a psoriatic disease of the skin on the ears and tails, which is first described in this work. All three diseases were investigated using immunohistochemistry and it was found that they have many similarities with human diseases including giant cell arteritis, Takayasu's arteritis, rheumatoid arthritis, and psoriasis. An inflammatory infiltrate composed of activated macrophages, activated CD4⁺ T-cells, dendritic cells and neutrophils were a feature in all three diseases, as was activated endothelium. The psoriatic disease had a mixed Th1/Th2 type cytokine profile, whilst the arteritis and arthropathy contained mainly Th1. Development of the phenotypes appears to be strain specific, since in this study only *Il1rn*^{-/-} mice bred on a Balb/c background develop the psoriatic and RA-like diseases.

This work provides evidence that *Il1rn*^{-/-} mice may provide suitable models for several human inflammatory diseases, including giant cell arteritis, Takayasu's arteritis, rheumatoid arthritis and psoriasis. The importance of the role of endogenous IL-1ra is reiterated, and a possible central role for dendritic cell activation by IL-1 in these disease mechanisms is proposed.

Acknowledgements

First and foremost, I'd like to thank my supervisor, Dr. Martin Nicklin, for his patience, unrivalled knowledge, and enthusiasm for science. I'd also like to thank (in no particular order!) Dr. Andy Heath for being my student advisor, Dr. David Hughes for finding the arteritic lesions in the first place, Dr. Howard Carter (University of Manchester) for the use of his bone-crunching cryostat, and Professor Yoichiro Iwakura (University of Tokyo) and Professor Emmet Hirsch (Columbia University) and their colleagues for sharing information about their IL-1ra deficient mice. Not forgetting Janine Timms, for bravely taking on the genotyping while I wrote this thesis, Hazel Holden for procuring a microtome, Dr "Maths" Mark Isles for help with...maths..., Dr. Jenny "Queen Irn Bru" Barton for lab tips when I was starting out and placation with sweets, and Orla Gallagher for her expert tuition and knowledge on all things histological. Thanks also to the staff of the Field labs., especially Barry, Lisa, Jane, Anne and Rachel for their help and for looking after the mice.

I'd also like to say a big "cheers!" to all the friends I've made in the Division who've come and gone, but especially Jim, Mark and Clare for shell animals, quizzers and accompanying me on many visits to see Dr. Booze. Thanks also to Jo and Jon Shepherd for letting me grow up thinking I can do anything if I give it a good go. Last but by no means least, Nicholas Bell for unending and unquestioning support and optimism, and also for Corduroy and encouraging all the magpies to gather around us at an alarming rate.

Thanks everyone!

Publications arising from this work

Shepherd, J., Iles, M.M., Hughes, D.E, and Nicklin, M.J.H. (2000). Inflammatory diseases in interleukin-1 receptor antagonist-deficient mice. *Eur. Cytokine Netw.* **11**:200 (Abs.)

Shepherd, J., Little, M.C., and Nicklin, M.J.H. (2002). Psoriasis-like lesions in Balb/c mice lacking interleukin-1 receptor antagonist (manuscript in preparation).

Abbreviations

aa	amino acids
AECA	anti-endothelial cell antibody
AP-1	activator protein-1
APC	antigen presenting cell
APES	3-Aminopropyltriethoxysilane
APP	acute phase protein
APR	acute phase response
bp	base pairs
CD40L	CD40 ligand
CDNA	complementary DNA
CIA	collagen induced arthritis
CIAP	calf intestinal alkaline phosphatase
COMP	cartilage oligomeric matrix protein
CREB	cyclic-AMP response element binding protein
CRH	corticotropin releasing hormone
CRP	C-reactive protein
CTL	cytotoxic T-lymphocyte
DAB	diaminobenzidine tetrahydrochloride
DC	dendritic cell
DNA	deoxyribonucleic acid
dNTP	deoxyribonucleic acid triphosphate
EC	endothelial cell
ECACC	european collection of animal cell cultures
ECM	extracellular matrix
EDTA	ethylenediamine tetraacetic acid
ELISA	enzyme linked immuno-sorbent assay
eNOS	endothelial nitric oxide synthase
ES	embryonic stem
GCA	giant cell arteritis
GlyCAM-1	glycosylation-dependent cell adhesion molecule-1
GM-CSF	granulocyte/macrophage-colony stimulating factor
H-2	histocompatibility-2
HLA	human leukocyte antigen
HPA axis	hypothalamic-pituitary-adrenal axis
HSP	heat shock protein
HUVEC	human umbilical vein endothelial cells
I κ B	inhibitor of κ B
ICAM-1	intercellular adhesion molecule-1
ICE	interleukin-1 converting enzyme
icIL-1ra	intracellular interleukin-1 receptor antagonist
IEL	internal elastic laminae
IFN γ	interferon gamma
Ig	immunoglobulin

IKK	IκB kinase
IL	interleukin
IL-1	interleukin-1
<i>Il1a</i>	gene encoding mouse IL-1α
<i>IL1B</i>	gene encoding human IL-1β
<i>Il1b</i>	gene encoding mouse IL-1β
<i>Il1r1</i>	mouse gene encoding IL-1R1
IL-1R1	type 1 interleukin-1 receptor
IL-1R2	type 2 interleukin-1 receptor
IL-1ra	interleukin-1 receptor antagonist
IL-1RAcP	interleukin-1 receptor accessory protein
IL1RN	human gene encoding interleukin-1 receptor antagonist
<i>Il1rn</i>	mouse gene encoding interleukin-1 receptor antagonist
iNOS	inducible nitric oxide synthase
IRAK	interleukin-1 receptor associated kinase
JNK	Jun N-terminal kinase
K	keratin
kb	kilobase
kDa	kilodalton
LC	Langerhans' cell
LFA-1	leukocyte function-associated antigen 1
LPS	lipopolysaccharide
MadCAM-1	mucosal addressin cell adhesion molecule 1
Mal	Myd88-adaptor-like
MAP kinase	mitogen activated protein kinase
MCAo	middle cerebral artery occlusion
MCP-1	monocyte chemoattractant protein-1
MHC	major histocompatibility complex
MIC	MHC class I chain-related
MIP-1	macrophage inflammatory protein
MMP	matrix metalloproteinase
Mog	myelin oligodendrocyte glycoprotein
MOPS	3-(N-morpholino)propanesulphonic acid
mRNA	messenger RNA
NFκB	nuclear factor κB
NF-IL6	nuclear factor of interleukin-6
NIH	neointimal hyperplasia
NIK	NFκB inducing kinase
NK	natural killer cell
NO	nitric oxide
PBMC	peripheral blood mononuclear cells
PBS	phosphate buffered saline
PCR	polymerase chain reaction
PDGF	platelet derived growth factor
PECAM-1	platelet/endothelial cell adhesion molecule-1
PGE ₂	prostaglandin E ₂

PMA	phorbol-12-myristate 13-acetate
PMR	polymyalgia rheumatica
PsA	psoriatic arthritis
PSGL-1	P-selectin glycoprotein ligand-1
RA	rheumatoid arthritis
RF	rheumatoid factor
rh	recombinant human
RNA	ribonucleic acid
RT-PCR	reverse-transcriptase polymerase chain reaction
SAA	serum amyloid A
SAP	serum amyloid P
SCID	severe combined immunodeficient
sIL-1ra	secreted interleukin-1 receptor antagonist
SLE	systemic lupus erythmatosus
sLE _x	sialyl Lewis _x
SMC	smooth muscle cell
SPF	specified pathogen free
SRBC	sheep red blood cells
SSRE	shear stress response element
TA	Takayasu's arteritis
TAK-1	TGF- β activated kinase
TCR	T-cell receptor
TEM	transendothelial migration
TGF- β	transforming growth factor beta
Th	T-helper cell
TIMP	tissue inhibitor of matrix metalloproteinase
TLR	<i>Toll</i> -like receptor
TNF- α	tumour necrosis factor-alpha
TRAF-6	TNF receptor associated factor-6
UIS	upstream induction sequence
UVR	ultraviolet radiation
VCAM-1	vascular cell adhesion molecule-1
VEGF	vascular endothelial growth factor
VSMC	vascular smooth muscle cell

Contents

Summary	i
Acknowledgements	ii
Publications arising from this work	iii
Abbreviations	iv

Section 1: Introduction

1.1: Interleukin-1 (IL-1)

1.1.1: The inflammatory response	p.2
1.1.2: Structure and processing of IL-1	p.2
1.1.3: Sources of IL-1	p.5
1.1.4: Biological effects of IL-1	p.9
1.1.5: Systemic effects of IL-1	p.10
1.1.6: Local effects of IL-1	p.13
1.1.7: Regulation of IL-1 expression	p.16
1.1.8: Interleukin-1 receptor antagonist	p.17
1.1.9: Forms of Il-1ra	p.17
1.1.10: Induction of IL-1ra expression	p.18
1.1.11: IL-1ra in health and disease	p.19
1.1.12: Therapeutic potential of IL-1ra	p.21
1.1.13: IL-1ra transgenic and IL-1ra deficient mice	p.22
1.1.14: IL-1 receptors	p.26

1.1.15: IL-1 receptor accessory protein	p.28
1.1.16: IL-1 signalling (NFκB pathway)	p.29
1.1.17: IL-1 signalling (MAP kinase pathways)	p.31
1.2: <i>Il1rn</i>^{-/-} mice, University of Sheffield	
1.2.1: Spontaneous inflammatory diseases in IL-1ra null mice from the University of Sheffield	p.32
1.2.2: Vasculitis	p.33
1.2.3: Giant cell arteritis	p.33
1.2.4: Characterisation of GCA lesions and the involvement of IL-1	p.34
1.2.5: Possible causes of GCA	p.37
1.2.6: Genetic susceptibility to GCA	p.39
1.2.7: Takayasu's arteritis	p.41
1.2.8: TA lesions	p.42
1.2.9: Possible aetiology of TA	p.42
1.2.10: Genetic susceptibility to TA	p.45
1.2.11: The influence of shear stress on vascular lesion development	p.47
1.2.12: Pathology and aetiology of rheumatoid arthritis (RA)	p.49
1.2.13: Involvement of IL-1 in RA	p.55
1.2.14: Psoriasis; psoriatic lesions	p.61
1.2.15: Causative factors in psoriasis	p.63
1.2.16: IL-1 in psoriasis	p.65
1.2.17: Animal models of psoriasis	p.68
1.2.18: Psoriatic arthritis	p.70

1.3: Summary and hypothesis	p.71
------------------------------------	------

Section 2: Materials and methods

2.1: Animals

2.1.1: Lines of mice used in studies	p.75
2.1.2: Housing and care of mice	p.75
2.1.3: Culling and dissection of animals	p.76

2.2: Preparation of genomic DNA

2.2.1: Preparation of genomic DNA from mouse ear clips	p.77
2.2.2: Preparation of high molecular weight genomic DNA from mouse splenocytes	p.78

2.3: Genotyping of mice by polymerase chain reaction (PCR)

2.3.1: Oligonucleotide primer design and preparation	p.80
2.3.2: Agarose gel electrophoresis	p.81
2.3.3: Optimisation of polymerase chain reactions	p.81
2.3.4: <i>Il1rn</i> genotyping by PCR	p.82
2.3.5: Haplotyping <i>H-2</i> by PCR	p.83

2.4: Analysis of PCR products

2.4.1: Extraction of DNA from agarose gel	p.89
2.4.2: Automated DNA sequencing	p.89

2.5: Radiolabelling DNA with ³²P

2.5.1: Radiolabelling 5' ends with ³² P	p.89
--	------

2.5.2: Random heptamer labelling of oligonucleotide probes with T7 quickprime kit	p.90
2.6: Genotyping of mice using Southern blot analysis	
2.6.1: Preparation of samples for Southern blot gel	p.90
2.6.2: Electrophoresis of high molecular weight genomic DNA	p.91
2.6.3: Southern blotting	p.91
2.6.4: Probing of Southern blot	p.92
2.6.5: Visualisation of Southern blot using a Phosphorimager	p.93
2.7: Cell culture	
2.7.1: Culture of RAW 264.7 mouse macrophage cells	p.93
2.7.2: Stimulation of cells with LPS	p.93
2.8: Immunohistochemistry for frozen sections	
2.8.1: 3-Aminopropyltriethoxysilane (APES) coating of slides	p.94
2.8.2: Cutting frozen sections – operation of cryostat	p.94
2.8.3: Cutting frozen sections from undecalcified joints	p.95
2.8.4: Haematoxylin and eosin staining of frozen sections	p.96
2.8.5: Haematoxylin and eosin staining of undecalcified frozen joints	p.96
2.8.6: Connective tissue staining of frozen sections	p.97
2.8.7: Immunohistochemical staining of frozen sections – optimisation of stains	p.98
2.8.8: Immunohistochemical staining of frozen sections – staining procedure with Vector ABC reagent kit	p.101
2.9: Immunohistochemistry for formaldehyde fixed sections	
2.9.1: Preparation of tissue samples for paraffin embedding	p.104

2.9.2: Preparation of paraffin wax blocks	p.105
2.9.3: Sectioning of paraffin blocks – operation of microtome	p.105
2.9.4: Histological staining of paraffin embedded sections	p.105
2.9.5: Naphthol AS-D chloroacetate esterase staining for neutrophils in paraffin embedded sections	p.106
2.9.6: Toluidine blue staining of formaldehyde fixed paraffin embedded sections	p.107
2.10: Analysis of RNA	
2.10.1: Preparation of RNA from cells	p.107
2.10.2: mRNA separation and Northern blot	p.108
2.11: Detection of <i>Helicobacter</i> species infection in mice	
2.11.1: PCR to detect <i>Helicobacter</i> spp. infection in mice	p.109
2.11.2: <i>Mbo</i> I digestion of <i>Helicobacter</i> spp. PCR products	p.110
2.12: Measurement of serum amyloid A (SAA) in mouse serum	
2.12.1: ELISA to detect levels of SAA in mouse serum	p.111

Section 3: Results

3.1: Southern blot analysis of two lines of <i>Il1rn</i>^{-/-} mice	p.114
3.2: Optimisation of immunohistochemical stains	
3.2.1: Positive controls	p.115
3.2.2: Positive control for IL-1 β	p.115
3.3: Arteritis in <i>Il1rn</i>^{-/-} mice	
3.3.1: Introduction	p.116
3.3.2: Animals used in arteritis studies	p.117

3.3.3:	Characterisation of arteritis in <i>Il1rn^{-/-}</i> mice – immunohistochemical study	p.117
3.3.4:	Arteritis time course study	p.127
3.3.5:	Carriage of <i>H-2</i> haplotype in relation to sensitivity to arteritis	p.133
3.3.6:	Helicobacter infection in <i>Il1rn^{-/-}</i> mice	p.139
3.3.7:	Measurement of the acute phase response in arteritis by measuring levels of SAA	p.140
3.4:	Psoriatiform disease in Balb/c <i>Il1rn^{-/-}</i> mice	
3.4.1:	Introduction	p.142
3.4.2:	Retrospective histological study of formaldehyde fixed ear sections	p.142
3.4.3:	Characterisation of psoriatiform lesions by immunohistochemistry	p.146
3.5:	<i>Il1rn^{-/-}</i> mice on a Balb/c background spontaneously develop a rheumatoid arthritis-like disease	
3.5.1:	Introduction	p.149
3.5.2:	Clinical signs of arthropathy	p.149
3.5.3:	Histological analysis of decalcified joint sections	p.150
3.5.4:	Immunohistochemical analysis of undecalcified joints	p.151
3.6:	<i>Il1rn^{-/-}</i> mice on a Balb/c background can develop arteritis, a psoriatiform disease and an RA-like disease simultaneously	p.153

Section 4: Discussion

4.1:	Mice lacking IL-1ra spontaneously develop inflammatory diseases	p.156
4.2:	Arteritis	
4.2.1:	Inflammatory artery disease in <i>Il1rn^{-/-}</i> mice	p.156

4.2.2: Initiating factors in the development of arteritis	p.158
4.2.3: Bacterial infection in heart disease	p.161
4.2.4: The influence of <i>H-2</i> haplotype on lethality of arteritis	p.162
4.3: Psoriasis	
4.3.1: Balb/c mice lacking IL-1ra suffer from a psoriasis-like disease	p.162
4.4: Rheumatoid arthritis	
4.4.1: Rheumatoid arthritis in Balb/c <i>IIIrn^{-/-}</i> mice	p.164
4.4.2: Comparison to RA in another colony of Balb/c <i>IIIrn^{-/-}</i> mice	p.165
4.5: Psoriatic arthropathy or psoriasis and arthritis?	p.166
4.6: Aetiology of inflammatory diseases in <i>IIIrn^{-/-}</i> mice – a possible central role for dendritic cells	p.167
4.7: Conclusions	p.175

Section 5: References

References	p.176
------------	-------

Appendix

List of Suppliers	p.222
-------------------	-------

List of Tables

Table 1:	PCR conditions for haplotyping across the murine <i>H-2</i>	p.88
Table 2:	Antibodies, positive controls and sera for mouse immunohistochemistry	p.99
Table 3:	Animals used in arteritis study	p.121
Table 4:	Animals used in arteritis time course study	p.127
Table 5:	SAA level in comparison to lesion development	p.141
Table 6:	Animals used in psoriasis study	p.144

List of Figures

- Figure 1:** Different forms of IL-1ra arise from alternative translational start sites and alternative splicing of a single gene
Facing p. 18
- Figure 2:** The generation of three different *Il1rn* null alleles in the mouse
Facing p. 22
- Figure 3:** Homology between *Drosophila* Toll and IL-1 signalling pathways
Facing p. 27
- Figure 4:** Signal transduction does not appear to occur following binding of IL-1 to the type 2 receptor, or following IL-1ra binding to IL-1
Facing p. 28
- Figure 5:** Schematic diagram of shear flow at an arterial bifurcation
Facing p. 47
- Figure 6:** Simplified physical map of the murine *H-2*
Facing p. 87
- Figure 7:** Southern blot analysis of two lines of *Il1rn*^{-/-} mice
Facing p. 114
- Figure 8:** Examples of positive controls for immunohistochemistry
Facing p. 115
- Figure 9:** Northern blot probed for IL-1
Facing p. 115
- Figure 10:** RAW 264.7 cells used as positive controls for IL-1 β staining
Facing p. 116
- Figure 11:** Demarcation of lesional area
Facing p. 118
- Figure 12:** Arteritic lesions close to valves
Facing p. 118
- Figure 13:** Formalin fixed, paraffin embedded aortic root sections
Facing p. 118

- Figure 14:** Examples of cellular infiltrate scores on haematoxylin and eosin stained frozen aortic root tissue
Facing p. 119
- Figure 15:** Examples of scores of elastin damage
Facing p. 119
- Figure 16:** Myocardial scar in *Il1rn*^{-/-} mouse
Facing p. 119
- Figure 17:** Large inflammatory infiltrates with relatively little elastin damage
Facing p. 120
- Figure 18:** Specificity of lesion development for large muscular arteries
Facing p. 120
- Figure 19:** Lack of cellular infiltrate or elastin damage in *Il1rn*^{+/+} aortic roots
Facing p. 120
- Figure 20:** F4/80⁺ macrophages and CD4⁺ T-cells in a lesion scoring 1 for cellular infiltrate
Facing p. 124
- Figure 21:** F4/80⁺ macrophages and CD4⁺ T-cells in a lesion scoring 3 for cellular infiltrate
Facing p. 124
- Figure 22:** Activated macrophages in arteritic lesions
Facing p. 124
- Figure 23:** Activated macrophages and CD4⁺ T-cells tend to co-localise in arteritic lesions
Facing p. 124
- Figure 24:** Co-localisation of production of IFN γ and IL-1 β in aortic root lesions of *Il1rn*^{-/-} mice
Facing p. 124
- Figure 25:** Sparse production of IL-4 or IL-5 in *Il1rn*^{-/-} aortic root lesion
Facing p. 124
- Figure 26:** Aortic root lesions with >5 IL-4 producing cells/section
Facing p. 124
- Figure 27:** Neutrophils in aortic root lesions of *Il1rn*^{-/-} mice
Facing p. 125

- Figure 28:** DEC 205⁺ dendritic cells in the arteritic lesions of *Il1rn*^{-/-} mice
Facing p. 125
- Figure 29:** Toluidine blue staining of paraffin embedded inflamed heart sections
Facing p. 125
- Figure 30:** CD19⁺ B-cells are relatively rare in the arteritic lesions of *Il1rn*^{-/-} mice
Facing p. 125
- Figure 31:** Chemokines and adhesion molecules in advanced arteritic lesions
Facing p. 125
- Figure 32:** Activated endothelium on both the luminal surface and within the microvasculature of arteritic lesions
Facing p. 125
- Figure 33:** Aortic roots from *Il1rn*^{+/+} mice contain circulating F480⁺ macrophages and CD4⁺ T-cells which are not activated
Facing p. 126
- Figure 34:** Uninflamed aortic root from a 151 day old *Il1rn*^{+/+} mouse
Facing p. 126
- Figure 35:** Pedigree of Sf3 animals used in arteritis studies
Facing p. 127
- Figure 36:** Aortic root from a 24 day old *Il1rn*^{-/-} mouse scoring 1 for cellular infiltrate
Facing p. 128
- Figure 37:** Uninflamed aortic root in a 23 day old *Il1rn*^{-/-} mouse
Facing p. 128
- Figure 38:** Small cellular infiltrates in aortic roots from 56-59 day old *Il1rn*^{-/-} mice
Facing p. 128
- Figure 39:** Activated macrophages and CD4⁺ cells in aortic root lesions of a 56 day old *Il1rn*^{-/-} mouse
Facing p. 128

- Figure 40:** Lack of inflammatory markers, other than small numbers of activated F480⁺ and CD4⁺ cells, in aortic root lesions of 56-59 day old *Il1rn*^{-/-} mice
Facing p. 128
- Figure 41:** Little IL-4 production in the aortic root lesion of a 59 day old *Il1rn*^{-/-} mouse
Facing p. 129
- Figure 42:** Aortic root lesions in 75-81 day old mice
Facing p. 129
- Figure 43:** Activated macrophages in aortic root lesions from 75-81 day old *Il1rn*^{-/-} mice
Facing p. 129
- Figure 44:** Activated CD4⁺ T-cells in aortic root lesions of 75-81 day old *Il1rn*^{-/-} mice
Facing p. 129
- Figure 45:** Chemokine and adhesion molecule production and expression in the aortic root lesions of *Il1rn*^{-/-} mice aged 75-81 days
Facing p. 129
- Figure 46:** Neutrophils and dendritic cells are present in the aortic root lesions of *Il1rn*^{-/-} mice aged 75-81 days
Facing p. 129
- Figure 47:** Few cells produce IL-4 or IL-5 in aortic root lesions of 75-81 day old *Il1rn*^{-/-} mice
Facing p. 130
- Figure 48:** Activated endothelium in aortic root lesions from 75-81 day old mice
Facing p. 130
- Figure 49:** Damaged aortic roots in *Il1rn*^{-/-} mice aged 105 days
Facing p. 130
- Figure 50:** Activated Th1 type CD4⁺ cells in the aortic root of a 105 day old *Il1rn*^{-/-} mouse
Facing p. 130
- Figure 51:** Neutrophils and activated macrophages in aortic root lesion of a 105 day old *Il1rn*^{-/-} mouse
Facing p. 130

- Figure 52:** Activated endothelium in the aortic root lesion of a 105 day old *Il1rn*^{-/-} mouse
Facing p. 130
- Figure 53:** Cellular infiltrates and elastin damage in aortic roots of *Il1rn*^{-/-} mice aged >125 days
Facing p. 130
- Figure 54:** Undamaged aortic root in one 154 day old *Il1rn*^{-/-} mouse
Facing p. 130
- Figure 55:** Activated CD4⁺ T-cells in aortic root lesions from *Il1rn*^{-/-} mice aged >125 days
Facing p. 131
- Figure 56:** Activated macrophages in aortic root lesion of *Il1rn*^{-/-} mouse aged >125 days
Facing p. 131
- Figure 57:** Dendritic cells and abundant neutrophils in aortic root lesion of *Il1rn*^{-/-} mouse aged >125 days
Facing p. 131
- Figure 58:** Activated endothelium in aortic root lesions from *Il1rn*^{-/-} mice aged >125 days
Facing p. 131
- Figure 59:** ICAM-1 production in aortic root lesions of *Il1rn*^{-/-} mice aged >125 days
Facing p. 131
- Figure 60:** Chemokine production in aortic root lesions of *Il1rn*^{-/-} mice aged >125 days
Facing p. 131
- Figure 61:** Polyacrylamide gel electrophoresis of radiolabelled *H2IEb* PCR
Facing p. 135
- Figure 62:** Sequence of larger PCR product of *H2IEb* (haplotype H-2^u) microsatellite locus
Facing p. 135
- Figure 63:** Sequence of smaller PCR product of *H2IEb* (haplotype H-2^b) microsatellite locus
Facing p. 135

- Figure 64:** Comparison of PCR products from *H2IEb* microsatellite amplification between strains
Facing p. 135
- Figure 65:** *H-2* and Longevity
Facing p. 135
- Figure 66:** Radiolabelled PCR amplification of *H2IEb* microsatellite
Facing p. 135
- Figure 67:** Amplification of microsatellite markers across *H-2* by PCR
Facing p. 135
- Figure 68:** PCR amplification and restriction enzyme analysis of *Helicobacter* spp. rRNA
Facing p. 140
- Figure 69:** Psoriatiform features in inflamed ear skin sections from Balb/c *Il1rn*^{-/-} mice
Facing p. 143
- Figure 70:** Epidermal neutrophilic infiltrate as identified by chloroacetate esterase activity
Facing p. 143
- Figure 71:** Haematoxylin and eosin scored ear skin sections
Facing p. 143
- Figure 72:** Toluidine blue staining of paraffin embedded ear skin sections
Facing p. 145
- Figure 73:** Psoriatiform Balb/c *Il1rn*^{-/-} ear sections contain a mixed dermal infiltrate
Facing p. 147
- Figure 74:** Mixed cytokine profile within dermal infiltrate of inflamed Balb/c ear skin sections
Facing p. 147
- Figure 75:** Chemokine and adhesion molecule expression in inflamed dermis of Balb/c *Il1rn*^{-/-} ear skin sections
Facing p. 147
- Figure 76:** Increased vascularity and activation of endothelial cells within the dermis of inflamed Balb/c *Il1rn*^{-/-} ear sections as compared to *Il1rn*^{+/+}
Facing p. 147

- Figure 77:** CD4⁺ T-cells infiltrating into the epidermis of lesional skin in *Il1rn*^{-/-} Balb/c mice
Facing p. 147
- Figure 78:** Epidermal Langerhans' cells appear to be activated and more numerous in psoriatiform *Il1rn*^{-/-} Balb/c ear skin than in *Il1rn*^{+/+}
Facing p. 147
- Figure 79:** Transverse epidermal skin sections of affected and unaffected mice stained for keratin 6
Facing p. 148
- Figure 80:** *Il1rn*^{+/+} Balb/c mice have a low level of inflammation in the ears
Facing p. 148
- Figure 81:** *Il1rn*^{+/+} Balb/c mice have no IL-4 or IL-5 production within the ears
Facing p. 148
- Figure 82:** Inflamed skin at the base of the tail in a Balb/c *Il1rn*^{-/-} mouse
Facing p. 149
- Figure 83:** Haematoxylin and eosin stained paraffin embedded skin sections from *Il1rn*^{-/-} and *Il1rn*^{+/+} Balb/c mice
Facing p. 149
- Figure 84:** Haematoxylin and eosin stained decalcified, paraffin embedded joint sections
Facing p. 151
- Figure 85:** Pannus in arthritic Balb/c *Il1rn*^{-/-} mouse joint
Facing p. 152
- Figure 86:** Activated macrophages in inflammatory infiltrate of a Balb/c *Il1rn*^{-/-} joint
Facing p. 152
- Figure 87:** Th1 type CD4⁺ T-cells within infiltrate of an arthritic Balb/c *Il1rn*^{-/-} joint
Facing p. 152
- Figure 88:** Immunohistochemical staining of a Balb/c *Il1rn*^{+/+} joint
Facing p. 153
- Figure 89:** Model of proposed involvement of dendritic cells
Facing p. 171

Section 1: Introduction

1.1: Interleukin-1 (IL-1)

1.1.1: The inflammatory response

Inflammation is a response by living tissue to infection or injury. It involves the release of multiple inflammatory mediators from numerous cells. As a part of the innate immune system, its overall effect is beneficial although some inflammatory reactions can have detrimental results on the host. The inflammatory mediators released at the site of the inflammatory response, which include pro-inflammatory cytokines, cause multiple physiological changes within the tissue. These changes include dilation of blood vessels and increased blood flow to the area, constriction of the efferent veins, activation of the endothelium of the vessels, recruitment and activation of leukocytes, and up-regulation of the synthesis and release or expression of other pro-inflammatory mediators. These events result in the classical symptoms of inflammation – pain, oedema, redness and heat. Many of the local reactions are potentially mediated by the pro-inflammatory cytokine IL-1, which is inhibited by its naturally occurring antagonist IL-1 receptor antagonist, IL-1ra. This thesis is an investigation of the effects of elimination of the IL-1ra gene, *Il1rn*, in mice.

1.1.2: Structure and processing of IL-1

There are two distinct but structurally homologous forms of the IL-1 protein, IL-1 α and IL-1 β , collectively known as IL-1. Another homologue, IL-1ra, acts as a natural inhibitor of the pro-inflammatory actions of IL-1 α and IL-1 β . IL-1ra acts by binding competitively but non-productively to the type 1 IL-1 receptor [Hannum *et al.*, 1990].

The genes for the agonists were cloned by screening an LPS stimulated human macrophage cDNA library and isolating the two distinct cDNAs for the proteins pro-IL-1 α and pro-IL-1 β . The amino acid sequences for human mature IL-1 α and IL-1 β showed only a 26% identity [March *et al.*, 1985]. The cloning and sequencing of a mouse IL-1 α cDNA based on the protein purified by Mizel [Mizel & Mizel, 1981] was also published [Lomedico *et al.*, 1984]. It showed 62% identity to the human IL-1 α but only 30% to human IL-1 β , demonstrating an ancient divergence. Complete nucleotide sequences of the genes for both human IL-1 α [Furutani *et al.*, 1986] and IL-1 β [Clark *et al.*, 1986] showed that they both contain 7 exons. The mouse genes have similar structures [Gray *et al.*, 1986; Telford *et al.*, 1986]. Neither the IL-1 α nor IL-1 β polypeptides possess the hydrophobic signal common to most secreted proteins. [Auron *et al.*, 1984; March *et al.*, 1985].

Although the predicted primary translation products are of Mr 30,606 and 30,479 for pro-IL-1 α and pro-IL-1 β respectively, the mature ~17kDa forms consist only of the carboxy terminal ends. These are biologically active. The precursor of IL-1 α , but not of IL-1 β , is also biologically active. [March *et al.*, 1985; Mosley *et al.*, 1987]. It was subsequently demonstrated that precursor forms of mouse IL-1 α [DeChiara *et al.*, 1986; Lomedico *et al.*, 1984] and IL-1 β [Gunther *et al.*, 1989] are also processed to the mature form.

The 271 aa pro-cytokine for IL-1 α can be cleaved *in vitro* in a calcium dependent manner by calpain, a neutral cysteine protease, into a 159 aa mature segment and 112 aa pro-sequence [March *et al.*, 1985; Kobayashi *et al.*, 1990; Watanabe & Kobayashi, 1994]. IL-

1 β converting enzyme (ICE, caspase-1) has also been suggested to process pro-IL-1 α , as ICE deficient mice display an impaired production of mature IL-1 α [Li *et al.*, 1995].

The 31kDa 269 aa IL-1 β precursor is cleaved intracellularly into a 116 aa pro segment and a 153 aa mature segment [March *et al.*, 1985; Thornberry *et al.*, 1992]. Different mechanisms have been postulated, the most recent of which is through the action of the protease ICE [Thornberry *et al.*, 1992]. Its activity was first reported in 1989 [Black *et al.*, 1989; Kostura *et al.*, 1989], and its specificity for IL-1 β was demonstrated [Sleath *et al.*, 1990]. The cDNA for the enzyme was subsequently cloned [Cerretti *et al.*, 1992]. The primary translation product is an inactive precursor molecule of 45kDa [Miller *et al.*, 1993] that is activated by processing into subunits of 10kDa and 20kDa. The heterodimer is capable of cleaving pro-IL-1 β [Wilson *et al.*, 1994]. ICE deficient mice lack the capacity to release mature IL-1 β [Kuida *et al.*, 1995; Li *et al.*, 1995], display an impaired production of IL-1 α [Li *et al.*, 1995], and are also unable to mount an efficient inflammatory response to clear *Shigella flexneri* infection [Sansone *et al.*, 2000]. However, the importance of IL-1 β processing in this last process is debatable because ICE also cleaves the precursor of IL-18, a member of the IL-1 family, into a biologically active mature form [Gu *et al.*, 1997]. IL-18 has recently been shown to be essential for the same response [Sansone *et al.*, 2000].

Pro-IL-1 β also appears to be secreted or possibly shed passively from dying cells [Hazuda *et al.*, 1988]. Extracellular activation by other proteases has been proposed, such as by a bacterial cysteine protease (from *Streptococcus pyogenes*) [Kapur *et al.*, 1993]

and by matrix metalloproteinases [Schonbeck *et al.* 1998]. Other proteinases were mainly proposed before the discovery of ICE, and their physiological relevance is difficult to assess. ICE remains the most likely candidate for the processing of pro-IL-1 β .

Despite the limited amino acid homology between IL-1 α and IL-1 β , their three dimensional structures, as determined by X-ray crystallography, are remarkably similar. IL-1 α and IL-1 β consist of a single domain, with pseudo 3-fold symmetry, of twelve anti parallel beta strands, six of which form a barrel, and six form a cap, closing the end [Prestle *et al.*, 1988; Priestle *et al.*, 1989; Finzel *et al.*, 1989; Veerapandian *et al.*, 1992; Graves *et al.*, 1990]. Mouse IL-1 β is structurally very similar to the human cytokine [Huang *et al.*, 1988; Van Oostrum *et al.*, 1991]. Mouse IL-1 β and human IL-1 β are both active on receptors from the other species [Sims *et al.*, 1993] and interact through conserved regions around the rim of the β -barrel [Veerapandian *et al.* 1992; Labriola-Tompkins *et al.*, 1993].

1.1.3: Sources of IL-1

IL-1 is produced predominantly by macrophages, but also a variety of other cell types including vascular endothelial cells [Miossec *et al.*, 1986], keratinocytes [Partridge *et al.*, 1991], synovial fibroblasts [Dalton *et al.*, 1989], glial cells [Fontana *et al.*, 1982] and epithelial cells [Waterhouse *et al.*, 1999]. A diverse range of both endogenous and exogenous agents have the ability to stimulate the production of IL-1. The best studied stimulus is the bacterial cell wall component LPS which rapidly activates IL-1 production by macrophages, monocytes and endothelial cells. The signal appears to be mediated

through the LPS binding protein CD14 [Wright *et al.*, 1990] and the *Toll*-like receptor, TLR4 [Chow *et al.*, 1999].

Monocytes, macrophages and fibroblasts

Although IL-1 production can be activated by microbial products (by signalling through the *Toll*-like receptors, TLRs), macrophages also respond to endogenous activators to produce IL-1. IL-1 has the ability to induce its own synthesis, either directly [Dinarello *et al.*; Dalton *et al.*, 1989] or via other cytokines such as interferon gamma (IFN γ) and tumour necrosis factor alpha (TNF- α), whose production is stimulated by IL-1. These cytokines can augment stimulation of further IL-1 production by LPS [Partridge *et al.*, 1991; Miossec & Ziff, 1986; Arenzana-Seisdedos *et al.*, 1985; Nawroth *et al.*, 1986].

The extracellular matrix (ECM) proteins collagen and fibronectin can activate IL-1 production in macrophages during tissue damage [Schiffer *et al.*, 1999]. During the inflammatory response, ECM proteins play a regulatory role at the site of tissue damage by regulating cell growth and differentiation, and the inflammatory activities of immunocompetent cells [Pakianathan, 1995]. The interactions between infiltrating leukocytes and ECM proteins may therefore influence the local inflammatory response. When monocytes bind through integrins *in vitro*, expression of IL- β and IL-8 (neutrophil chemotactic factor) is induced [Rosales & Juliano, 1995].

Keratinocytes

IL-1 α is produced constitutively in the skin [Ansel *et al.*, 1988; Partridge *et al.*, 1991]. Ultraviolet irradiation (UVR) stimulates IL-1 production in cultured human keratinocytes [Kupper *et al.*, 1987] and in a murine keratinocyte cell line [Ansel *et al.*, 1988]. The increase of both IL-1 mRNA and protein in keratinocytes exposed to UV irradiation probably contributes to skin tissue damage following solar irradiation. IL-1 α induced by UVR was shown to upregulate expression of the type 1 IL-1 receptor on keratinocytes, making them more responsive to IL-1. The increased responsiveness was demonstrated to be necessary for upregulation of intercellular adhesion molecule-1 (ICAM-1, a cell surface adhesion molecule which binds to lymphocytes) expression on keratinocytes following IL-1 α stimulation [Krutmann & Grewe, 1995]. Thus, UVR increases production of IL-1 α , which leads to upregulation of ICAM-1 thereby increasing keratinocyte-leukocyte interactions.

Endothelial cells

Stimulation of human umbilical vein endothelial cells (HUVEC) with LPS, either directly or indirectly, induces the release of IL-1 β *in vitro*. Both the direct and indirect pathways are dependent on CD14. The direct pathway, which is serum dependent, involves the binding of LPS to the LPS binding protein (LPB). The complex then interacts with soluble CD14, and the complex then interacts with TLR4 on the endothelial cell surface. The indirect pathway involves the LPS induced release of IL-1 from macrophages, following its interaction with membrane bound CD14 on the mononuclear cell surface,

which can then activate endothelial cells directly resulting in the further release of IL-1 [Pugin *et al.*, 1993].

Mast cell tryptase stimulation of HUVEC induces expression of mRNA for both IL-1 β and IL-8 [Compton *et al.*, 1998]. Upon activation by antigen binding to IgE, mast cells release various inflammatory mediators such as proteases, histamine and cytokines. Tryptase, a serine protease, is released in large quantities by mast cells upon degranulation, and it appears to have potent effects on surrounding cells, including causing microvascular leakage (possibly by causing the release of histamine) and neutrophil accumulation at injection sites in guinea pigs [He & Walls, 1997; He, 1997], induction of type 1 collagen synthesis in fibroblasts [Cairns & Walls, 1997; Gruber, 1997], and stimulation of release of the chemokine IL-8 and upregulation of ICAM-1 expression on epithelial cells [Cairns & Walls 1996]. Despite detecting an increase in IL-1 β mRNA expression in tryptase treated HUVEC, Compton *et al.* could not detect IL-1 β in supernatants. They suggest that tryptase may prime endothelial cells for release of IL-1 β after a secondary stimulus, or the endothelial cells may require simultaneous stimulation by several different stimuli. The artificial experimental conditions used make it difficult to tell if this is the case but it seems possible, since at sites of mast cell activation endothelial cells will be exposed to more than one stimulus. In addition, histamine released by mast cells upon degranulation has a number of effects, one of which is to activate immature dendritic cells transiently, inducing the expression of IL-1 β , IL-6, IL-8, monocyte chemoattractant protein-1 (MCP-1) and MIP-1 α [Caron *et al.*,

2001] and the enhancement of synthesis of IL-1 β in IL-1 α stimulated peripheral blood mononuclear cells (PBMC) [Vannier & Dinarello, 1993].

1.1.4: Biological effects of IL-1

One of the earliest observations associated with IL-1 was that it causes the proliferation of T-cells in mixed lymphocytic cell cultures [Gordon & MacLean, 1965; Gery & Waksman, 1972; Watson *et al.*, 1979]. It has since been shown that IL-1 has numerous local and systemic effects. It activates multiple cell types including T-cells, which can then produce other cytokines, such as IL-2 [Gillis & Mizel, 1981] and IL-6 [Helle *et al.*, 1988]. In response to IL-1, B-cells are activated and proliferation is induced [Lipsky *et al.*, 1983]; fibroblasts produce IL-6 and IL-11 [Mino *et al.*, 1998], collagenase and prostaglandin E₂ (PGE₂) [Balavoine *et al.*, 1986; Postlethwaite *et al.*, 1988], and synovial cells [Mizel *et al.*, 1981; Dayer *et al.*, 1986] and endothelial cells [Bevilacqua *et al.*, 1985] are activated. Chemokines such as IL-8 and MCP-1 are also produced following IL-1 stimulation [Sica *et al.*, 1990].

It has recently been shown that IL-1 also enhances T-cell dependent antibody production. *IL-1^{-/-}* mice (deficient in both IL-1 α and IL-1 β) on a Balb/c background were challenged with sheep red blood cells (SRBC) and the resulting antibody titres measured. In IL-1 deficient mice, antibody production was reduced, an effect which could be reversed by the administration of an agonistic anti-CD40 monoclonal antibody. This implies an essential role for CD40 ligand (CD40L, CD154), produced in response to IL-1, in antibody production. Antigen presenting cells (APCs) from IL-1 null mice were

incapable of activating SRBC specific T-cells, and it was subsequently demonstrated that IL-1 induces CD40L, a molecule expressed on the surface of activated T-cells which is involved in T-cell priming and which binds to CD40 on B-cells [Nakae *et al.*, 2001].

IL-1 also has numerous effects on dendritic cells (DC). One primary effect is to trigger the maturation and migration of DC to the draining lymph nodes where they can encounter and prime naïve T-cells [Cumberbatch *et al.*, 1997]. IL-1 enables Langerhans' cells (DC resident in the epidermis) to dissociate from epidermal keratinocytes by causing a decrease in the expression of E-cadherin, a DC adhesion molecule [Jakob & Udey, 1998], thus allowing them to migrate.

1.1.5: Systemic effects of IL-1

On a systemic level, one of the early responses to infection or injury is a complex set of reactions known as the acute phase response (APR). APR is characterised by fever and the release of proteins by the liver termed the acute phase proteins (APP). These include human C reactive protein (CRP), the serum amyloid A (SAA) proteins and serum amyloid P (SAP). IL-1 released by activated macrophages is a potent inducer of the hepatic APR [Bornstein, 1982]. Early research by Bornstein *et al.* demonstrated that a single intravenous dose of purified IL-1 in the rabbit resulted in increased plasma concentrations of C-reactive protein, haptoglobin and fibrinogen after 24 hours [Bornstein, 1982].

The murine “SAA inducer” released by macrophages in response to LPS, which triggered SAA release from hepatocytes, was identified as IL-1 in 1981 [Sztein *et al.*, 1981]. Induction of murine SAA by IL-1 was demonstrated in mice injected with murine recombinant IL-1. Levels of SAA mRNA rose in a dose dependent manner, and IL-1 could also stimulate SAA production in C3H/HeJ mice, which are resistant to endotoxin, demonstrating that IL-1 and not endotoxin was the stimulus. mRNA levels for apolipoprotein E, a constitutive hepatic protein which is not involved in the APR, were also measured and were not affected by IL-1 administration [Weinstein & Taylor, 1987]. This supported earlier observations by Kampshmidt *et al.* who demonstrated the release of acute phase proteins after injection with partially purified IL-1 in C3H/HeJ mice [Kampschmidt *et al.*, 1980], and by Ramadori *et al.* who showed that IL-1 upregulates SAA mRNA levels and downregulates albumin gene expression (a negative acute phase protein) *in vivo* in C3H/HeJ mice and *in vitro* in primary mouse hepatocyte cultures [Ramadori *et al.*, 1985].

Fever induction by IL-1 is due to its ability to act on the hypothalamic-pituitary-adrenal axis (the “HPA” axis). It alters the temperature set-point in the hypothalamus by stimulation of PGE₂ release from endothelial cells. [Reviewed in Dinarello & Wolff, 1982]. In rats, elevated temperature in response to IL-1 is caused at least in part by activation of thermogenesis in brown adipose tissue [Dascombe *et al.*, 1989]. PGE₂, a potent vasolidator, is also released from fibroblasts and synovial cells [Mizel *et al.*, 1981; Dayer *et al.*, 1986; Balavoine *et al.*, 1986; Postlethwaite *et al.*, 1988] along with collagenase in response to IL-1. This release is involved in the pathogenesis of

rheumatoid arthritis, discussed in section 1.2.13. Many of the febrile responses to IL-1 are now known to be indirect, via IL-1-induced IL-6. For instance, IL-6 deficient mice are incapable of producing fever in response to intraperitoneal injection of LPS or IL-1 β or intracerebroventricular injection of IL-1 β , but do have a fever response to intracerebroventricular injection of IL-6 [Chai *et al.*, 1996]. Circulating IL-6 has also been shown to mediate the febrile response to localised LPS-induced inflammation in rats, which can be abolished by pre-treatment with IL-6 antiserum [Cartmell *et al.*, 2000].

IL-1, along with IL-6 and TNF α produced after LPS stimulation in mice, can also induce the release of corticotropin-releasing hormone (CRH) from the hypothalamus. CRH stimulates the secretion of corticotropin from the pituitary which causes the release of corticosterone from the adrenal cortex [Besedovsky *et al.*, 1986; Perlstein *et al.*, 1993]. The glucocorticoids then act in a negative feedback, as will be discussed in section 1.1.7. IL-1 β is an inducer of hepatic nitric oxide (NO) synthesis. NO is an antimicrobial, antiviral and antiparasitic effector molecule of the immune system [Reviewed in Schmidt & Walter, 1994], and is produced in large amounts by inducible NO synthase (iNOS) during inflammation. IL-1 α and IL-1 β , as well as IFN γ and TNF- α , are endogenous activators of iNOS transcription [Geller *et al.*, 1995; Ding *et al.*, 1988]. IL-1 also increases synthesis of nitric oxide synthase (and therefore nitric oxide) in vascular smooth muscle cells [French *et al.*, 1991], thereby reducing vascular contractility. Vasodilation mediated by NO and PGE $_2$ results in increased blood flow at areas of inflammation.

1.1.6: Local effects of IL-1

Many of the local reactions in the inflammatory process are potentially mediated by IL-1. For example, circulating leukocytes must attach to and extravasate through the vessel walls, then localise into the damaged tissue. IL-1 can stimulate vascular endothelial cells to become more adhesive for circulating leukocytes [Bevilacqua *et al.*, 1985] through several pathways.

IL-1 upregulates the expression of the vascular adhesion molecule E-selectin (CD62E) on endothelial cells [Kupper & Groves, 1995]. E-selectin expression is also induced by TNF- α [Weller *et al.*, 1992]. There are two other selectins, L- and P-selectin (CD62L and CD62P). L-selectin is expressed continuously on the leukocyte cell surface while P-selectin is stored in granules (Weibel-Palade bodies) in platelets and endothelial cells and is rapidly transported to the cell surface in response to histamine, components of the complement pathway, TNF- α or IL-1 [Weller *et al.*, 1992]. L- and P-selectin weakly interact with their carbohydrate ligands, such as the mucin-like molecules MadCAM-1, GlyCAM-1 and CD34 for L-selectin, and P-selectin glycoprotein ligand-1 (PSGL-1), to cause the “rolling” motion of leukocytes observed along the vessel wall [Shimizu & Shaw, 1993; Borges *et al.*, 1997; Baumhueter *et al.* 1994; Sako *et al.*, 1993]. E-selectin then creates a stronger adherence of the leukocytes to the vascular wall by binding to its ligand sialyl Lewis_x (sLe_x) [Sako *et al.*, 1993].

IL-1 stimulates the release of chemotactic factors (chemokines) from many cell types including vascular endothelial cells, which recruit leukocytes into the area and then

increase the low-affinity interactions between adhesion molecules on the endothelial cells and their ligands on leukocytes [Grabovsky *et al.*, 2000]. Chemokines whose production is stimulated by IL-1 (and TNF) include IL-8 and MCP-1 [Sica *et al.*, 1990]. IL-8 and MCP-1 in turn activate integrins on the leukocytic cell surface [Jiang *et al.*, 1992; Gerszten *et al.*, 1999; Seo *et al.*, 2001].

The integrins involved in leukocyte adhesion are primarily β_2 (CD18)-integrins. The β_2 -integrins are four heterodimers, LFA-1 (CD11a/CD18), Mac-1 (CD11b/CD18), p150,95 (CD11c/CD18) and CD11d/CD18. Integrins bind with a high affinity to endothelial cell adhesion molecules such as ICAM-1 (CD54), which although present at low levels on the surface of normal endothelial cells, has greatly increased expression in response to stimulation by IL-1 [Dustin *et al.*, 1986; Bochner *et al.*, 1991] and other pro-inflammatory cytokines.

After firm attachment of the leukocytes to the endothelial cells they must migrate across the endothelium, a process known as diapedesis. Most of the leukocytes squeeze through the endothelial cell junctions, regulated largely by homophillic interactions of platelet/endothelial cell adhesion molecule-1 (PECAM-1 or CD31), which is expressed diffusely on the surfaces of migrating leukocytes and on the borders of endothelial cells [Muller & Randolph, 1999]. Transendothelial migration (TEM) is also thought to be controlled by IL-1 induced chemokine gradients across the endothelium, directing the leukocytes across and into the target tissue [Weber *et al.*, 1999].

IL-1 can also induce the expression of matrix metalloproteinases (MMPs) from monocytes, fibroblasts and endothelial cells [Zhang *et al.*, 1998; Rajavashisth *et al.*, 1999]. MMPs are a large family of proteases which between them can degrade all components of the extracellular matrix, and are naturally inhibited by the tissue inhibitors of metalloproteinases (TIMPS) [reviewed in Brew *et al.*, 2000]. The chemokine MCP-1 can also enhance the synthesis of MMP-1 (interstitial collagenase) in fibroblasts *in vitro*, mediated by IL-1 α , since addition of IL-1ra prior to MCP-1 almost completely inhibits MMP-1 production by fibroblasts [Yamamoto *et al.*, 2000]. Localised degradation of ECM components by IL-1 induced MMPs may facilitate the migration of leukocytes to the target area.

Thus, IL-1 acts at a local level as a mediator of the change from low affinity “rolling” of leukocytes along the vessel wall to firm adhesion following activation of the endothelium, then diapedesis through the intercellular junctions and extravasation into the damaged tissue.

Despite the numerous biological effects of IL-1, few essential functions have been identified. IL-1 null mice develop normally, are viable and do not as yet appear to develop any spontaneous disease, although their responses to challenges such as LPS [Fantuzzi *et al.*, 1996], turpentine [Zheng *et al.*, 1995; Horai *et al.*, 1998], and 2,4,6-trinitrochlorobenzene (TNCB) (which induces contact hypersensitivity) [Nakae *et al.*, 2001], are altered compared to wild type mice.

1.1.7: Regulation of IL-1 expression

IL-1 β expression is very rapid after stimulation of monocytes (for example with LPS), and is regulated on several levels. A number of transcription factors have been shown to play a role in regulation of the *IL1B* gene, including NF κ B, NF-IL6, CREB and Spi-1 [Godambe *et al.*, 1994; Tsukada *et al.*, 1994; Kominato *et al.*, 1995]. Glucocorticoids negatively regulate the expression of IL-1 [Snyder & Unanue, 1982]. This occurs at the transcriptional level by glucocorticoids inhibiting the activity of the *IL1B* upstream induction sequence (UIS), which is the regulatory region controlling the induction of *IL1B* located between positions -3134 and -2729 upstream of the transcription start site [Auron & Webb, 1994].

Other cell products arising from IL-1 activity on target cells can also regulate IL-1 expression in a negative feedback loop – for example, nitric oxide (NO). Stimulation of mouse RAW 264.7 cells (a murine macrophage cell line) with LPS and concomitant inhibition of iNOS results in an increase in IL-1 α and IL-1 β secretion. Also, addition of a NO-generating compound reduces concentrations of IL-1 α and IL-1 β in supernatants [Obermeier *et al.*, 1999]. As protein levels correlate with mRNA expression under these experimental conditions, this suggests another possible control at the transcriptional level. NO has been shown to inhibit NF κ B, which controls transcription of IL-1, by stabilising I κ B and preventing its dissociation from NF κ B (a process necessary for NF κ B activation) [Peng *et al.*, 1995].

1.1.8: Interleukin-1 receptor antagonist (IL-1ra)

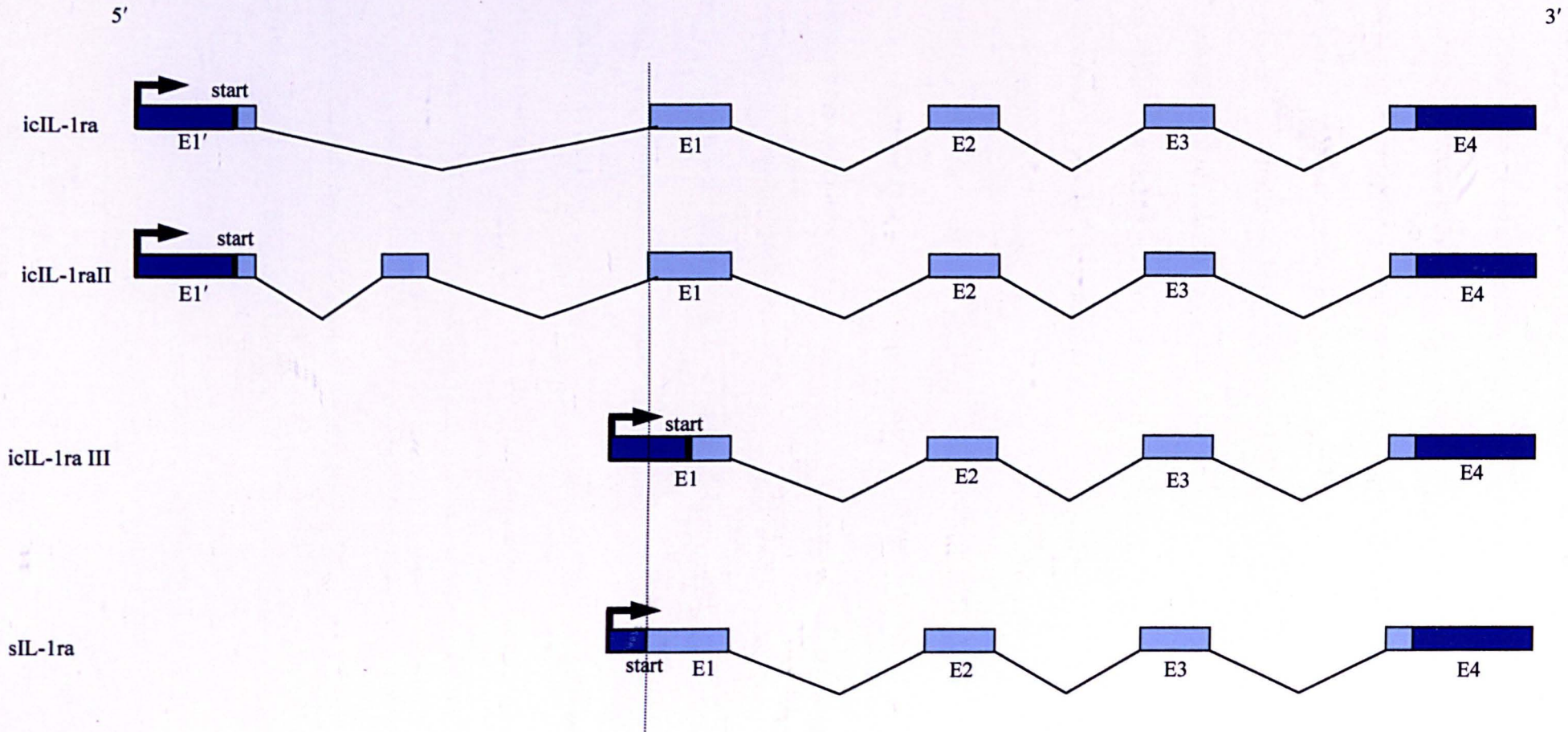
Identification of IL-1ra

The potent effects of IL-1 on host physiology suggest a requirement for its tight regulation in order to avoid potential damage. As well as regulation of IL-1 activity at the level of synthesis, there were reports of inhibitors which could regulate the activity of IL-1 directly. In 1987 Seckinger *et al.* [Seckinger *et al.*, 1987a] reported that urine from febrile patients contained an inhibitor of IL-1 biological activity, measured as PGE₂ and collagenase production by fibroblasts and synovial cells. They partially purified the inhibitor and found it to be 18 – 25kDa. Hannum *et al.* [Hannum *et al.*, 1990] purified three monocyte derived proteins from IgG stimulated cells with an IL-1 inhibitory activity which they termed protein inhibitors α (18kDa), β (22kDa) and γ (22kDa). After partial sequencing they showed them to be glycosylation variants of the same protein, which bound to the IL-1 receptor with no detectable consequences. Seckinger *et al.* tested the mechanism of inhibition in EL-46.1 cells (a murine thymoma line that produces IL-2 in response to IL-1). They observed that IL-1 activity was still inhibited after EL4-6.1 cells were pre-incubated with the inhibitor and washed, which suggested that the inhibitor was bound to a surface structure. They postulated the most economical hypothesis, that the inhibitor binds to the IL-1 receptor [Seckinger *et al.*, 1987b]. They named the activity interleukin-1 receptor antagonist (IL-1ra).



1.1.9: Forms of IL-1ra

It is now known that IL-1ra is a homologue of IL-1 α and IL-1 β , and that it exists in at least four forms, which are all products of a single gene. The 22kDa secreted form (sIL-

Figure 1: Different forms of IL-1ra arise from alternative translational start sites and alternative splicing of a single gene



Key:

-  Coding region
-  Non-coding region

E Exon

start Translation start site

1ra) of the protein shares 26% amino acid identity to IL-1 β , and 19% identity to IL-1 α . It is synthesised as a protein of 177 amino acids, which includes a conventional signal sequence of 25 amino acids that is removed to leave 152aa - the 22kDa protein [Eisenberg *et al.*, 1990]. The other three forms are intracellular. Two of these, icIL-1ra and icIL-1raII (18kDa and 25kDa) lack signalling sequences and remain in the cytoplasm of activated cells. They are transcribed from an upstream promoter [Haskill *et al.*, 1991; Butcher *et al.*, 1994; Muzio *et al.*, 1995]. The third, 16kDa icIL-1ra (icIL-1raIII) has been identified in neutrophils and monocytes [Malyak *et al.*, 1998b]. It binds to the IL-1 receptor with a lower affinity than that of sIL-1ra or icIL-1ra [Malyak *et al.*, 1998a]. icIL1raIII is derived from a translation initiation site at the second AUG of sIL-1ra mRNA (Figure 1).

1.1.10: Induction of IL-1ra expression

Various stimuli induce expression of IL-1ra – some also induce expression of IL-1, such as LPS [Andersson *et al.*, 1992] and others, for example adherent IgG [Arend *et al.*, 1991] or granulocyte/macrophage-colony stimulating factor (GM-CSF) [Poutsika *et al.*, 1991], stimulate production of IL-1ra but not IL-1. This indicates separate regulatory mechanisms for the induction of expression of IL-1 and IL-1ra. Human monocytes, stimulated with LPS, can produce IL-1 and IL-1ra simultaneously, as has been seen in double staining of cells visualised by fluorescence microscopy [Anderson *et al.*, 1992].

Th1 type T cells preferentially produce pro-inflammatory cytokines such as IL-12 and IFN γ . They induce IL-1 β production rather than IL-1ra production in the monocytic cell line THP-1 after stimulation of the THP-1 cells with the membranes of antigen activated

Th1 primed cells. In contrast, Th2 cells, characterised by production of anti-inflammatory cytokines including IL-4, IL-5, IL-10 and IL-13, preferentially induce production of IL-1ra over that of IL- β in the same experiment [Chizzolini *et al.*, 1997]. In primary hepatocytes and hepatoma HepG2 cells, stimulation with IL-4 or IL-13 in combination with IL-1 β augments the effect of IL-1ra production in response to IL-1 β [Gabay *et al.*, 1999]. IL-4 stimulation also increases IL-1ra production in human PMN activated by LPS [Marie *et al.*, 1996]. These results suggest co-operation between Th2 type cytokines and IL-1ra in their anti-inflammatory activities.

There is also evidence that IL-1ra down-regulates the acute phase response through antagonising IL-1. For example, when IL-1ra is co-injected with silver nitrate (silver nitrate induces an inflammatory response) into C57BL/6 mice, induction of hepatic mRNAs for the acute phase proteins SAA and SAP is partially blocked, and circulating protein levels decreased [Grehan *et al.*, 1997].

1.1.11: IL-1ra in health and disease

IL-1ra appears to act solely as a natural anti-inflammatory inhibitor of IL-1 by competitively binding to the type 1 IL-1 receptor without initiating any signal transduction. Strong evidence for a requirement for endogenous IL-1ra comes from transgenic mouse models, in which the gene for IL-1ra is non-functional. These animals suffer from inflammatory diseases including arteritis, rheumatoid arthritis and, as we first describe here, a psoriasis-like disease, as discussed in section 1.2.

IL-1ra can be detected in the plasma of healthy individuals [Hurme & Santtila, 1998] and in normal cells – for example intestinal epithelial cells (IECs) from normal mucosa constitutively produce low levels of icIL-1ra, but no IL-1 [Bocker *et al.*, 1998].

Significantly elevated levels of both IL-1ra mRNA and serum protein have been demonstrated in patients with active stage polymyositis and dermatomyositis (PM/DM) (inflammatory muscle diseases) [Son *et al.*, 2000], and in diseased human coronary arteries, where the protein co-localises with IL-1 β in the endothelium. *In vitro* stimulation of HUVEC and human coronary artery endothelial cells with LPS/PMA or TGF- β *in vitro* leads to accumulation of icIL-1ra mRNA [Dewberry *et al.*, 2000].

IL-1ra also appears to be neuroprotective. After focal cerebral ischaemia by middle cerebral artery occlusion (MCAo) in the rat, low amounts recombinant human IL-1ra (rhIL-1ra) injected directly into the brain, and higher amounts of rhIL-1ra administered peripherally, can significantly inhibit infarct size and cerebral oedema formation [Relton *et al.*, 1996]. The expression of IL-1ra mRNA is rapidly induced in the rat brain following focal cerebral ischaemia and blocking of IL-1ra by anti-rat IL-1ra antiserum before MCAo greatly increases ischaemic brain damage [Loddick *et al.*, 1997]. Conversely, overexpression of IL-1ra via gene transfer can reduce brain injury after focal cerebral ischaemia in the mouse.

1.1.12: Therapeutic potential of IL-1ra

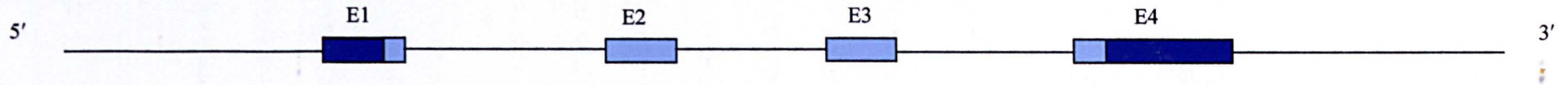
A well-studied therapeutic use of IL-1ra has been in the treatment of rheumatoid arthritis (RA). As discussed in section 1.2.13, there is a large body of evidence implicating IL-1 in the pathogenesis of RA in humans, rabbits, rats and mice. In animals, arthritis has been treated with IL-1ra in several models. Gene therapy using IL-1ra delivered in a recombinant adeno-associated virus vector (rAAV) suppressed LPS induced arthritis in rats [Pan *et al.*, 2000]. In type 2 collagen induced arthritis (CIA) in mice, an animal model for RA, administration of IL-1ra reduces incidence of CIA, and suppresses antibody response to IL-1 when administered to animals with established disease [Wooley *et al.*, 1993]. Importantly, mice deficient in IL-1ra spontaneously develop arthropathy resembling RA [Horai *et al.*, 2000; this work] as discussed in sections 1.1.13 and 1.2.

In humans, clinical trials involving subcutaneous injection of human recombinant IL-1ra into patients improves RA symptoms and significantly reduces the rate of joint damage as compared to patients receiving a placebo [Bresnihan *et al.*, 1998; Jiang *et al.*, 2000].

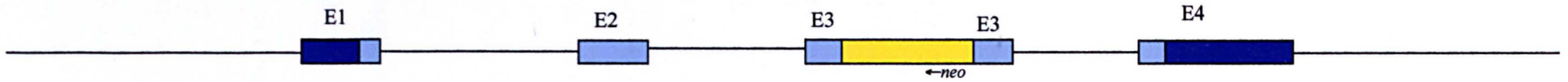
Therefore, various cell and tissue types in the normal, healthy individual produce IL-1ra and this production is upregulated during infection or inflammation. Blocking of IL-1ra generally exacerbates disease, whereas multiple inflammatory conditions have shown improvement after treatment with IL-1ra. Clinical trials have been performed or are underway to test the efficacy of using IL-1ra therapeutically in humans.

Figure 2: The generation of three different *Il1rn* null alleles in the mouse

Wild type *Il1rn* locus



Hirsch *et al.*, PNAS 1996



Horai *et al.*, J.Exp.Med 1998



Nicklin *et al.*, J.Exp.Med 2000



1.1.13: IL-1ra transgenic and IL-1ra deficient mice

Three groups have produced mice with altered expression of IL-1ra (Figure 2). Hirsch *et al.* (New York) have produced both IL-1ra null and overproducing mice [Hirsch *et al.*, 1996]. Transgenic mice were made that contained sIL-1ra under control of its endogenous elements in a 9kb DNA fragment. The IL-1ra null mice have a deletion in the open reading frame from the beginning of exon 3.

IL-1ra null and overexpressing mice were viable and appeared normal, although the mean body weight of *Il1rn*^{-/-} mice was lower compared to wild type littermates. There seems to be no obvious reason for this finding, but the authors postulate that IL-1 somehow plays a role in normal growth and development. IL-1ra null mice were highly susceptible to LPS injection, and IL-1ra overexpressors were less susceptible than wild type controls to LPS-induced shock. After challenge with LPS, circulating levels of IL-1 α and IL-1 β were lowered in IL-1ra null mice compared with wild-type controls, and higher in IL-1ra overexpressors as compared to wild type controls. This suggests that IL-1ra somehow positively regulates IL-1 expression during endotoxic shock. The most obvious way is through antagonising direct or indirect (for example, through the HPA axis) negative feedback on IL-1 expression.

Following infection with the intracellular bacterium *Listeria monocytogenes*, IL-1ra null mice showed increased survival, and IL-1ra overproducers showed decreased survival, in relation to wild type littermates. This suggests that in the absence of IL-1ra, macrophages are more sensitive to activation by IL-1, and in this case it is an advantage since the

increased activation of the macrophages enables the animals to clear the bacteria more efficiently. IL-1 plays an important role in the clearance of infection by *L.monocytogenes*. In further experiments, Irikura *et al.* demonstrated that during primary listeriosis, IL-1ra appeared to play a regulatory role with respect to macrophage activation. IL-1ra overproducing mice showed decreased class II major histocompatibility complex (MHC) expression on macrophages, implying that IL-1 is necessary for macrophage activation in listeriosis [Irikura *et al.*, 1999].

Horai *et al.* (University of Tokyo) have also produced IL-1ra null mice as well as mice deficient in IL-1 α , IL-1 β or both IL-1 α and β [Horai *et al.*, 1998]. For the IL-1ra null mice, they produced a construct in which a 5.3kb DNA fragment of the gene containing exons 1-4 was deleted and a neomycin resistance cassette inserted in its place. 129/Sv derived chimeras were crossed with female C57BL/6, and the F1 generation was inbred to produce homozygous null F2 mice. Again, IL-1ra null mice were viable and appeared healthy, but had lower body weight than wild type littermates, which became more apparent with age. When injected with turpentine, which causes a local inflammation and fever, IL-1ra null mice had a higher body temperature than control mice and still had an increased body temperature one week after injection. IL-1 has been implicated as a mediator of turpentine induced fever by activation of the HPA axis (see section 1.1.5). Horai *et al.* showed that IL-1 β deficient mice (but not IL-1 α) displayed no rise in body temperature after injection with turpentine, and also that there was no rise in serum corticosterone level as compared to control mice 8 hours after injection. This would suggest that IL-1 β deletion is epistatic to IL-1ra deletion (the two genes lie on the same

phenotypic pathway). There was however a similar initial increase in corticosterone levels between wild type and IL-1 β null mice post injection, suggesting that IL-1 is not uniquely required to activate the HPA axis. That data coupled with that for IL-1ra suggest an essential role for IL-1 in mediating turpentine induced fever, and IL-1ra in regulating that induction.

In further experiments with the *Il1rn*^{-/-} mice, Horai *et al.* backcrossed the knockout mice extensively onto C57BL/6J, DBA/1 and Balb/cA backgrounds to investigate the effects of strain differences. They discovered that the *Il1rn*^{-/-} mice on a Balb/cA background (but not C57BL/6J or DBA/1) developed a spontaneous arthropathy resembling rheumatoid arthritis [Horai *et al.*, 2000]. From 35 days of age, the animals' joints and especially the hind ankles, became swollen, red and stiff. Histological examination revealed many characteristics of RA; synovial inflammation with proliferation of synovial lining cells, a mixed inflammatory infiltrate containing lymphocytes and neutrophils which formed a pannus, activation of osteoclasts, and bone erosion where the bone was replaced with fibroblastic cells. By 91 days of age, all *Il1rn*^{-/-} mice on a Balb/cA background had developed the RA-like disease, whereas none of the or the wild type, heterozygous or any C57Bl/6J mice had by 112 days of age. By 336 days of age, 2/7 remaining C57Bl/6J *Il1rn*^{-/-} mice had developed arthropathy. Unsurprisingly, by 112 days, there was a marked (10-fold) increase in IL-1 β mRNA levels in the arthritic joints of Balb/cA knockout mice, and there was also an increase of IL-6 and to a lesser extent TNF- α mRNA levels. This suggested that the unopposed IL-1 could induce expression of other proinflammatory cytokine genes in the arthritic joints.

Horai *et al.* showed a significant increase in antibody levels against the autoantigens dsDNA and type 2 collagen, and IgG class RF in the *Il1rn*^{-/-} mice on a Balb/cA background as compared to wild type and heterozygous mice. No elevation in autoantibody levels were seen in C57BL/6J *Il1rn*^{-/-} mice. Their data shows that there is a very low basal expression of IL-1 in the joints which is presumably normally antagonised by IL-1ra, and also that *Il1rn*^{-/-} mice develop inflammatory conditions which are background specific, results which have been supported by our own observations.

The third group to prepare *Il1rn*^{-/-} animals is our laboratory at the University of Sheffield [Nicklin *et al.*, 2000], in collaboration with the University of Edinburgh. The main body of this work characterises the spontaneous inflammatory diseases (arteritis, a psoriatic disease and an RA-like disease) observed in these animals, and their phenotypes are discussed in sections 3 and 4.

The animals were generated by the creation of a replacement construct (as were the other two colonies), which replaced parts of exon 3 and exon 4 with a cassette containing the G418 resistance gene and a β -actin promoter (β -*Neo*) in reverse orientation, disrupting the reading frame and generating a null allele. 129/Ola embryonic stem (ES) cells containing the construct were injected into C57BL/6 blastocysts which were implanted into pseudopregnant females. Two sets of chimeric offspring were obtained from distinct ES colonies. An animal from one set was backcrossed twice onto a 129/Ola background, before mating with outbred Swiss MF1 albino females. An animal from the other set was

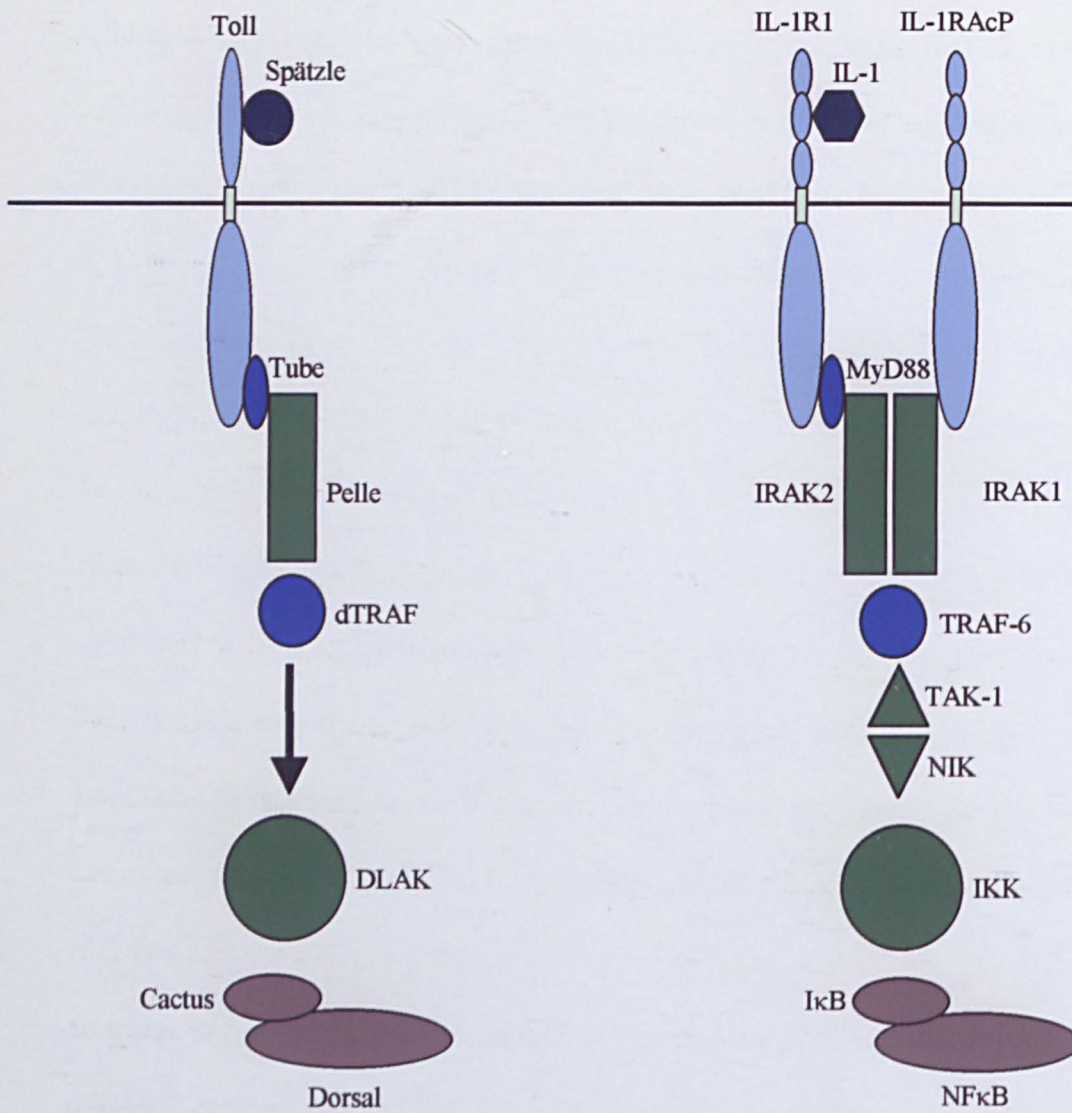
directly mated with MF1. Mice homozygous for the null allele were generated by inbreeding. Lines were inbred from these original animals, and the heterozygosity of the *Il1rn* locus was maintained during the inbreeding process. Animals were initially genotyped by Southern blotting, and subsequently genotyped by PCR performed on DNA extracted from routine ear clippings. Animals from these sublines were also backcrossed onto Balb/c and C57BL/6 backgrounds. All mice are viable, but early death amongst *Il1rn*^{-/-} mice was observed. The analysis of the phenotypes is described in this work (section 1.2, section 3 and section 4).

1.1.14: IL-1 Receptors

IL-1 α and IL-1 β both compete for the same receptor [Dower *et al.*, 1986; Kilian *et al.*, 1986], which explains their shared biological activities. There are two distinct IL-1 receptors which are products of different genes, [Chizzonite *et al.*, 1989], the IL-1 type 1 receptor (IL-1R1) and the type 2 receptor (IL-1R2).

The extracellular portions of both IL-1 receptors are encoded with similar intron/exon structures in the human, suggesting both genes arise from a common ancestor [Sims *et al.*, 1995]. The receptors are predominantly expressed on different cell types – for example IL-1R1 is the major IL-1 receptor on T-cells, epithelial cells and fibroblasts, whereas B-cells predominantly express IL-1R2 [Chizzonite *et al.*, 1989; Bomszyk *et al.*, 1989].

Figure 3: Homology between *Drosophila* Toll and IL-1 signalling pathways



Key:

- Ligand
- Receptor complex
- Adaptor protein
- Kinase
- Rel protein family member

Figure 3: Homology between *Drosophila* Toll and IL-1 signalling pathways

The signalling cascades through the type 1 IL-1 receptor in humans and through Toll in *Drosophila* are very similar. In *Drosophila*, after binding of the ligand Spätzle to the Toll receptor [Morisato & Anderson, 1994], Pelle and Tube (a functional homologue of Myd88) are the intermediate signal transducers required in Dorsal (NF-κB-like) activation signalling through Toll (IL-1R1-like) [Galindo *et al.*, 1995]. Pelle (IRAK-like) becomes activated and then, via the *Drosophila* homologue of TRAF-6, dTRAF-6, [Means *et al.*, 2000] it induces a protein kinase cascade involving DLAK (*Drosophila* LPS-activated kinase, structurally related to IKK) [Kim *et al.*, 2000]. DLAK phosphorylates Cactus (IκB-like) [Geisler *et al.*, 1992]. On phosphorylation, IκB and Cactus dissociate from NFκB and Dorsal respectively, which translocate to the nucleus to increase gene expression of inflammatory and immune mediators. Dorsal and NFκB are both members of the Rel family of inducible transactivators.

Binding of IL-1 to the type 1 receptor initiates biological effects. Mice deficient in the type 1 IL-1 receptor have no abnormal resting phenotype [Glaccum *et al.*, 1997] but they fail to respond to IL-1 and show an overall reduced inflammatory response [Labow *et al.*, 1997]. *Il1r1^{-/-}* mice are however quick to resolve cutaneous infection by the protozoan parasite *Leishmania major* by an enhanced Th2 response, indicating a role for IL-1 in normal regulation of Th1/Th2 responses [Satoskar *et al.*, 1998].

The type 1 receptor is an 80kDa transmembrane protein consisting of an extracellular portion, 319 aa in length and composed of three immunoglobulin-like domains [Sims *et al.*, 1988; Sims *et al.*, 1989], a 22 aa transmembrane region and a 217 aa cytoplasmic *Drosophila* Toll-like domain, TIR (Toll/IL-1 receptor homologous region) [Medzhitov & Janeway, 2000]. The intracellular domains of IL-1R1 and the Toll receptor show a 25% amino acid identity [Gay & Keith, 1991]. The protein Toll is involved in dorsoventral polarity in the *Drosophila* embryo [Hashimoto *et al.*, 1988], and antifungal responses [Lemaitre *et al.*, 1996]. The signal transduction pathways downstream of IL-1R1 and Toll are strikingly similar (Figure 3). There are at least 9 members of the IL-1-like receptor family [reviewed in Sims, 2002], and at least 10 other human and mouse Toll-like receptors (TLRs) [Reviewed by O'Neill & Greene, 1998, and Akira *et al.*, 2001].

The type 2 receptor was first cloned from B cells, where it is the predominant binding receptor for IL-1, but is also present on other cell types, including monocytes, keratinocytes, peripheral blood T- cells and the hepatoma cell line HepG2 [McMahan *et al.*, 1991]. Like IL-1R1, it has an extracellular ligand-binding portion, 334 aa in length,

Figure 4: Signal transduction does not appear to occur following binding of IL-1 to the type 2 receptor, or following IL-1ra binding to IL-1R1

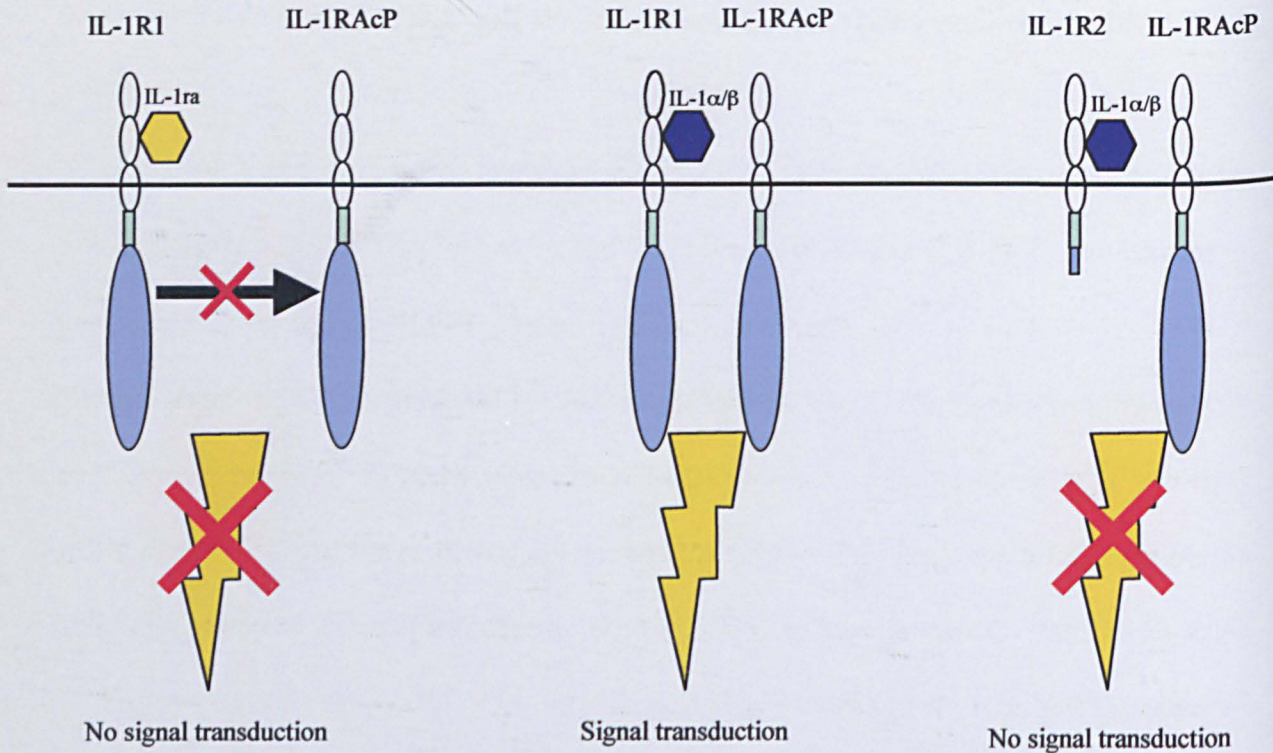


Figure 4: Binding of IL-1 α or IL-1 β to the extracellular domain of the type 1 receptor, IL-1R1, results in the recruitment of the IL-1 receptor accessory protein, IL-1RAcP. Heterodimers of the intracellular domains of IL-1R1 and IL-1RAcP subsequently recruit further adaptor and kinase molecules required for IL-1 signalling.

When IL-1ra binds to the extracellular domain of IL-1R1, IL-1RAcP is not recruited to the complex, the cytoplasmic heterodimer is not formed, and no signal transduction is achieved.

IL-1 α or IL-1 β binding to the extracellular domain of the type 2 decoy receptor, IL-1R2, results in recruitment of IL-1RAcP. However, since IL-1R2 has a truncated intracellular cytoplasmic domain, again the heterodimer is not formed and there is no subsequent signal

consisting of three immunoglobulin-like domains and a short 22 aa transmembrane region, but only has a 29 aa cytoplasmic domain and no Toll-like domain [McMahan *et al.*, 1991]. No evidence has been obtained to suggest that IL-1R2 is a signalling receptor.

IL-1 initiates biological effects only by binding to the type 1 receptor as judged by induction of NF κ B by IL-1 on murine cell lines, bearing predominantly either IL-1R1 (EL4.NOB.1) or IL-1R2 (70Z/3) [Stylianou *et al.*, 1992]. Subsequent experiments showed that using monoclonal antibodies capable of blocking binding to both receptors, it was possible to block responses to IL-1 completely when directed against the type 1 receptor, but that no inhibitory effect was seen upon blocking of the type 2 receptor [Sims *et al.*, 1993]. Occupancy of only a few type 1 receptors per cell is enough to elicit a response [Re *et al.*, 1996].

1.1.15: IL-1 Receptor accessory protein

A second subunit of the IL-1 receptor complex, the IL-1 receptor accessory protein (IL-1RAcP) is required for signalling via IL-1R1 (Figure 4). A monoclonal antibody, isolated by Greenfeder *et al.*, blocked the binding and bioactivity of human and murine IL-1 β to the receptor in murine cells. The antibody recognised a protein distinct from both the type 1 and type 2 IL-1 receptors. The target of the antibody was identified as a novel protein required for IL-1 responses, the IL-1 receptor accessory protein [Greenfeder *et al.*, 1995]. Cell lines which did not express IL-1RAcP were unresponsive to IL-1 [Wesche *et al.*, 1996]. Transfection of IL-1RAcP cDNA into non-responsive cells restored their ability to initiate biological activity after stimulation with IL-1, indicating requirement for the

second subunit [Korherr *et al.*, 1997; Hofmeister *et al.*, 1997]. Mice lacking IL-1RAcP and IL-1RAcP-deficient fibroblasts fail to produce a biological response when challenged with IL-1, although IL-1 α and IL-1 β still bind to IL-1R1. IL-1RAcP shows a structure similar to that of IL-1R1.

Murine IL-1 β shows a 70 fold reduction in affinity for the type 1 receptor in IL-1RAcP deficient fibroblasts, demonstrating that the presence of IL-1RAcP is also required for high affinity binding of IL-1 to IL-1R1 [Cullinan *et al.*, 1998]. IL-1RAcP stabilises the IL-1/IL-1R1 complex by protecting IL-1 in the ligand-binding site of IL-1R1 [Wesche *et al.*, 1998]. Immunoprecipitation studies showed that IL-1 can be cross-linked to both IL-1R1 and IL-1RAcP, but that IL-1ra can only be seen cross-linked to IL-1R1 and not the accessory protein, which suggests that IL-1ra does not bind to the IL-1RAcP or form a trimeric complex with IL-1R1 and IL-1RAcP [Greenfeder *et al.*, 1995].

1.1.16: IL-1 Signalling (NF κ B pathway)

The most well characterised signalling pathway resulting from formation of the trimeric IL-1/IL-1R1/IL-1RAcP complex leads to the activation of the transcription factor NF κ B (nuclear factor κ B) (Figure 3). After binding to the IL-1R/IL-1 complex, the two intracellular Toll-like domains of IL-1R1 and IL-1RAcP are brought into close contact. The resulting scaffold of the cytoplasmic tails of IL-1R1/IL-1RAcP recruits the adapter protein Myd88. The C terminal domain of Myd88 binds with high affinity to the heterocomplex (but not to IL-1R1 or IL-1RAcP alone) following IL-1 binding, and it then

functions as an adapter to recruit unphosphorylated IL-1 receptor associated kinases (IRAK1 and IRAK2) [Wesche *et al.*, 1997].

Another molecule, Myd88-adapter-like (Mal) has recently been shown to be required for signal transduction through TLR-4. Mal associates with TLR-4, possibly in a dimer with MyD88, and activates NF κ B by recruiting IRAK2 (but not IRAK1). Mal is therefore an additional component to MyD88 in TLR-4 mediated signalling, and its discovery explains why, in cells from MyD88 deficient mice, NF κ B and JNK are still activated after stimulation with LPS (which signals through TLR-4). Mal is not, however, involved in IL-1 or IL-18 signalling [Fitzgerald *et al.*, 2001].

After association with the MyD88/IL-1R1 complex, both IRAKs are phosphorylated [Cao *et al.*, 1996] and IRAK-1 then appears to disassociate from the complex to interact with the downstream adapter TRAF-6 (TNF-receptor-associated-factor-6) [Muzio *et al.*, 1997].

Two MAP3K (MAP kinase kinase kinase) related proteins, TAK-1 (TGF- β activated kinase) and NIK (NF κ B inducing kinase) then act downstream of TRAF-6. TAK-1 associates with TRAF-6 as demonstrated by immunoprecipitation and then associates with and phosphorylates NIK [Ninomiya-Tsuji *et al.*, 1999].

The ubiquitous transcription factor NF κ B (nuclear factor κ B) exists in a latent state bound by the inhibitory proteins collectively known as I κ B (inhibitor of κ B) which mask

its nuclear localisation signal. In response to signalling by the kinases collectively termed IKK (I κ B kinase), which interact with NIK [Regnier *et al.*, 1997; Mercurio *et al.*, 1997; Woronicz *et al.*, 1997], I κ B is phosphorylated, which serves as a signal for its capture and destruction by proteosomes [DiDonato *et al.*, 1997; Zandi *et al.*, 1997]. NF κ B is thus released.

However, other experiments have shown that NIK is not necessarily required for the activation of NF κ B. In cultured human macrophages, the adenoviral mediated expression of kinase deficient NIK did not affect NF κ B activation following stimulation by IL-1 α or TNF- α , although it was necessary for NF κ B activation following LPS stimulation. In addition, kinase deficient NIK did not affect the spontaneous secretion of TNF- α from rheumatoid arthritis derived synoviocytes [Smith *et al.*, 2001].

Upon degradation of I κ B, it dissociates from NF κ B. NF κ B then translocates into the nucleus to increase gene expression of numerous inflammatory and immune mediators [Beg *et al.*, 1993]. Inflammatory mediators induced by NF κ B include the cytokines IL-1, IL-2, IL-6, IL-8, TNF- α and GM-CSF, acute phase proteins such as the C3 component of complement and SAA, and cell adhesion molecules such as ICAM-1, E-selectin and VCAM-1 [reviewed in Kopp & Ghosh, 1995].

1.1.17: IL-1 Signalling (MAP kinase pathways)

IL-1 can induce at least three MAP kinase pathways as well as the NF κ B pathway. The MAP kinase pathways identified result in activation of JNK (Jun N-terminal kinase)

which is also known as SAPK (stress activated protein kinase), p38 and ERK2. These kinases activate several transcription factors and transcription factor subunits. The most well characterised is the JNK pathway, which phosphorylates the N-terminal domain of c-jun, a subunit of the AP-1 (activator protein 1) transcription factor. This is involved in IL-2 gene regulation amongst others [reviewed in Brooks & Mizel, 1994].

1.2: *Il1rn*^{-/-} mice, University of Sheffield

1.2.1: Spontaneous inflammatory diseases in IL-1ra null mice from the University of Sheffield

As discussed in section 1.1.14, three groups have produced mice deficient in IL-1ra. Our original colony of IL-1ra null mice (“Sf”) is derived from inbreeding a cross between a 129/Ola chimaera and an outbred MF1 mouse. The IL-1ra null mice suffer from inflammation of the aorta and its main branches [Nicklin *et al.*, 2000]. Two lines, derived from this original cross (Sf2 and Sf3) are studied in this work.

Backcrossing of *Il1rn*^{-/-} onto a Balb/c background produces IL-1ra null mice which develop a spontaneous RA-like condition, particularly in the hind limbs. This is in agreement with Horai *et al.* [Horai *et al.*, 2000]. Our Balb/c backcrossed *Il1rn*^{-/-} mice also suffer from arteritis and an additional psoriasis-like disorder of the skin on their ears and occasionally tails. The arterial inflammation is also seen in cadavers of mice from the Horai group [Nicklin, Hughes, Iwakura, unpublished data]. The three diseases, and relevance of IL-1 to their aetiology are discussed below.

1.2.2: Vasculitis

In the human there are approximately 20 different disorders which can be classed as vasculitides, including giant cell arteritis (GCA), vasculo-Behçet's disease, polyarteritis nodosa, Kawasaki's disease, Churg-Strauss syndrome and Takayasu's arteritis (TA). Blood vessels affected in human vasculitides range from the smallest blood vessels in the skin (for example in Churg-Strauss) to the aorta (GCA, TA). Vasculitis also commonly occurs as a secondary feature of other diseases such as RA and systemic lupus erythematosus (SLE) [Savage *et al.*, 1997]. GCA and TA are here discussed in more detail as they affect the aorta, in a similar manner to the arteritis observed in our *Il1rn^{-/-}* mice.

1.2.3: Giant cell arteritis

GCA (also known as temporal arteritis) is the most common of the arteritides in adult humans, with an incidence of ~200/million/population/year [Savage *et al.*, 2000]. It preferentially affects the medium and large sized branches of the upper aorta, particularly in the extracranial arteries [Hunder & Michet, 1985]. Sufferers, who are consistently aged over 50, display a range of symptoms including headache, joint pain, facial pain, fever and impaired vision. Patients respond well to glucocorticoids, but if left untreated complications can include blindness, stroke, aneurysms or ischaemia resulting from arterial stenosis [Huston *et al.*, 1978; Hunder *et al.*, 1990; Kaiser *et al.*, 1998]. The inflammatory lesions in GCA are often granulomatous, and tend to occur in a discontinuous pattern, "skipping" areas of the vessel.

Arrangement of the arterial vessel wall

There are three concentric layers in large arterial vessel walls – the intimal layer (closest to the lumen), the medial layer and the adventitial layer. The intimal layer consists of endothelium, and connective tissue layers including several layers of well-defined elastin, the internal elastic lamina (IEL). The medial layer is composed of circular arrays of smooth muscle cells, and the adventitial layer, furthest into the tissue, contains small blood vessels known as the vasa vasorum which supply the muscle around the main vessel. The medial-adventitial junction also contains an elastic layer, the external elastic lamina, but it is not as distinct as the intimal-medial junction.

1.2.4: Characterisation of GCA lesions and the involvement of IL-1

The infiltrates in GCA are composed mainly of CD4⁺ T-cells and macrophages which are found in all layers of the arterial wall, but the inflammation tends to be focused at the area of the internal elastic lamina. Multinucleated giant macrophages are frequently observed. Neutrophils tend to be less abundant within GCA lesions. Mast cells are also frequently present, and are almost exclusively found in the adventitia rather than in the medial or intimal layers [Banks *et al.*, 1983]. Aortic aneurysms can occur in GCA due to necrosis of the smooth muscle cells and degradation of the elastic layers of the vessels. Fragments of elastin have been identified within giant cells [Banks *et al.*, 1983].

The fragmentation of the intimal elastin layers may be due to the action of several products of CD68⁺ (microsialin) macrophages. Although classically used as a macrophage marker, CD68 may also be expressed by some myeloid-derived dendritic

cells [Thompson *et al.*, 2002]. There appears to be two subsets of CD68⁺ cells active in GCA lesions – one set, which expresses iNOS and secretes MMP-2 (Gelatinase-A) [Weyand *et al.*, 1996], and elevated levels of MMP-9 (Gelatinase-B) [Nikkari *et al.*, 1996], localises preferentially to the intimal layer and intimal-medial junction (the site of tissue destruction), whereas another subset which secrete IL-1 β , IL-6 and transforming growth factor β -1 (TGF β -1) but which do not secrete MMP-2 nor express iNOS, co-localise to the adventitia with IFN γ producing CD4⁺ T-cells [Wagner *et al.*, 1994; Weyand *et al.*, 1996].

The localisation of cells that are probably macrophages and activated CD4⁺ T-cells to the adventitia, with concurrent upregulation of chemokines and adhesion molecules induced by IL-1 β in this area suggests that inflammatory cells are recruited into the lesional area via the vasa vasorum in the adventitia rather than through the main vessel wall. MCP-1 production, probably stimulated by IL-1 and IFN γ , has been shown associated with mononuclear cells in all layers of the vessel wall, and also with endothelial cells, giant cells and some smooth muscle cells [Ellingsen *et al.*, 2000]. The levels of MCP-1 production differed between the three layers in this study, with higher numbers of cells staining positively for MCP-1 in the intimal and adventitial layers than the medial layer. Since a gradient of chemokine concentration is required for chemotaxis, the differing levels of MCP-1 production seen may indicate leukocyte trafficking between the adventitia and intima.

As well as fragmentation of the IEL (resulting in aneurysm), intimal growth, which can lead to vascular occlusion and stenosis, is observed in GCA. In atherosclerosis, this growth is associated with the release of platelet-derived growth factor (PDGF), a potent chemoattractant for vascular smooth muscle cells (VSMCs), from macrophages and giant cells along the medial intimal junction [Kaiser *et al.*, 1998]. Intimal thickening is due to migration of VSMCs from the media into the intima where they proliferate and secrete an excess of matrix proteins such as collagen [McCaffrey *et al.*, 1995]. This process is mediated by PDGF [Ross *et al.*, 1986; Jawien *et al.*, 1992]. IL-1 α and IL-1 β are potent mitogens for VSMCs, inducing their proliferation [Libby *et al.*, 1988; Beasley & Cooper., 1999], due to their induction of the release of PDGF [Ikeda *et al.*, 1990; Raines *et al.*, 1989]. Human VSMC themselves produce IL-1 in an autocrine loop following stimulation with IL-1 [Warner *et al.*, 1987].

The intimal hyperplasia is associated with the formation of new vasa vasorum. The vasa vasorum are normally restricted to the adventitial layer, but in GCA microvasculature is seen forming in the media and intima. The degree of angiogenesis correlates with medial thickening, destruction of the IEL and with the release of vascular endothelial growth factor (VEGF) from the giant cells and macrophages clustered along the medial intimal junction. The amount of neovasculature also correlates closely with the levels of IFN γ production within the lesion [Kaiser *et al.*, 1999].

1.2.5: Possible causes of GCA

The initiating factors and mechanisms of GCA progression are not well defined. Some lines of evidence suggest that GCA is a T-cell driven, autoimmune disease. CD4⁺ T-cells have been shown to be critical in the disease process. Brack *et al.*, using xenografts of human GCA temporal artery biopsies onto SCID mice, showed that the elimination of tissue infiltrating T-cells from the arterial grafts results in the eradication of vasculitis development, and adoptive transfer of CD4⁺ T-cells from diseased human tissue into SCID mice results in upregulation of pro-inflammatory mediators [Brack *et al.*, 1997a, 1997b].

Analysis of the T-cell receptor (TCR) molecules present on tissue infiltrating T-cells from GCA lesions showed that T-cells with identical beta chains could be isolated from distinct areas of lesions, suggesting that the CD4⁺ T-cells involved in lesion formation in GCA may recognise an antigen or autoantigen within the vessel wall. However, these results were from only one temporal biopsy [Weyand *et al.*, 1994]. In support of this work, IFN γ producing CD4⁺ T-cells from the adventitia were immunohistologically stained for the IL-2 receptor α -chain (CD25) and talin. The α -chain of the IL-2 receptor is expressed after TCR-mediated stimulation, and talin is a cytoskeletal protein which is reorganised in T-cells after interaction with antigen presenting cells (APCs). It was shown that the majority of the IFN γ producing T-cells expressed CD25, some had reorganised talin, and a subset was also undergoing proliferation as identified by expression of the Ki-67 nuclear antigen [Wagner *et al.*, 1996]. Ki-67 is a protein expressed in all stages of the cell cycle apart from G₀, so it can be used as a marker of

actively proliferating cells. Thus, a fraction of the T-cells present in the lesional areas of GCA appear to have been activated by stimulation of their antigen specific receptors.

Putative antigens in GCA

There are many possible exogenous antigens, which might trigger an inflammatory disease in the aorta that may then develop into a chronic autoimmune disease. One of these is *Chlamydia pneumoniae*. The bacterium has been identified in atherosclerotic lesions [Ong *et al.*, 1996], and associated with coronary artery disease [Dahlen *et al.*, 1995]. *C. pneumoniae* was detected by both immunohistochemistry and PCR in 8 out of 9 temporal artery tissues from patients with GCA, whereas control specimens were all negative. The eight positive results all came from patients with upper respiratory tract symptoms, which are often reported in GCA sufferers. The bacteria localised to the adventitial layers of the vessels, and when serial sections were stained for dendritic cells it was shown that dendritic cells were also predominantly found in the adventitia, localised with or near the bacteria [Wagner *et al.*, 2000]. Dendritic cells, as well as being efficient antigen presenting cells, are capable of stimulating naïve T-cells [Van Voorhis *et al.*, 1983]. Immune responses to *Chlamydia* infection are T-cell dependent, and in these infections monocytes are stimulated to produce IL-1 β [Rothermel *et al.*, 1989].

Therefore, in GCA, *C. pneumoniae* present in the vessel walls may act as an antigen that is presented by dendritic cells, which also stimulate naïve T-cells. Production of IL-1 β by monocytes is induced, which may further stimulate dendritic cells, and the response is enhanced. However, other infectious agents have also been implicated in GCA such as

parvovirus B19 [Gabriel *et al.*, 1999] and *Mycoplasma pneumoniae* [Elling *et al.*, 1996]. It is a possibility that infection generally is a risk factor in the development of GCA. In a study of GCA in Olmsted County, Minnesota, it was found that the incidence of GCA tended to have cyclical peaks every 6-7 years [Salvarani *et al.*, 1995] which could indicate concurrence with unidentified infections which also tend to occur in cycles within a community. It is also possible that the elderly patients with GCA are more susceptible to infection, and that it is not an initiating factor but rather a result of GCA. Our IL-1ra null mice which suffer from arteritis are housed in specified pathogen free conditions, which although not sterile are free of several microorganisms, including mouse *Chlamydia*.

1.2.6: Genetic susceptibility to GCA

The involvement of possible antigen presentation by dendritic cells and macrophages, along with evidence that GCA is a T-cell driven disease, suggests a possible role for HLA (human leukocyte antigen) gene polymorphism in susceptibility to arteritis. HLA genes are numerous and highly polymorphic, and code for the components of the human major histocompatibility complex (MHC). T-cells recognise peptide fragments bound to the MHC on antigen presenting cells, which makes analysis of the MHC and its interactions central to much immunological investigation.

GCA has been shown to be associated with specific variants of the HLA-DRB1 locus, which codes for the HLA-DR β 1 chain of the MHC class II complex [Weyand *et al.*, 1992]. The HLA-DR β 1 chain associates with the HLA-DR α chain to form a complex

which presents peptides to CD4⁺ T-cells. The HLA-DRB1 variants associated with GCA all relate to a region on the β -pleated sheet of the antigen presentation site. Therefore the formation of specific peptide binding grooves on the MHC class II molecules may affect antigen presentation in individuals carrying the alleles.

Genetic studies on the susceptibility to other vascular disorders have suggested that a variation in the IL-1ra locus itself might play a role. It was shown that carriage of the rare allele (allele 2) of *IL1RN* in humans shows a strong association with single vessel coronary artery disease [Francis *et al.*, 1999]. IL-1RN*2 carriage is also associated with a number of other inflammatory diseases including psoriasis [Tarlow *et al.*, 1997], alopecia areata [Tarlow *et al.*, 1994], Graves' disease [Blakemore *et al.*, 1995], SLE [Blakemore *et al.*, 1994], and polymyalgia rheumatica (PMR) [Boiardi *et al.*, 2000]. PMR is often found (in up to 50% of cases) in patients with GCA, and has similar symptoms but no temporal artery lesions [Gonzalez-Gay *et al.*, 1999]. In SLE, IL-1RN*2 carriage together with MHC class II variants DR17 and DQ2 increases the risk of development of SLE by seven fold [Tjernstrom *et al.*, 1999]. However, it currently seems likely that IL-1RN*2 acts more as a marker for disease susceptibility rather than having a functional consequence, since where tested, (in keratinocytes), levels of IL-1ra mRNA production do not appear to differ with *IL1RN* genotype [Clay *et al.*, 1996].

There are contradictory reports, however, that protein levels of IL-1ra are both elevated [Danis *et al.*, 1995] and lowered [Dewberry *et al.*, 2000] in association with IL-1RN*2. IL-1RN*2 has also been shown to be associated with increased production of IL-1 β from

monocytes after stimulation with phorbol dibutyrate [Santtila *et al.*, 1998]. The mechanism for this association has not been investigated.

It is likely that a number of factors are involved in the development of GCA. Ageing, genetic susceptibility and possibly a trigger (such as an infection) for onset of the disease may all contribute to pathogenesis of GCA.

1.2.7: Takayasu's arteritis

Takayasu's arteritis was first described in 1908 by Mikito Takayasu. It is also occasionally referred to as "pulseless disease" since patients with TA can have a peripheral pulse which is difficult to detect, due to stenosis of the arteries involved. TA typically affects females under 40 years of age. It is a rare disease, with 2-3 cases per million people each year in Caucasian populations although it has a higher incidence amongst Oriental, Asian and Indian populations [Arend *et al.*, 1990; Lie, 1998]. It involves the aorta (particularly the aortic arch) and its major branches [Numano *et al.*, 2000], although about 10% of patients also have coronary artery disease [Byrne *et al.*, 2001].

Patients initially present with systemic symptoms such as fever, weight loss and fatigue. During this phase, TA often goes undetected or is misdiagnosed due to the generalised nature of the symptoms [Sharma *et al.*, 1996]. The systemic phase is followed by the occlusive phase, where the pulse becomes difficult to detect and patients experience

symptoms caused by narrowing of the affected arteries such as claudication (aching on exertion) in the limbs [Kerr *et al.*, 1994].

1.2.8: TA lesions

TA is histologically similar to GCA. The medial and adventitial layers become dense and fibrous, and this change is accompanied by inflammatory infiltrates. These consist of numerous T-cells, CD68⁺ cells (macrophages) and dendritic cells within the aortic vessel walls. Lymphocytes tend to co-localise with dendritic cells, particularly around the neovessels seen in the adventitia, and granulocytes also accumulate in the adventitial layer. Neovascularisation is seen within the adventitia and the intima [Inder *et al.*, 2000]. Lesions tend to end in fibrosis, and fresh active lesions can be seen in close proximity to older fibrotic ones [Hotchi, 1992]. Healed arteritis in TA is indicated by the presence of extensive scarring in the media [Lie, 1990].

1.2.9: Possible aetiology of TA

Although the initiating factors and mechanisms of TA are yet to be defined, some research suggests an immune response to an antigenic factor within the vessel wall, which may be an autoantigen. For instance, there was found to be a significantly raised level of an antibody that binds an aorta-specific antigen in TA patients compared to normal controls and patients with RA or SLE. Following collagenase treatment of the aorta, antiaorta antibody titres fell almost to the level of that in normal controls, suggesting that collagen in the vessel wall may be acting as an autoantigen [Dhingra *et*

al., 1998]. However, anti-aorta antibodies were not found in the sera of 35 TA patients in another study [Baltazares *et al.*, 1998].

Other work has shown the presence of high levels of anti-endothelial cell antibodies (AECA) in the sera of patients with TA, as measured by ELISA using HUVEC as a target [Sima *et al.*, 1994; Eichorn *et al.*, 1996; Nityanand *et al.*, 1997]. The presence of AECA has also been demonstrated in RA [Bodolay *et al.*, 1989], SLE [Rosenbaum *et al.*, 1988] and Wegener's granulomatosis [Ferraro *et al.*, 1990]. AECA from patients with Wegener's granulomatosis can stimulate endothelial cells to produce MCP-1, IL-1 β , IL-6 and IL-8, as well as upregulate expression of adhesion molecules (E-selectin, ICAM-1 and VCAM-1 (vascular cell adhesion molecule-1, found on activated endothelium)) [Del Papa *et al.*, 1996].

Blank *et al.* prepared six monoclonal AECA (mAECA) from a TA patient that together recognised all of the epitopes on HUVEC targeted by the patients' whole IgG-AECA. They showed immunohistochemically that the autoantibodies bound specifically to HUVEC, and to human aortic endothelial cells. Immunoprecipitation revealed that a wide range of HUVEC target molecules were recognised by the mAECA. Four of the mAECA were capable of activating the HUVEC, as measured by IL-6 production. In addition, E-selectin, ICAM-1 and VCAM-1 expression and NF κ B activation were all increased following incubation with the antibodies [Blank *et al.*, 1999]. After incubation with mAECA, there was increased monocyte adherence to HUVEC due to the elevated levels of adhesion molecules.

Interestingly, none of the six mAECA isolated showed significant anti-microvascular activity as they did not bind to TrHBMEC (bone marrow endothelial cells), unlike positive controls from a patient with a vasculitis of the microvasculature [Blank *et al.*, 1999]. This observation is compatible with the fact that TA affects large arteries (the aorta), and suggests that TA is an antibody driven disease. AECA may well play a key role in TA by activating endothelial cells. The enhancement of NF κ B activation following AECA activation of endothelial cells may lead to increased production of IL-1, which in turn further upregulates expression of endothelial cell adhesion molecules, induces production of chemokines, and activates T lymphocytes, thus increasing damage to the affected area.

It seems plausible that IL-1 could induce endothelial cell antigens that are recognised by AECA in arteritides such as TA. AECA may then play a part in at least perpetuating the disease.

Seko *et al.* proposed another possible mechanism for vascular injury in TA involving direct damage to the vascular wall by the release of perforin from natural killer (NK) cells, cytotoxic T-lymphocytes (CTLs, CD8⁺ T-cells) and gammadelta (γ : δ) T-cell receptor (TCR) T-cells [Seko *et al.*, 1994]. The majority of T-cells recognise antigen through their α : β /CD3 TCR complexes but a subset of T-cells, γ : δ T-cells (representing <5% of the T-cell population), possess an alternative form of the TCR (γ : δ /CD3). Whilst α : β ⁺ T-cells also tend to have the CD4 or CD8 coreceptors, γ : δ T-cells do not. γ : δ T-cells

may be able to recognise antigen directly without assistance from APCs, and they are found abundantly within epithelial tissues. Peripheral blood $\gamma:\delta$ T-cells have also been shown to constitutively express perforin protein in their cytoplasmic granules [Nakata *et al.*, 1990]. Seko *et al.*, using immunohistochemistry, showed that there was a roughly equal number of $\alpha:\beta$ TCR ($CD4^+$ or $CD8^+$) T-cells to $\gamma:\delta$ T-cells in the infiltrate of TA lesions. They also demonstrated the presence of a 65kDa heat shock protein (HSP-65) in the aortic tissue. HSPs are produced by cells in response to various stresses such as a rise in temperature, UV radiation or viral infection. Recognition of HSP-65 by $\gamma:\delta$ T-cells may play a part in autoimmunity as they have been shown to respond to mycobacterial HSP (HSP-65) in the presence of APCs *in vitro* [Haregewoin *et al.*, 1989]. Therefore killer cells may release perforin in response to recognition of autologous HSP-65, directly injuring the vascular wall by forming pores in the plasma membranes of target cells, perforating them so that cells die by colloid-osmotic lysis [Liu *et al.*, 1996].

Subsequent analysis of the TCR V- α and V- β genes in the infiltrating $\alpha:\beta$ T-cells in TA showed that their usage was restricted [Seko *et al.*, 1996]. This indicates that a dominant antigen may be being presented on the MHC molecules of APCs in TA.

1.2.10: Genetic susceptibility to TA

Further evidence for cell mediated autoimmunity in TA comes from studies which suggest that specific HLA molecules are associated with the disease, although there are discrepancies in the reports. A positive association is seen with the HLA-B5 molecule, an HLA class I antigen in North Indian patients [Mehra *et al.*, 1996], and with both of its

two subtypes HLA-B51 and HLA-B52 [Mehra *et al.*, 1998]. HLA-B52 has also been proposed as a susceptibility marker for TA in Mexico [Vargas-Alarcon *et al.*, 2001], Thailand [Charoenwongse *et al.*, 1998] and Japan (as well as HLA-B39) [Kimura *et al.*, 1996; Kitamura *et al.*, 1998].

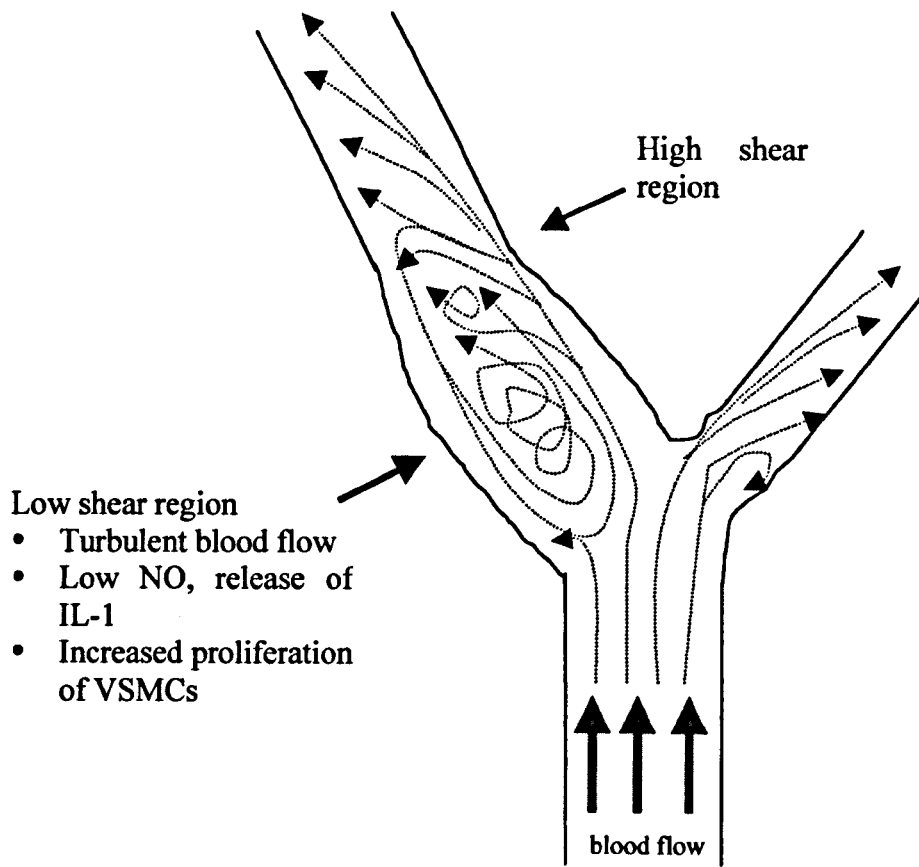
HLA-DRB1 and HLA-DPB1 were also found to be associated with TA in Japan [Kimura *et al.*, 1996], but this is probably due to DRB1 and DPB1 being in strong linkage disequilibrium with HLA-B52 in the Japanese population.

However, in another study involving 21 TA patients, HLA typing showed no significant differences between the patients and normal controls [Kerr *et al.*, 1994].

Polymorphisms in a HLA-linked gene, MICA (MHC Class I chain-related A) have also been associated with TA [Kimura *et al.*, 1998]. Stress-induced MICA and MICB molecules have been shown to be recognised by $\gamma\delta$ T-cells in human intestinal epithelium [Groh *et al.*, 1998]. In the Japanese population, MICA was shown to be in strong linkage disequilibrium with HLA-B [Kimura *et al.*, 1998], so it is possible that polymorphisms in MICA and not HLA-B are susceptibility markers for TA. An additional argument against HLA-B involvement is that $\gamma\delta$ T-cells do not use MHC class I restriction in their targeting of HSPs, so if an immune reaction against HSPs is a cause of TA, this means any association with HLA-B5 is irrelevant.

TA, like GCA, appears to be a multifactorial disease with the possible involvement of autoimmunity. IL-1 may play an inflammatory role at various stages of the pathology,

Figure 5: Schematic diagram of shear flow at an arterial bifurcation



from upregulation of adhesion molecules, integrins and chemokines to the induction of release of MMPs which destroy the IEL. It may also induce endothelial cell antigens recognised by AECA. Although the two diseases are histologically similar and appear to have similar pathologies, GCA affects the temporal arteries of patients aged over 50, whereas TA affects predominantly young females.

1.2.11: The influence of shear stress on vascular lesion development

The inflammatory arterial disease seen in our *Il1rn^{-/-}* mice occurs mainly at specific sites, such as branches and bifurcations, which are also more susceptible to the development of atherosclerotic lesions in humans [Zarins *et al.*, 1983]. Atherosclerosis is a widely prevalent inflammatory disease which involves the medium and large arteries [Berliner *et al.*, 1995; reviewed in Ross, 1999].

In arterial sites, such as branches and bifurcations, which are prone to lesion development, there is an alteration in blood flow, with a decrease in the normally high shear stress and an increase in turbulence (Figure 5). Evidence for the contribution of low shear stress to atherogenesis comes partly from the use of “drag reducing polymers” (DRPs), such as Separan AP-30, in animal models of atherosclerosis. DRPs have been shown to reduce lesion size in hyperlipidemic rabbits and guinea pigs [Faruqui *et al.*, 1987; Ertepinar *et al.*, 1990]. This was later demonstrated to be a result of increasing shear in areas, which are normally exposed to low, chaotic shear stress [Sawchuck *et al.*, 1999]. In human patients, measurement of wall shear stress in the carotid arteries of hypertensive patients also revealed that the number of lesions and the intima/media

thickness in the arteries were significantly negatively correlated to shear stress levels [Jiang *et al.*, 1999].

The exact mechanisms by which shear stress affects the development of vascular lesions are unclear, however several pathways have been proposed. Nagel *et al.*, using a fluid shear stress model to replicate flow at arterial bifurcations, demonstrated that endothelial cells under disturbed laminar shear stress (replicating chaotic blood flow) displayed elevated levels of nuclear localised NF κ B, early growth response-1 (Egr-1, a transcription factor) and c-Jun and c-Fos which dimerise to form AP-1. They identified transcriptional regulatory elements, which they termed “shear stress response elements” (SSREs), within the promoter regions of some endothelial cell genes (such as the genes for ICAM-1 and PDGF-B). The transcription factors NF κ B, AP-1 and Egr-1 can interact with the SSREs, regulating expression of SSRE containing genes presumably as well as others with which they are known to interact, such as the genes for IL-1 and MCP-1 [Nagel *et al.*, 1999]. Thus it seems shear flow can modulate the expression of various genes, at least partly by upregulating expression of transcription factors.

Endothelial dysfunction is often characterised by decreased vasodilation. High shear stress is known to be a potent inducer of the vasodilator NO by upregulating eNOS (endothelial nitric oxide synthase) [Topper & Gimbrone, 1999]. NO downregulates IL-1 α and IL-1 β expression, possibly by inhibiting the nuclear translocation of NF κ B [Peng *et al.*, 1995]. Therefore in areas of low shear stress, less NO is produced, resulting in decreased vasodilation and less regulation of IL-1. Production of NO at areas of high

shear stress may be vasoprotective, and the decreased NO production in areas of low shear stress may contribute to vascular lesion development.

Increasing shear stress has also been demonstrated to inhibit smooth muscle cell proliferation *in vitro*, whereas SMC proliferation increases with lower shear stress [Sterpetti *et al.*, 1993]. As shear stresses are felt directly only by endothelial cells lining the vessels, they must release a factor which induces SMC proliferation under low shear. A study by Rectenwald *et al.* confirms the importance of low shear stress induced IL-1 in neo-intimal hyperplasia (NIH). Experimentally induced low shear stress in the common carotid arteries of mice lacking IL-1R1 results in attenuated NIH as compared to wild-type controls. In addition, they showed by RT-PCR that IL-1 α mRNA expression is induced after experimental low shear stress induction in the carotid arteries in wild-type animals [Rectenwald *et al.*, 2000].

The contribution of low, turbulent shear stress to atherosclerotic lesion development seems likely to be substantial, but the complex mechanisms still need to be elucidated. It is possible that IL-1 plays a role in low shear stress induced vascular lesion development, by being upregulated by low-shear induced nuclear translocation of NF κ B and exerting its various effects on surrounding endothelial cells and leukocytes.

1.2.12: Pathology and aetiology of rheumatoid arthritis (RA)

RA is a well documented and prevalent chronic disease, although its cause remains unknown. RA affects nearly three times as many women as men, and mostly occurs

between the ages of 29 and 50 [Schiff, 2000]. Symptoms include joint stiffness and pain, tenderness and swelling of the affected joints. It is characterised by an inflammatory infiltrate in the synovial joints, with formation of a pannus that eventually leads to cartilage and bone destruction in the joint. The synovial lining of the joint space (which normally consists of macrophage-like cells and fibroblasts) becomes thickened (hyperplastic) as the synovial lining cells proliferate at an increased rate [Mohr *et al.*, 1975] and more macrophages and lymphocytes are recruited from the peripheral blood [Henderson *et al.*, 1988]. The synovial infiltrate is composed mainly of activated T-cells intimately associated with APCs, PMNs, mast cells, B-cells and plasma cells [Tak *et al.*, 1997]. The destructive pannus which forms is composed mainly of fibroblast-like synoviocytes and macrophages [Bresnihan, 1999]. The cartilage-pannus junction is the site of cartilage erosion; in this area mast cells [Bromley *et al.*, 1984] and PMNs are observed as well as macrophage- (type A synoviocytes) and fibroblast-like (type B synoviocytes) synovial cells [Shiozawa *et al.*, 1983]. The synovium becomes increasingly vascular, and the observed neovascularisation has been associated with the expression of VEGF in synovial macrophages and endothelial cells of the small vessels found within the pannus, possibly induced by IL-1 or TNF- α [Paleolog, 1996]. The macrophages activate T-cells which stimulate synovial fibroblasts to produce inflammatory cytokines including IL-1 [Breedveld, 1998], which induce the release of MMPs from synoviocytes [Zvaifler & Firestein, 1994]. MMPs found in RA synovium include MMP-1 and MMP-9, which are induced by IL-1, as well as MMP-13 (collagenase 3, which degrades type II collagen and aggrecan) and MMP-15 (membrane-type 2 MMP (MT2-MMP) which activates proMMP-2 and proMMP-13, and is involved in TNF- α processing) [Kontinen

et al., 1999]. IL-1 α and β can also induce MMP-13 secretion from fibroblasts *in vitro* [Uria *et al.*, 1997].

Activated B-cells are also involved in RA. Most RA patients have IgM autoantibodies that recognise the Fc region of IgG. These autoantibodies are known as rheumatoid factor (RF) and their presence lends support to RA being an autoimmune disease. The precise contribution of RF to the pathogenesis of RA remains to be elucidated, and it has also been demonstrated in other diseases such as Sjorgen's syndrome [Feldmann *et al.*, 1996].

Genetic susceptibility to RA

There has been great deal of research into genetic susceptibility to RA, since there is a degree of familial clustering [del Junco *et al.*, 1984]. The HLA-DR locus has been shown to have a large contribution to predisposition to RA, as a large number of Caucasian RA patients are HLA-DR4 or HLA-DR1 positive compared to controls [Ollier *et al.*, 1984; Gao *et al.*, 1990; Schiff *et al.*, 1982]. For example, in an investigation using 100 controls and 139 seropositive RA patients, the relative risk (odds ratio) of carriage of HLA-DR4 and development of RA was calculated as 10.5 [Wordsworth *et al.*, 1989]. In another investigation of HLA-DR4 in 52 RA patients and 59 controls, the DR4 subtype Dw4 was found in 86.5% of the patients and 55.9% of the controls, giving an odds ratio of 5.07 [Gao *et al.*, 1990]. HLA-DR1 was found in 30.6% of 49 Jewish RA patients as opposed to 11.1% of 90 controls ($p = <10^{-3}$) [Schiff *et al.*, 1982]. HLA-DR genes encode MHC class II molecules with non-polymorphic α -chains and polymorphic β -chains. Sequencing of HLA-DR subtypes associated with RA (DR4 subtypes Dw4(DRB1*0401),

Dw14(DRB1*0404), Dw14a(DRB1*0408), Dw15(DRB1*0405) and DR1) has revealed that they share amino acid similarities at residues 70-74 of their HLA-DR β 1 exons [Sherrit *et al.*, 1996], suggesting that *DRB1* is an influential susceptibility locus within the HLA class II region [Wordsworth *et al.*, 1989].

This supports the theory of carriage of an HLA “shared epitope” being related to RA susceptibility in humans [Gregerson *et al.*, 1987]. The conserved amino acids are thought to convey disease susceptibility by acting as a binding epitope for a specific peptide (which may be a self-peptide), or by acting as an immuogen itself.

Other HLA genes have also been proposed to influence susceptibility to RA, such as those encoding HLA-DQ. There is strong linkage disequilibrium between the loci *DQB1*, *DQA1* and *DRB1* and it has been suggested that that the extended HLA-DQ-DR haplotype contributes to RA susceptibility rather than *DRB1* haplotype alone [Zanelli *et al.*, 1998]. HLA genotype appears to contribute >30% of the genetic component of the disease [Deighton *et al.*, 1989] and the influence of other possible susceptibility loci are under examination including polymorphisms in the IL-1 gene cluster [Cox *et al.*, 1999; Jouvenne *et al.*, 1999; Cantagrel *et al.*, 1999].

T-cell involvement in RA

T-cells are implicated as a playing a major role in RA, since the only role of HLA-DR molecules is to present antigen to T-cells. There are, however, conflicting reports as to their importance in RA pathology. Despite their large numbers in the synovial infiltrate, it

has proved difficult to detect their activation markers. For instance, although most synovial T-cells express MHC class II antigens, very few also express the IL-2 receptor [Pitzalis *et al.*, 1987]. On the other hand there is an abundance of macrophage activation markers such as TNF- α and IL-1 production [Salmon & Gaston, 1995]. Of the T-cells present in the infiltrates, most tend to display a Th1 type cytokine profile [Simon *et al.*, 1994]. A small proportion of CD4⁺ T-cells within the perivascular areas express IL-2 and IFN γ (but also IL-4 to a small extent). CD8⁺ T-cells are distributed throughout the synovium [Steiner *et al.*, 1999].

One of the earliest observations in the pathogenesis of RA is that endothelial cells swell and form high endothelial venules, with elevated expression of adhesion molecules which leads to increased cell migration [Iguchi & Ziff, 1986]. P- and E-selectin facilitate the migration of Th1 rather than Th2 T-cells [Austrup *et al.*, 1997], leading to heightened recruitment of Th1 T-cells into the inflamed joint. It is possible that only a small number of activated T-cells are required to maintain the disease.

Putative autoantigens in RA

In the search for an autoantigen in RA, several candidates have been suggested. One is human cartilage glycoprotein-39, HC gp39, which is secreted from chondrocytes. PBMC from RA patients proliferate in response to HC gp39, and it induces arthritis upon injection in incomplete Freund's adjuvant in Balb/c mice [Verheijden *et al.*, 1997]. Type II collagen is also a potential autoantigen. Type II CIA is a well established model of RA in rodents and monkeys [Trentham *et al.*, 1977; Courtenay *et al.*, 1980; Yoo *et al.*, 1988].

Immunisation of animals with type II collagen in complete Freund's adjuvant results in a severe arthritis that affects several joints in the same animal. The arthritis is similar to that seen in humans, with joint swelling, synovial hyperplasia, formation of pannus and cartilage and bone erosion [Courtenay *et al.*, 1980].

CIA in animal models is strain dependent, and only animals of certain MHC class II genotypes develop the disease [Wooley *et al.*, 1981] suggesting that only certain MHC molecules are capable of presenting type II collagen. The mouse MHC cluster is generally known as H-2 (histocompatibility-2). For example, Balb/c mice, which are H-2^d, are not susceptible to type II CIA, whereas DBA/1 mice (H-2^q) are highly susceptible. This is in accordance with the observed link between RA susceptibility and certain HLA haplotypes in humans. Extracts of articular cartilage specimens from RA patients were found to contain antibodies to both native and denatured type II collagen as well as RF [Jasin, 1985]. Synovial cells from RA lesions secrete the antibodies, most frequently in patients who are also seropositive for RF [Tarkowski *et al.*, 1989]. Testing of T-cell clones from RA synovial joints over a period of 3 years showed a persistence in the specificity of these clones to type II collagen [Londei *et al.*, 1989], which suggests the continual stimulation of T-cells in the RA joint by APCs bearing the autoantigen.

Recently, it was shown that 64% of RA patients, but not controls, had increased levels of anti-GPI IgG in their serum and synovial fluid [Schaller *et al.*, 2001]. GPI, glucose-6-phosphate isomerase, was initially identified as an autoantigen in spontaneous inflammatory arthritis in K/BxN TCR transgenic mice, which shares many features of

human RA. In this model, animals develop joint specific arthritic disease despite having systemic autoreactivity to the MHC class II allele I-A^{g7} [Kouskoff *et al.*, 1996]. Transfer of anti-GPI antibodies into healthy mice induces arthritis [Korganow *et al.*, 1999]. It is possible that infectious organisms may express GPI that has homology to host GPI, leading to cross-reactivity with self-GPI.

Although the cause of RA remains unknown, it is likely to be multifactorial, with a substantial genetic element to susceptibility, and the possible influence of environmental factors such as infections which may lead to autoimmune cross-reactivity.

1.2.13: Involvement of IL-1 in RA

IL-1 in human RA

IL-1 involvement in the pathogenesis of RA is well established. Its presence and activity has been measured in joints affected by RA in many studies. Synovial fluid from patients with RA contains IL-1 [Wood *et al.*, 1983; Nouri *et al.*, 1984] which is biologically active [Hopkins *et al.*, 1988]. IL-1 activity has been demonstrated in the culture supernatants from the synovium of RA patients, where the IL-1 production correlated with degree of joint damage and inflammation [Miyasaka *et al.*, 1988].

Plasma levels of IL-1 β are increased in RA patients compared to control individuals, and the level of circulating IL-1 β appears to positively correlate with clinical signs of the disease [Eastgate *et al.*, 1988]. TNF α and TNF β mRNA are found, along with IL-1 α and

IL-1 β mRNA, in mononuclear synovial cells isolated from RA patients [Buchan *et al.*, 1988].

TNF and IL-1 proteins both induce the activation and proliferation of synovial fibroblasts *in vitro* [Gitter *et al.*, 1989], and they also both induce collagenase production from synovial cells [Mizel *et al.*, 1981; Dayer *et al.*, 1985; Dayer *et al.*, 1986], stimulate bone resorption *in vitro* [Gowen *et al.*, 1983; Bertolini *et al.*, 1986] and inhibit proteoglycan synthesis in articular chondrocytes [Saklatvala, 1986]. Proteoglycan is a structural component of the cartilage which allows it to withstand mechanical forces by providing compressible and elastic properties.

IL-1 stimulates collagenase and PGE₂ production in human synovial cells [Mizel *et al.*, 1981; Dayer *et al.*, 1986] and fibroblasts [Postlethwaite *et al.*, 1988]. Treatment of synovial fibroblasts from human RA pannus with IL-1 α , IL-1 β or TNF- α *in vitro* stimulates them to produce stromelysin and collagenase [MacNaul *et al.*, 1990]. Collagenase and stromelysin mRNA are expressed at the synovial lining in RA patients [Gravallese *et al.*, 1991].

IL-1 in animal models of RA

A line of transgenic mice, that express human TNF- α protein in their joints and other tissues, develops chronic polyarthritis [Keffer *et al.*, 1991]. The additional requirement of IL-1 to TNF- α in disease development was demonstrated. Administration of a blocking antibody to IL-1R1 resulted in prevention of development of the disease [Probert *et al.*,

1995]. TNF- α levels were also decreased in these experiments, demonstrating a positive loop of TNF induction by IL-1. Other experiments have shown that TNF- α induces IL-1 production in synoviocytes from RA patients, since anti-TNF- α treatment results in a decrease in IL-1 production [Brennan *et al.*, 1989].

Animal models of arthritis have consistently shown that administration of IL-1 into the joint space either induces or exacerbates the disease. For instance, administration by mini-osmotic pumps of recombinant human IL-1 β to DBA/1 mice (H-2^d) previously immunised with type II collagen significantly exacerbates the type II CIA. Onset of the disease is earlier and histological examination reveals a more severe inflammatory reaction [Hom *et al.*, 1988].

Intra-articular injection of human and porcine IL-1 into the knees of rabbits results in a rapid accumulation of leukocytes in the joint space and loss of cartilage proteoglycan [Pettipher *et al.*, 1986; Dingle *et al.*, 1987]. Similar effects are seen when murine recombinant IL-1 is injected intra-articularly into C57BL/10 mice, which are exacerbated after repeated injections of IL-1 [Van de Loo & Van den Berg, 1990]. In addition to proteoglycan breakdown, dose-dependent inhibition of proteoglycan synthesis is observed.

Transgenic mice (on a C3H/HeJ background) which constitutively produce human IL-1 α under the control of the cytomegalovirus enhancer gene develop an arthritic disease and by 56 days of age, hyperplastic synovium and the formation of destructive pannus is

observed. The hyperplastic synovial membrane is composed mainly of macrophages expressing human IL-1 α , which is also expressed by the synovial fluid monocytes and the synovial lining fibroblasts [Niki *et al.*, 2001].

Chemokines and adhesion molecules in RA

Synovial fluid from RA patients is chemotactic for both T-cells and B-cells, and the chemotactic qualities of the fluid are largely removed by treatment with anti-IL-1 antibody [Miossec *et al.*, 1986]. High levels of the chemokine MCP-1, whose mRNA expression and secretion from fibroblast-like synovial cells is induced by IL-1, have been detected in the synovial fluid of RA patients. MCP-1 injected into the knee joints of rabbits induces the accumulation of mononuclear cells in the synovial lining, demonstrating that MCP-1 is an important chemotactic factor in RA for the migration of macrophages into the synovium [Akahoshi *et al.*, 1993].

IL-1 β , TNF- α and IFN γ all induce ICAM-1 and VCAM-1 expression on cultured fibroblast-like synoviocytes derived from the synovial lining of RA patients [Morales-Ducret *et al.*, 1992]. VCAM-1 mediates the recruitment of T-cells into the synovium by interacting with its ligand, the integrin VLA-4 ($\alpha_4\beta_1$) on T-cells [Morales-Ducret *et al.*, 1992]. Therefore the cytokines present in RA tissue, including IL-1, enhance expression of adhesion molecules and thereby facilitate the recruitment of leukocytes into the synovium.

Blocking the action of IL-1 in RA in vitro

Further evidence for the involvement of IL-1 in RA comes from studies in which disease incidence and severity can be ameliorated by administration of IL-1 inhibitors, such as IL-1ra or blocking antibodies to IL-1. Antibodies to IL-1 β , IL-6 and TNF- α inhibit cartilage degradation *in vitro* by fibroblasts obtained from RA patients, demonstrating their activity in activating fibroblasts to release metalloproteinases [Scott *et al.*, 1997].

Blocking the action of IL-1 in RA in vivo

In LPS induced arthritis in rabbits, injection of rabbit IL-1ra partially ameliorates the disease. There is a marked decrease in leukocyte infiltration and articular cartilage destruction [Matsukawa *et al.*, 1993]. In the murine type II CIA model, neutralisation of IL-1 by rabbit anti-mouse IL-1 α and IL-1 β antibodies during established disease results in significant suppression of disease activity [Joosten *et al.*, 1999]. Anti-IL-1 α and IL-1 β antibodies in combination injected before onset of established CIA completely prevents disease [Van den berg *et al.*, 1994]. Intraperitoneal injections of IL-1ra into mice 14 days after administration of type II collagen results in a delay in the onset of CIA and a reduction in disease severity, along with a reduction in serum levels of the anti-type II collagen antibody [Wooley *et al.*, 1993].

Following antibody neutralisation of IL-1 in established CIA, there is a marked decrease in serum cartilage oligomeric matrix protein (COMP), a marker released from cartilage during cartilage turnover, demonstrating IL-1 involvement in cartilage breakdown in CIA. Bone erosion, as indicated by radiological analysis, is also prevented in anti-IL-1

treated animals. On the other hand, blocking of TNF- α by administration of soluble TNF binding protein does not affect serum COMP levels or bone erosion. It does however reduce the influx of inflammatory cells [Joosten *et al.*, 1999]. This data suggests that TNF- α is important in the initial influx of inflammatory cells into the synovial space, whilst the role of IL-1 is primarily involvement in cartilage and bone destruction in CIA. Although neutralisation with anti-IL-1 β results in a marked suppression of arthritis in CIA, and only a small effect is seen with anti-IL-1 α , the optimal suppression is achieved using anti-IL-1 α and anti-IL-1 β together. This suggests that although IL-1 β plays the greater role in the progression of RA, both forms are involved [Joosten *et al.*, 1996].

In IL-1ra transgenic mice, overexpression of IL-1ra leads to a reduction in the incidence and severity of CIA, whereas deletion of *Il1rn* results in a significantly earlier onset of disease with heightened severity, indicating a role for endogenous IL-1ra in protection against CIA [Ma *et al.*, 1998]. IL-1ra null mice on a Balb/C background develop a spontaneous RA-like disease [Horai *et al.*, 2000, this work] (see section 1.1.14). Interestingly, these mice are not susceptible to CIA.

IL-1ra in clinical trials as therapy for RA

The beneficial effects of using IL-1ra in animal models has led to clinical trials in human RA patients. In one trial involving 472 patients with active RA, daily subcutaneous injections of IL-1ra significantly reduced the symptoms of RA by 24 weeks [Schiff, 2000]. Treating human RA patients with recombinant IL-1ra results in a decrease in the numbers of infiltrating macrophages in the inflamed synovial tissue, and a decrease in the

number of endothelial cells expressing E-selectin and the number of mononuclear cells expressing VCAM-1 and ICAM-1. Clinically, in this study some patients who received IL-1ra also had an arrest in the progression of joint damage [Cunnane *et al.*, 2001]. Anti-TNF- α therapy (using a monoclonal antibody) also improves the symptoms of RA [Elliot *et al.*, 1994] in part due to the reduction of induction of IL-1.

IL-1, acting in conjunction with other cytokines such as TNF- α , plays a major role in several aspects of RA. Anti IL-1 treatment is very effective at preventing disease progression in animal models of RA and humans, supporting the hypothesis that IL-1 is a key mediator of inflammation-induced damage in RA.

1.2.14: Psoriasis: Psoriatic lesions

Psoriasis is a chronic skin disease, which is characterised by inflammation and scaling of the skin, affecting up to 2% of the Caucasian population. Plaque psoriasis (psoriasis vulgaris) is the most common form, with the plaques being patches of thick, reddened skin covered in silvery scales. The major cause of the psoriasis plaque is altered epidermal keratinocyte differentiation and hyperproliferation of the keratinocytes, leading to a thickened epidermis (“acanthosis”). The hyperproliferative keratinocytes form characteristic elongations which reach down into the dermis, known as “rete ridges” or “rete pegs”. Histopathology reveals a mixed dermal inflammatory infiltrate composed of T-cells, monocytes and macrophages [Bjerke *et al.*, 1978]. Neutrophils infiltrate the epidermis and may aggregate underneath the stratum corneum (the horny, top layer of skin) at the top of rete ridges to form sterile Munro microabscesses. There is

hyperkeratosis, a thickening of the stratum corneum, and also retention of nuclei in the stratum corneum (“parakeratosis”). The dermal papillae are elongated and club shaped and fit in between the rete ridges of the epidermis [Baden, 1984]. There is also increased vascularity of the dermis with a change in shape of the small vessels to a more tortuous morphology [Barker, 1991].

T-cell involvement in psoriasis

In active lesions, T-cells tend to be CD4⁺ [Baker *et al.*, 1984]. CD4⁺ T-cell clones derived from the epidermis of psoriasis patients have a Th1 phenotype [Vollmer *et al.*, 1994, Schlaak *et al.*, 1994]. In skin biopsies from psoriasis patients, mRNA for IFN γ but not IL-4 or IL-10 can be detected [Schlaak *et al.*, 1994]. PCR and immunostaining also show elevated levels of Th1-type cytokines in lesional skin, with production of IL-1, IL-2, IFN γ and TNF- α and no significant levels of IL-4, IL-5 or IL-10. Increased levels of IL-1 α and IL-1 β have also been shown in non lesional psoriatic skin [Uyemura *et al.*, 1993]. This may indicate an early role for IL-1 in psoriasis lesion development.

Vollmer *et al.* detected the production of IL-5 in T-cell clones derived from lesional psoriatic skin. The production of IL-5 from T-cells does not fit in with a Th1 cytokine profile. This may suggest that a novel subset of T-cells is involved in psoriasis, which produce a complex cytokine profile and are able to enhance keratinocyte proliferation since this profile was observed in T-cell clones whose supernatants were capable of acting as mitogens for keratinocytes *in vitro* [Vollmer *et al.*, 1994]. Another study suggests a mixture of Th1 and Th2 T-cells in psoriasis lesions. Measurement of IFN γ and

IL-4 production T-cell clones prepared from the psoriatic plaques of two patients revealed the presence of Th0, Th1 and Th2 T-cell subsets [Barna *et al.*, 1994]. However, the Th2 type cytokines measured in these studies may be involved in the resolution of the plaques.

Psoriasis is generally agreed to be a T-cell driven disease, since cyclosporin is an effective treatment [Griffiths *et al.*, 1989] and blocking T-cell binding to LFA-3 (leukocyte function associated antigen-3, an adhesion molecule) on APCs appears to be an effective therapy for psoriasis in clinical trials [Magilavy, 1999].

1.2.15: Causative factors in psoriasis

Genetic susceptibility to psoriasis

Like GCA, TA and RA, the cause of psoriasis is unknown. It, too, appears to have a genetic input into susceptibility to the disease. Monozygotic and dizygotic twins have a concordance rate of ~40% and ~10% respectively [Farber *et al.*, 1974]. There are two cohorts with different average ages of onset for psoriasis, type 1 with a mean age at onset of 16-20, and type 2 with a mean age at onset of 55-60. Various HLA antigens have been suggested to be associated with psoriasis, particularly those of class I. The early onset psoriasis displays more familial inheritance than the late onset type, and appears to be linked with the HLA class I antigen CW6 [Henseler *et al.*, 1985; Schmitt-Egenolf *et al.*, 1993].

The *S* gene (encoding corneodesmosin), located only 160kb from HLA-C within the MHC, has also been suggested to be linked to psoriasis [Tazi Ahnini *et al.*, 1999a]. Corneodesmosin is expressed during keratinocyte differentiation and its cleavage appears to play a major part in desquamation. Polymorphisms in allele 5 (at +619, +1240 and +1243) have been linked to psoriasis [Tazi Ahnini *et al.*, 1999a; Jenisch *et al.*, 1999; Allen *et al.*, 1999]. Analysis of the relative contributions of the *S* gene and HLA-CW6 shows that they both independently exert effects on susceptibility to psoriasis [Tazi-Ahnini *et al.*, 1999b].

Five different loci are so far thought to contain psoriasis susceptibility genes, PSOR1 on 6p21.3 (which includes the *S* gene), PSOR2 on 17q, PSOR3 on 4q12-q13, PSOR4 on 1cen-q21 and PSOR5 on 3q21 [Henseler, 1997]. In a Chinese population, the A5.1 allele of the MHC-associated MICA gene was also found to be significantly associated with psoriasis [Cheng *et al.*, 2000].

Psoriasis is now believed to be a complex disease, with the input of several genetic factors and an additional environmental influence such as infection. It is possible that trigger factors such as psychological stress, skin injury from sunburn or surgery, bacterial infection such as streptococcal infection (with bacterial endotoxin acting as a superantigen), yeast or viral infection [reviewed in Ortonne, 1999] induce the onset of psoriasis in genetically susceptible individuals.

1.2.16: IL-1 in psoriasis

Endothelial cells

IL-1 α derived from the stratum corneum of normal skin upregulates the expression of the endothelial cell molecules ICAM-1, VCAM-1 and ELAM-1 (endothelial leukocyte adhesion molecule-1) when injected intradermally into healthy skin [Groves *et al.*, 1992].

Keratinocytes

Keratinocytes of the epidermis proliferate at the basal layer, after which they migrate up through the epidermal layers where they stop dividing and undergo various morphological and biochemical changes. The top layer of the epidermis, the stratum corneum, is made up of layers of dead, terminally differentiated keratinocytes. As the cells progress through the various stages, they express different keratins. Keratins are a family of proteins expressed in pairs, which form 8-10nm structural filaments in the cytoplasm of all epidermal cells. Normally, cells at the basal layer express K14 and K5. Cells undergoing terminal differentiation express K1 and K10. During hyperproliferation however, as in psoriasis, there is a reduction in K1 and K10 expression and K6 and K16 are expressed at high levels in the suprabasal layers of hyperproliferative epidermis [Weiss *et al.*, 1984; Stoler *et al.*, 1988]. K6 and K16 mRNA is expressed at low levels in normal epidermis without production of the proteins, except for around the outer root sheath of hair follicle and on the nail bed [Stoler *et al.*, 1988].

Upon injury, cytoplasmic IL-1 α or pro-IL-1 β is released from keratinocytes [Murphy *et al.*, 2000]. As keratinocytes do not contain active ICE [Mizutani *et al.*, 1991a], the IL-1 β released is presumably processed in an ICE-independent manner. One candidate is stratum corneum chymotryptic enzyme (SCCE) which has chymotrypsin-like activity. Chymotrypsin and chymotrypsin-like proteases have been shown to be capable of processing pro-IL-1 β to the mature form *in vitro* [Mizutani *et al.*, 1991b]. Biologically active IL-1 β is present in psoriatic scales, as measured by ELISA and its ability to induce E-selectin expression on HUVEC [Lundqvist & Egelrud, 1997].

Although most of the IL-1 activity observed in psoriatic lesions is attributed to IL-1 α , *in vitro* IL-1 β induces the psoriatiform epidermal phenotype in skin organ cultures derived from healthy skin and non lesional psoriatic skin. The phenotype includes induction of keratin 16 and keratin 17 markers on keratinocytes, and induction of expression of ICAM-1 and HLA-DR on basal keratinocytes [Wei *et al.*, 1999].

IL-1 activates keratinocytes, causing them to proliferate and become migratory [Kupper & Groves, 1995] and express K6 and K16, ICAM-1, integrins and fibronectin [Komine *et al.*, 2001; reviewed in Freedberg *et al.*, 2001]. GM-CSF produced in T-cells after IL-1 stimulation, is also capable of inducing keratinocyte proliferation [Hancock *et al.*, 1988]. IL-1 stimulated cultured human fibroblasts secrete the mitogen keratinocyte growth factor which stimulates keratinocyte growth and proliferation [Werner & Smola, 2001]. IL-1 and IL-1-induced TNF- α from keratinocytes can maintain keratinocytes in the activated state [Nickoloff & Turka, 1993] by stimulating NF κ B and C/EBP which act as

a complex to induce K6 expression [Komine *et al.*, 2000; La & Fischer, 2001; Komine *et al.*, 2001].

IL-1 released from keratinocytes in the epidermis downregulates the expression of E-cadherin on Langerhans' cells (epidermal dendritic cells), inducing their migration into the dermis and draining lymph nodes. E-cadherin mediates the adhesion of Langerhans' cells to keratinocytes, and the downregulation induced by IL-1 allows the Langerhans' cells to migrate out of the epidermis [Jakob & Udey, 1998]. IL-1 α in combination with GM-CSF has been shown to enhance the epidermal Langerhans' cell dependent activation of T-cells in murine skin *in vitro* [Heufler *et al.*, 1988].

IL-1 also acts on other cells in the skin. TNF- α , IL-1 β , IFN γ , CD40 ligand or IL-17 can all induce the expression of the chemokine macrophage inflammatory protein-3 alpha (MIP-3 α , CCL20) *in vitro* on cultured primary keratinocytes, dermal fibroblasts, dermal microvascular endothelial cells and dendritic cells. MIP-3 α expression is upregulated on keratinocytes in psoriasis. The receptor for MIP-3 α , CCR6, is also found expressed in increased amounts as compared to normal skin on the surface of skin-homing memory T-cells from psoriatic skin [Homey *et al.*, 2000]. Upregulation of the chemokine MIP-3 α by IL-1 could increase T-cell recruitment into the psoriatic lesions.

1.2.17: Animal models of psoriasis

There is no known naturally occurring animal disease, which has all of the immunopathogenic and phenotypic hallmarks of human psoriasis. Several animal models of psoriasis now exist which reflect various aspects of the disease. They can be split into four groups of spontaneous mutations, transgenic animals, xenotransplantation models and T-cell transfer models. Examples of some of these models are given below.

Spontaneous mutations

Spontaneous mouse mutation models include flaky skin mouse (*fsn*) and the chronic proliferative dermatitis (*cpd*) and asebia (*ab/ab*) mutations. Of these, flaky skin mice have the phenotype most like that of human psoriasis with epidermal hyperproliferation, a mixed inflammatory infiltrate composed of monocytes, macrophages, mast cells, T-cells and neutrophils, epidermal microabscesses with neutrophil accumulation, expression of ICAM-1 and GM-CSF, and dilated dermal vasculature [Morita *et al.*, 1995; Schon *et al.*, 2000]. The lesions are found over the whole body surface, and are particularly pronounced on the dorsal skin. IL-1 β levels are markedly increased in psoriatiform lesions in flaky skin mice, and administration of a blocking monoclonal antibody against IL-1 β results in a decrease in epidermal thickness, numbers of infiltrating CD4⁺ and CD8⁺ T-cells, and a decreased number of Munro microabscesses [Schon *et al.*, 2001]. Unlike human psoriasis however, it seems T-cells do not play a role in the development of the flaky skin phenotype, since *fsn* mice backcrossed onto SCID mice still develop the disease [Schon, 1999].

Transgenic models

There are several transgenic mouse models for the study of psoriasis. For instance, mice which overexpress IL-1 α in the basal epidermis display dermal infiltrates of monocytes and macrophages, upregulation of ICAM-1 and limited acanthosis [Groves *et al.*, 1995]. Lesions in these mice are found on the head, trunk, and limbs and hair growth is sparse. Transgenic mice which overexpress IL-1R1 on the basal epidermal keratinocytes show an increased level of epidermal thickening in comparison to control mice, and a large inflammatory dermal infiltrate when stimulated with PMA on the skin. [Groves *et al.*, 1996]. When these animals are crossed with the IL-1 α overexpressors, mice which expressed both transgenes develop a spontaneous skin inflammation with acanthosis and a dermal inflammatory infiltrate [Groves *et al.*, 1996].

Xenotransplantation models

Psoriatic plaques from human disease can be successfully xenotransplanted onto SCID mice and maintained for several months [Nickoloff *et al.*, 1995]. Histologically the resulting lesions are very similar to human psoriatic plaques, with hyperkeratosis, Munro microabscesses, increased vascularity and dermal infiltrates composed of mononuclear cells, CD4⁺ and CD8⁺ T-cells, and dermal dendritic cells. Further experiments showed that after grafting non-lesional skin from psoriasis patients onto SCID mice, injection of blood derived autologous immunocytes, activated by IL-2 and superantigens, caused the plaques to become psoriatic. The changes observed included marked acanthosis, parakeratosis, elongation of rete ridges, Munro microabscesses and dermal and epidermal infiltrates [Wrone-Smith & Nickoloff, 1996]. These data suggest that psoriasis is caused

by dysregulation of the immune system and requires a circulating immune factor or cell, rather than being due solely to abnormal epidermal keratinocytes.

T-cell transfer models

Transfer of naïve mouse CD4⁺ T-cells with a minor histocompatibility mismatch into SCID mice results in a skin disorder affecting most of the body surface which has various phenotypic similarities to human psoriasis including lymphocytic infiltrates (with abundant CD4⁺ T-cells) in the dermis and epidermis, accumulation of dermal neutrophils, acanthosis, hyperkeratosis and an increase in vascularity. Expression of K6 is observed on the hyperproliferative keratinocytes, and an increase in ICAM-1 and MHC class II expression is also seen within the epidermis. TNF- α , IFN γ , IL-6 and IL-1 α expression are also upregulated [Schon *et al.*, 1997].

It seems clear that IL-1 can play several roles in psoriasis pathogenesis. It acts as a proinflammatory mediator, upregulating leukocyte recruitment and production of cytokines, and it also activates keratinocytes and induces the production of TNF- α , which maintains the keratinocytes in an activated state.

1.2.18: Psoriatic arthritis

The distinction between psoriatic arthritis (PsA) and arthritis with concurrent psoriasis is not clear, although clinicians agree that not all patients presenting with psoriasis and inflammatory arthritis have psoriatic arthritis, which is a separate disease [Patel *et al.*, 2001]. PsA affects about 0.02-0.1% of the UK population [O'Neill and Silman, 1994].

Up to 20 years can separate the onset of the psoriasis and the arthritis, and some PsA patients never present with skin manifestations [Pitzalis 1998]. One way of distinguishing PsA from RA is by the appearance of the vasculature in early synovitis. In PsA patients (and reactive arthritis patients), the synovial vessels have a much more tortuous and bushy appearance than those in RA [Reece *et al.*, 1999]. In addition PsA patients are usually sero-negative, and have asymmetrical arthritis which often affects the spine, unlike RA [Gladman & Brockbank, 2000]. The bone and joint destruction in PsA is less complete than in RA, as there is a lower release of aggrecan and COMP, reflecting a lower cartilage turnover [Mansson *et al.*, 2001]. In general however the psoriatic and arthritic symptoms and pathologies are very similar in PsA to psoriasis and RA. Generally the distinction between PsA and RA with psoriasis remains unclear.

1.3: Summary and hypothesis

IL-1 is a pleiotropic, pro-inflammatory cytokine that exerts its effects after binding to the type 1 IL-1 receptor. Its action is inhibited by IL-1ra, which binds to IL-1R1 without any resulting signal transduction, possibly due to the failure of the IL-1ra/IL-1R1 complex to recruit the essential IL-1 receptor accessory protein subunit.

IL-1 acts upon many cell types, inducing their growth and proliferation, or inducing or upregulating the expression, production and secretion of adhesion molecules, chemokines, and other cytokines. Many of the proteins induced or upregulated by IL-1 are also pro-inflammatory, such as TNF α . A large part of the action of IL-1 in inflammation is the upregulation and induction of expression of various adhesion

molecules and integrins on endothelial cells and circulating leukocytes, as well as the induction of the secretion of chemokines that recruit leukocytes to the inflamed area.

Due to the central role that IL-1 plays in inflammation, we hypothesised that the generation of mice lacking the natural inhibitor to IL-1, IL-1ra, would suffer from inflammatory disease as a result of the unopposed action of IL-1. IL-1 has been implicated as playing major roles in several inflammatory diseases including vasculitis, RA and psoriasis.

Here, the susceptibility of *Il1rn*^{-/-} mice to inflammatory disease is investigated, and the phenotypes of the spontaneous inflammatory diseases observed in Sf3 and Balb/C *Il1rn*^{-/-} mice are characterised, in order to compare them with human diseases and consider their possible use as models for these diseases. The arterial disease is characterised histologically to compare it with human diseases such as GCA and TA. A time course study of the development of arterial lesions was undertaken, to test the hypothesis that endothelial cell activation due to turbulent blood flow is a key initiating factor in development of the disease, and to investigate the progression of the disease to attempt to elucidate a mechanism of disease development. Since SAA levels are increased during an inflammatory response, it was also hypothesised that measurement of SAA levels could provide a prognostic marker for development of arteritis in *Il1rn*^{-/-} mice. Due to the observed genetic influence of the MHC on autoimmune inflammatory diseases in humans, it was also hypothesised that there is a possible contribution of *H-2* into

inflammatory disease susceptibility in *Il1rn*^{-/-} mice, and this was investigated by haplotyping animals of different susceptibilities at loci across the *H-2* cluster.

A histological study of the psoriatiform disease observed in our Balb/c *Il1rn*^{-/-} animals was undertaken, to compare the features with those found in human psoriatic lesions and to attempt to elucidate the mechanism of disease development. Finally, a histological comparison of the arthropathy found in our Balb/c *Il1rn*^{-/-} mice with that previously observed in Balb/c *Il1rn*^{-/-} mice [Horai *et al.* 2000] was also performed, to attempt to evaluate the hypothesis that the development of RA in Balb/c mice is due to the result of the interaction of the Balb/c genetic background and not environmental factors with *Il1rn* deficiency. It is proposed that IL-1, with no competition for its receptor in the form of IL-1ra, plays a central role in the pathogenesis of the three diseases in IL-1ra deficient mice.

Section 2: Materials and Methods

2.1: Animals

2.1.1: Lines of mice used in studies

Il1rn^{-/-} mice were generated as previously described [Nicklin *et al.*, 2000]. *Il1rn*^{-/-}, ^{+/-} and ^{+/+} mice were bred on two genetic backgrounds. The first (as described previously) was derived from crossing a 129/Ola-bearing chimera (heterozygote) with an outbred MF1 female. Subsequently several lines were established and were sib-sib inbred. One of these was used in this study (“Sf3”). Several mice from another line (“Sf2”) were also used in the arteritis study, but this line could not be sustained. All the mice from the stock described here (unless otherwise stated) are from the tenth or greater inbred generation. It is possible to calculate the likely degree of residual heterozygosity in these animals compared to F1 as 10.7% at F10 (the earliest generation used) and 4.6% at F14. *IL1rn*^{-/-} Sf3 mice were also then bred onto a Balb/c background and then inbred, to create Balb/c *Il1rn*^{-/-} animals. Animals used here were from generations N5 to N9. Mice were fed a standard diet, and were identified by ear punches.

2.1.2: Housing and care of mice

Animals were housed in specified pathogen free (SPF) conditions in the University of Sheffield. Sera from mice from the colony have been tested for evidence of infection by viruses including adeno-, cytomegalo-, ectromelia, hantaan, hepatitis, K-, lymphocytic choriomeningitis, minute, parainfluenza-, pneumonia, polyoma-, Sendai virus, Theilers' virus, mouse rotavirus, and reovirus 3. The sera were also tested for bacteria including *Clostridium piliformis*, *Mycoplasma pulmonis*, and mouse *Chlamydia*. The intracellular eukaryotic parasite *Encephalitozoon cuniculi* was also tested for. All were found

negative. Mice from both our colony and from the colony generated by Hirsch *et al.* were also tested for evidence of infection by *Helicobacter* spp. and found to be carriers of *H. hepaticus* (see section 3.3.6).

The project was covered by the necessary Project and Personal Home Office licences.

2.1.3: Culling and dissection of animals

Mice that died suddenly were dissected by a longitudinal cut along the thoracic and abdominal cavities and fixed in 3.7% neutral buffered formaldehyde (10% formaldehyde, 0.03 M sodium dihydrogen orthophosphate dihydrate, 0.06 M sodium phosphate). Mice killed prospectively and animals which appeared to be ill (typically displaying a poor coat, hunching, “wheezy” breathing or swollen limbs) were humanely culled either by cervical dislocation or, if a serum sample was required, by overdosing on anaesthetic (Pentobarbitone forte). Blood samples were taken either from the tail vein or by cardiac puncture whilst the animals were under terminal anaesthesia. Animals culled due to ill health were dissected along the thoracic cavity and stored in 3.7% neutral buffered formaldehyde until examination.

Mice killed prospectively were kept on ice and dissected within 1 hr. Prior to dissection, the outward appearance of the animal under examination was checked for obvious signs of ill health, such as swollen limbs, reddened ears, or a poor coat. The animal was then pinned and opened by making an incision through the skin and peritoneal lining from a point anterior to the urethral opening. A cut was then made with scissors up the mid-ventral line of the animal until there was a cut from the groin to the chin. Two further

incisions were then made from the start of the first incision down toward the knees. The skin and muscle layers were then reflected back to reveal the inner anatomy of the animal. The appearance of the major organs (heart, lungs, liver, spleen etc) was examined for obvious abnormalities in size or colour, then the desired organs or other parts of the animal were removed.

The organs and parts removed were either snap frozen in liquid nitrogen followed by storage at -70°C , or they were fixed in 3.7% neutral buffered formaldehyde. Blood samples taken were centrifuged at $16,000 \times g$ for 15 min and the serum removed and stored at -20°C .

2.2: Preparation of genomic DNA

2.2.1: Preparation of genomic DNA from mouse ear clips

To obtain genomic DNA for genotyping, circles of skin, 2 mm in diameter, were saved from the routine ear punch mouse identification procedure and digested in a proteinase K digestion mixture at 53°C . 0.5 ml microfuge tubes containing the skin samples were first pulsed in a microfuge to ensure the sample was at the bottom of the tube, then 100 μl of proteinase K digestion mixture (containing 0.1 M sodium chloride, 0.01 M Tris pH 8.0, 0.025 M diaminoethanetetra-acetic acid (EDTA) pH 8.0, 0.5% sodium dodecyl sulphate and 100 μg proteinase K) were added to each sample. The samples were incubated with shaking at 55°C for 24 hr then mixed by vortexing, pulsed in a microfuge and returned to the incubator for a further 24 hr.

After incubation, the digest mixture was diluted by the addition of 100 μ l sterile water and mixed by vortexing. Deproteinisation of the solution was achieved by the addition of an equal volume of phenol, mixing by vortexing of the contents until an emulsion formed, then centrifugation in a microfuge at 16,000 x g for 5 min. The aqueous phase was transferred to a clean tube, then an equal volume of chloroform was added to remove any traces of phenol. An emulsion was formed by vortexing, which was again centrifuged in a microfuge at 16,000 x g for 5 min at room temperature. The DNA was then precipitated by taking the aqueous phase into a tube and adding 0.1 volume of 3 M sodium acetate and 2.5 volumes of 100% ethanol, followed by mixing, chilling in a -70°C freezer for 15 min and then centrifuging in a microfuge for 15 min at 16,000 x g. The resulting DNA pellet was washed with 70% ethanol, allowed to dry and then resuspended in 30 μ l TE (6 mM Tris hydrochloric acid (Tris-HCl), 4 mM Tris base, 1 mM EDTA). The DNA samples were stored at -20°C until needed.

2.2.2: Preparation of high molecular weight genomic DNA from mouse splenocytes

a) Isolation and proteolysis of splenocytes

Spleens were removed from freshly killed mice and were washed in 10 ml cold saline (0.9% sodium chloride) in a universal vial. Each spleen was tipped into a petri dish and bathed in 10 ml cold saline, then cut into pieces with a sterile scalpel and the portions ground between the ends of two microscope slides. The ground tissue was rinsed off into a petri dish with cold saline. The resulting tissue and cell suspension was placed into a 15 ml tube.

The larger pieces of tissue were allowed to sediment for 60 s, and the cell suspension was taken into a 15 ml tube. This was centrifuged at 16,000 x g at 4°C for 15 min and the supernatant removed. The pellet was resuspended in the dregs of the saline by tapping and 4 ml of splenocyte DNA digestion buffer (0.1 M sodium chloride, 0.005 M Tris base, 0.005 M Tris-HCl, 0.025 M trisodium EDTA, 0.5% SDS, 10 mg proteinase K) added to each pellet. The cells were incubated at 55°C for 17 hr to allow digestion.

b) Protein extraction and dialysis of splenocyte DNA

An equal volume of phenol was added to the extract polypeptides from the digestion mixture and emulsified by vortexing. Phases were separated by centrifugation at 16,000 x g for 10 min and the resulting viscous aqueous phase (containing DNA) was removed with a disposable pasteur pipette into a universal vial.

For the dialysis, one length of ~30 cm of Spectra/Por molecular porous membrane (size 6,000-8,000) was cut for each sample. The dialysis tubing was prepared by soaking in 1 l 2.5% ammonium bicarbonate solution which was brought to the boil and simmered for 10 min. Liquid was decanted and the tubing rinsed several times in deionised water. DNA samples were dialysed with stirring in dialysis tubing against two changes of TE buffer (500 ml) over 24 hr. 50 µl of each sample was taken into a 1.5 ml microfuge tube, diluted 1:20 in TE. Using these aliquots, the absorbence at 260nm was measured in a spectrophotometer to determine the DNA concentration in each sample.

2.3: Genotyping of mice by polymerase chain reaction (PCR)

2.3.1: Oligonucleotide primer design and preparation

Oligonucleotide primers were designed using MacVector software version 4.5.3 (Eastman Kodak Co.) from the genomic DNA sequences of the genes of interest. Sequences were obtained from the Genbank database at the National Centre for Biotechnology Information (NCBI) (<http://www.ncbi.nlm.nih.gov>). Primer design was based on several constraints, including a primer length of 18 to 30 bases, a GC content of approximately 50% and a final product size of 100 bp to 1000 bp. Primer pairs were checked with MacVector software for similar predicted annealing and melting temperatures, and were also checked for their potential to anneal to each other, Primers were rejected if they had a high potential to form dimers. To check primer specificity, the basic local alignment search tool (BLAST) at the NCBI was used. Primers were rejected if they could potentially bind to inappropriate sequences in the mouse genome.

The primer oligonucleotides were synthesised within the Division of Genomic Medicine on a 394 DNA/RNA synthesiser (ABI Applied Biosystems) and were supplied desiccated, and re-suspended before use in 400 µl of sterile distilled water. 200 µl of the solution were stored at -20°C for future use, and the remaining 200 µl precipitated with ethanol. The resulting pellet was washed with 70% ethanol, air dried and resuspended in 200 µl sterile distilled water.

The primer concentration was calculated from the extinction coefficient by diluting an aliquot 1:500 in water and taking spectrophotometric readings at 260nm (Eppendorf

Biophotometer). A working concentration of 20 μM was used for subsequent PCR reactions. Working dilutions and stock primers were stored at -20°C .

2.3.2: Agarose gel electrophoresis

Agarose was dissolved with heating in a microwave in 1 x TAE buffer (40 mM Tris acetate, 1 mM EDTA) or 1 x TBE buffer (90 mM Tris, 90 mM boric acid, 1 mM EDTA), cooled to $\sim 50^{\circ}\text{C}$, and 0.5 $\mu\text{g/ml}$ ethidium bromide added. The agarose mixture was poured into a tray with combs providing the required number of wells in place and allowed to set. Electrophoresis was run in 1 x TAE or TBE buffer and the samples and DNA size markers ($\Phi\text{X174}/\text{HaeIII}$ or pt7) loaded into the wells in 1 x loading buffer (5 x buffer contains 80% glycerol, 60 mM EDTA, 0.1% xylene cyanole FF). The gels were run at a constant 10 V/cm, and the DNA/ethidium complexes were visualised by orange fluorescence under illumination at 320nm.

2.3.3: Optimisation of polymerase chain reactions

PCRs were optimised in 25 μl reactions, containing 250-500 ng genomic DNA extracted from ear clips (as described in section 2.2.1), 0.5-3 μM each primer, 1-6 mM magnesium chloride, 0.2 mM dNTPs (from a stock 2.5 mM mixture of dATP, dCTP, dGTP and dTTP in equal amounts), 1 x buffer, as supplied by manufacturer (20 mM Tris-HCl pH 8.4/0.1 mM potassium chloride) and 0.625 units of *Thermus aquaticus* (*Taq*) DNA polymerase. The mixtures were overlaid with 2 drops of paraffin oil to prevent evaporation. All reactions, unless otherwise stated, had an initial denaturation step of 5 min at 94°C , followed by 1 minute at 94°C , 1 minute at a range of annealing

temperatures around the predicted optimum, and either 1 or 2 min elongation at 72°C. All reactions underwent 35 cycles (unless otherwise stated) in a DNA thermocycler machine (either a Trio-Thermoblock (Biometra) or a DNA Thermal Cycler 480 (Perkin Elmer)). PCR products were then electrophoresed on agarose gel.

2.3.4: *Illrn* genotyping by PCR

To detect the wild type *Illrn* gene, a 25 µl PCR reaction was used as in section 2.3.3, containing 2 mM magnesium chloride and 1 µM each of the forward (5' TCT TGA GGG ATT AGC TGG ACA AAC 3') and reverse (5' TGG TGG TTT CAT CAA AAA GCC C 3') primers. This reaction amplifies a region between +4187 and +5035 of the wild type mouse *Illrn* sequence, which is partly deleted in the null allele, so that the reverse primer site is not present. The product is 848 bp.

For the null allele, 2 mM magnesium chloride and 2 µM each of the forward (5' CGG CAT CAG AGC AGA TTG TAC TG 3') and reverse (5' TTG GTC TGG ACT GTG GAA GTG CAG 3') primers were used. This reaction amplifies a region between +2263 within the sequence of the cloning vector pBR322 (part of the replacement vector construct used to generate the null allele) to +4912 of the wild-type sequence. All reactions were cycled using 1 minute annealing at 60°C and 1 minute primer extension at 72°C. All samples were electrophoresed on a 1% TBE agarose gel. The product is 412 bp.

2.3.5: Haplotyping *H-2* by PCR

i) H2IEb (MHC Class II)

a) Primary PCR reaction

A microsatellite of two repeating tetranucleotides (TGGA and GGCA) exists in the murine *H2IEb* gene (encoding the β -chain of MHC class II) at the 3' end of intron 2. The number of each repeat varies between haplotypes, therefore allowing distinction between *H2IEb* haplotypes by the size of PCR product [Saha *et al.*, 1993].

To amplify the microsatellite in the murine *H2IEb* gene, a 25 μ l PCR reaction was used containing 2 mM magnesium chloride and 1 μ M each of the forward (5' ATT CCT CCT GAG AGT GGA GCT GAC 3') and reverse (5' TGC GTC TTT GTG GGG TAC ACA G 3') primers. The primers amplify a region that includes the microsatellite. The mixture was cycled with a 1 minute annealing step at 58°C and 1 minute primer extension at 72°C. The products were electrophoresed on a 2% TAE agarose gel.

Using this method, the *H2IEb* alleles can be distinguished corresponding to the H-2 haplotypes: *b*, *d*, *f*, *j*, *k*, *p*, *q*, *r*, *s*, *u*, *v*, and *w*. Haplotype *b* (e.g., for C57BL/6) gives a product of 240bp in this reaction. Results were used in a Kruskal-Wallis analysis of variance test, to determine statistically whether any particular haplotypes influence susceptibility to disease.

b) Amplification of a microsatellite in the mouse H2IEb gene using secondary radiolabelled PCR

In order to obtain higher resolution of the PCR products resulting from the primary *H2IEb* PCR reactions, a secondary PCR was performed with radiolabelled primers, and the primary PCR products as templates. The forward primer (10 pmol) for the *H2IEb* PCR was 5' end labelled with ³²P using T4 polynucleotide kinase (see section 2.5.1) and was diluted to 100 µl with sterile water and stored at -20°C for up to 4 weeks.

Dephosphorylation of 5' ends of a ΦX174/HaeIII DNA size marker

In order to create a radiolabelled DNA size marker for the secondary radiolabelled PCR reaction, the 5' ends of ΦX174/*HaeIII* were first dephosphorylated using calf intestinal alkaline phosphatase (CIAP).

The number of 5' ends in 1 µg of ΦX174/*HaeIII* were first calculated. For the dephosphorylation reaction, 1.6 µg ΦX174/*HaeIII*, 1 x supplied CIAP reaction buffer (50 mM Tris-HCl pH 9.3, 1 mM magnesium chloride, 0.1 mM zinc chloride, 1 mM spermidine) and 0.05 u of CIAP were incubated together at 37°C for 20 min, then 56°C for 20 min to ensure access to the 5' ends. Another 0.05 u of CIAP was then added and again the mixture incubated at 37°C for 20 min followed by 56°C for 20 min. The reaction was stopped by the addition of 300 µl of CIAP stop buffer (10 mM Tris pH 7.5, 1 mM EDTA, 200 mM sodium chloride, 0.5% SDS).

Phenol:chloroform (350 μ l) (a solution of 50% buffered phenol, 48% chloroform and 2% isoamyl alcohol overlaid with an equal volume of 50 mM Tris-HCl pH 8.0) was added mixed by vortexing. Phases were separated by centrifugation at 16,000 x g for 5 min, after which the DNA was ethanol precipitated from the aqueous phase. The resulting pellet was washed with 70% ethanol, dried, and resuspended in 5 μ l water.

The 5' dephosphorylated Φ X174/*Hae*III was then end-labelled using T4 polynucleotide kinase as described in section 2.5.1. The purified radiolabelled marker was stored at -20°C in a lead container for up to 4 weeks.

Creation of an alternative DNA size marker for radiolabelled secondary H2IEb PCR (pNEB193/HpaII)

In order to size the radiolabelled secondary *H2IEb* PCR products more accurately, an alternative DNA size marker was created. 1 μ g of the pNEB193 plasmid was digested with 10 u of *Hpa*II in 10 μ l sterile water containing 1 x *Hpa*II buffer (6 mM Tris-HCl (pH 7.4), 6 mM magnesium chloride, 6 mM sodium chloride, 1 mM DL-Dithiothreitol (DTT)) for 1 hr at 37°C. Digestion of pNEB193 with *Hpa*II results in 14 fragments, of sizes 489, 453, 404, 331, 242, 190, 147, 127, 110, 67, 48, 34, 26, and 11nt. The fragments were then radiolabelled by adding 2 μ l of γ -[³²P] dCTP and 5 u of Klenow fragment (a 5' - 3' DNA polymerase, used to fill in 5' overhanging ends with radiolabelled dNTPs) and incubating at room temperature for 10 min. 1 μ l of 0.2 mM dNTPs was then added and the mixture again left at room temperature for 10 min. The enzyme was inactivated by heating to 75°C for 10 min. The solution was then diluted into

50 μ l of sterile water and purified through a Sephadex G50 spin column. The radiolabelled DNA size marker was stored at -20°C in a lead container until use.

Secondary radiolabelled PCR for H2IEb

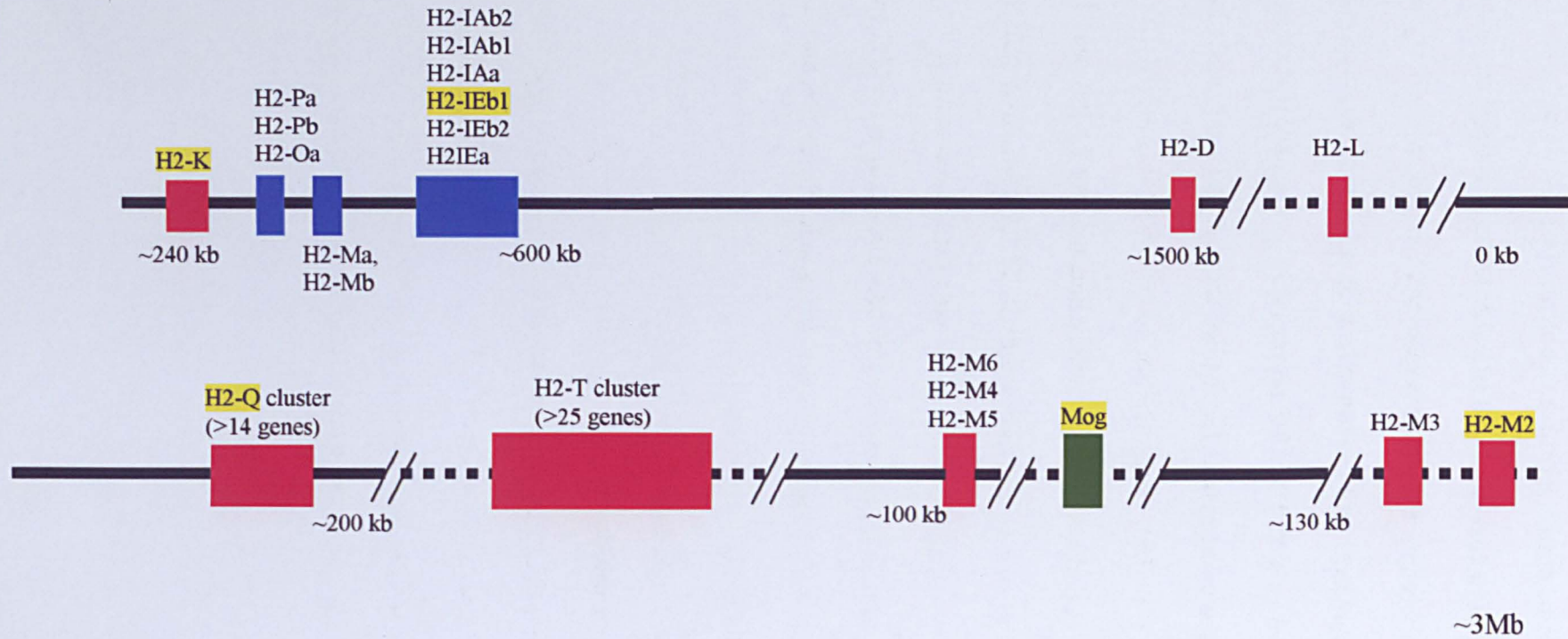
0.2 pmol of labelled forward oligonucleotide primer and 5 pmol of the unlabelled reverse primer were added to 1 μ l of product from the primary PCR reaction. The mixture was then made up to 10 μ l with 2 mM magnesium chloride, 1.25 units of *Taq* polymerase, 1 x *Taq* polymerase buffer and 0.2 mM dNTPs. The reaction was cycled with an initial 5 min at 94°C followed by 1 minute at 94°C , 1 minute at 60°C and 1 minute 72°C for 10 cycles.

The 10 μ l of PCR product mixture was then ethanol precipitated to concentrate the mixture. This was achieved by adding 10 μ g glycogen as a carrier for the nucleic acid precipitation, 0.4 volumes 3 M sodium acetate and 4 volumes of 100% ethanol to each reaction. The mixtures were cooled at -70°C for 10 min then centrifuged in a microcentrifuge at 16,000 x g for 10 min. The supernatant was decanted and the pellet redissolved in 5 μ l 8 M urea/1 x TBE. Urea is used to denature the nucleic acids, so that they run on electrophoresis as single strands.

Size determination of radiolabelled secondary PCR products on an 8% polyacrylamide gel

An 8% polyacrylamide solution containing 30:1 acrylamide/Bis-acrylamide and 8 M urea was prepared and stirred with mixed bed resin deionising beads. The solution was

Figure 6: Simplified physical map of the murine H-2



Key:

- MHC Class I genes
- MHC Class II genes
- Genes containing markers used in study
- Non-MHC gene

decanted into a clean flask. 1 x TBE was added and the gel stored until use in dark glass bottle at 4°C.

50 ml of the polyacrylamide mixture, containing 45 µl N,N,N',N'-Tetramethylethylenediamine (TEMED) and 450 µl of 20% ammonium persulfate was used to pour each gel. The polymerised gel was clamped upright in a gel rig and an aluminium plate clamped onto the front to improve heat distribution across the gel. The gel was warmed by pre-running with 1 x TBE buffer at 38 watts for 30 min. Prior to loading, the samples were heated at 100°C for 2 min, then 0.5 µl formamide loading buffer (xylene cyanole FF 1 mg/ml, bromophenol blue 1 mg/ml, 0.01 M EDTA in deionised formamide) was added to each. Radiolabelled marker (2 µl) was loaded alongside the samples. The gel was electrophoresed at 38 W for 2 hr. After running, the gel was fixed in 10% acetic acid/10% methanol. It was then lifted onto filter paper, covered in P.V.C wrap and dried in a gel drier (Model 583, Bio-Rad) at 80°C for at least 1 hr. The dried gel was placed on autoradiograph film in a shielded cassette, and stored at -70°C for 1 week until developing.

ii) Haplotyping of other genes within H-2

Mice were haplotyped, using PCR, for 4 markers across the H-2 cluster, 3 of which lie in MHC Class I genes (*H2K*, *H2M2*, *H2Q4*) and one that lies within the *H2M* (MHC Class I) cluster, but encodes murine oligodendrocyte glycoprotein, which is not an MHC molecule (*Mog*) (Figure 6). Markers were found using by searching for PCR

polymorphisms within the *H-2* cluster on chromosome 17 on the Jackson Laboratory mouse genome informatics website (<http://www.informatics.jax.org/>).

All PCR reactions were in 25 μ l and underwent 35 cycles of amplification with a 1 min primer extension step at 72°C, and were electrophoresed in 2% TAE agarose gels.

Table 1: PCR conditions for haplotyping across the murine *H-2*:

Gene	Region amplified	Forward (F) and reverse (R) primers	Primer concn. (μM)	Magnesium chloride concn. (mM)	Annealing temp.	End product size
<i>H2K</i>	(CA) _n within the promoter region	(F) 5'ACT CAG GAC TCA GAA TGA AGA TCC3' (R) 5' ATT CCT AGA TGA AAA GTC TGT GGC3'	1	1	56°C	e.g. 120bp (<i>H-2K^b</i>), 104bp (<i>H-2K^d</i>),
<i>H2M2</i>	(CA) _n within intron 3	(F) 5' ACC TCT CAC CTC TCT CTG TG 3' (R) 5' TGG AGA GAC GTC CTA TGA TG 3'	2	2	58°C	e.g. 142bp (<i>H-2M2^d</i>), 126bp (<i>H-2M2^b</i>)
<i>H2Q4</i>	(TTC) _n \times (CT) _n	(F) 5' CCT GCA GGA ATA TCA ATA GTG 3' (R) 5' ATA CAG AGA AAC CCT ATC TCA A 3'	2	2	56°C	*
<i>Mog</i>	Microsatellite located near the 3' end of intron 2	(F) 5' GGT GTC CAC AAT CCA AAT TCC 3' (R) 5' CTC CCC AAA TTT TAT TCA GTG 3'	2	2	58°C	~164 bp or ~155bp

* Different haplotypes can be distinguished using this reaction if tested simultaneously, however there is no method of identifying single haplotypes

2.4: Analysis of PCR products

2.4.1: Extraction of DNA from agarose gel

After running PCR products on a TAE agarose gel, the band of interest was visualised under UV light at 320nm and excised from the gel with a scalpel. The agarose gel slice was chopped finely, then centrifuged through silanised glass wool at 4000 x g for 5 min. The eluate was then ethanol precipitated. The resulting DNA pellet was washed in 70% ethanol, air dried and resuspended in 10 µl water.

2.4.2: Automated DNA sequencing

DNA samples were sequenced in the Division of Genomic Medicine. Template DNA (0.25 µg-0.5 µg) was amplified using the ABI PRISM Ready Reaction DyeDeoxy Terminator Cycle Sequencing kit (PE Applied Biosystems) according to the manufacturers instructions. The samples were separated by electrophoresis on a 6% polyacrylamide gel and analysed on an ABI 377 DNA sequencer (PE Applied Biosystems) using PRISM DNA sequencing software version 3.2 (PE Applied Biosystems).

2.5: Radiolabelling DNA with ³²P

2.5.1: Radiolabelling 5' ends with ³²P:

To catalyse the transfer of radiolabelled phosphates to the 5' terminus of a polynucleotide, T4 polynucleotide kinase (PNK) was used. The oligonucleotide or DNA size marker to be end labelled (10 pmol), 10 units of T4 PNK and 1 x supplied kinase buffer (70 mM Tris-HCl pH 7.5, 10 mM magnesium chloride, 5 mM DTT, 0.1 mM

EDTA, 0.1 μ M ATP, 50% (v/v) glycerol) were added together in a 10 μ l reaction. 3 μ l γ -[³²P] ATP were added and the mixture incubated at 37°C for 30 min, then 68°C for 20 min to inactivate the kinase. Unincorporated nucleotides were removed by centrifugation through a Sephadex G50 spin column at 1200 x g for 5 min.

2.5.2: Random heptamer labelling of oligonucleotide probes with T7 Quickprime kit:

DNA probes were labelled with α -[³²P] dCTP (NEN), with random heptamer primers. 10 μ l of the supplied T7 reagent mix (containing buffer, dNTPs and random heptamers), 50 ng/50 μ l reaction of the oligonucleotide probe, 1 μ l T7 DNA polymerase and 5 μ l α -[³²P] dCTP per reaction were mixed on ice, and incubated in a 37°C water bath for 15 min to allow the polymerase extension from the heptamer primers. Following incubation, 2 μ l of 0.5 M EDTA and 50 μ l sterile water were added and the mixture heated to 100°C in a boiling water bath for 1 min to stop the reaction. Unincorporated nucleotides were removed by centrifugation through a Sephadex G50 spin column.

2.6: Genotyping of mice using Southern blot analysis

2.6.1: Preparation of samples for Southern blot gel

For each sample, 10 μ g of high molecular weight DNA extracted from splenocytes was placed into a 1.5 ml microfuge tube and diluted to 176 μ l with TE. Buffer, 20 μ l 10 x *Apa*I buffer (6 mM Tris-HCl (pH 7.4), 6 mM magnesium chloride, 6 mM sodium chloride, 1 mM DTT) and 40 u of *Apa*I were added, mixed gently and incubated at 37°C overnight to allow *Apa*I digestion. The remainder of the dialysed DNA was stored at 4°C.

Following *ApaI* digestion, an equal volume of phenol:chloroform was added to each sample and mixed by inversion for 30 s, the mixture centrifuged at 16,000 x g for 5 min, and the aqueous phase transferred to 1.5 ml microfuge tubes. DNA was precipitated using ethanol. The pellets were washed with 70% ethanol, dried and resuspended in 25 µl TE.

2.6.2: Electrophoresis of high molecular weight genomic DNA

5 µl of sample buffer (60 mM EDTA pH 8.0, 60% glycerol, bromophenol blue) was added to each sample and to 0.5 µg of a *HindIII* digested λ DNA size marker. All tubes were heated at 55°C for 5 min to disrupt any newly formed double strands, prior to loading onto a 0.7% TBE agarose gel. The gel was run at 20V for 40 hr, with a change of buffer after 20 hr.

The gel was then stained with ethidium bromide by incubating the gel in a tank of 1 x TBE containing 0.5 µg/ml ethidium bromide for 1 hr. The gel was then examined under UV light at 320nm to monitor the size range of the DNA in the gel. The gel was subsequently washed for 15 min in 0.4 M hydrochloric acid (to partially depurinate the DNA), rinsed in sterile water then washed for 2 x 15 min in 0.5 M sodium hydroxide to hydrolyse the DNA at depurinated sites and denature the double stranded DNA.

2.6.3: Southern blotting

A glass plate was placed over a reservoir of 0.5 M sodium hydroxide in a large tray and filter paper laid onto the glass with wicks hanging down either side into the sodium hydroxide. The gel was placed upside down onto the filter paper, and Saran wrap laid

over the gel with a window cut out over the running area of the gel. Zetaprobe GT, a positively charged nylon membrane soaked in sterile water was laid over the window onto the gel and covered with 2 layers of filter paper soaked in 0.5 M sodium hydroxide, followed by an 8 cm thick layer of paper towels, topped with a glass plate. The stack was left overnight. The following day, the membrane was washed briefly in 200 mM sodium phosphate (1M sodium phosphate buffer consists of 0.2 M NaH_2PO_4 /0.4 M Na_2HPO_4) to neutralise the DNA, then dried in an oven, between two sheets of filter paper, at 80°C. When dry, the membrane was sealed in a plastic bag until probing.

2.6.4: Probing of Southern blot

The membrane was rolled up into a hybridisation bottle containing 20 ml of hybridisation solution (500 mM sodium phosphate, 7% sodium dodecyl sulphate). The membrane was pre-hybridised by rolling at 65°C overnight.

The oligonucleotide probe was randomly labelled with α -[^{32}P] dCTP using a T7 Quickprime kit (section 2.5.2) A further 50 μl of sterile water were added and the mixture centrifuged at 1200 x g through a Sephadex G50 spin column to remove unincorporated dCTP. The radiolabelled probe was heated to 100°C in a boiling water bath for 5 min to denature any newly formed double stranded DNA. 50 μg of mouse *Cot1* DNA was added (to suppress the hybridisation of repetitive DNA sequences).

The labelled probe, 10 pmol, was then mixed into 10 ml hybridisation solution (pre-warmed to 65°C). The hybridisation bottle containing the membrane was drained and the

hybridisation fluid containing the labelled probe was passed through a 0.2 µm filter into the bottle. This was found necessary, in order to avoid the appearance of a radioactive background on the blot. The membrane was then hybridised with the probe for 16 hr. The membrane was then washed in hybridisation solution at 65°C for 3 x 20 min, then sealed into a plastic bag.

2.6.5: Visualisation of Southern blot using a phosphorimager

Screens (molecular imaging screen, Bio-Rad) were erased for 15 min in a GS-250 screen eraser (Bio-Rad) prior to use. The blot was left overnight to irradiate the screen in a sample loading dock (Bio-Rad). The screen was scanned using a GS-250 molecular imager (Bio-Rad) and the scan visualised on a computer using Molecular Analyst software version 2.0.1 (Bio-Rad).

2.7 Cell culture

2.7.1: Culture of RAW 264.7 mouse macrophage cells

Stocks of RAW 264.7 cells (ECACC) were kept frozen in liquid nitrogen. Aliquots were thawed and cultured in RPMI1640 medium containing 100 u/ml penicillin, 100 µg/ml streptomycin and 10% heat inactivated foetal calf serum. Cells were grown at 37°C/5% CO₂ and passaged every 6 days.

2.7.2: Stimulation of cells with LPS

In order to activate them, RAW 264.7 cells were stimulated with LPS by replacing LPS-free medium with that containing 100 ng/ml *Escherichia coli* LPS. Cells were stimulated

for 4 and 18 hr. Separate aliquots of cells were not stimulated with LPS as negative controls.

2.8 Immunohistochemistry for frozen sections

2.8.1: 3-Aminopropyltriethoxysilane (APES) coating of slides

It is necessary to coat slides in APES or a similar compound in order to make slides more adherent for frozen sections. This process ensures that sections are not washed off slides during the staining procedure. Microscope slides were dipped for 15 s each in 95% ethanol/2% APES, 95% ethanol and deionised water, dried at 37°C and subsequently stored at room temperature.

2.8.2: Cutting frozen sections – operation of cryostat

Sections were cut with a 16 cm blade (Leica) in a cryostat (cryocut-E, Reichart-Jung), pre-cooled to -25°C. The section was embedded in optimum cutting temperature (O.C.T) compound on a pre-cooled chuck, which was then mounted in the chuck holder after the O.C.T block containing the tissue had completely frozen.

The block was trimmed at depths of 20 µm until the desired area of tissue was reached. At this stage, 4-5 sections were cut at 6 µm to smooth the block. 6 µm sections could then be taken, by collecting on room temperature APES coated slides. The slides were labelled and stored in microscope slide boxes at -70°C.

2.8.3: Cutting frozen sections from undecalcified joints

It was necessary to cut sections from undecalcified joints in order to allow immunohistology of sensitive antigens. This process uses a powerful cryo-microtome (School of Dentistry, University of Manchester) capable of cutting thin sections of samples containing undecalcified bone, which would otherwise shatter within the sample or damage the blade of a normal cryostat.

Specimens were mounted by first cooling a chuck, inside a metal case, in liquid nitrogen for 2 min. The chuck was covered in 1.6% carboxymethyl cellulose, which was allowed to cool. The sample was then placed in the desired position onto the cold carboxymethyl cellulose, and was then covered with more paste by syringing it over the sample. When the paste had frozen, the chuck and case were removed from the liquid nitrogen and the case removed. The partially formed block was held upside down in metal tongs and dipped in the liquid nitrogen, followed by dipping in more paste, and the process repeated until a smooth block was achieved. The specimen was allowed to warm slightly before placing in the cryostat (Cryo-microtome 450-MP, PMV (Stockholm)) which was pre-cooled to -20°C . Slides were coated in a thin layer of Sellotape glue which was allowed to dry for 2 min, after which they were labelled and placed inside a slide rack inside the cryostat to cool.

The block was trimmed, and $10\ \mu\text{m}$ sections were then collected. To collect the sections, a thin layer of water soluble glue was scraped across the top of the block using the edge of a clean slide. A cut piece of cigarette paper (Rizla) was then pressed onto the top of the

section leaving a small overhang over the blade. The overhang was held with tweezers and the block moved through the blade to cut the section. As it was being cut, the section was guided over the blade with the tweezers. The section was then pressed down onto a glue-coated slide in a smooth motion. The slides were stored at -70°C until required.

2.8.4: Haematoxylin and eosin staining of frozen sections

To examine the general cellularity of frozen tissue sections, they were stained with haematoxylin and eosin. Slides at room temperature were submerged in Gill's No.1 haematoxylin for 5 min. The slides were rinsed in running tap water for 1 minute, then submerged in Scott's solution (20 g/l of sodium bicarbonate and 3.5 g/l of magnesium sulphate 7-hydrate) for 30 s. The slides were then rinsed in running tap water for 1 min, submerged in aqueous 1% Eosin Y for 5 min, rinsed in running tap water for 1 min and dehydrated by submerging in 70% ethanol, 95% ethanol and 100% ethanol for 1 min each. Finally, the slides were cleared by submersion in xylene for 1 minute and coverslips mounted using Eukitt mounting medium.

Cell nuclei stain blue/purple while eosin stains acidophilic tissue components pink/red colours.

2.8.5: Haematoxylin and eosin staining of undecalcified frozen joint sections

Slides were allowed to reach room temperature. They were then stained with haematoxylin and eosin as above but not dehydrated. It was found that dehydration through an ethanol series had an adverse effect on the glue, causing it to become cloudy.

Instead, after staining with eosin, the slides were rinsed in running tap water for 1 min then air dried and coverslips mounted using a glycerol-based aqueous mounting medium (Aquamount, BDH).

2.8.6: Connective tissue staining of frozen sections

To identify elastin and collagen in sections simultaneously, the elastic/van Gieson staining technique was employed. Slides were allowed to reach room temperature, after which they were incubated with 5 g/l potassium permanganate on a rack at room temperature for 5 min. The slides were rinsed with distilled water then decolourised by incubating with 1% oxalic acid for 2 min at room temperature. The slides were then rinsed in running tap water for 2 min followed by dehydration by rinsing with 95% ethanol and incubation in Miller's solution at room temperature for 1.5 - 4 hr.

The slides were then rinsed briefly in 95% ethanol, then 75% ethanol, then washed in running tap water for 1 min. They were then counterstained on a rack with van Gieson solution (2.5 g/l acid fuschin, picric acid to saturation) at room temperature for 5 min, blotted dry using filter paper and dehydrated by submerging in 100% ethanol for 1 min, then cleared by submerging in xylene for 1 min. Specimens were mounted using Eukitt mounting medium. This protocol stains elastin black, collagen red and muscle yellow.

2.8.7 Immunohistochemical staining of frozen sections - optimisation of stains

PBS/0.1% saponin

All incubations and washes unless otherwise stated were in fresh PBS/0.1% saponin. Saponin acts as a detergent allowing intracellular antigens to be detected. Although some antigens were on the cell surface, saponin did not appear to have any effect on the staining for these antigens. Saponin was therefore used in all staining procedures for ease of performing multiple stains simultaneously. PBS/0.1% saponin consists of 8 g/l sodium chloride, 0.2 g/l potassium chloride, 0.9 g/l anhydrous disodium hydrogen phosphate, 0.2 g/l potassium dihydrogen phosphate, and 1g saponin. The solution was stirred for at least 20 min before use to disperse the saponin.

To optimise immunohistochemical stains, the procedure given in section 2.8.8 was carried out on appropriate positive control slides, as listed in table 2. At the point of incubation with primary antibody, a range of concentrations of the primary antibody was used in order to determine optimal concentration – i.e., the concentration of antibody which gave the clearest specific staining without inappropriate background staining. Negative control slides were co-incubated with PBS/0.1% saponin in place of primary antibody. The optimal concentrations for each primary antibody are given in table 2.

Table 2: Antibodies, positive controls and sera for mouse immunohistochemistry

Primary antibody	Clone	Supplier	Target antigen	Concn. for use ($\mu\text{g/ml}$)	Positive controls	Normal serum used in block	Biotinylated secondary antibody	Concn. for use ($\mu\text{g/ml}$)
Rat anti-mouse IL-1 β	30311.11	R&D	IL-1 β	2.5	LPS stimulated RAW 264.7 cells	Rabbit (Vector)	Rabbit α -rat	2.5
Rat anti-mouse F4/80	CI:A3-1	Caltag	Macrophages	1	Mouse spleen	Rabbit (Vector)	Rabbit α -rat	2.5
Rat anti-mouse CD4	H129.19	Pharmingen	CD4+ T cells	0.5	Mouse spleen/thymus	Rabbit (Vector)	Rabbit α -rat	2.5
Rat anti-mouse CD8a	53-6.7	Pharmingen	CD8+ T cells	0.5	Mouse spleen/thymus	Rabbit (Vector)	Rabbit α -rat	2.5
Rat anti-mouse IFN γ	XMG1.2	Pharmingen	IFN γ	1	Mouse thymus	Rabbit (Vector)	Rabbit α -rat	2.5
Rat anti-mouse IL-4	BVD6-24G2	Immuno Kontact	IL-4	2	Immunised mouse spleen	Rabbit (Vector)	Rabbit α -rat	2.5
Rat anti-mouse IL-5	TRFK5	Caltag	IL-5	2	Immunised mouse spleen	Rabbit (Vector)	Rabbit α -rat	2.5
Rat anti-mouse CD31	MEC 7.46	HyCult	PECAM-1 (endothelial cells)	0.5	Heart tissue	Rabbit (Vector)	Rabbit α -rat	2.5
Rat anti-mouse CD62e	10E9.6	Pharmingen	E-selectin	10		Rabbit (Vector)	Rabbit α -rat	2.5
Rat anti-mouse CD19	1D3	Pharmingen	B cells	1.6	Mouse spleen	Rabbit (Vector)	Rabbit α -rat	2.5

Primary antibody	Clone	Supplier	Target antigen	Concn. for use (µg/ml)	Positive controls	Normal serum used in block	Biotinylated secondary antibody	Concn. for use (µg/ml)
Rat anti-mouse neutrophils	7/4	Serotec	Neutrophils	0.33		Rabbit (Vector)	Rabbit α-rat	2.5
Rat anti-mouse DEC205	NLDC-145	Serotec	Dendritic cells, thymic epithelial cells, follicular DC's of B cell follicles	S/N. 1:100 dilution used	Mouse skin	Rabbit (Vector)	Rabbit α-rat	2.5
Hamster anti-mouse MCP-1	2H5	Serotec	MCP-1	5	Induced granuloma in mouse thigh tissue	Goat (Sigma)	Goat α-hamster	5
Hamster anti-mouse CD54	3E2	Pharmingen	ICAM-1	10	Induced granuloma in mouse thigh tissue	Goat (Sigma)	Goat α-hamster	5
Rabbit anti-mouse keratin 6	Polyclonal	Covance	Keratin 6	5	Mouse skin, mouse tongue	Goat (Sigma)	Goat α-rabbit	5

For staining frozen joint sections, antibody concentrations were increased since the adhesive used and fixing step seems to mask some antigen. In these sections, α -IL-1 β was used at 5 μ g/ml, α -F4/80 at 2 μ g/ml, α -CD4 at 2 μ g/ml, α -CD8a at 2 μ g/ml, α -IFN γ at 2 μ g/ml, and α -IL-4 at 5 μ g/ml. The secondary antibody (rabbit α -rat) was used at 5 μ g/ml.

2.8.8: Immunohistochemical staining of frozen sections - staining procedure with Vector ABC reagent kit

Slides stored at -70°C freezer were allowed to reach room temperature. They were fixed in acetone at room temperature for 10 min and dried on a rack. Frozen joint sections were fixed for 20 min in methanol at 4°C , as acetone was found to destroy the adhesive.

The slides were rinsed briefly with PBS then washed 3 x 3 min. In order to quench endogenous peroxidase by auto-oxidation, the slides were then incubated for 20 min at room temperature in 0.9% v/v hydrogen peroxide (1.2% hydrogen peroxide for frozen joint sections). If sections were to be stained using the alkaline phosphatase method, the quenching step with hydrogen peroxide was omitted. After quenching, the slides were washed 3 x 3 min. To avoid loss of reagents from the slides, a hydrophobic barrier was created around each sample with a paraffin pen (PAP pen, Hybaid). Frozen joint sections were dried only on the back of the slide, to avoid disturbing the glue holding the section in place. To block inappropriate reactivity to the secondary antibody, the slides were then incubated for 30 min at room temperature in a humidified chamber with 200 μ l per slide of 7% appropriate normal serum (10% for frozen joint sections) (see table 2). The

serum used corresponded to the species in which the secondary antibody was made.

The slides were then blocked for inappropriate staining of endogenous biotin within the sections. The slides were drained and 1 drop of avidin from an avidin/biotin blocking kit (Vector) was added to each slide. After 15 min incubation at room temperature the slides were rinsed with PBS and 1 drop of biotin from the same kit was added to each slide. After 15 min incubation at room temperature, the slides were rinsed with PBS and washed 3 x 3 min. This procedure binds any endogenous biotin in the tissue (which would otherwise create false positive results by reacting with the ABC complex) with avidin, then blocks any remaining biotin binding sites on the avidin with biotin.

The appropriate primary antibody (see table 2) in 200 μ l, at the optimal concentration, was added to each section and the slides incubated either for 15 hr at 4°C, or for 2 hr at room temperature, both in a humidified chamber.

Following incubation with primary antibody, the slides were washed 3 x 3 min and incubated in a humidified chamber at room temperature with the appropriate biotinylated secondary antibody (all supplied by Vector) for 30 min (see table 2).

At this point the ABC reagents (VECTASTAIN Elite ABC kit, Vector) were mixed and incubated at 4°C for 30 min to form an avidin DH biotinylated horseradish peroxidase H complex. The avidin binds to the biotinylated secondary antibody, whilst the peroxidase reacts with the chromagen DAB to produce a brown precipitate. To mix the ABC reagents, the amount required was first

calculated (100 µl per slide). The appropriate amounts of reagent A and reagent B were added to PBS/0.1% saponin as follows:

For diaminobenzidine tetrahydrochloride (DAB) staining (brown/black staining of positive cells), 2 µl each of reagent A and reagent B were added to each 100 µl.

For alkaline phosphatase staining (red staining of positive cells) the VECTASTAIN ABC-AP kit (Vector) was used, and in this case 1 µl each of reagent A and reagent B were added to each 100 µl. This combines avidin DH with biotinylated alkaline phosphatase H. The phosphatase catalyses the hydrolysis of the phosphate-containing Vector Red (Vector) substrate to form a red product.

After incubation with the biotinylated secondary antibody, the slides were washed 3 x 3 min. 100 µl of the ABC reagent was added to each slide and these were then incubated in a humidified chamber at room temperature for 30 min. The slides were then washed 3 x 3 min, then 2 x 3 min in PBS. The slides were then incubated with and 200 µl of substrate solution at room temperature.

For DAB staining, 1 drop of buffer, 2 drops of DAB substrate reagent and 1 drop of hydrogen peroxide substrate reagent as supplied (Vector) were added to each 5 ml of water. If a black rather than brown stain was required, 1 drop of the supplied nickel II chloride solution was also added. The slides were incubated with the substrate for 5-10 min.

For alkaline phosphatase staining, 2 drops each of Vector Red substrate reagents 1, 2 and 3 were added to 5 ml of 100 mM Tris-HCl, pH 8.2-8.5. 1 drop of the phosphatase inhibitor levamisole (Vector) was also added to each 5 ml of solution to block inappropriate staining. The slides were incubated with the substrate for 20-30 min.

The slides were rinsed with deionised water, then washed in deionised water for 1 min. They were then rinsed in running tap water for 1 min. Slides were counterstained with Gill's haematoxylin for 1 min, washed in running water for 1 min, allowed to turn blue in Scotts' solution for 10 s, rinsed in running tap water for 1 min then dehydrated through an ethanol series (1 min each in 70%, 95% and 100% ethanol). The slides were cleared in xylene for 1 min then mounted in Eukitt mounting medium.

Frozen joint sections were not dehydrated; after rinsing in running water following incubation in Scotts' solution, the sections were air dried and mounted in a glycerol based aqueous mounting medium.

2.9: Immunohistochemistry for formaldehyde fixed sections

2.9.1: Preparation of tissue samples for paraffin embedding

Tissue was fixed for >24 hr in 3.7% neutral buffered formaldehyde, or dissected from formaldehyde fixed cadavers. The tissue was placed inside a cassette and processed to paraffin automatically in a Citadel 2000 tissue processor (Shandon).

If the required samples contained bone, they were decalcified in daily changes of 0.53 M EDTA/sodium hydroxide (pH 8.0) for > 1 week prior to processing to

paraffin. Before decalcification, fur and skin were removed from the tissue in order to allow the decalcifying solution to permeate the tissue.

2.9.2: Preparation of paraffin wax blocks

Processed tissue samples were incubated at 65°C in a Tissue-Tek thermal console. Each specimen was orientated in a metal mould and molten paraffin (at 65°C) dispensed into the mould using a Tissue-Tek dispensing console, before cooling on a Tissue-Tek cryo-console at -5°C for 10 min, and removing blocks from the mould for storage at room temperature.

2.9.3: Sectioning of paraffin blocks – operation of microtome

The face of the block to be cut was chilled before being placed in the block holder of the microtome (model 820, American Optical Corporation). Disposable microtome blades (Feather) were used. The block was then trimmed by removing 20 µm thick sections until the desired area of tissue was exposed, when 6 µm thick sections were cut, floated on deionised water at 50°C and collected onto the surface of microscope slides. Sections were labelled, dried at 37°C overnight then subsequently stored at room temperature.

2.9.4: Histological staining of paraffin embedded sections

Sections were deparaffinised in xylene for 2 x 5 min, rehydrated by soaking in 100% ethanol for 2 x 5 min, 95% ethanol for 5 min, 75% ethanol for 5 min and running tap water for 1 min. For haematoxylin and eosin staining, the slides were then placed in Gill's haematoxylin. The procedure thereafter followed that for

frozen sections (section 2.8.4). Alternatively, the connective tissue staining method was followed (section 2.8.6).

2.9.5: Naphthol AS-D chloroacetate esterase staining in paraffin embedded sections

This technique detects a specific cellular esterase contained within neutrophils and the granules of mast cells. Naphthol AS-D chloroacetate esterase causes the enzymatic hydrolysis of naphthol AS-D chloroacetate (naphthol 3-hydroxy-2-naphthoic acid *o*-toluidide) to a naphthol compound. This then reacts with a diazonium salt, forming insoluble red deposits at the sites of enzyme activity. Neutrophils and mast cells can be identified in formaldehyde fixed, paraffin embedded sections [Yam *et al.*, 1971; Li *et al.*, 1973]. Sections were deparaffinised and rehydrated. Meanwhile 80 ml of deionised water were warmed to 37°C in a water bath. Immediately before use, 2 ml 0.1 M sodium nitrite solution was added to diazotise 2 ml fast red violet LB base solution (15 mg/ml fast red violet LB base in 0.4 M hydrochloric acid) in a universal vial and incubated for 2 min at 37°C. This solution was then diluted with the 80 ml warmed deionised water. TRIZMAL 6.3 buffer concentrate (10 ml) and 2 ml naphthol AS-D chloroacetate solution (8 mg/ml) were added. The mixture was poured over the slides, which were then incubated at 37°C in the dark for 15 min. The slides were then washed in deionised water for 2 min, and counterstained with haematoxylin for 2 min. Slides were rinsed in tap water, air dried and coverslips mounted using an aqueous mounting medium.

2.9.6: Toluidine blue staining of formaldehyde fixed paraffin embedded sections

Toluidine blue forms a characteristic purple complex with sulphated glycoproteins that are abundant in mast cells and basophils. Sections were deparaffinised and rehydrated, and stained in 0.01% aqueous toluidine blue solution for 30 s before rinsing in running water. Sections were dehydrated by dipping in 70%, 95% and 100% ethanol for 3 s each, then cleared by dipping in xylene and mounted. Mast cells appear violet, with a blue staining background.

To compare numbers of mast cells between skin sections, numbers were counted under a light microscope and divided by the approximate area of the skin visible in each field.

2.10: Analysis of RNA

2.10.1: Preparation of RNA from cells

Cells, from tissue culture, were pelleted by centrifugation and resuspended in a small volume of medium. 3 ml of RNAzol B was added to each cell suspension and mixed. The cell suspensions were transferred to sterile tubes on ice and 0.1 volume of chloroform added. The mixtures were vigorously mixed by vortexing for 30 s, then left on ice for 20 min, and centrifuged at 16,000 x g for 10 min at 4°C. The resulting aqueous phases were transferred to sterile tubes. Isopropanol, one volume, was added to each tube and the mixtures centrifuged at 16,000 x g for 15 min at 4°C. The resulting pellets were washed in 70% ethanol, allowed to dry and resuspended in 100 µl sterile water. 1 µl of the RNA sample was diluted 1:500 in sterile water. The concentration was measured spectrophotometrically at 260nm.

2.10.2: mRNA separation and Northern blot

a) Running of agarose gel and capillary transfer to membrane

A 250 ml gel tank and tray were soaked in 1 M sodium hydroxide for 30 min then rinsed out with sterile water. Baked glassware was used to make up a 1.2% agarose gel containing 0.1 M deionised formaldehyde and 5 ml 10 x 3-[N-Morpholino]propanesulfonic acid (MOPS) at pH 7.0 (500 ml 10x MOPS: 41.8 g MOPS/6.8 g sodium acetate/1.86 g disodium EDTA/3.2 g sodium hydroxide). 10 µg of each RNA sample were made up to 5 µl with sterile water. 20 µl loading buffer (12.5% 10 x MOPS, 9% formaldehyde, 62.5% formamide, 2.5% water, bromophenol blue) were added to each sample and appropriate RNA size marker.

Samples were heated to 70°C for 2 min then loaded into the gel. The gel was run for 2 hr at 70 volts in a tank containing a buffer composed of 1 x MOPS and 0.1 M deionised formaldehyde in water. After running, the gel was washed for 30 min in sterile water to remove formaldehyde, then washed for 30 min in 20 x sodium citrate buffer (SSC) (0.3 M trisodium citrate/3 M sodium chloride). A stack was then created, as for Southern blotting (section 2.6), with the difference that 10 x SSC was used in the capillary transfer, and the stack was topped with a weight of ~400 g. RNA transfer was allowed to proceed for 12 hr.

The stack was dismantled and the membrane washed in 2 x SSC, then baked between two sheets of filter paper for 30 min at 80°C. The blot was stored flat and sealed until probing.

b) Probing Northern blot

An IL-1 β mouse coding region probe was radiolabelled with α -[³²P] dCTP using the T7 Quickprime kit (section 2.5.2). The blot was rolled up into a hybridisation bottle, where it was pre-hybridised with 20 ml hybridisation solution at 65°C. The procedure as for probing Southern blots (section 2.6) was then followed. After probing, the damp blot was sealed in a plastic bag and placed on autoradiograph film in a light proof cassette at -70°C and developed after 24 hr.

2.11 Detection of *Helicobacter* species infection in mice

2.11.1: PCR to detect *Helicobacter* spp. infection in mouse

Helicobacter is not amongst the pathogens routinely investigated by the University of Sheffield SPF field laboratories. To detect if there was any *Helicobacter* infection, a PCR assay was employed [Riley *et al.*, 1996] to detect bacterial rRNA in faecal DNA. A 50 μ l PCR reaction was used which contained roughly 1 μ g DNA extracted from murine faeces, 4 mM magnesium chloride as supplied, 1 x buffer as supplied, 0.2 mM dNTPs, 2.5 units *Taq* DNA polymerase and 0.5 μ M each of the forward (5' CTA TGA CGG GTA TCC GGC 3') and reverse (5' ATT CCA CCT ACC TCT CCC A 3') primers. This reaction amplifies a stretch of the 16S rRNA gene which is conserved across members of the genus *Helicobacter*. The mixture was cycled with an initial DNA denaturation step at 94°C for 5 min, followed by a 2 s denaturation step at 94°C, 2 s annealing at 53°C and 30 s primer extension at 72°C. After 35 cycles, giving an end product of 375 bp for positive reactions, the samples were cooled to 4°C then stored at 4°C until running on a 2% TAE agarose gel.

2.11.2: *Mbo*I digestion of *Helicobacter* spp. PCR products

To determine which species of *Helicobacter* was present in the tested mice, the PCR products were digested with the restriction enzyme *Mbo*I. Using this method, *H. hepaticus* yields fragments of 348 bp and 27 bp, *H. muridarum* yields the unfragmented product of 375bp, and *H. bilis* gives fragments of 348 and 27 bp which can be further fragmented by the restriction enzymes *Hha*I and *Mae*I to yield fragments of 251 bp, 71 bp, 27 bp and 26 bp [Riley *et al.*, 1996].

The PCR product, 25µl, was run on a 2% TAE agarose gel to ensure the reaction had worked and the other 25 µl stored at 4°C. When the reaction had been confirmed, the remaining 25 µl was diluted with 65 µl sterile water and the DNA purified by phenol/chloroform extraction, followed by ethanol precipitation. The resulting pellet was resuspended in 10 µl TE. The sample was split into two aliquots of 5 µl and to one set 9.8 µl water, 2 µg BSA, 2 µl 10 x NEB buffer 3 (100 mM sodium chloride, 50 mM Tris-HCl, 10 mM magnesium chloride, 1 mM DTT pH 7.9) and 3µl (15 u) *Mbo*I were added. The other set were used as controls and had no enzyme added. These were incubated at 37°C for 3 hr, and the reaction stopped by the addition of 4 µl loading dye containing 80% glycerol/60 mM EDTA. The samples run on a 2% TBE agarose gel containing 0.5 µg/ml ethidium bromide and bands were visualised under ultraviolet radiation at 320nm.

2.12: Measurement of serum amyloid A (SAA) in mouse serum

2.12.1: Enzyme linked immunosorbent assay (ELISA) to detect levels of SAA in mouse serum

To attempt to measure the acute phase response in mice suffering from arteritis, levels of SAA in samples of mouse serum were measured using an SAA ELISA kit (Biosource) as per the kit instructions. Working solutions of the supplied wash buffer and diluent were prepared, then the supplied conjugated anti-SAA monoclonal antibody was prepared by diluting in diluent. Standards (at 3.8 µg/ml, 1.9 µg/ml, 0.950 µg/ml, 0.475 µg/ml, 0.233 µg/ml and 0 µg/ml) were prepared as per instructions, as well as 1:50 dilutions in (diluent buffer) of each serum sample. The supplied wells (pre-coated with a monoclonal antibody against mouse SAA) were washed twice with the working wash buffer. 50 µl of conjugated anti-SAA was added to all wells except blank controls, to which 100 µl of diluent was added. 50 µl of either standards or samples (all in duplicate) were then added to the wells (except blank controls). The wells were then covered with the supplied adhesive plastic over and incubated at 37°C for 1 hr.

Following incubation, the wells were emptied and washed 3 times with working wash buffer. A working PNPP (4-nitrophenyl phosphate) substrate solution was then prepared (1 mg/ml) in the supplied PNPP substrate buffer. 100 µl of PNPP solution was then added to all wells, and the wells covered and incubated at 37°C for 1 hr. 50 µl of the supplied stop solution (3 M sodium hydroxide) were added to all wells, and the absorbance read for each well at 405nm on an ELISA plate reader (MRX, Dynatech Laboratories). Results were analysed using Biolyinx

software (Dynatech Laboratories) version 2.20, and levels of SAA in each sample calculated from a graph constructed from the standards.

Section 3: Results

Figure 7: Southern blot analysis of two lines of *Illrn*^{-/-} mice

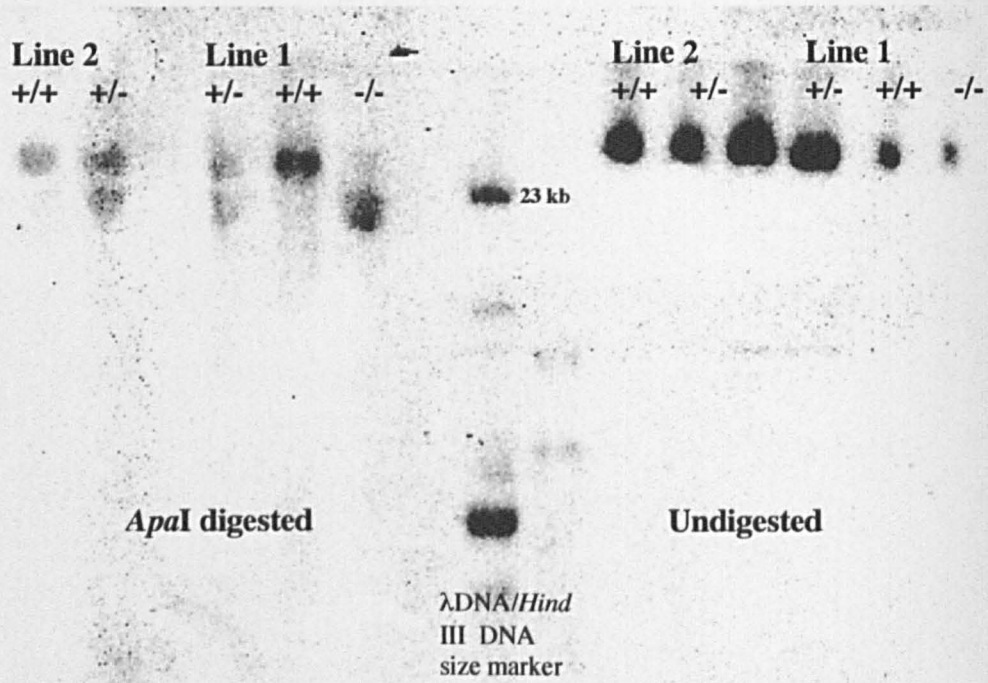


Figure 7: *ApaI* digestion of high molecular mass genomic DNA from two lines of *Illrn*^{-/-} mice, followed by Southern blot analysis using a radiolabelled 3' flanking probe, demonstrates that both lines contain the same null allele.

3.1: Southern blot analysis of two lines of *Il1rn*^{-/-} mice

The colony of IL-1ra deficient mice at the University of Sheffield is derived from the progeny of a single chimaera and an outbred MF1 female. In order to confirm that arteritis would arise in a second line, another chimaeric mouse was derived from a second G418 resistant embryonic stem cell colony. The mouse was backcrossed twice onto 129/Ola, then mated with a second outbred MF1 mouse. *Il1rn*^{-/-} progeny from this second mating were also confirmed as having arteritis [Nicklin *et al.*, 2000].

To compare the null alleles carried by the two lines, high molecular weight DNA was extracted from the spleens of mice from both lines. The DNA was then digested with *Apa*1 and the restriction fragments probed on a Southern blot with a radiolabelled 3' flanking probe (containing nucleotides ~13,300 to ~14,600).

Hybridisation of the probe to the Southern blot confirmed that the two lines contained the same null allele (Figure 7). Since *Il1rn*^{-/-} animals from both lines suffer from arteritis, and both contain the same null allele, it is reasonable to assume that the illness is due to the known null allele, and not an erroneously selected susceptibility gene.

Further evidence is currently being gathered through investigating whether a null allele in the IL-1 type 1 receptor gene (*Il1r1*) is able to suppress the *Il1rn*^{-/-} phenotype, by crossing *Il1rn*^{-/-} mice with *Il1r1*^{-/-} animals. This study is in progress.

Figure 8: Examples of positive controls for immunohistochemistry

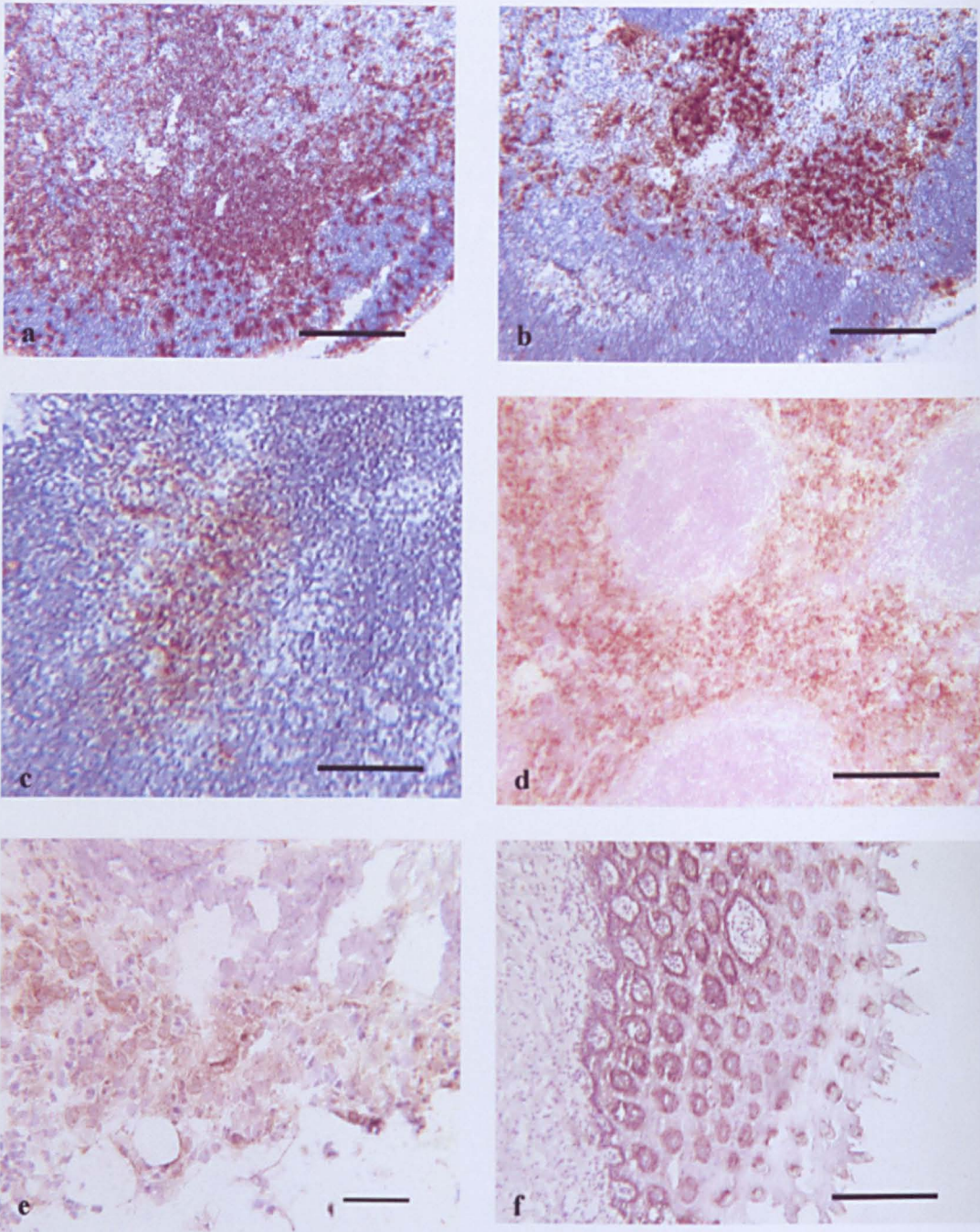


Figure 8: Examples of positive control stains for immunohistochemistry on frozen sections of mouse tissue. a) CD4⁺ cells, mouse thymus. b) CD8⁺ cells, mouse thymus. c) IFN γ ⁺ cells, mouse thymus. d) F4/80⁺ cells, mouse spleen. e) MCP-1 production, induced granuloma in mouse thigh muscle. f) keratin-6, mouse tongue. In all cases brown indicates positive staining, all counterstained with haematoxylin (purple/blue). Scale bars in a-d and f = 200 μ m, scale bar in e = 40 μ m. Scale bars throughout all figures are approximate.

Figure 9: Northern blot probed for IL-1 β

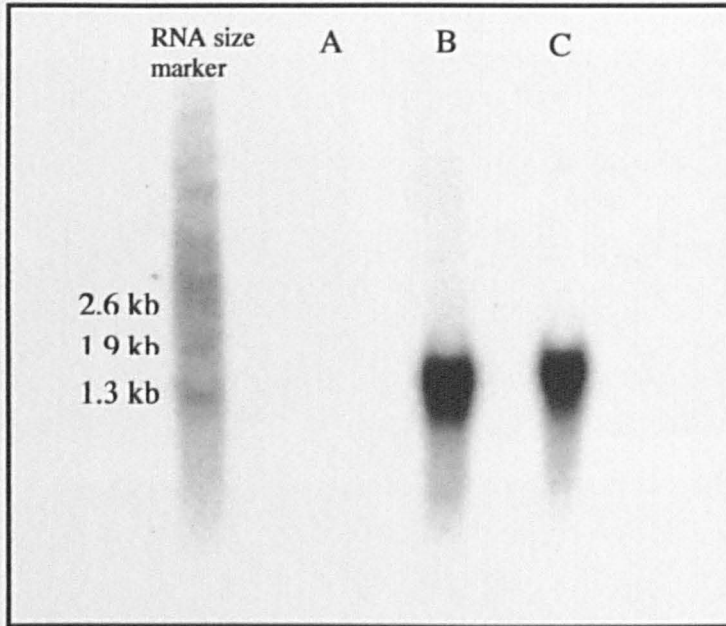


Figure 9: Northern blot prepared from 10 μ g RNA extracted from RAW 264.7 cells which had been either stimulated with 0.1 μ g/ml LPS or left unstimulated (cultured in LPS-free media). The blot was probed using a radiolabelled IL-1 β mouse coding region probe. Lane A, unstimulated RAW 264.7 cells. Lane B, RAW 264.7 cells after 4 hr stimulation with LPS. Lane C, RAW 264.7 cells after 18 hr stimulation with LPS. IL-1 β RNA is detectable in RAW 264.7 cells following LPS stimulation, but not before.

3.2: Optimisation of immunohistochemical stains

3.2.1: Positive controls

Several of the monoclonal antibodies used in this study had not been previously reported as suitable for immunohistochemical staining of frozen mouse tissue. In addition, antibodies which were previously used in protocols elsewhere still need to be optimised. Stains were optimised on an appropriate frozen tissue section. Most antibodies which had not been reported as used in staining frozen mouse tissue in the trade literature worked well after optimisation, as did those which had been used previously by other workers (Figure 8).

3.2.2: Positive control for IL-1 β

As a positive control for the anti IL-1 β antibody, RAW 264.7 (mouse macrophage) cells were grown on coverslips, stimulated with LPS then stained for IL-1 β . Negative controls were provided by simultaneously growing RAW 264.7 cells on coverslips in LPS-free medium. To test IL-1 β RNA production in these cells with and without LPS stimulation, to ensure they would make a viable positive control, a Northern blot assay was performed. RNA was extracted from RAW 264.7 cells 0 hours, 4 hours and 18 hours post stimulation with 100 ng/ml LPS. The RNA was used to create a Northern blot which was probed for IL-1 β RNA, using a radiolabelled probe. The resulting autoradiograph shows production of IL-1 β RNA in RAW 264.7 cells following LPS stimulation (Figure 9). For a positive control, the cells were stained for the macrophage antigen F4/80. Note that the expression of F4/80 is uniform, but IL-1 β is strong in some cells, but not in others (Figure 10).

Figure 10: RAW 264.7 cells used as positive controls for IL-1 β staining

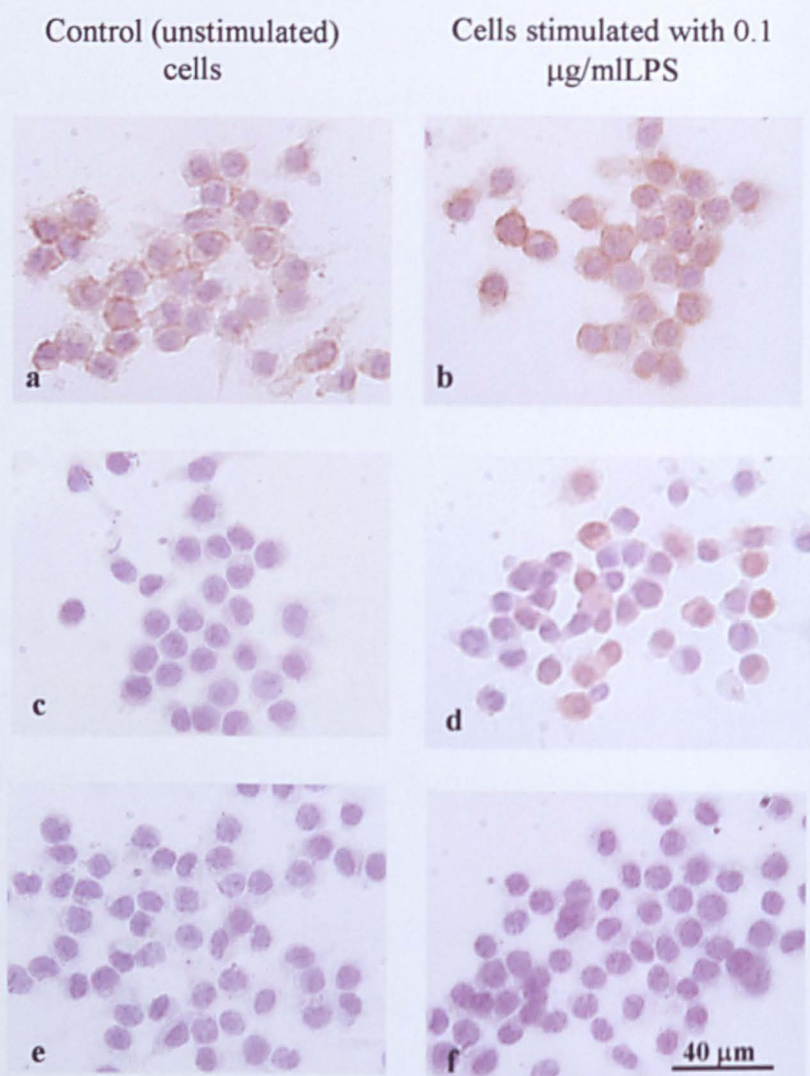


Figure 10: RAW 264.7 cells, either stimulated for 4 hr with 0.1 $\mu\text{g/ml}$ LPS or unstimulated (controls) were stained for F4/80 (positive control), IL-1 β , or CD4 (negative control). a) and b) are stained for F4/80, c) and d) for IL-1 β , and e) and f) for CD4. All cells stain positively for F4/80, none stain for CD4, and ~30% stain positively for IL-1 β following LPS stimulation. Scale bar applies to a-f.

Following this confirmation, RAW 264.7 cells were grown on coverslips, and either stimulated with LPS for 4 hours or left unstimulated. They were then stained with the anti-IL-1 β antibody. This procedure worked well (Figure 10), even after coverslips covered in LPS stimulated RAW 264.7 cells had been stored for several weeks in 100% ethanol at 4°C. Unstimulated cells did not stain for IL-1 β , nor did any cells stain for CD4 (used as an additional control). LPS stimulated RAW 264.7 cells thus served as positive controls for IL-1 β staining.

3.3 Arteritis in *Il1rn*^{-/-} mice

3.3.1: Introduction

Il1rn^{-/-} mice spontaneously develop arteritis, particularly in the aorta and its main branches. Lesions are often located at areas of turbulent blood flow such as flexures and bifurcations [Nicklin *et al.*, 2000]. The predilection for arteritic lesions to develop at these sites in our *Il1rn*^{-/-} mice is similar to that of GCA, TA and atherosclerotic lesion development in the human. *Il1rn*^{-/-} mice tend to die suddenly, from organ infarction, particularly myocardial, and less often as a result of internal haemorrhage from ruptured aneurysms.

The hypothesis being tested is that inflammatory arterial lesions arise in *Il1rn*^{-/-} mice as a result of the unopposed action of IL-1. The aim of this investigation was to further characterise the inflammatory lesions observed in arteritic *Il1rn*^{-/-} mice [Nicklin *et al.*, 2000], in order to obtain insight into the mechanisms by which arterial lesions result from the activity of IL-1. A further aim was to compare the disease with inflammatory lesions in human arteritides such as giant cell arteritis (GCA) and Takayasu's arteritis (TA), to test the hypothesis that the pathology of

the *Il1rn*^{-/-} mice may provide a suitable animal model for the study of human inflammatory artery disease.

3.3.2: Animals used in arteritis studies

Animals killed prospectively appeared outwardly healthy. Animals culled because of ill health and later confirmed as suffering from arteritis typically had poor coats, appeared hunched and lethargic, or had audible breathing.

In total, aortic roots from 70 animals were examined (40 from the Sf3 line that we are developing, 9 from the Sf2 line, and 21 Balb/c). 64/70 aortic roots were frozen and sectioned, and 6/70 were formaldehyde fixed, paraffin embedded, and sectioned.

Of the 64 animals examined in frozen sections, 8 were *Il1rn*^{+/+} Sf3, 4 were *Il1rn*^{+/-} Sf3, and 28 were *Il1rn*^{-/-} Sf3 animals. 6 were *Il1rn*^{+/+} Balb/c, 2 were *Il1rn*^{+/-} Balb/c, and 7 were *Il1rn*^{-/-} Balb/c. 2 were *Il1rn*^{+/+} Sf2, and 7 were *Il1rn*^{-/-} Sf2.

3.3.3: Characterisation of arteritis in *Il1rn*^{-/-} mice - immunohistochemical study

In all cases the aortic root was studied as it proved to be a frequently affected area, particularly around valves (an area of turbulent blood flow). Some formaldehyde fixed paraffin embedded sections were used, but the majority of the study used immunohistochemical staining techniques with frozen sections. Though the histology of these sections is less clear, they allowed us to define cell types, cytokines, chemokines and adhesion molecules present at the lesional site. In addition, a time course study was performed to attempt to define initiating factors

in the disease and to examine the progress of the lesions. It was hoped that by identifying the earliest features of the lesions, it would be possible to provide insights into how lesions develop in the arteries of *Il1rn*^{-/-} animals, and also to compare the lesions in more detail to those found in human GCA and TA.

General cell distribution

Frozen sections were stained with haematoxylin and eosin to locate lesions and to examine the general cellularity of the area. In affected *Il1rn*^{-/-} animals, haematoxylin and eosin staining of the aortic root revealed a large cellular infiltrate around affected vessels, particularly within the adventitial and medial layers. These results are similar to those described previously elsewhere in the arterial system [Nicklin *et al.*, 2000]. The boundaries of the infiltrate were often clearly defined (Figure 11). Lesions were frequently observed in areas of the vessels containing valves, which are sites of turbulent blood flow (Figure 12). Staining of formaldehyde-fixed paraffin embedded sections with haematoxylin and eosin gave a better impression of the structural morphology of the lesions (Figure 13). Lesions were seen in 4/6 paraffin embedded sections from *Il1rn*^{-/-} mice.

The haematoxylin and eosin stained sections were scored for the extent of cellular infiltrate as follows: 0 denotes no cellular infiltrate, and 1 denotes a small infiltrate of activated immune cells (<50) in the outer layer of the vessel wall. A score of 2 denotes a larger, more densely packed infiltrate, comprising approximately 25-50% of the area of the vessel, within the outer/medial layers. 3

Figure 11: Demarcation of lesional area

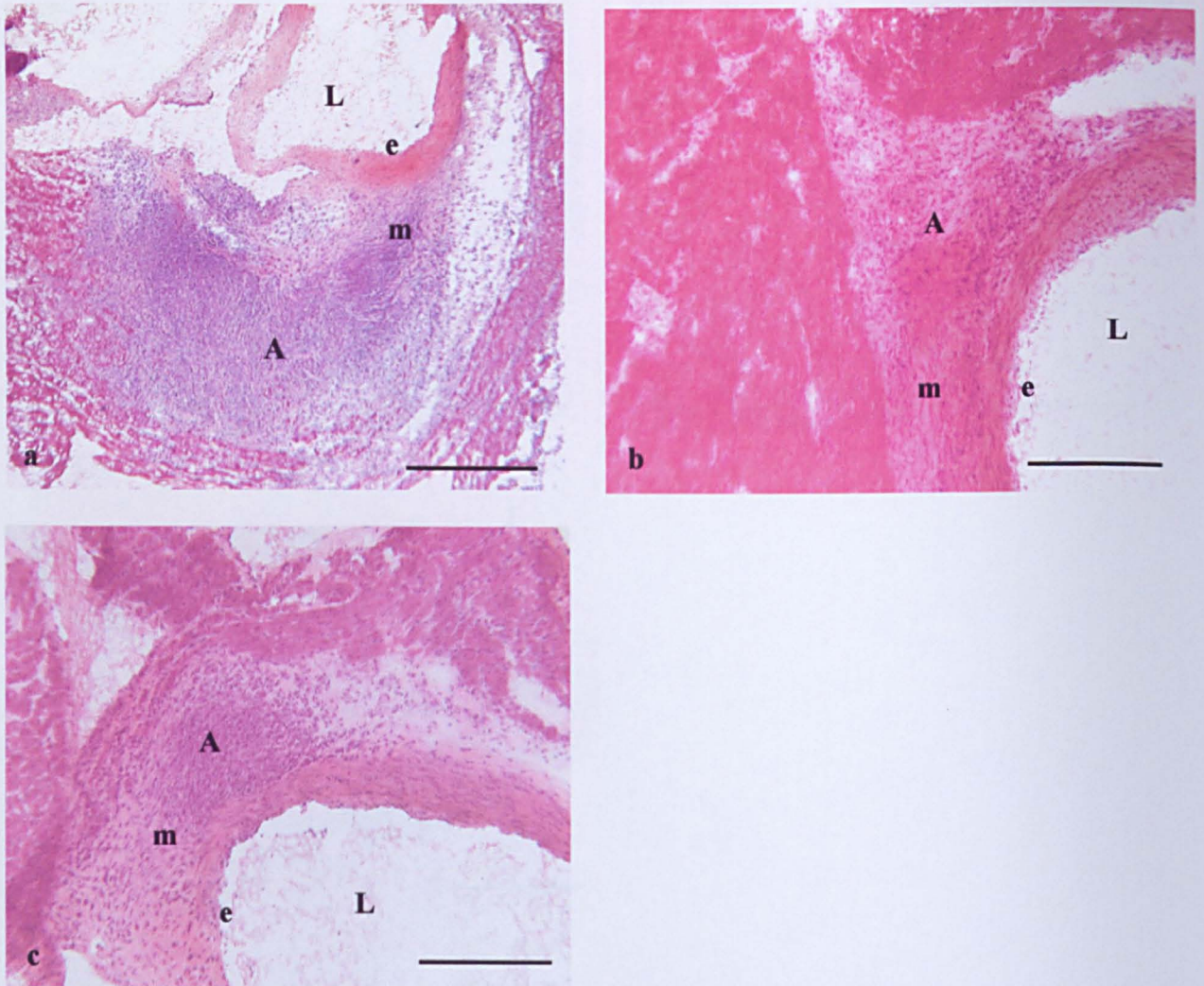


Figure 11: Haematoxylin and eosin stains of frozen aortic root sections from *Illrn*^{-/-} mice show clear demarcation of the lesional area (A) from surrounding tissue. L = vessel lumen, e = endothelium, m = media. Sections are from the aortic root lesions of *Illrn*^{-/-} mice aged a) 155 days (female), b) 125 days (male) and c) 203 days (male). Scale bar = 200 μ m.

Figure 12: Arteritic lesions close to valves

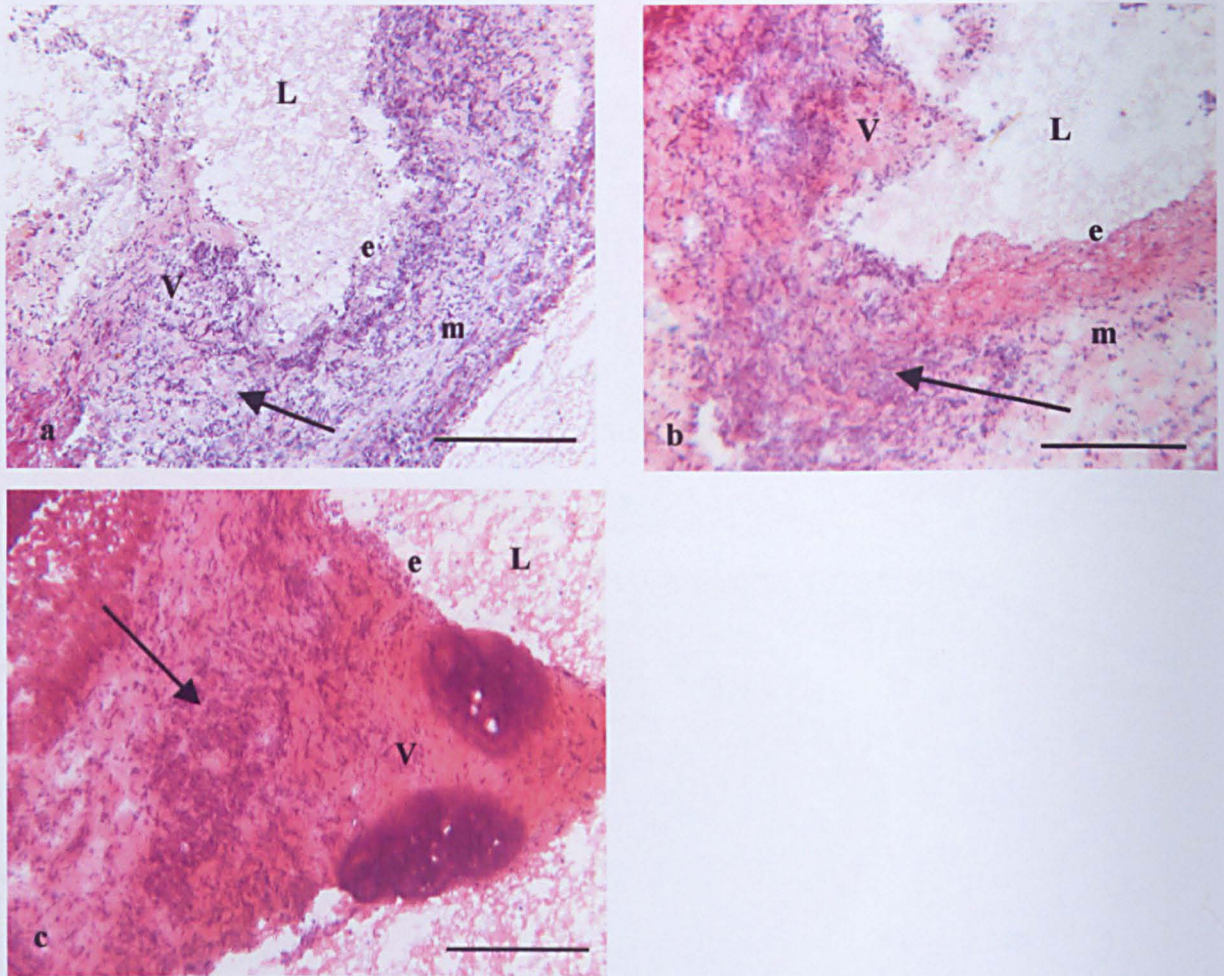


Figure 12: Haematoxylin and eosin stained aortic root lesions, from 3 *Il1rn*^{-/-} mice, demonstrating their frequent appearance around valves (V). L = vessel lumen, e = endothelium, m = media, arrows = inflammatory infiltrate. The examples shown are aortic root sections from *Il1rn*^{-/-} mice aged a) 221 days (female), b) 174 days (male) and c) 179 days (female). Scale bars = 200 μ m.

Figure 13: Formalin fixed, paraffin embedded aortic root sections

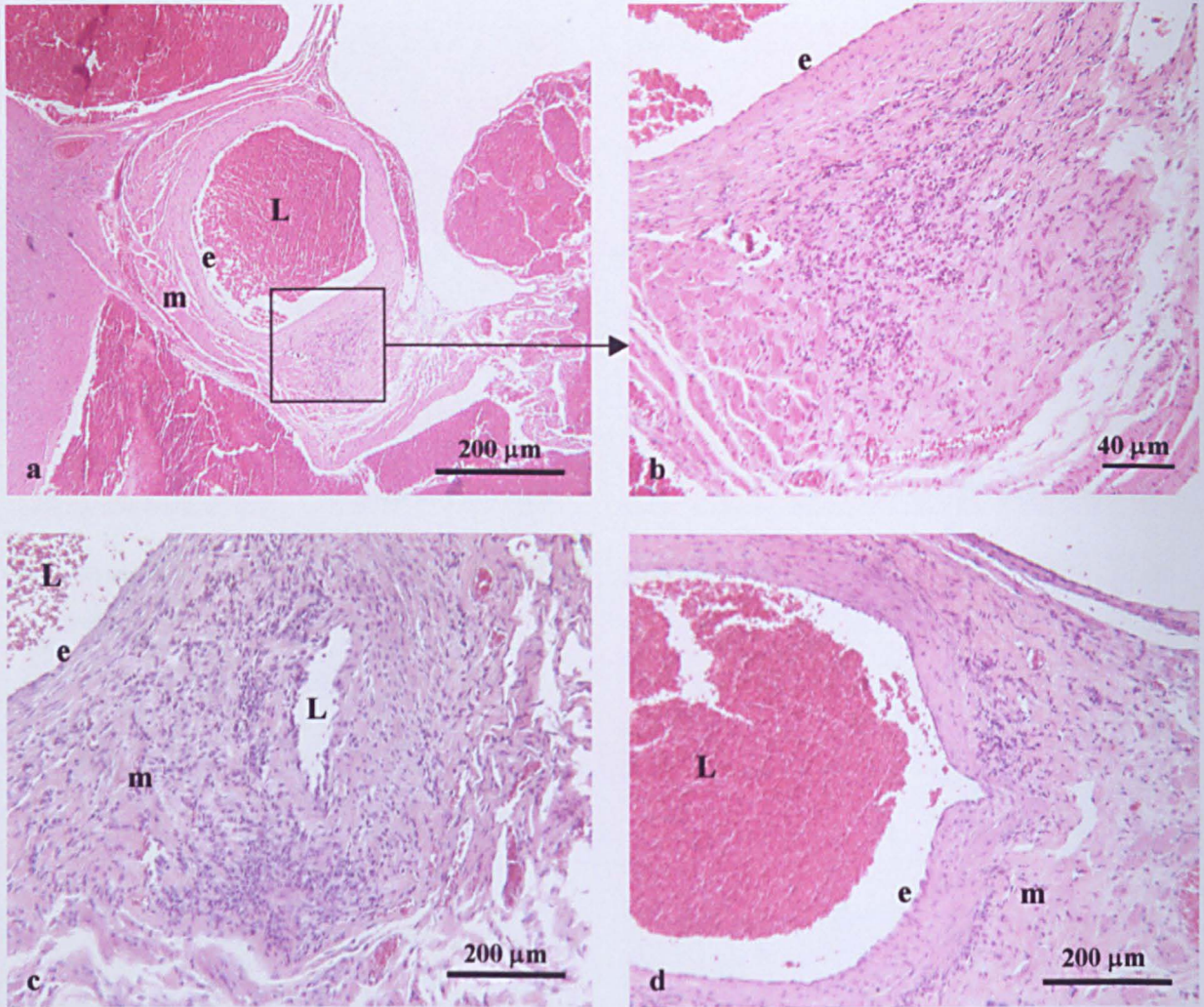


Figure 13: Haematoxylin and eosin staining of paraffin embedded sections of aortic root from *Illrn*^{-/-} animals showing inflammatory infiltrates around the large vessels. L = vessel lumen, e= endothelium, m = media. a) aortic root section from a 199 day old male *Illrn*^{-/-} mouse. b) higher power magnification of boxed area in a. c) aortic root section from a 174 day old female *Illrn*^{-/-} mouse. d) aortic root section from a 172 day old male *Illrn*^{-/-} mouse.

Figure 14: Examples of cellular infiltrate scores on haematoxylin and eosin stained frozen aortic root tissue

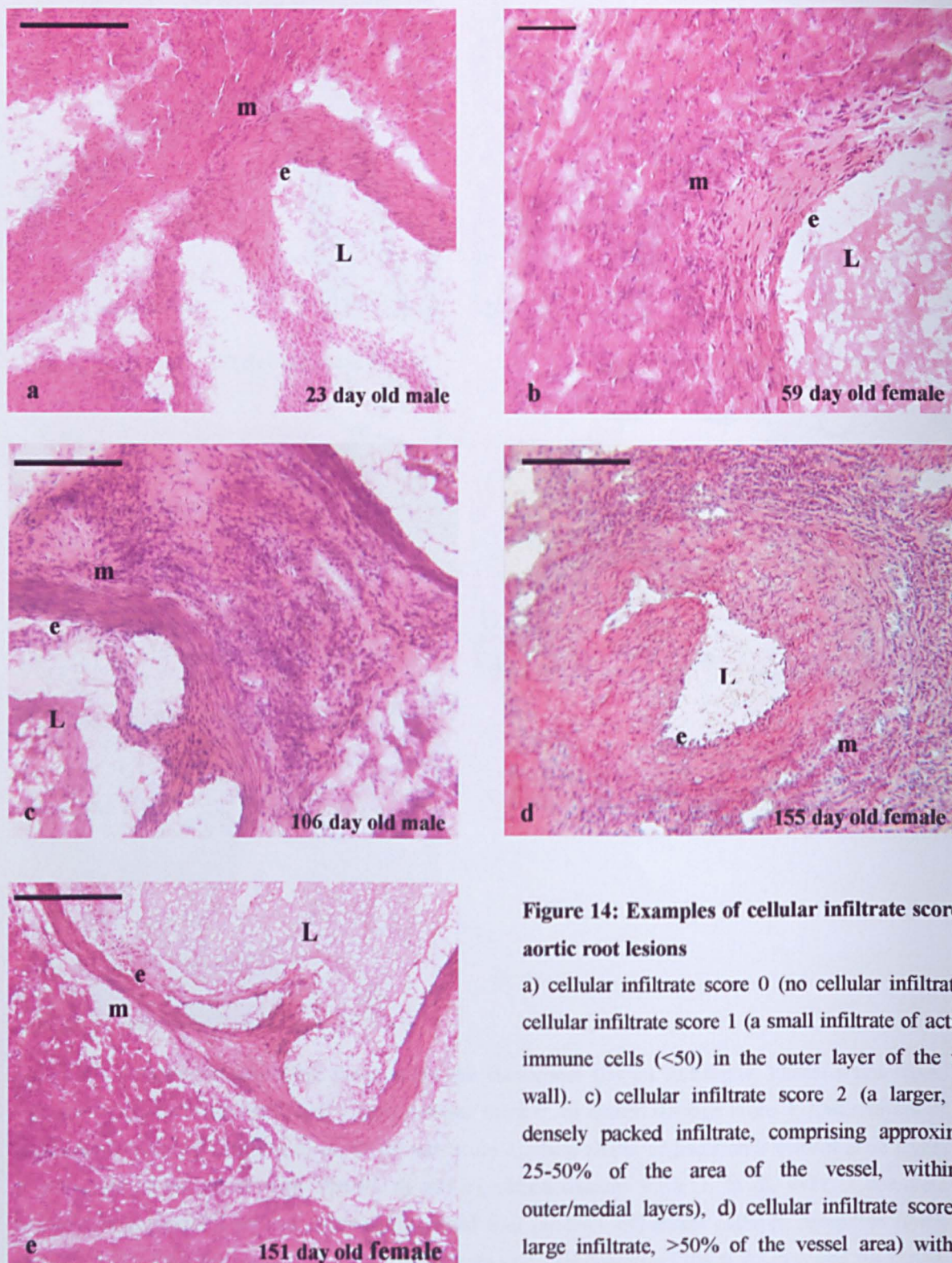


Figure 14: Examples of cellular infiltrate scores for aortic root lesions

a) cellular infiltrate score 0 (no cellular infiltrate). b) cellular infiltrate score 1 (a small infiltrate of activated immune cells (<50) in the outer layer of the vessel wall). c) cellular infiltrate score 2 (a larger, more densely packed infiltrate, comprising approximately 25-50% of the area of the vessel, within the outer/medial layers), d) cellular infiltrate score 3 (a large infiltrate, >50% of the vessel area) with cells infiltrating all layers of the vessel wall). e) *Il1rn*^{+/+} aortic root, score 0. All haematoxylin and eosin stained. Scale bar = 200 μ m except in b = 40 μ m. L = vessel lumen, e = endothelium, m = media.

Figure 15: Examples of scores of elastin damage

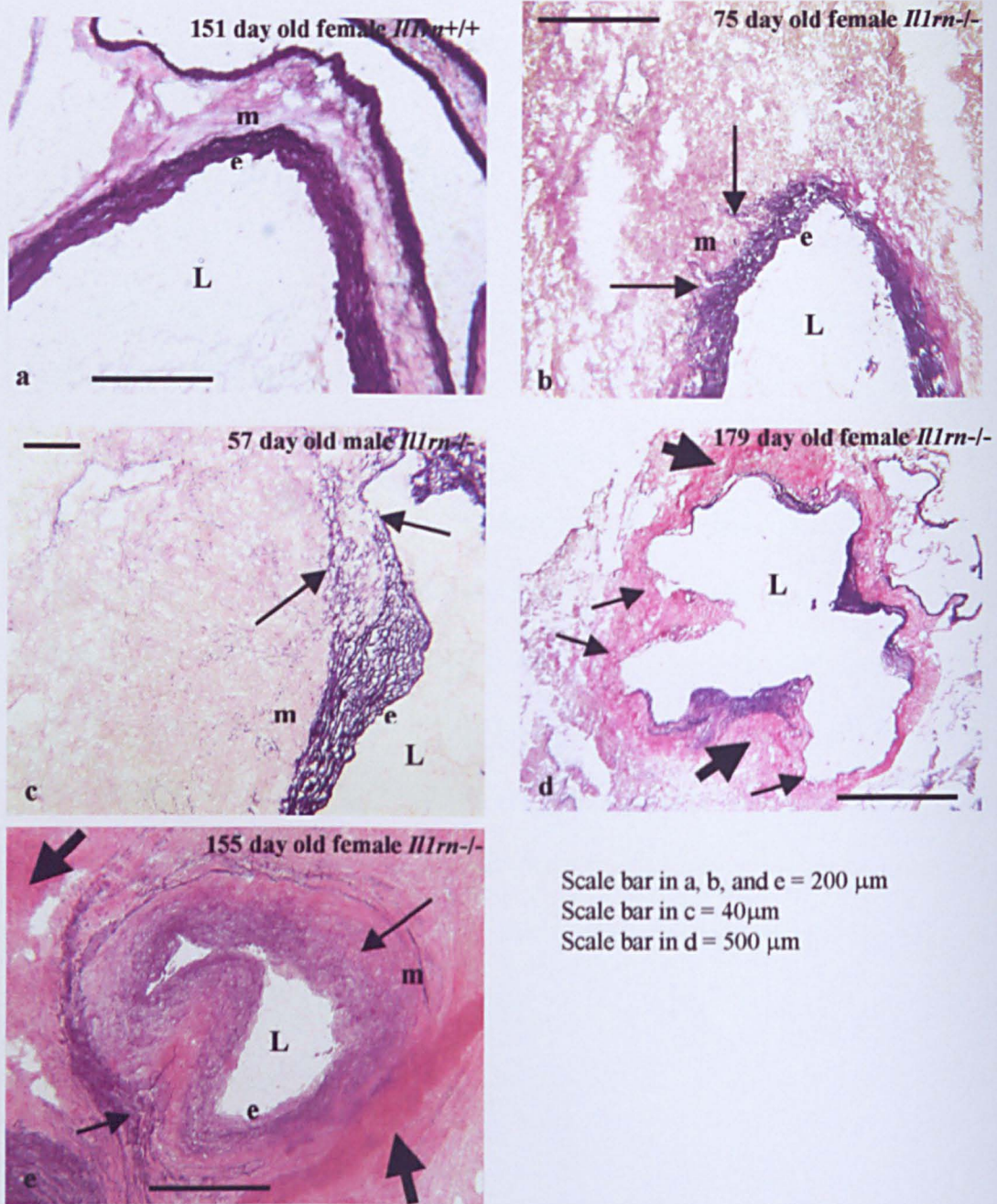


Figure 15: staining of connective tissue using the elastic/van Gieson technique. Elastin stains black, collagen red and muscle yellow. a) elastin damage score 0. b) elastin damage score 1. Outer layers of elastin are fragmented (arrows). c) elastin damage score 2, where elastin degradation is evident in all layers at one point of the vessel wall (arrow). d) and e), elastin damage score 3. In d), there is complete degradation of elastin at several points of the vessel wall (arrows) and excess collagen deposition (thick arrows). In e), there is evidence of repair with excess collagen deposition (thick arrows) and thickened, disorganised elastin layers (arrows). L = vessel lumen, e = endothelium, m = media.

Figure 16: Myocardial scar in *Il1rn*^{-/-} mouse

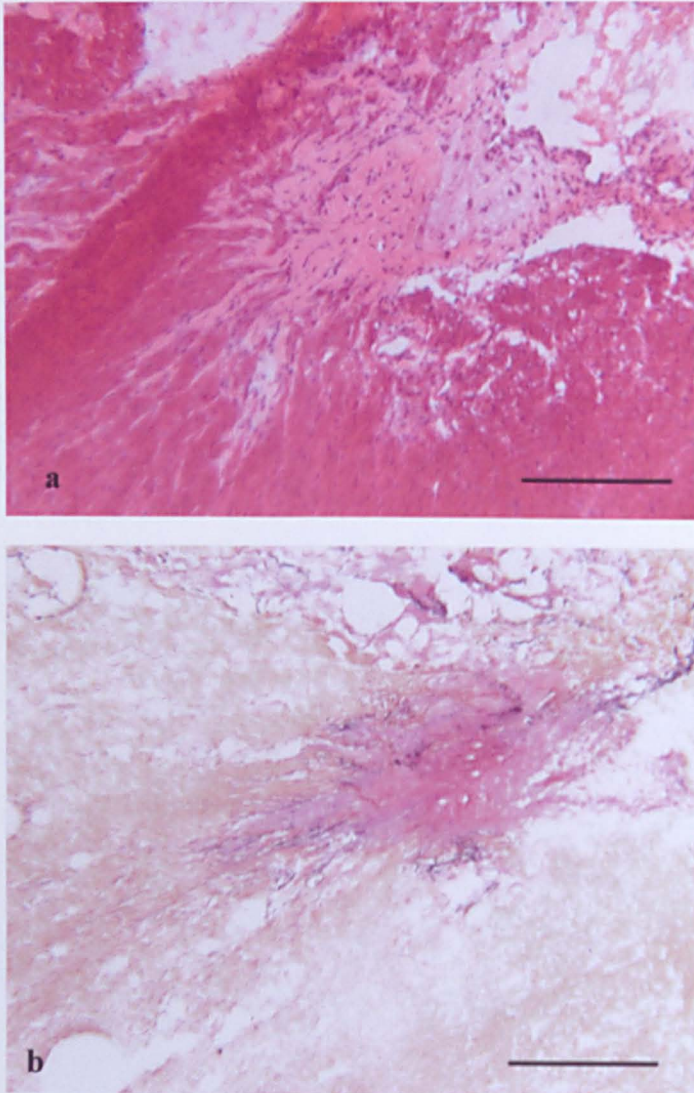


Figure 16: Myocardial scar in a 165 day old female *Il1rn*^{-/-} mouse, indicating a previous non-lethal inflammatory event. a) haematoxylin and eosin stain, b) connective tissue stain. Scale bar = 200 μ m.

denotes a large infiltrate (>50% of the vessel area) with cells infiltrating all layers of the vessel wall (Figure 14).

Il1rn^{+/-} mice appeared to be mildly affected by arteritis, with 3/4 of the animals from which frozen sections were taken scored scoring 1 for cellular infiltrate.

In *Il1rn*^{+/+} mice, no inflammatory infiltrates were observed, in any animals. All results were in keeping with previous observations [Nicklin *et al.*, 2000].

Connective tissue

Frozen sections were also stained for connective tissue in order to examine damage to the elastin layers of the vessel walls, and to detect signs of repair to damaged connective tissue.

Connective tissue staining showed that the elastic layers of the outer elastic laminae and internal elastic laminae were often partially fragmented or completely destroyed in affected animals (Figure 15), whilst in some lesions from older animals there was evidence of repair to the damaged elastin with excess collagen deposition and fibrosis, as well as thickened and disorganised elastin layers (Figure 15), suggesting that repair of the vessel walls follows degradation caused by the inflammatory infiltrate. Destruction of the elastic layers is presumably due to the production of MMPs and other proteases from cells (such as macrophages or neutrophils) within the infiltrate. In some cases there was also evidence of myocardial scarring, indicating a previous non-lethal inflammatory event (Figure 16). These results confirm earlier published results [Nicklin *et al.*, 2000].

Figure 17: Large inflammatory infiltrates with relatively little elastin damage

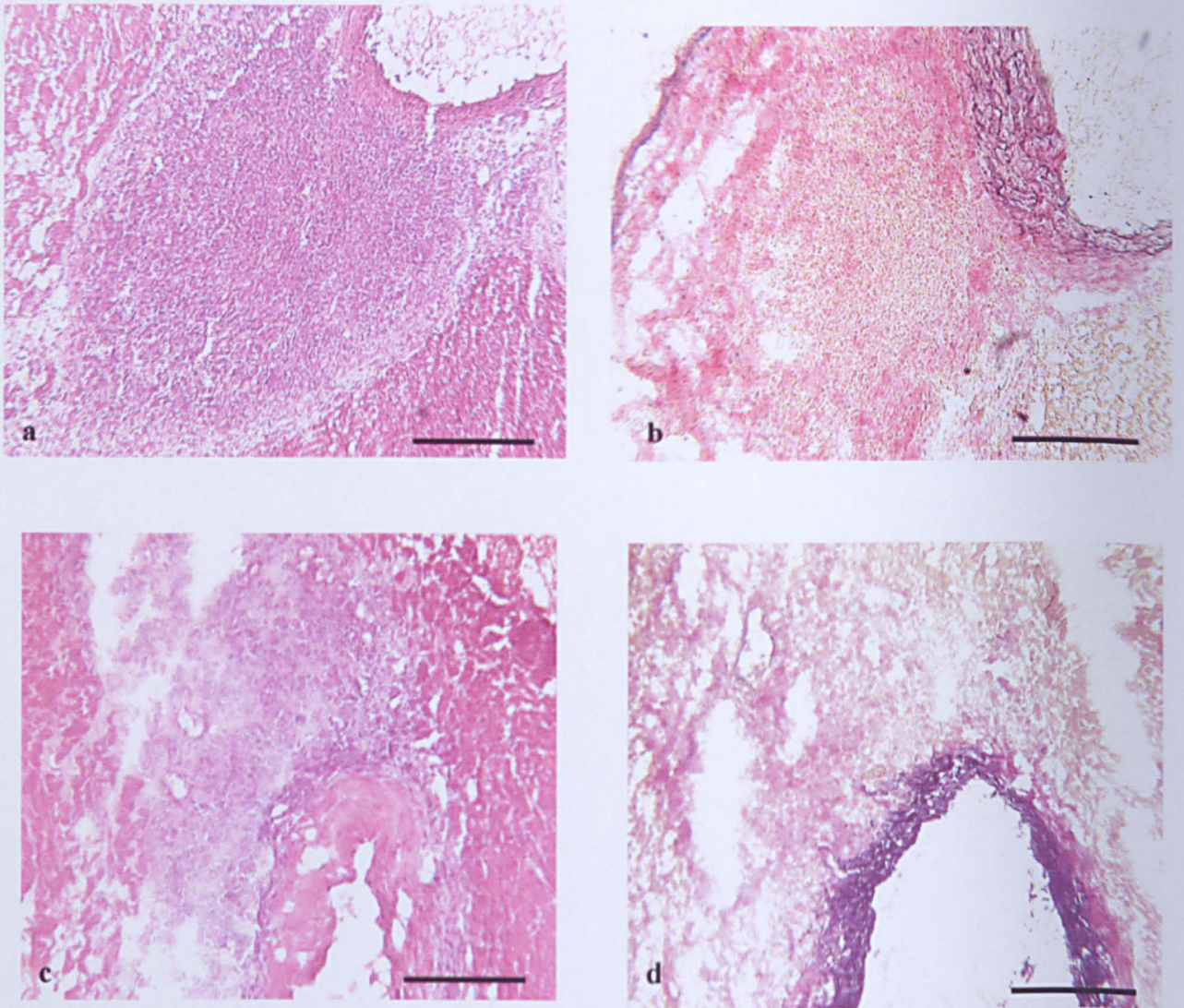


Figure 17: a) & c) haematoxylin and eosin stained aortic root lesions. b) & d), the same aortic root lesions stained for connective tissue. From cases such as this, it appears that inflammatory infiltrates precede elastin damage. a and b) aortic root lesion sections from a 131 day old male *Il1rn^{-/-}* mouse. c and d) aortic root lesion sections from a 75 day old female *Il1rn^{-/-}* mouse. Scale bar = 200 μm .

Figure 18: Specificity of lesion development for large muscular arteries

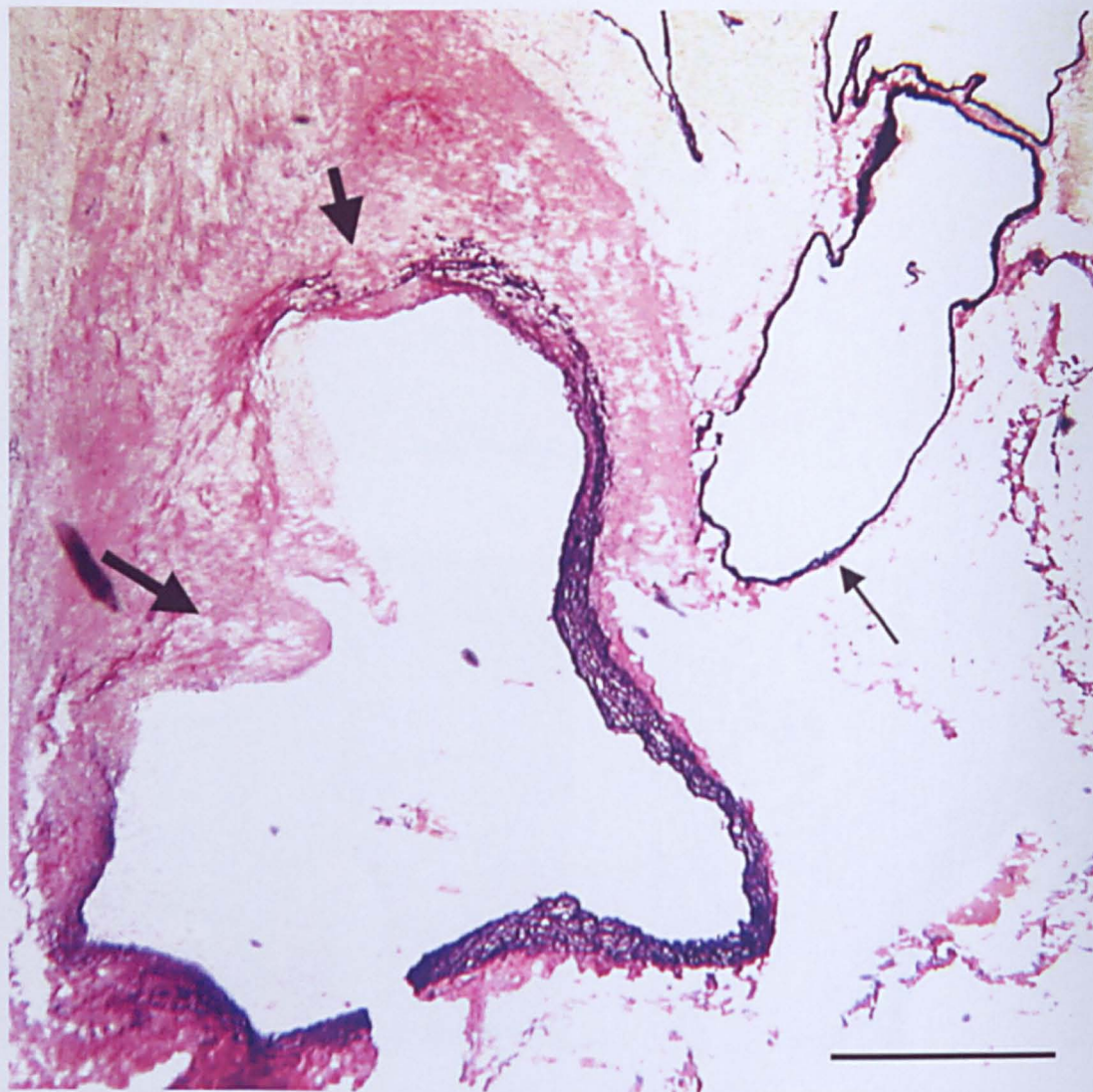


Figure 18: Connective tissue staining shows the predilection for lesion development at the large muscular arteries. Note complete degradation of the elastin layers at several points of the large artery (thick arrows) as well as excess collagen deposition (red staining). Compare to a neighbouring vein (thin arrow) which remains unaffected. The example shown is a section of an aortic root lesion from a 155 day old female *Illrn*^{-/-} mouse. Scale bar = 500 μm .

Figure 19: Lack of cellular infiltrate or elastin damage in *Il1rn*^{+/+} aortic roots

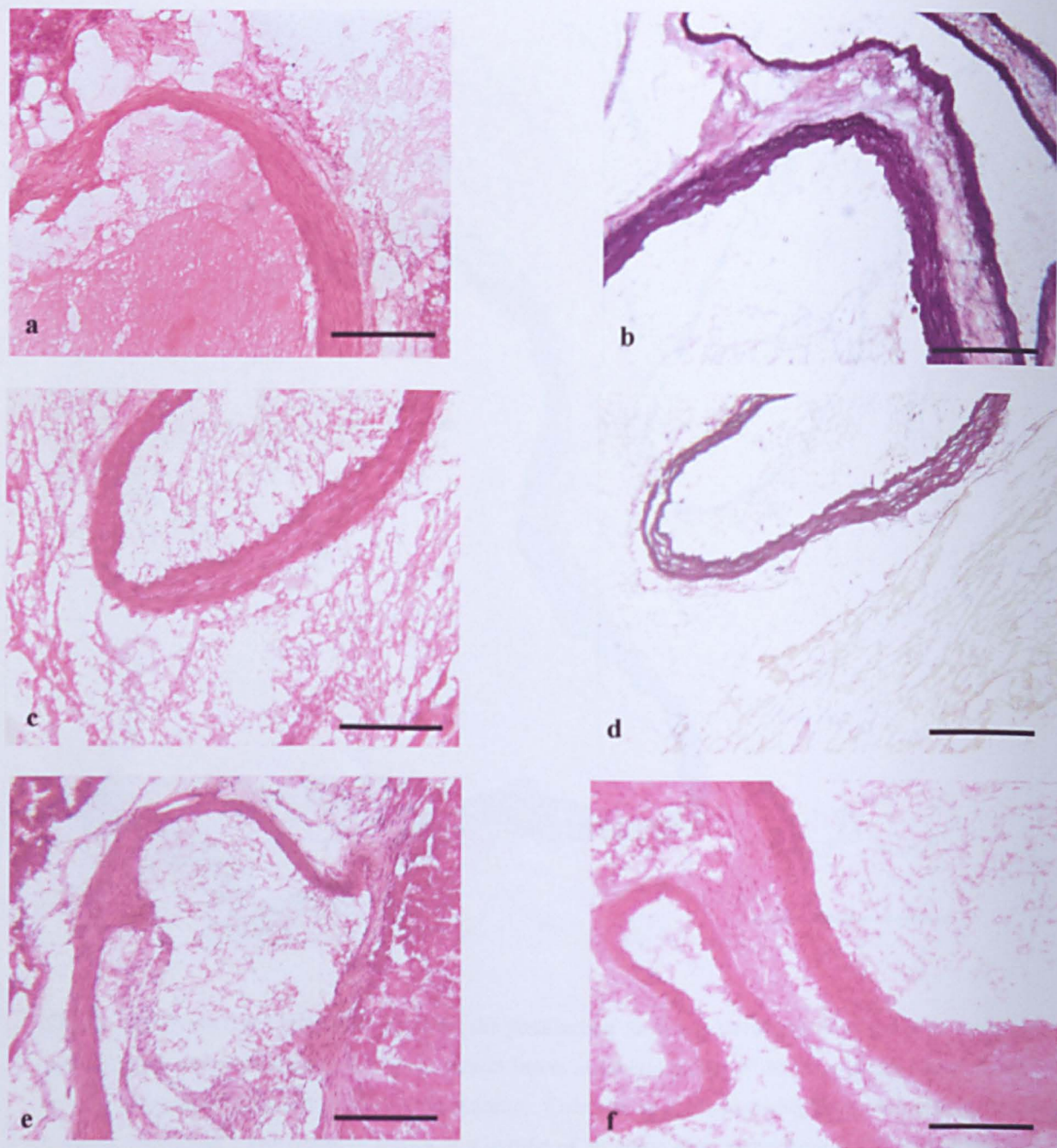


Figure 19: Aortic roots from *Il1rn*^{+/+} mice show no cellular infiltrates or elastin damage. a) and b) haematoxylin and eosin and connective tissue staining of the aortic root from a 151 day old female *Il1rn*^{+/+} mouse. c) and d) haematoxylin and eosin and connective tissue staining of the aortic root from a 108 day old male *Il1rn*^{+/+} mouse. e) and f) haematoxylin and eosin stained aortic root from a second, female, 108 day old *Il1rn*^{+/+} mouse. In all note the lack of cellular infiltrates and the undamaged elastin layers, which remain clearly organised and unfragmented. Also note lack of excess collagen deposition. Scale bar = 200 μm .

In support of the hypothesis that the infiltrate arises from the adventitial layer, in some lesions it was possible, in some cases, to observe a large infiltrate within the outer layers of the vessel wall, but no degradation of the internal elastic laminae, and a lack of inflammatory cells at the luminal surface of the aorta (Figure 17).

Neighbouring veins and arterioles were unaffected by the inflammation, demonstrating the specificity of the inflammatory disease for the large muscular arteries (Figure 18).

All *Il1rn*^{+/+} mice examined had undamaged vessel walls. In all cases the elastin layers were clearly defined and organised in concentric layers, with no evidence of fragmentation. There was also no evidence of excess collagen deposition in any *Il1rn*^{+/+} animal (Figure 19).

Scores for elastin damage were also given on these sections as follows: 0 denotes no damage to elastin, a score of 1 denotes fragmentation of the outer layers, 2 denotes complete degradation at one point of the vessel wall, and 3 denotes complete degradation at >1 point of the vessel wall and/or evidence of repair (Figure 15).

All scores (for cellular infiltrate and elastin degradation) were performed blind to the animals' genotype or age. The scores, and subsequent immunohistochemical analysis, all refer to the most affected area of the vessel seen.

Table 3: Animals used in arteritis study

Mouse I.D number	Back-ground	<i>Illrn</i> genotype	Age at death (days)	Sex	Cellular infiltrate at site of section	Elastin degradation at site of section	Used in time course study
134-08	Sf3	-/-	23	M	0	0	*
137-03	Sf3	-/-	24	M	1	0	*
138-03	Sf3	-/-	24	F	0	n/d	*
150-01	Sf3	-/-	56	M	1	0	*
150-05	Sf3	-/-	56	M	1	n/d	*
154-04	Sf3	-/-	59	F	1	2	*
154-08	Sf3	-/-	59	F	1	n/d	*
144-04	Sf3	-/-	75	F	2	1	*
144-05	Sf3	-/-	75	F	1	1	*
151-01	Sf3	-/-	81	M	0	0	*
151-02	Sf3	-/-	81	M	3	3	*
133-02	Sf3	-/-	105	M	3	3	*
133-08	Sf3	-/-	105	F	0	n/d	*
149-01	Sf3	-/-	106	M	2	n/d	*
149-03	Sf3	-/-	106	M	0	1	*
115-01	Sf3	-/-	125	M	3	3	*
115-02	Sf3	-/-	125	M	3	1	*
104-02	Sf3	-/-	128	F	3	3	*
123-03	Sf3	-/-	131	M	3	3	*
123-05	Sf3	-/-	131	M	3	n/d	*
140-01	Sf3	-/-	154	M	3	2	*
140-02	Sf3	-/-	154	M	0	n/d	*
154-02	Sf3	-/-	163	M	3	n/d	*
110-04	Sf3	-/-	179	F	3	3	*
110-05	Sf3	-/-	179	F	2	n/d	*
134-06	Sf3	-/-	203	M	2	n/d	*
104-05	Sf3	-/-	221	F	3	3	*
104-07	Sf3	-/-	221	F	3	3	*
134-10	Sf3	+/-	23	F	0	n/d	*
150-06	Sf3	+/-	56	M	1	n/d	*
149-04	Sf3	+/-	106	F	1	n/d	*
115-03	Sf3	+/-	125	M	1	n/d	*
137-01	Sf3	+/+	24	M	0	0	*
137-02	Sf3	+/+	24	M	0	0	*
148-03	Sf3	+/+	108	M	0	0	*
148-06	Sf3	+/+	108	F	0	0	*
145-02	Sf3	+/+	151	M	0	0	*
145-03	Sf3	+/+	151	F	0	1	*
153-06	Sf3	+/+	193	F	0	n/d	*
151-09	Sf3	+/+	220	F	0	n/d	*
108-02	Sf2	-/-	57	M	3	1	*
98-05	Sf2	-/-	155	F	3	3	*
98-06	Sf2	-/-	155	F	3	3	*
98-07	Sf2	-/-	155	F	3	3	*

Mouse I.D number	Back-ground	<i>Illrn</i> genotype	Age at death (days)	Sex	Cellular infiltrate at site of section	Elastin degradation at site of section	Used in time course study
108-03	Sf2	-/-	165	F	3	3	
106-01	Sf2	-/-	174	M	3	2	
106-03	Sf2	-/-	174	M	3	n/d	
108-04	Sf2	+/+	165	F	0	n/d	
106-02	Sf2	+/+	174	M	0	0	
B8IC-01	Balb/c	-/-	115	M	2	n/d	
B8IC-02	Balb/c	-/-	115	M	2	n/d	
B8IC-04	Balb/c	-/-	115	M	1	n/d	
B6I3-04	Balb/c	-/-	132	F	0	n/d	
B8IA-02	Balb/c	-/-	155	M	3	3	
B6I1-04	Balb/c	-/-	172	M	2	n/d	
B6I0-06	Balb/c	-/-	174	M	0	n/d	
B6I0-07	Balb/c	-/-	174	F	3	n/d	
B5I5-03	Balb/c	-/-	199	M	0	0	
B5I5-11	Balb/c	-/-	199	F	0	0	
B8I9-01	Balb/c	-/-	216	M	3	3	
B8I9-07	Balb/c	-/-	216	F	3	3	
B8I9-08	Balb/c	-/-	216	F	2	n/d	
B8IB-07	Balb/c	+/-	136	F	0	n/d	
B8IA-09	Balb/c	+/-	155	F	1	n/d	
B8IA-10	Balb/c	+/+	155	F	0	n/d	
B8IA-11	Balb/c	+/+	155	F	0	n/d	
B8IA-12	Balb/c	+/+	155	F	0	n/d	
B8I8-02	Balb/c	+/+	171	M	0	n/d	
B8I8-04	Balb/c	+/+	171	M	0	n/d	
B8I9-05	Balb/c	+/+	216	M	0	n/d	

n/d =stain not performed

Composition of the inflammatory infiltrate

Frozen sections were immunohistochemically stained to identify cell types and products present within the cellular infiltrate, in order to attempt to establish the mechanisms by which the lesions arise. Cell types identified included macrophages (by detection of the macrophage specific antigen F4/80), CD4⁺ T-cells, CD8⁺ T-cells, dendritic cells (by identification of the dendritic cell antigen DEC205), B-cells (by detecting CD19), and neutrophils (by identifying the neutrophil antigen 7/4).

To further define the activation status and Th1/Th2 polarity of the CD4⁺ T-cells, IFN γ (Th1), IL-4 (Th2) and IL5 (Th2) were also detected.

Since the hypothesis is that the arterial lesions arise as a direct effect of the unopposed action of IL-1, cell localised IL-1 β was also identified by immunohistochemistry within the infiltrates.

To reveal activated endothelium, possibly as a result of activation by IL-1, the antigens CD31 (PECAM-1, to detect all endothelial cells) and CD62E (E-selectin, to detect activated endothelium) were identified. In some cases, sections were double-stained for CD31/E-selectin.

In addition, the inflammatory markers MCP-1, a chemokine that induces the migration of T-cells into the affected area, and the adhesion molecule ICAM-1 (on leukocytes) were detected.

Paraffin embedded sections were stained with toluidine blue to identify basophils/mast cells, to compare with toluidine blue stained ear skin sections in which there are large numbers of mast cells (see section 3.4.2). In addition, increased numbers of mast cells (and their degranulation) have been reported in vasculitides such as in a mouse model of IL-1 β /TNF- α induced vascular inflammation in the brain [Rhodin *et al.*, 1999], and in various cutaneous inflammatory diseases such as necrotising vasculitis [Soter, 1976] and Behçets' disease [Lichtig *et al.*, 1980].

Figure 20: F4/80⁺ macrophages and CD4⁺ T-cells in a lesion scoring 1 for cellular infiltrate

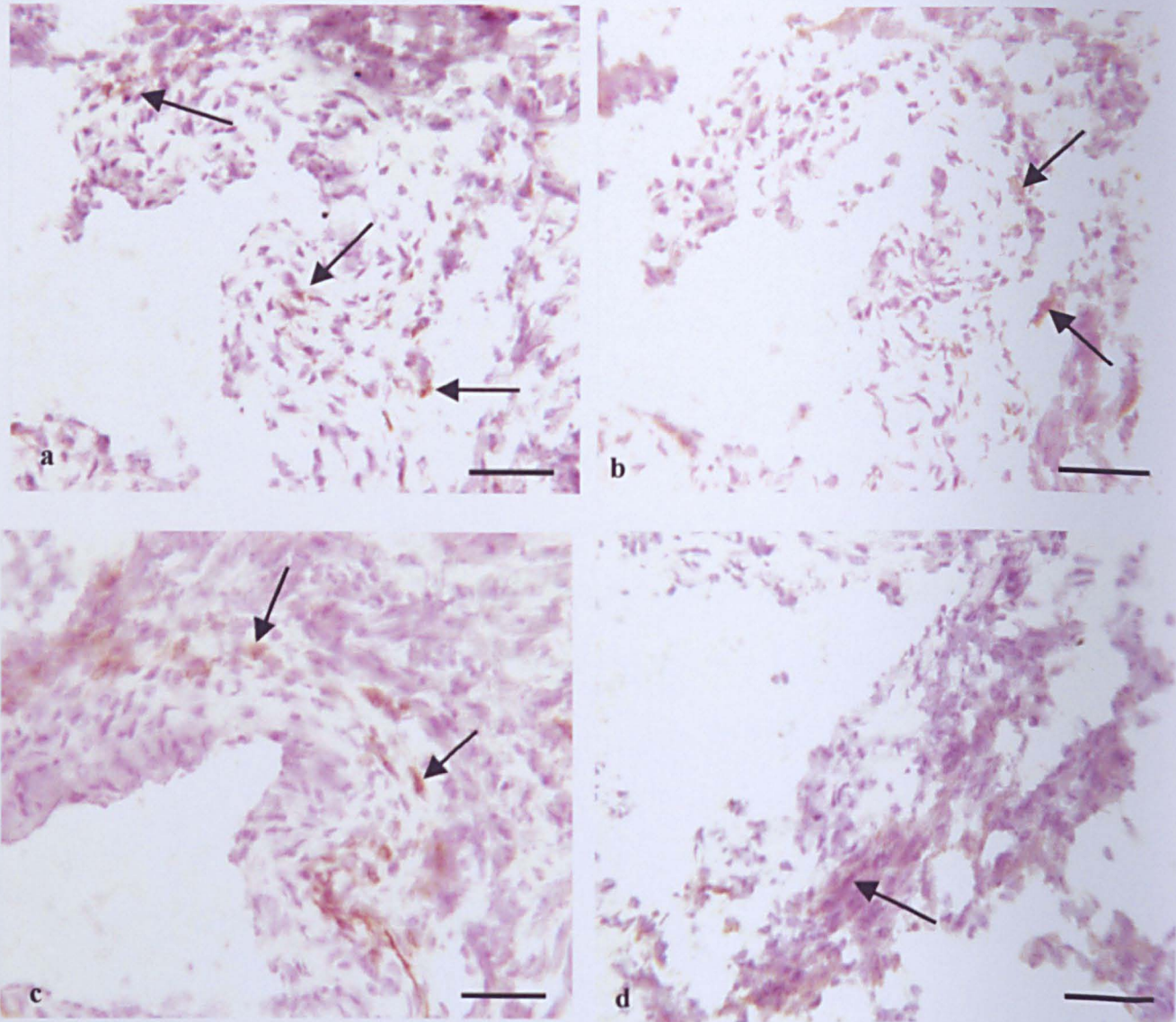


Figure 20: Lesion scoring 1 for cellular infiltrate in the aortic root of a 59 day old *Illrn*^{-/-} mouse. Sections are stained for a) F4/80⁺ cells, b) IL-1β⁺ cells, c) CD4⁺ cells, d) IFNγ⁺ cells. Arrows indicate examples of positively stained cells, which appear brown. There are <50 CD4⁺ or F4/80⁺ cells per section, some of which are activated. Scale bar = 40 μm.

Figure 21: F4/80⁺ macrophages and CD4⁺ T-cells in a lesion scoring 3 for cellular infiltrate

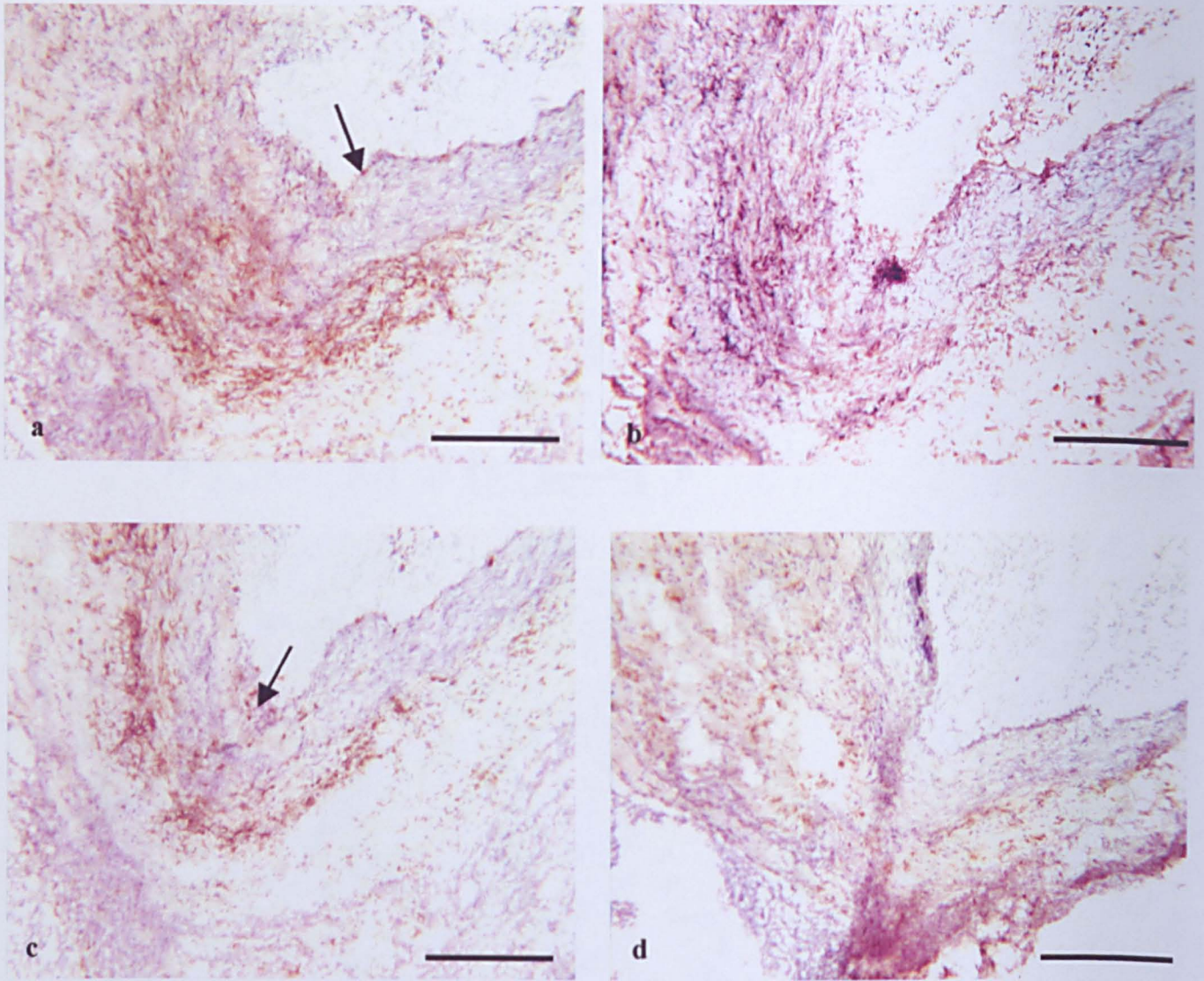


Figure 21: Aortic root from a 174 day old male *Il1rn*^{-/-} mouse scoring 3 for cellular infiltrate. Sections are stained for a) F4/80⁺ macrophages, b) IL-1β⁺ cells, c) CD4⁺ T-cells, and d) IFNγ⁺ cells. In all cases a brown colour indicates a positively stained cell. In aortic roots scoring 3 for cellular infiltrate, the inflammatory cells are visible in all layers of the vessel walls, including the intimal layer (closest to the lumen) and may be present on the luminal surface (examples indicated by arrows). Scale bar = 200 μm.

Figure 22: Activated macrophages in arteritic lesions

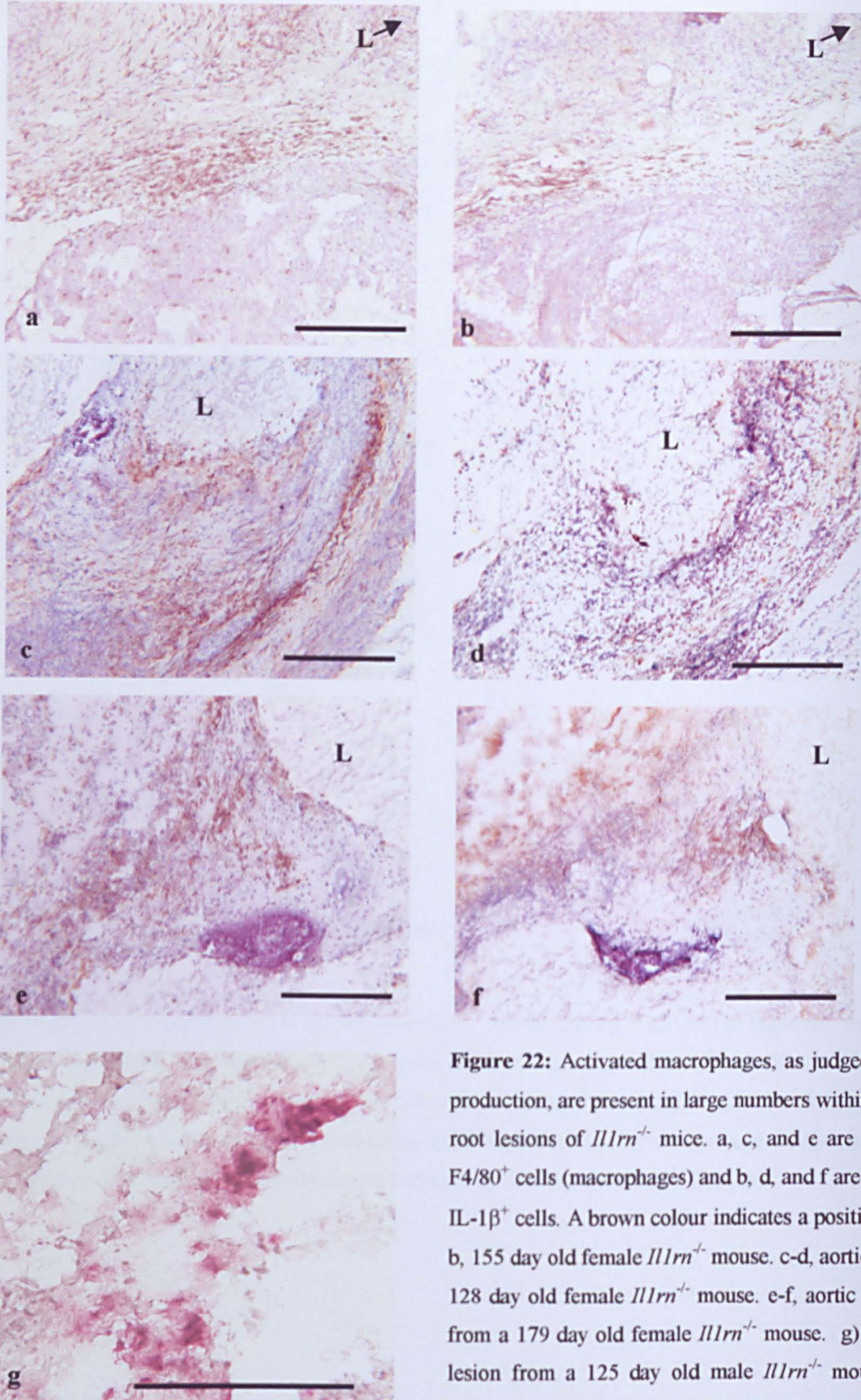


Figure 22: Activated macrophages, as judged by IL-1β production, are present in large numbers within the aortic root lesions of *Illrn*^{-/-} mice. a, c, and e are stained for F4/80⁺ cells (macrophages) and b, d, and f are stained for IL-1β⁺ cells. A brown colour indicates a positive stain. a-b, 155 day old female *Illrn*^{-/-} mouse. c-d, aortic root from 128 day old female *Illrn*^{-/-} mouse. e-f, aortic root lesion from a 179 day old female *Illrn*^{-/-} mouse. g) aortic root lesion from a 125 day old male *Illrn*^{-/-} mouse double stained for F4/80 (red) and IL-1β (black). L = vessel lumen. Scale bar a-f = 200 μm, g = 40 μm.

Figure 23: Activated macrophages and CD4⁺ T-cells tend to co-localise in arteritic lesions

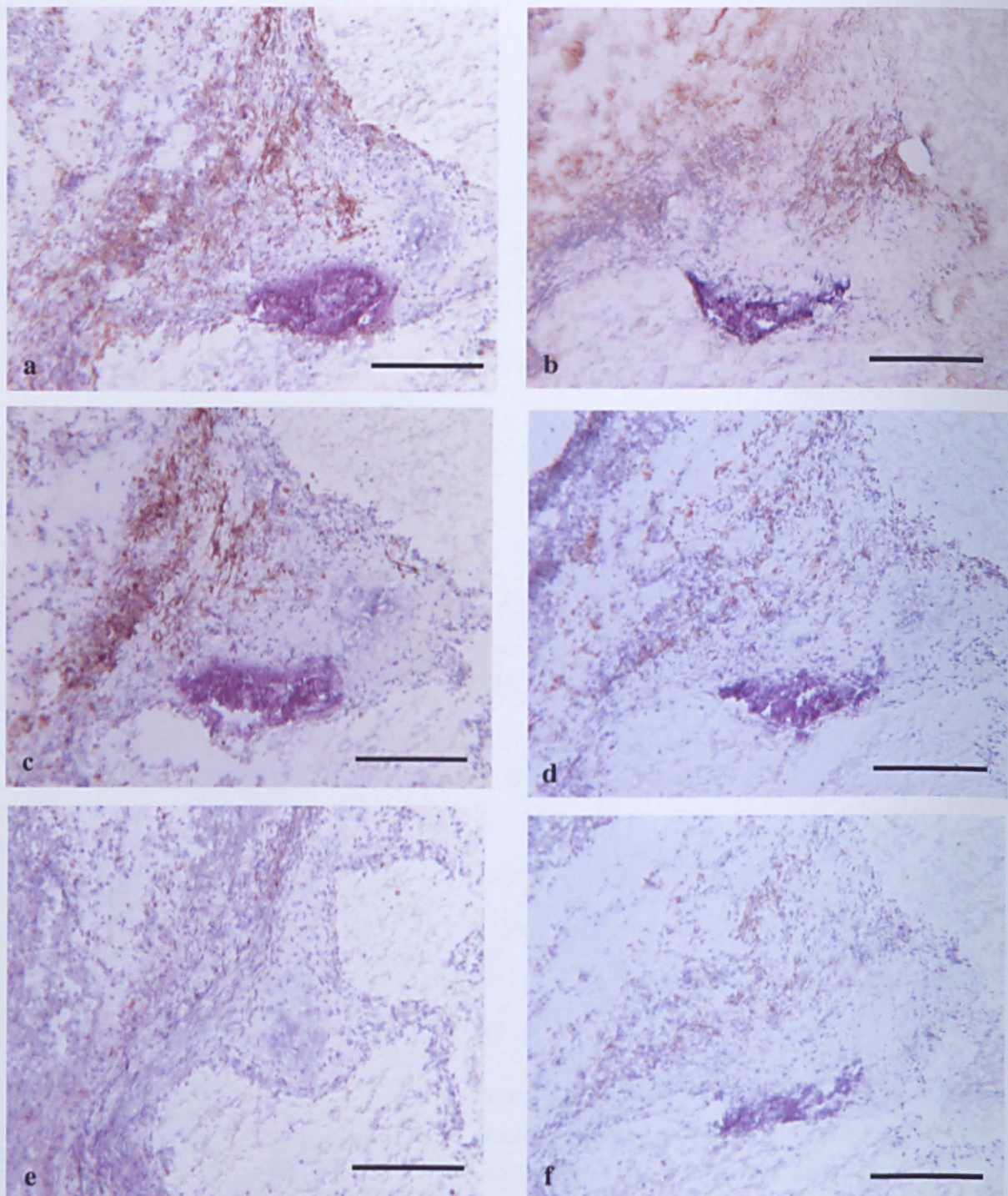


Figure 23: Aortic root from 179 day old female *Il1rn*^{-/-} mouse showing co-localisation of activated macrophages and CD4⁺ T-cells. a) F4/80⁺ cells, b) IL-1β⁺ cells, c) CD4⁺ cells, d) IFNγ⁺ cells. The relatively low number of CD8⁺ cells is shown in e). This animal was one of the three that showed higher IL-4 production (in 10-100 cells), shown in f). In all cases brown colouration indicates positive staining. Scale bar = 200 μm.

Figure 24: Co-localisation of production of IFN γ and IL-1 β in aortic root lesions of *Il1rn*^{-/-} mice

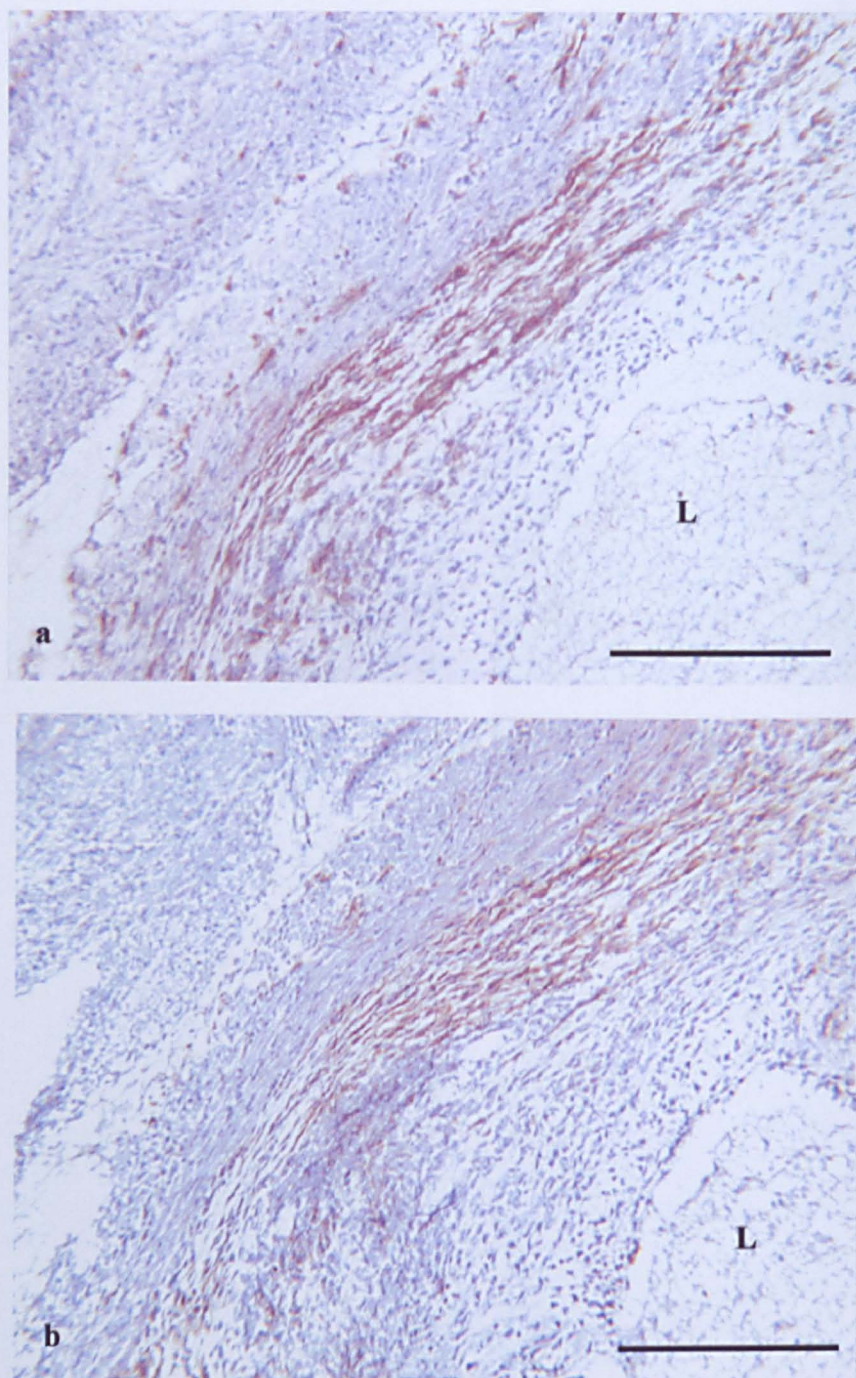


Figure 24: Cells producing IFN γ and IL-1 β tend to co-localise in aortic root lesions of *Il1rn*^{-/-} mice. The examples above are sections from the aortic root lesion of a 128 day old female *Il1rn*^{-/-} mouse. Brown staining indicates a) IFN γ ⁺ cells, and b) IL-1 β ⁺ cells. L = vessel lumen. Scale bar = 200 μ m.

Figure 25: Sparse production of IL-4 or IL-5 in *Il1rn*^{-/-} aortic root lesions

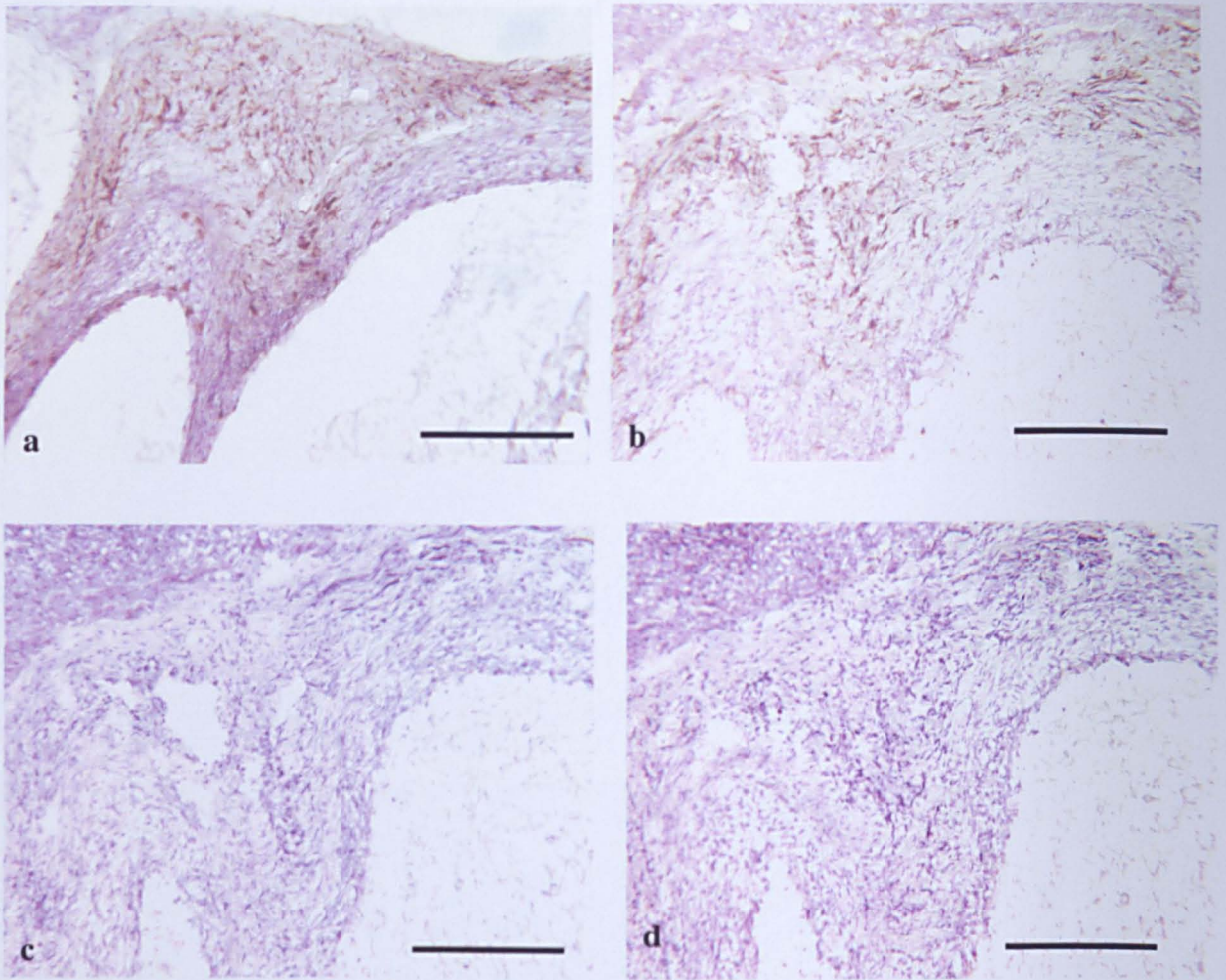


Figure 25: Aortic root lesions in *Il1rn*^{-/-} mice contain very few cells that produce IL-4 or IL-5. a-d are serial sections of an aortic root lesion from a 158 day old male *Il1rn*^{-/-} mouse. Brown staining indicates a) CD4⁺ cells, b) IFN γ ⁺ cells, c) IL-4⁺ cells, and d) IL-5⁺ cells. CD4⁺ T-cells appear to be of the Th1 type rather than Th2, as there is abundant production of IFN γ but little or no IL-4 or IL-5. Scale bar = 200 μ m.

Figure 26: Aortic root lesions with >5 IL-4 –producing cells/section

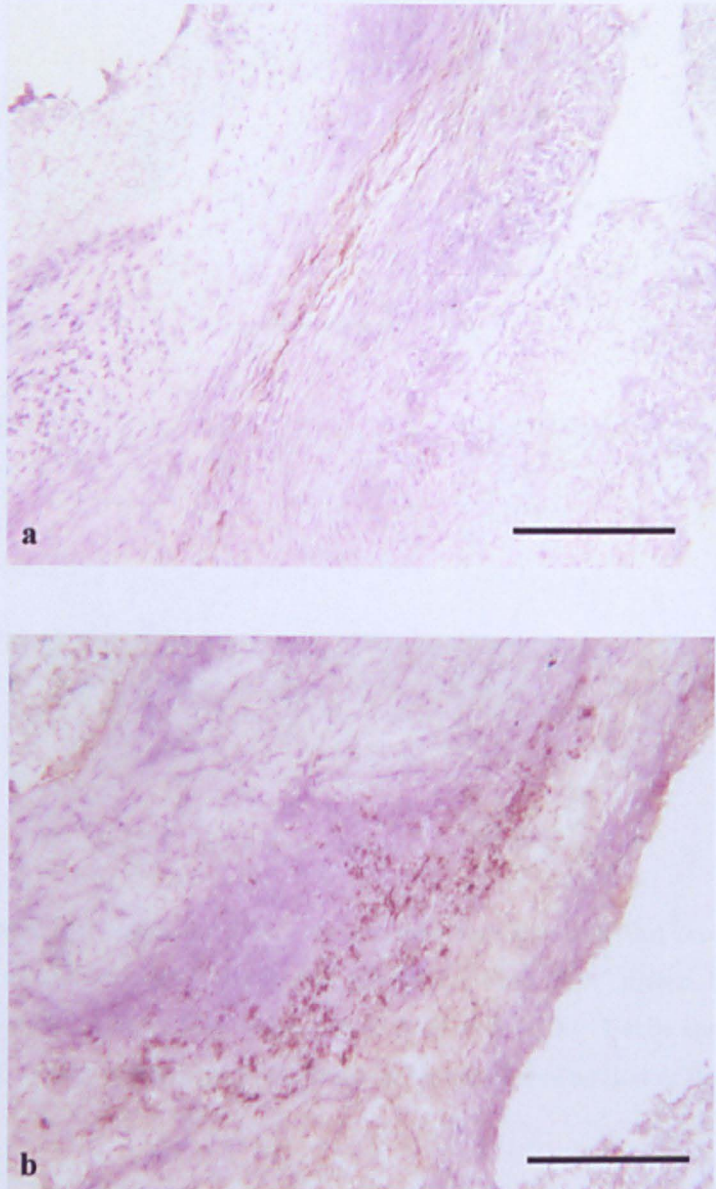


Figure 26: Of all *Il1rn*^{-/-} mice examined, 3 had aortic root lesions in which >5 cells were producing IL-4. a) 128 day old female, b) 221 day old female. The third example is shown in Figure 23 (179 day old female). Scale bar = 200 μ m.

Macrophages

Arterial lesions of score 1 contained <50 cells per section staining positive for F4/80, of which at least some were activated and producing IL-1 β (Figure 20). No other inflammatory cells or markers were seen within these infiltrates, (other than T-cells, see below), which were not dense, and which localised to the outer layers of the vessel wall. Inflammatory lesions of score 2 and above contained large numbers of activated macrophages that contained IL-1 β , although not all of the macrophages present were IL-1 β producers (Figure 21). The macrophages located to the adventitial and medial layers of the vessel walls, and in more advanced lesions (score 3) had also infiltrated through the intimal layers and could be seen on or near the luminal surface (Figure 21). In most cases however, those that contained IL-1 β appeared to localise mainly to the outer layers (Figure 22).

T-cells

Arterial lesions of score 1 contained <50 cells per section staining positive for CD4, of which at least some were activated and producing IFN γ . Within infiltrates scoring 2 or above there were also large numbers of activated CD4⁺ T-cells producing IFN γ , localising in the same areas as the IL-1 β -producing macrophages (Figures 21, 23 and 24). Generally <5 cells per 6 μ m section produced IL-4 or IL-5 (Figure 25), with the exception of lesions in 3 mice in which 10-100 cells stained positively for IL-4 (but no IL-5) (Figure 26). The lesions in which IL-4 production was seen were in the aortic roots of older mice, aged 128, 179 and 221 days. CD8⁺ T-cells, although present within the lesions at the same locations as CD4⁺ T-cells, were far fewer in number (<~10% of the number of CD4⁺ T-cells) (e.g, see Figure 44). Therefore, the vast majority of T-cells present were activated

Figure 27: Neutrophils in aortic root lesions of *Il1rn*^{-/-} mice

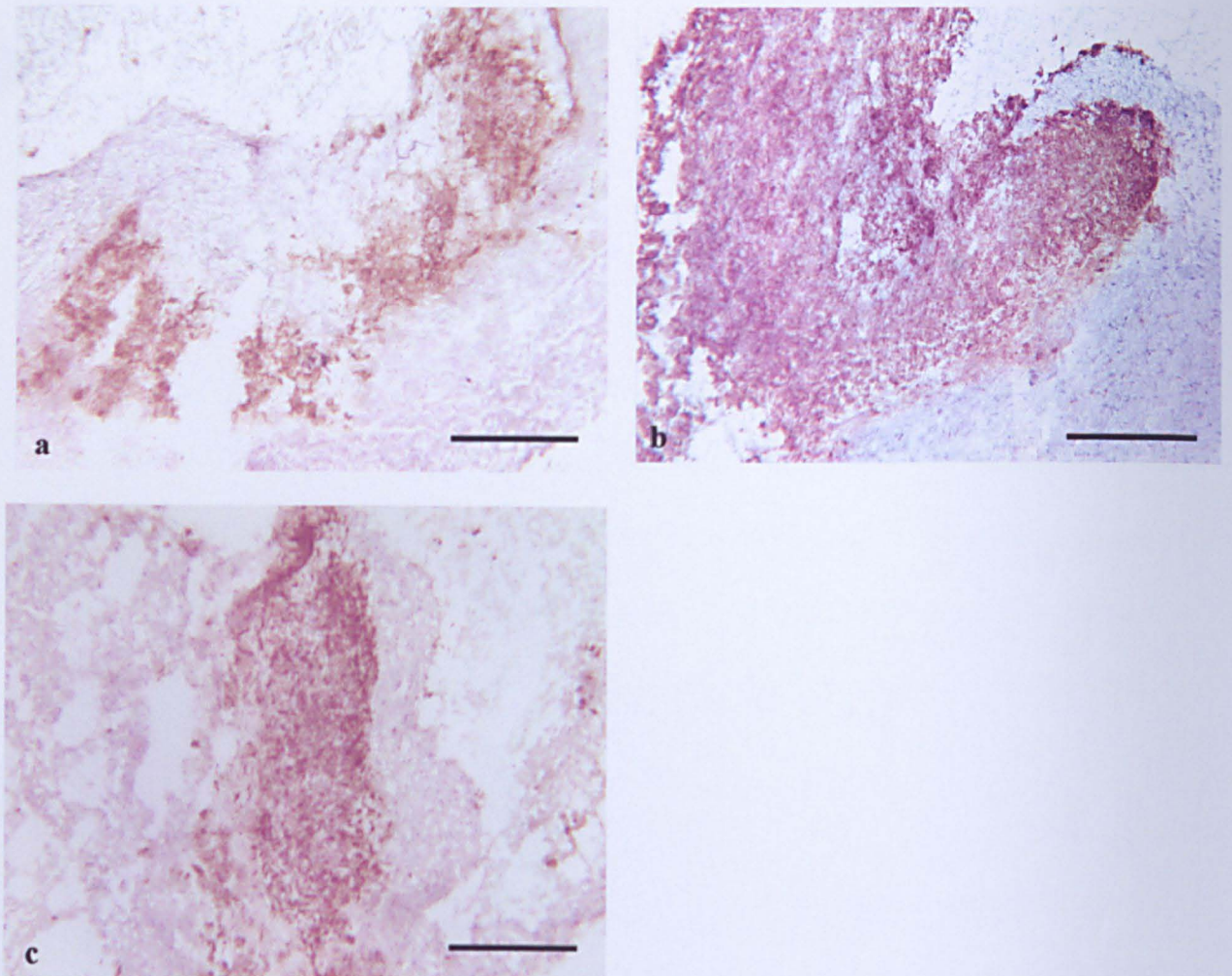


Figure 27: Sections of lesional aortic root from three male *Il1rn*^{-/-} mice aged a) 105 days, b) 131 days and c) 174 days, stained for neutrophils. Brown colouration indicates cells staining positively. Neutrophils are abundant throughout advanced lesions and form an area which is clearly demarcated from non-lesional tissue. Scale bar = 200 μm.

Figure 28: DEC 205⁺ dendritic cells in the arteritic lesions of *Il1rn*^{-/-} mice

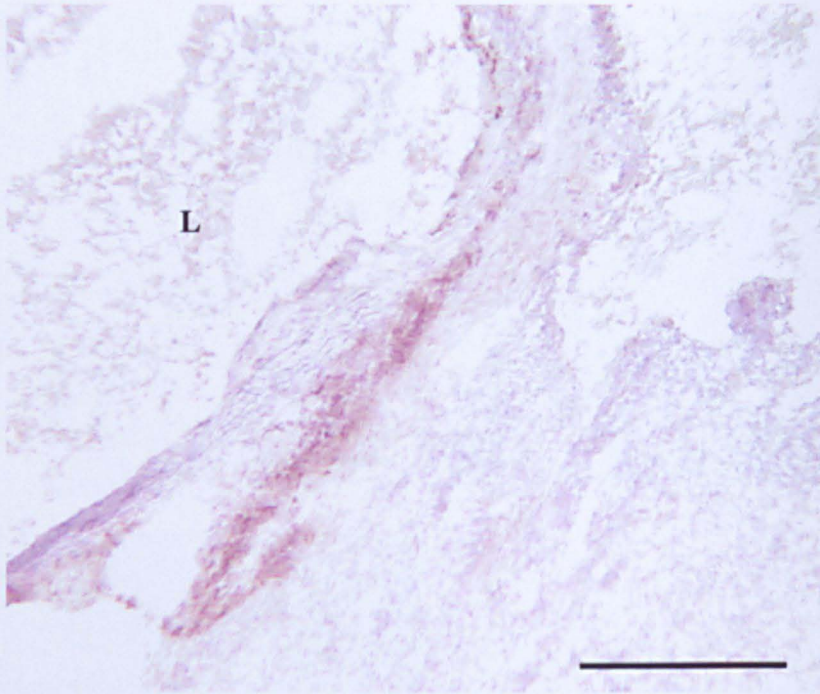


Figure 28: Dendritic cells are abundant in the arteritic lesions of *Il1rn*^{-/-} mice. The example shown is from the lesional aortic root of a 179 day old female *Il1rn*^{-/-} mouse. A brown stain indicates cells that are stained positively for DEC205, a dendritic cell marker which is upregulated on activated DC. L = vessel lumen. Scale bar = 200 μ m.

Figure 29: Toluidine blue staining of paraffin embedded inflamed heart sections

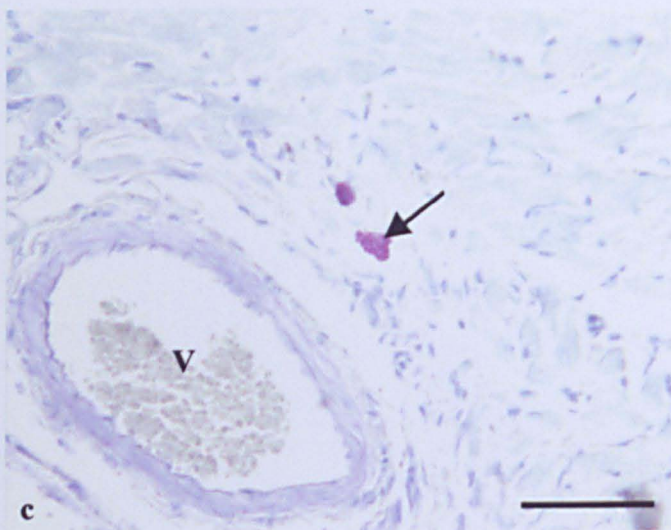
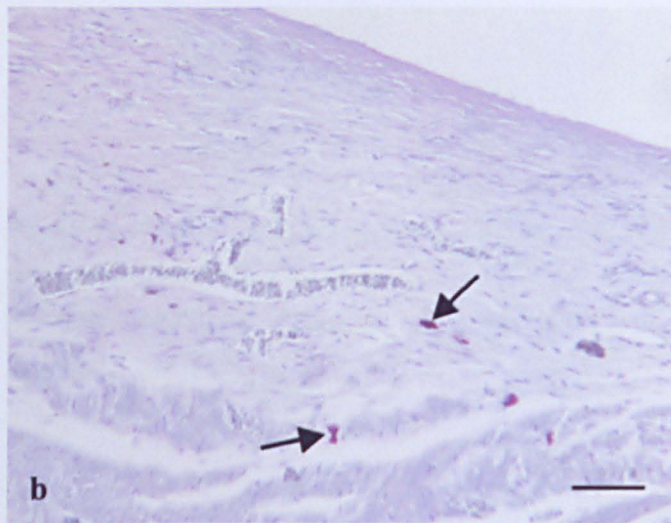
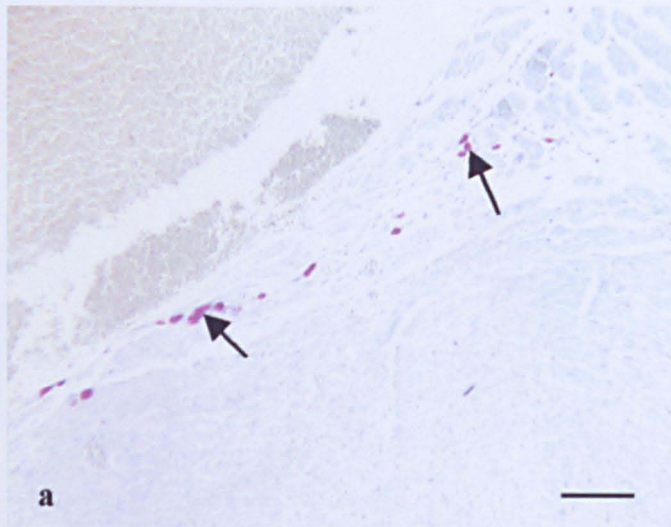


Figure 29: Toluidine blue staining of paraffin embedded sections of inflamed mouse heart reveals the presence of a small number of mast cells (arrows) around the inflamed areas and in the vicinity of adjacent small blood vessels (V). The sections are from the aortic roots of a) a 199 day old male *Illrn*^{-/-} mouse, b) a 172 day old male *Illrn*^{-/-} mouse, and c) a 199 day old female *Illrn*^{-/-} mouse. Scale bars = 40 μ m.

Figure 30: CD19⁺ B-cells are relatively rare in the arteritic lesions of *Il1rn*^{-/-} mice

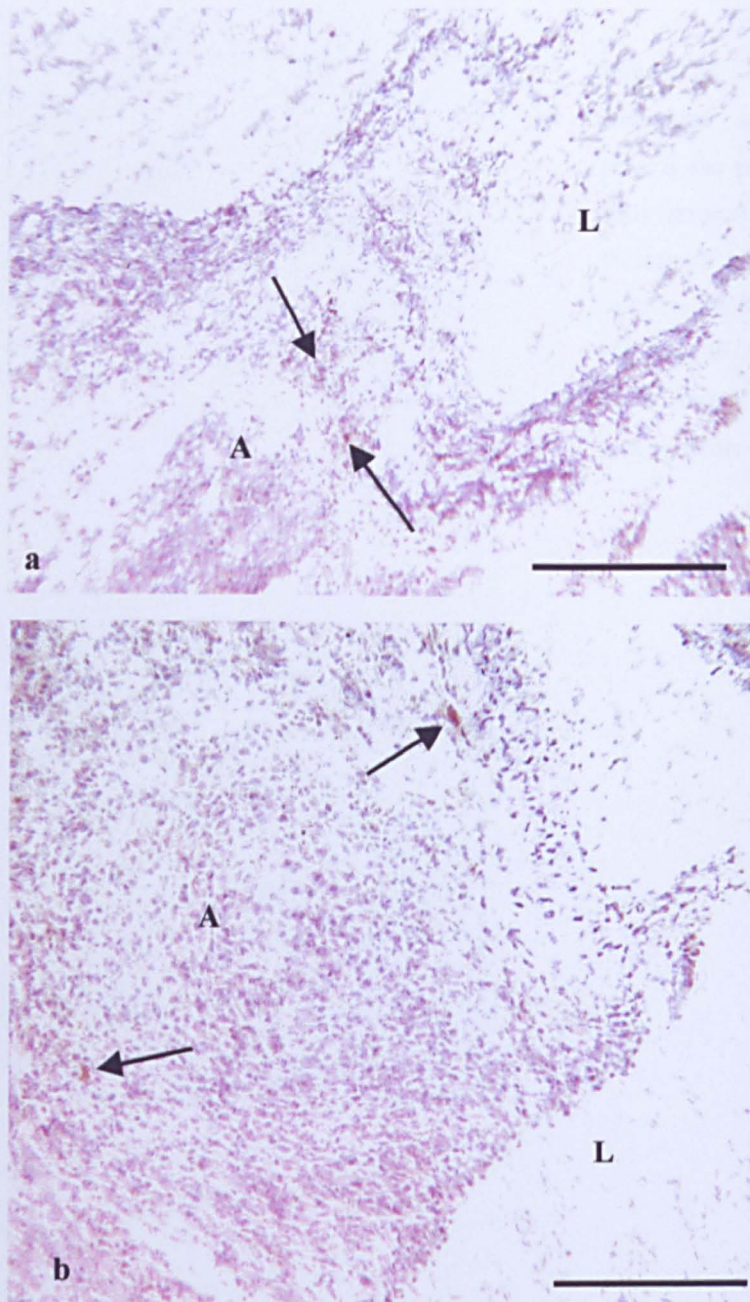


Figure 30: CD19⁺ B-cells are relatively rare within the arteritic lesions of *Il1rn*^{-/-} mice. Advanced lesions from two *Il1rn*^{-/-} mice are shown, aged a) 179 days and b) 131 days. Cells staining positively are indicated by arrows. A = lesional area, L = vessel lumen. Scale bar = 200 μ m.

Figure 31: Chemokines and adhesion molecules in advanced arteritic lesions

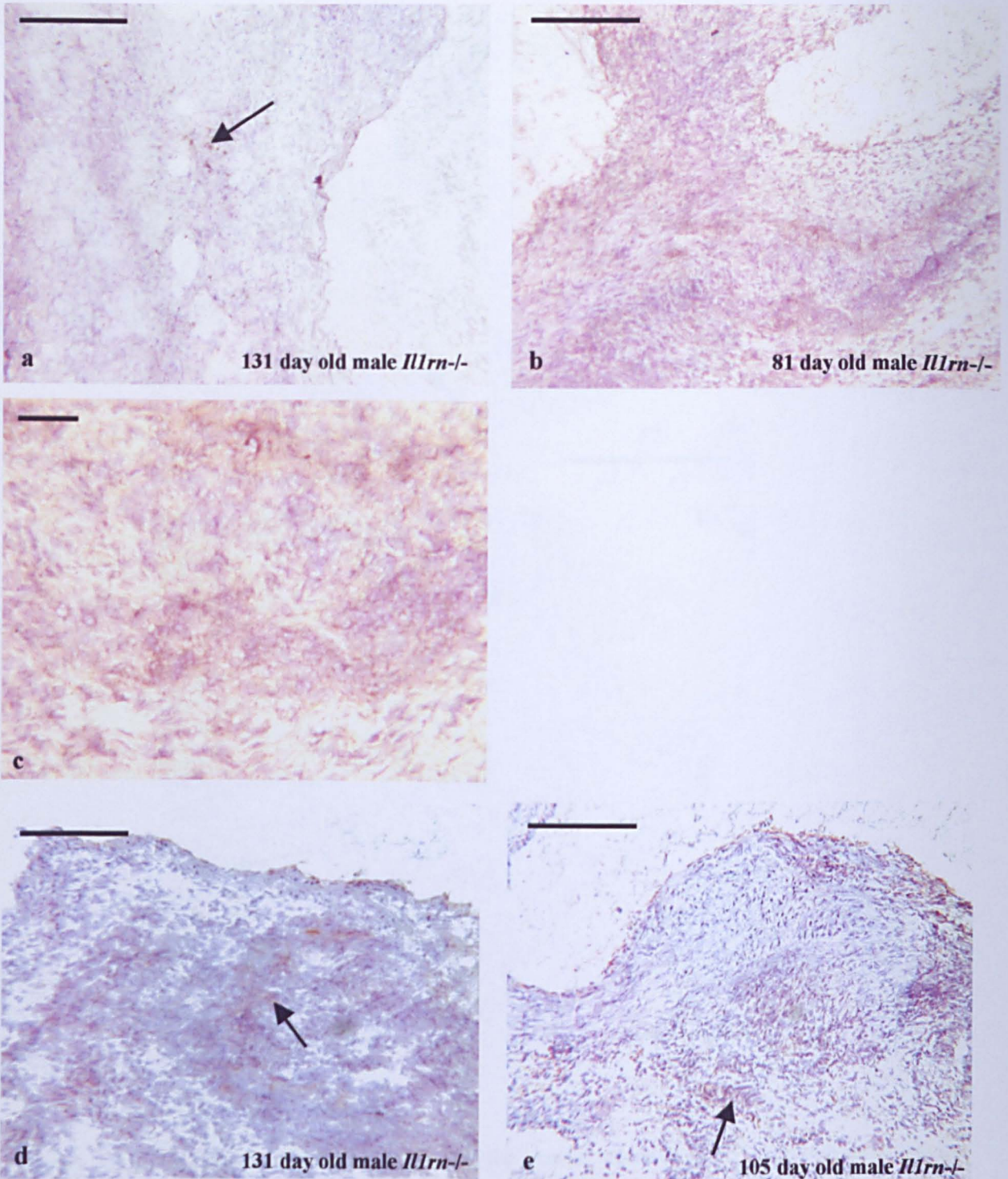


Figure 31: Chemokine and adhesion molecule production and expression in advanced aortic root lesions of *Il1rn*^{-/-} mice. a, b, c) MCP-1⁺ cells (stained in brown). d, e) CD54 (ICAM-1)⁺ cells (stained in brown). c is a higher power magnification of the section shown in b. Scale bar in a, b, d, e = 200 μm, scale bar in c = 40 μm

Figure 32: Activated endothelium on both the luminal surface and within the microvasculature of arteritic lesions

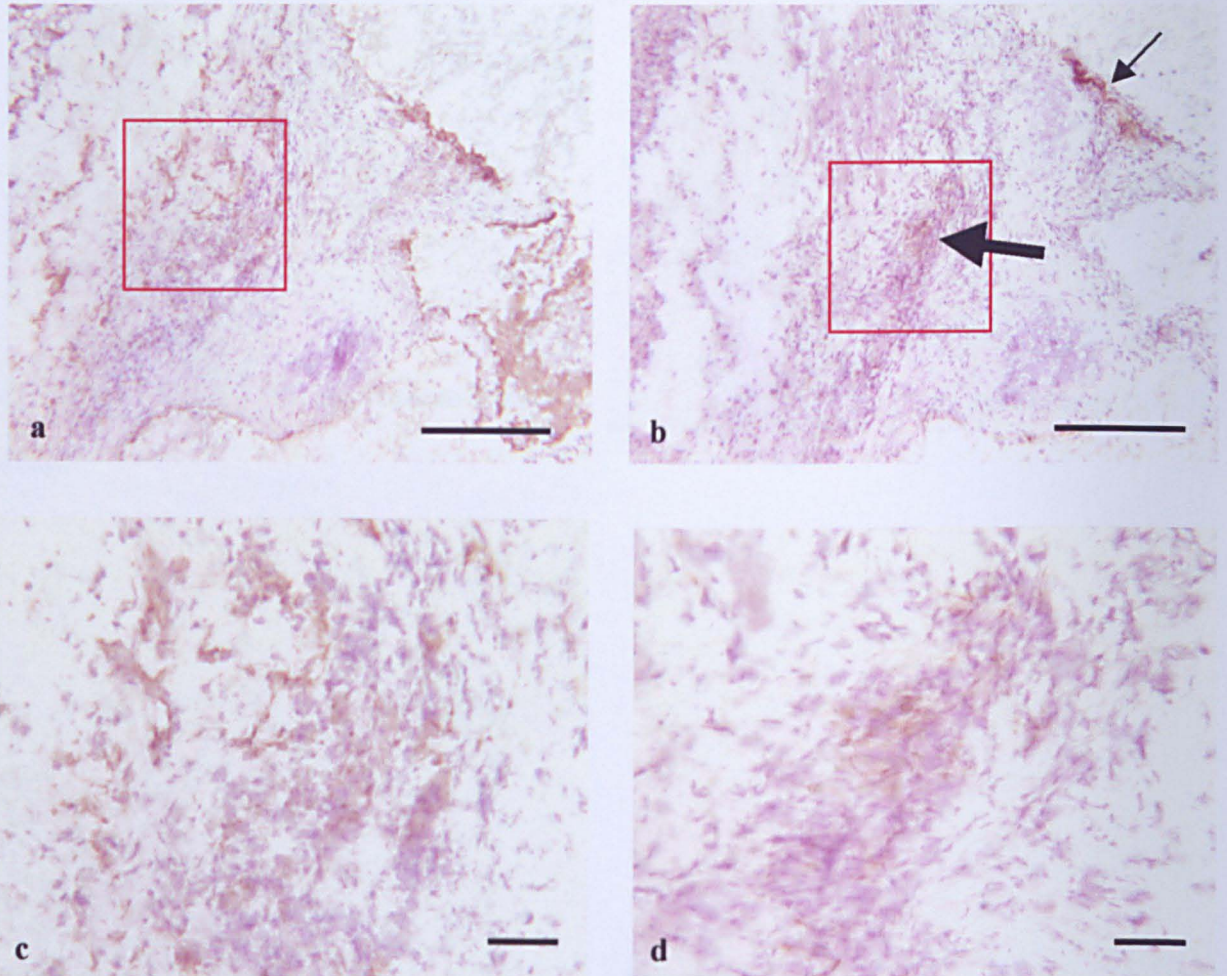


Figure 32: Sections stained for a) $CD31^+$ cells, and b) $CD62e^+$ (E-selectin) cells. c) and d) are higher power magnifications of the boxed areas in a) and b). b) shows activated endothelium both on the luminal surface of the large vessel (thin arrow) and within the microvasculature (thick arrow). In all cases brown indicates a positive stain. Sections are taken from the lesional aortic root of a 179 day old female $Il1rn^{-/-}$ mouse. Scale bar in a and b = 200 μm , scale bar in c and d = 40 μm .

CD4⁺ T-cells with a Th1 type cytokine profile. However, not all of the CD4⁺ T-cells present within the lesions showed evidence of IFN γ production. This could indicate memory CD4⁺ T-cells relocating to the tissue.

Abundant neutrophils and dendritic cells were also present within the frozen sections of the lesions scoring 2 or 3, again with clear demarcation from unaffected tissue (Figure 27, Figure 28). The neutrophils appeared in similar numbers throughout the lesional area, without localising to any particular layers of the vessel wall. Toluidine blue staining of paraffin sections also demonstrated the presence of small numbers of mast cells within the inflammatory infiltrate and adjacent to surrounding microvasculature and small veins (Figure 29). B-cells were present but were observed in far less abundance than CD4⁺ T-cells, macrophages, dendritic cells or neutrophils within the frozen sections (Figure 30).

Production of MCP-1 (Figure 31) was observed within lesions scoring 2 or 3, within the medial and adventitial layers in the same areas as the macrophages, which are a major source of the chemokine. Expression of ICAM-1 (Figure 31) was also observed within similar areas of the lesions, which suggests its cytokine-induced expression on the surfaces of the infiltrating antigen presenting cells, and possibly on the endothelial cells of the microvasculature. The expression of E-selectin on CD31⁺ endothelial cells, both on the luminal surface of the affected aorta, and on the endothelial cells of the vasa vasorum within the adventitial layer and on microvasculature in the surrounding tissue (Figure 32), also indicates endothelium activated by cytokines. Again, E-selectin and ICAM-1 expression were only seen in lesions scoring 2 or 3.

Figure 33: Aortic roots from *Il1rn*^{+/+} mice contain circulating F4/80⁺ macrophages and CD4⁺ T-cells which are not activated

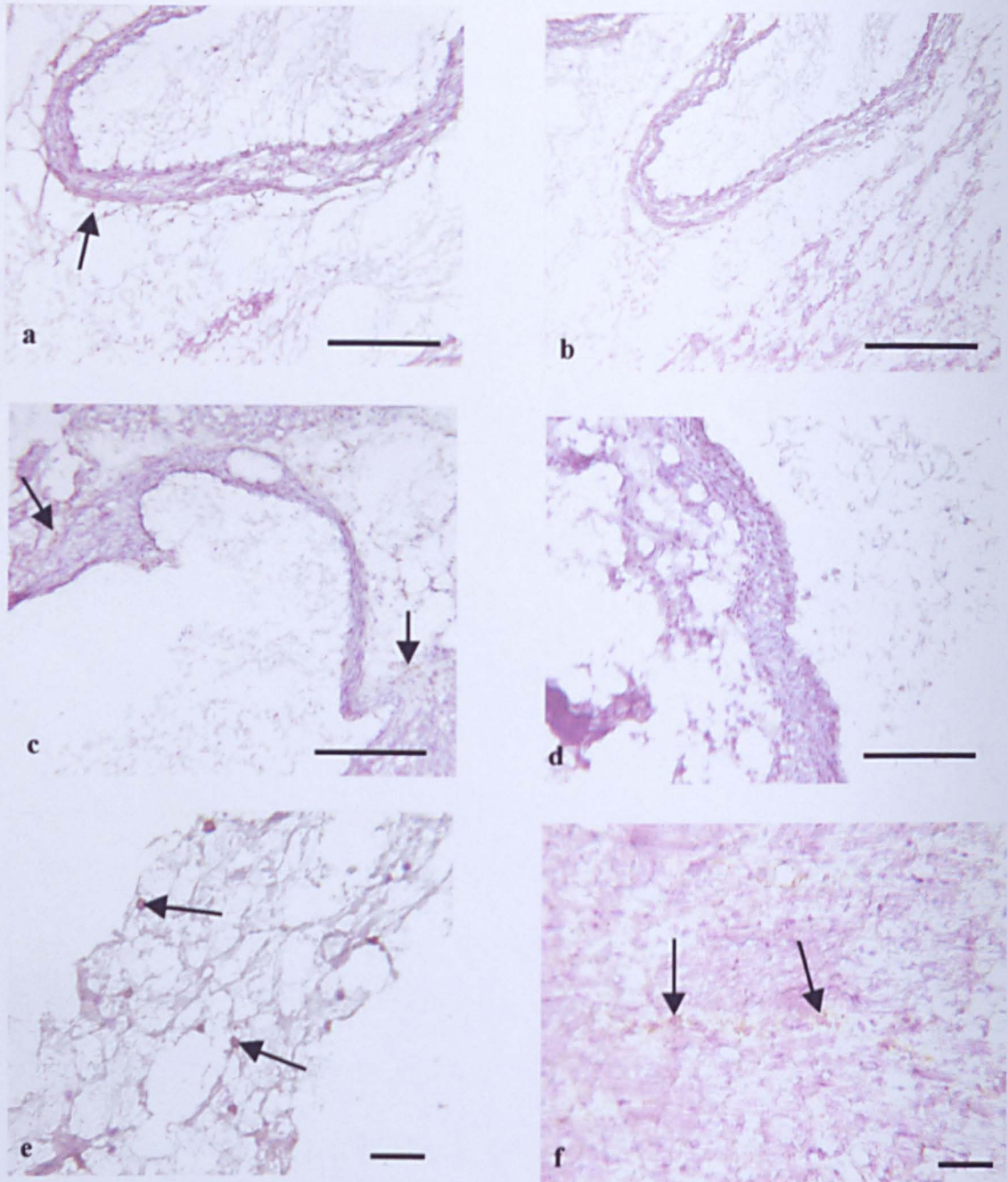


Figure 33: Circulating CD4⁺ T-cells and F4/80⁺ macrophages in *Il1rn*^{+/+} aortic roots are not activated. a) and b) aortic root of a 108 day old *Il1rn*^{+/+} mouse stained for CD4 and IFN γ . c) and d) Aortic root of a second 108 day old *Il1rn*^{+/+} mouse stained for F4/80 and IL-1 β . e) circulating CD4⁺ T-cells in the bloodstream of a 108 day old *Il1rn*^{+/+} mouse. f) F4/80⁺ macrophages resident in the heart tissue of a 108 day old *Il1rn*^{+/+} mouse. Examples of cells staining positively are indicated by arrows. Scale bar a-d = 200 μ m, scale bar e and f = 40 μ m.

Figure 34: Uninflamed aortic root from a 151 day old *Il1rn*^{+/+} mouse

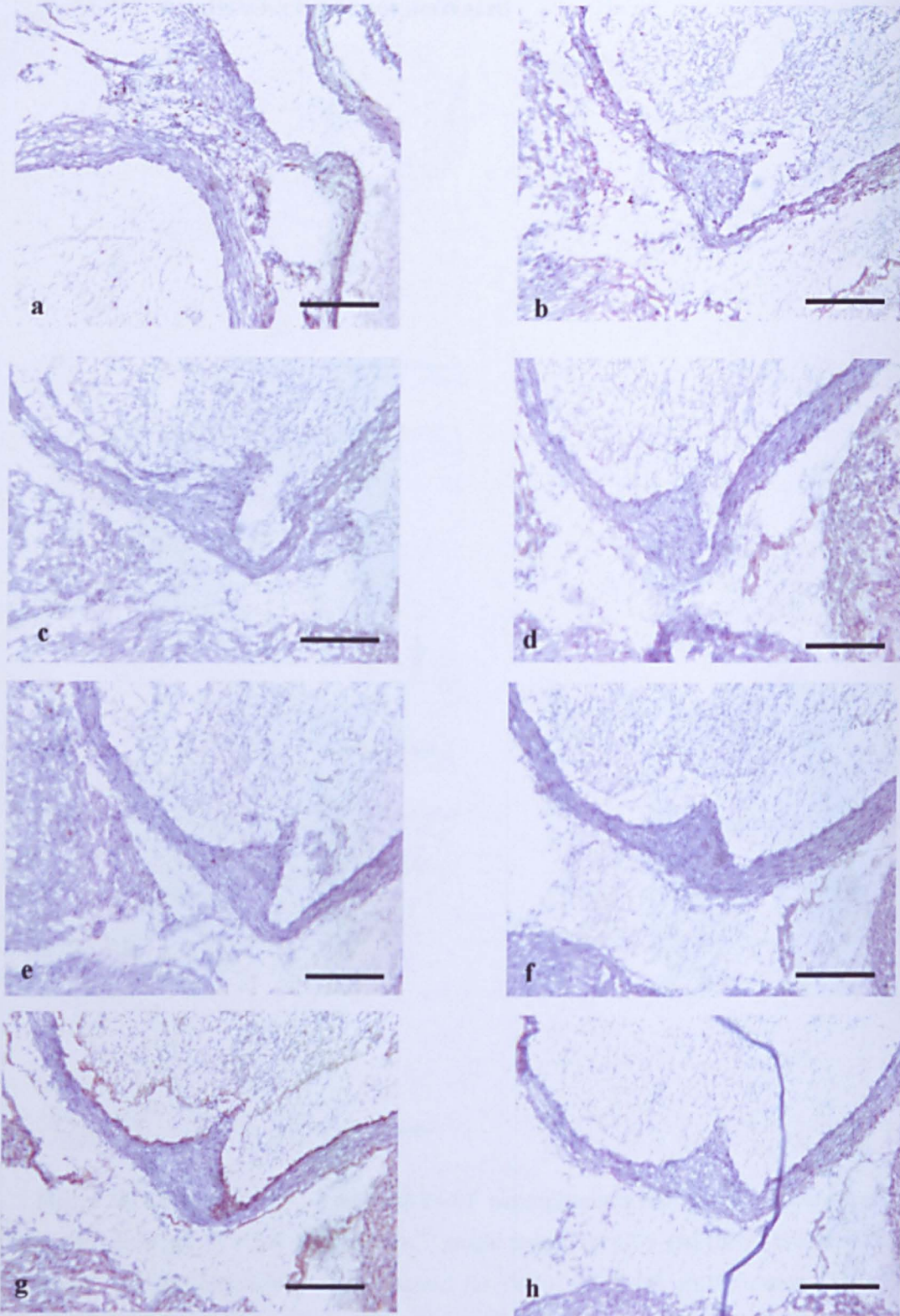


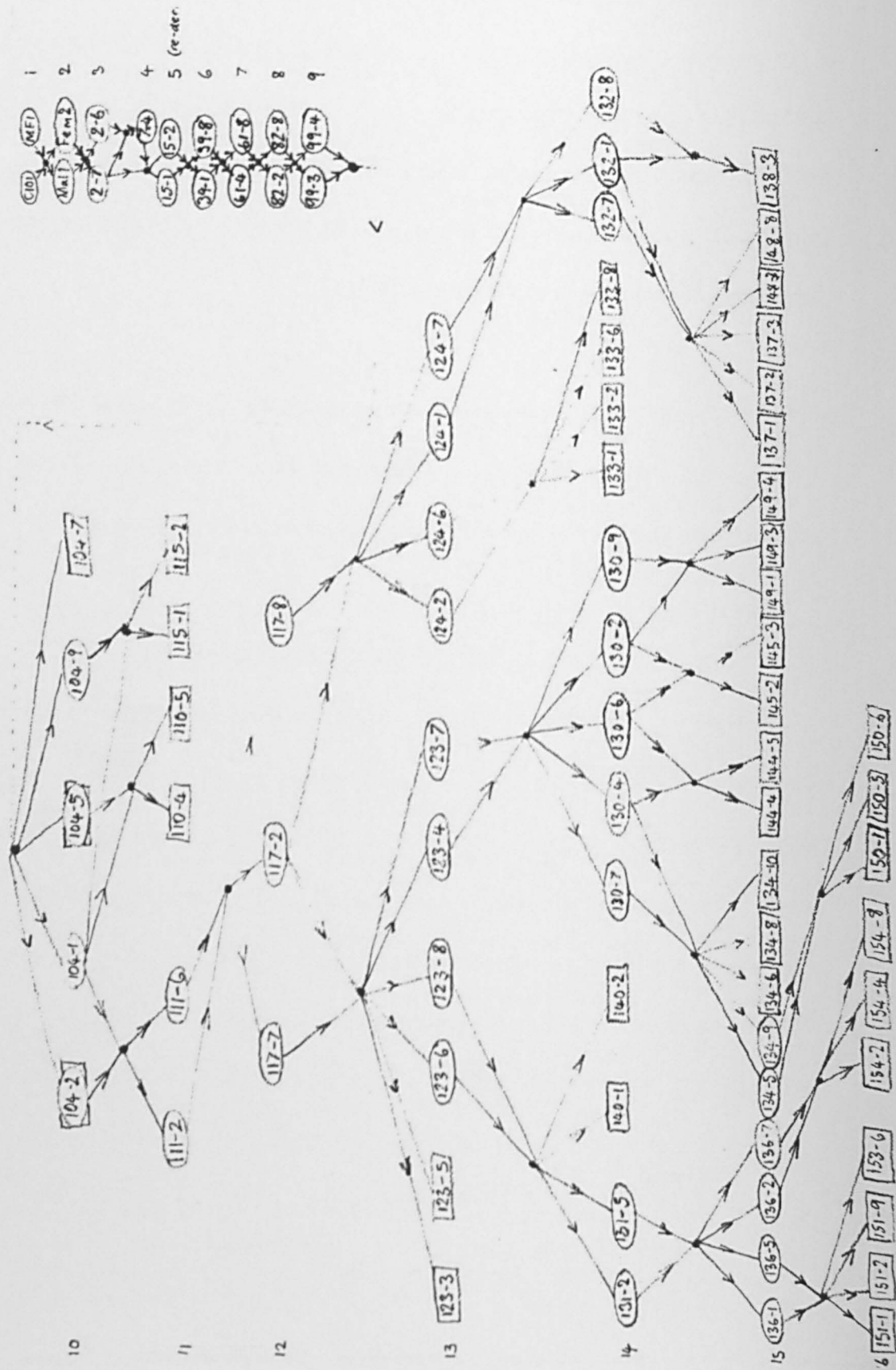
Figure 34: Immunohistochemical staining of aortic root from a 151 day old female *Il1rn*^{+/+} mouse. Sections are stained for a) CD4, b) F4/80, c) IFN γ , d) IL-1 β , e) IL-4, f) MCP-1, g) CD31, h) E-selectin. All show few or no cells staining positively, apart from CD31 (PECAM-1, endothelial cells). Scale bar = 200 μ m.

Activated endothelium on the vasa vasorum would suggest that the cellular infiltrate locates to the lesional site via the microvasculature within the adventitial layer, rather than being recruited from the main vessel. This is in accordance with observations that the infiltrate appears concentrated in the adventitial layer prior to destruction of the elastin layers within the intima. This seems to be histologically similar to observations in sections from temporal arteries of human GCA patients, which also suggest that the inflammatory infiltrate arrives at the lesion via the vasa vasorum deep within the adventitial layer.

Il1rn^{+/-} mice (4/6) were mildly affected with the disease. They had small cellular infiltrates (of <50 cells) which were composed of activated CD4⁺ T-cells and macrophages. No other inflammatory markers were seen in these mice.

Il1rn^{+/+} littermates of affected *Il1rn*^{+/-} mice displayed no outward signs of illness, and immunohistochemical examination of aortic roots from wild type animals demonstrated a lack of inflammatory artery disease at this site. In all wild type sections examined, a small number of CD4⁺ T-cells and macrophages were observed throughout the tissue. No cells stained positive for IL-1 β , IFN γ , IL-4 or IL-5 suggesting that these circulating macrophages and T-cells were not activated (Figure 33, Figure 34). This suggests that there is no strain-specific tendency for inflammatory lesions to form in the aorta. All other immunohistochemical stains were also negative (Figure 34), other than that for CD31 (endothelial cells).

Figure 35: Pedigree of Sf3 animals used in arteritis studies



Lesions in *Il1rn*^{-/-} mice on both the Sf3 and Balb/c backgrounds were histologically and immunohistologically similar. All markers were detected in both strains in animals of a similar stage of disease.

3.3.4: Arteritis time course study

To attempt to characterise the initiating factors and progression of the disease, an immunohistochemical time course study was performed on frozen sections of aortic roots dissected from Sf3 mice.

The time course study consisted of 35 animals, with 8 *Il1rn*^{+/+}, 23 *Il1rn*^{-/-} and 4 *Il1rn*^{+/-} animals. The family tree of the animals used is shown in Figure 35. Animals were culled in 5 age ranges, each divided by ~25 days (see table 4).

Table 4: Animals used in arteritis time course study

Set	Days of age	Nos. of <i>Il1rn</i> ^{+/+} animals	Nos. of <i>Il1rn</i> ^{+/-} animals	Nos. of <i>Il1rn</i> ^{-/-} animals	<i>Il1rn</i> ^{+/+} cellular infiltrate scores	<i>Il1rn</i> ^{+/-} cellular infiltrate scores	<i>Il1rn</i> ^{-/-} cellular infiltrate scores
1	23-24	2	1	3	0,0	0	0,0,1
2	56-59	0	1	4		1	1,1,1,1
3	75-81	0	0	4			0,1,2,3
4	105-108	2	1	4	0,0	1	0,0,2,3
5	≥125	4	1	8	0,0,0,0	1	0,2,3,3,3, 3,3,3

Serial frozen sections were stained immunohistochemically (as section 3.3.3) to evaluate cellular processes occurring over time.

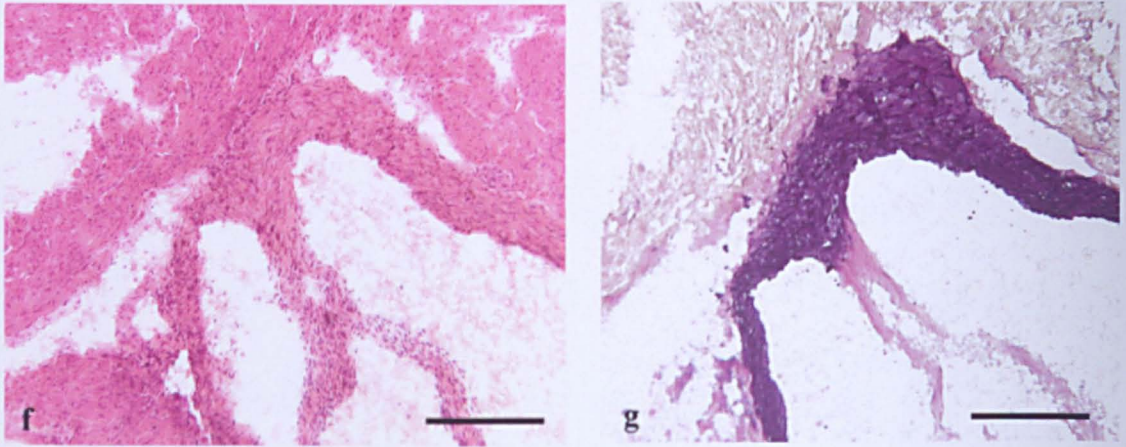
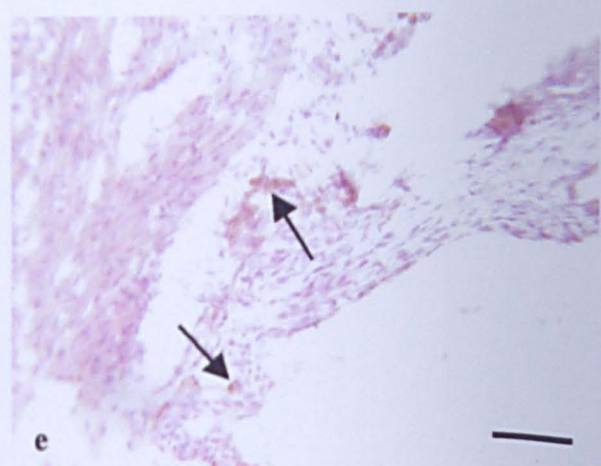
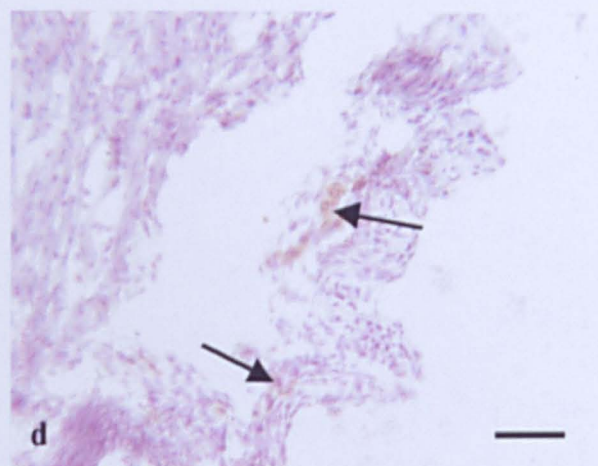
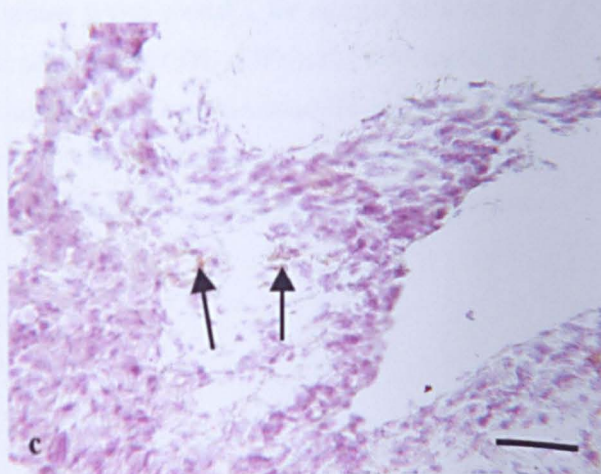
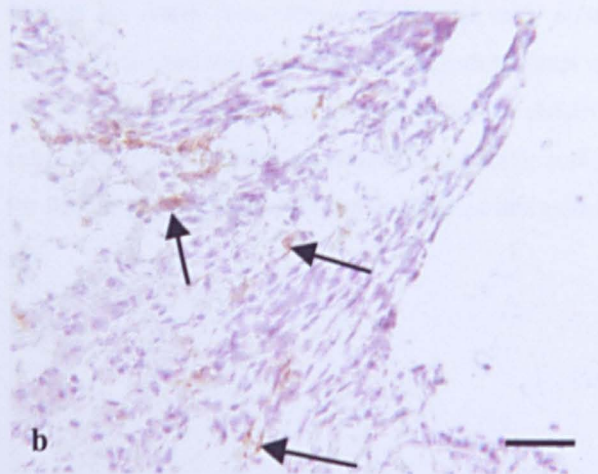
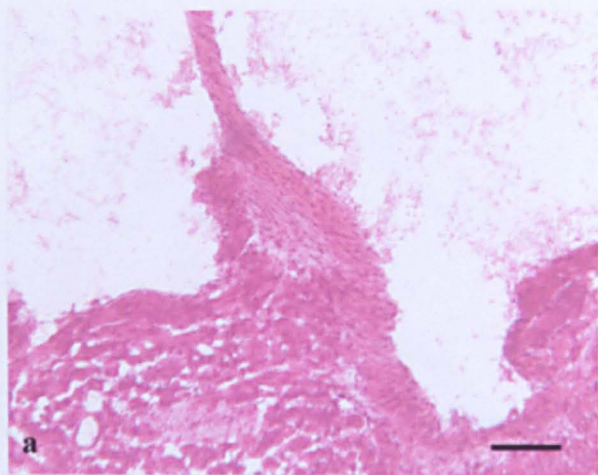


Figure 36: Aortic root from a 24 day old male *Illrn*^{-/-} mouse which scored 1 for cellular infiltrate. a) haematoxylin and eosin staining. Aortic root sections were stained for b) CD4, c) IFN γ , d) F4/80, and e) IL-1 β . Examples of positively stained cells are shown by arrows. f) & g) haematoxylin and eosin and connective tissue staining on an unaffected aortic root from a 23 day old male *Illrn*^{-/-} mouse (see figure 37 for further immunohistochemical analysis of this example). Scale bar a-e = 40 μ m. Scale bar f and g = 200 μ m.

Figure 36: Aortic root from a 24 day old *Il1rn*^{-/-} mouse scoring 1 for cellular infiltrate



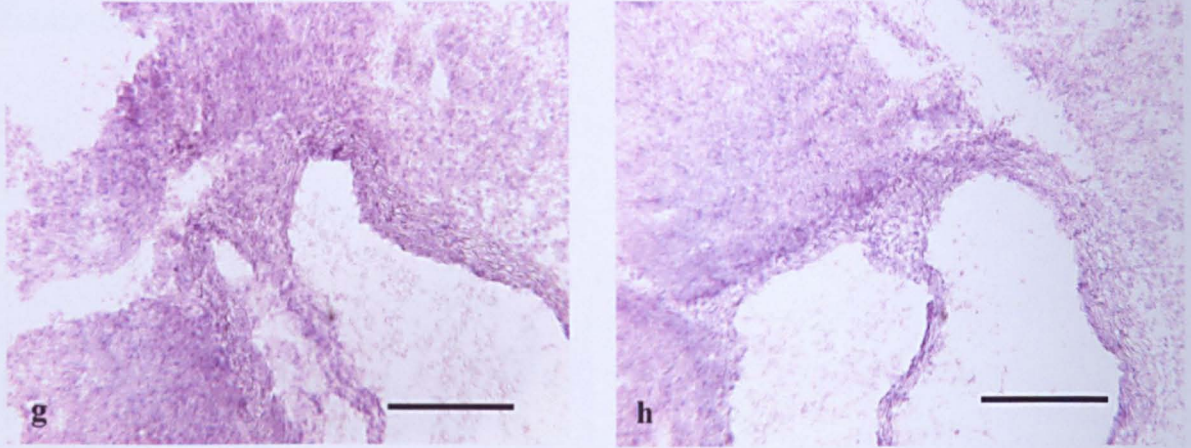


Figure 37: Immunohistochemical staining of the aortic root from a 23 day old male *Illrn*^{-/-} mouse reveals a lack of inflammatory markers. Sections are stained for a) F4/80, b) IL-1 β , c) CD4, d) IFN γ , e) CD31, f) CD62e (E-selectin), g) IL-4, h) negative control. Some circulating F4/80⁺ and CD4⁺ cells can be seen (arrows) but are not concentrated on any particular areas and are not activated. Endothelium (CD31⁺) is also not activated as judged by the lack of cells staining positively for E-selectin. Scale bar = 200 μ m.

Figure 37: Uninflamed aortic root in a 23 day old *Il1rn*^{-/-} mouse

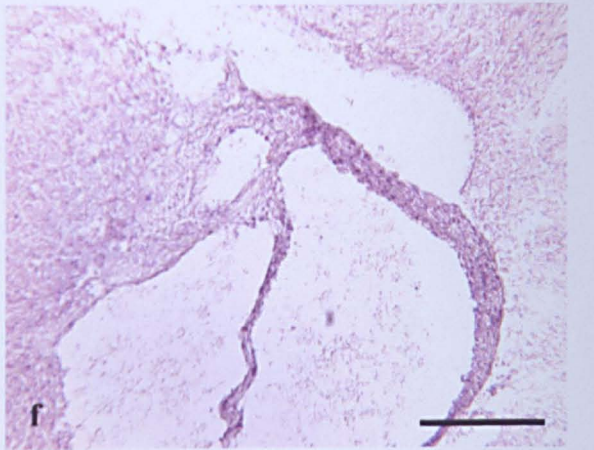
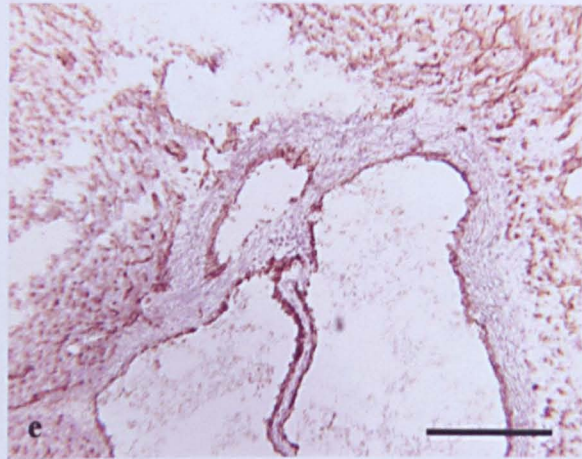
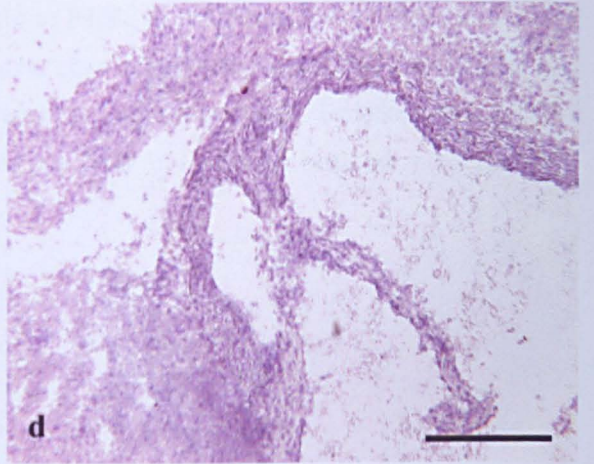
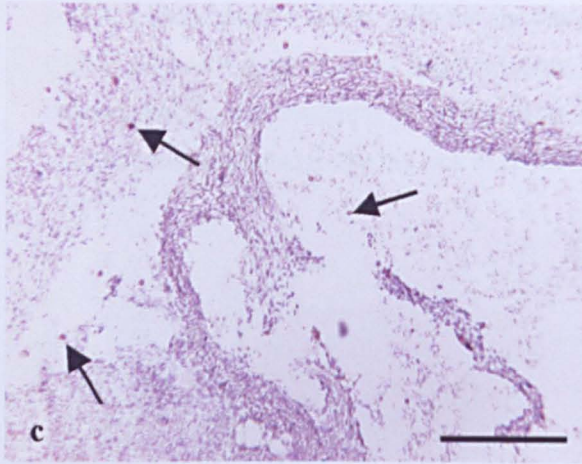
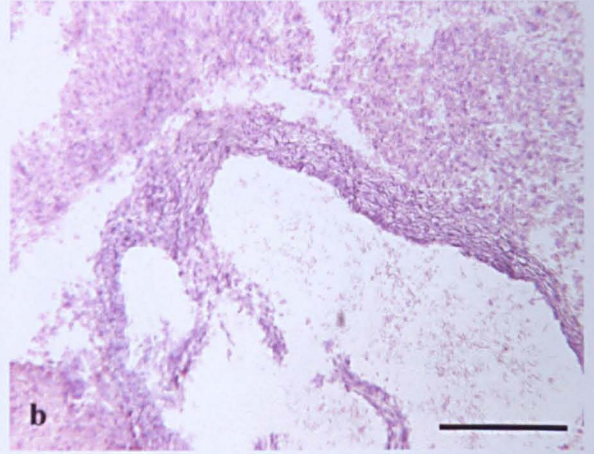
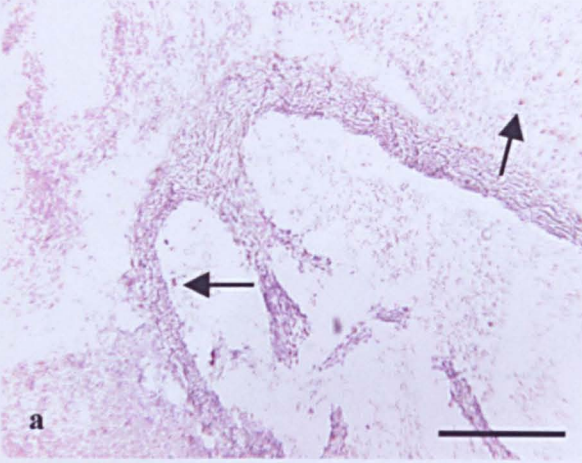


Figure 38: Small cellular infiltrates in aortic roots from 56-59 day old *Il1rn*^{-/-} mice

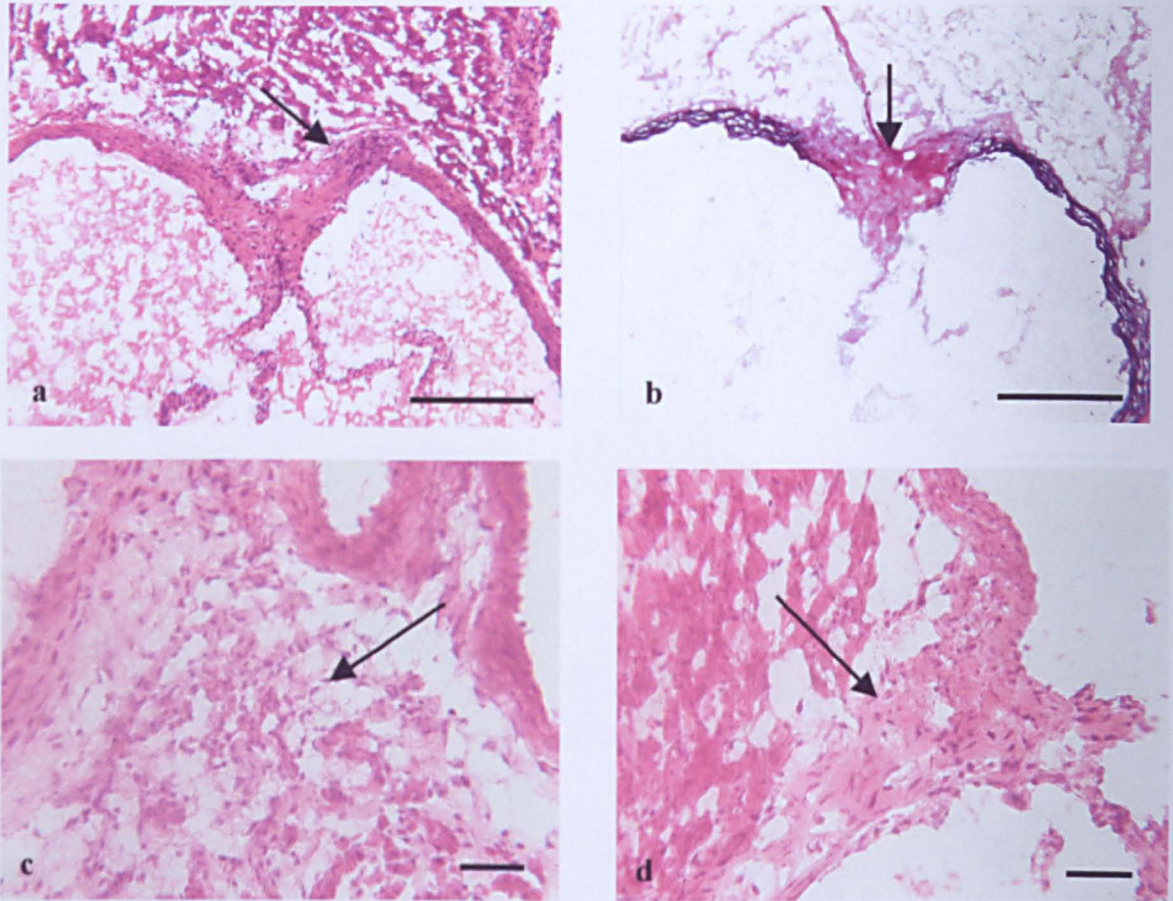


Figure 38: Aortic roots from 56-59 day old *Il1rn*^{-/-} mice have small cellular infiltrates. a and b) sections from a 59 day old female *Il1rn*^{-/-} mouse which was assigned a cellular infiltrate score of 1 and an elastin damage score of 2. The elastin appears to be completely degraded at one point of the vessel wall (arrow in b), although there is only a small cellular infiltrate (arrow in a). c and d are haematoxylin and eosin stained sections of aortic root from two male 56 day old *Il1rn*^{-/-} mice. The areas of the small cellular infiltrates are indicated by arrows. Scale bar a & b = 200 μ m, c & d = 40 μ m.

Figure 39: Activated macrophages and CD4⁺ cells in aortic root lesions of a 56 day old *Il1rn*^{-/-} mouse

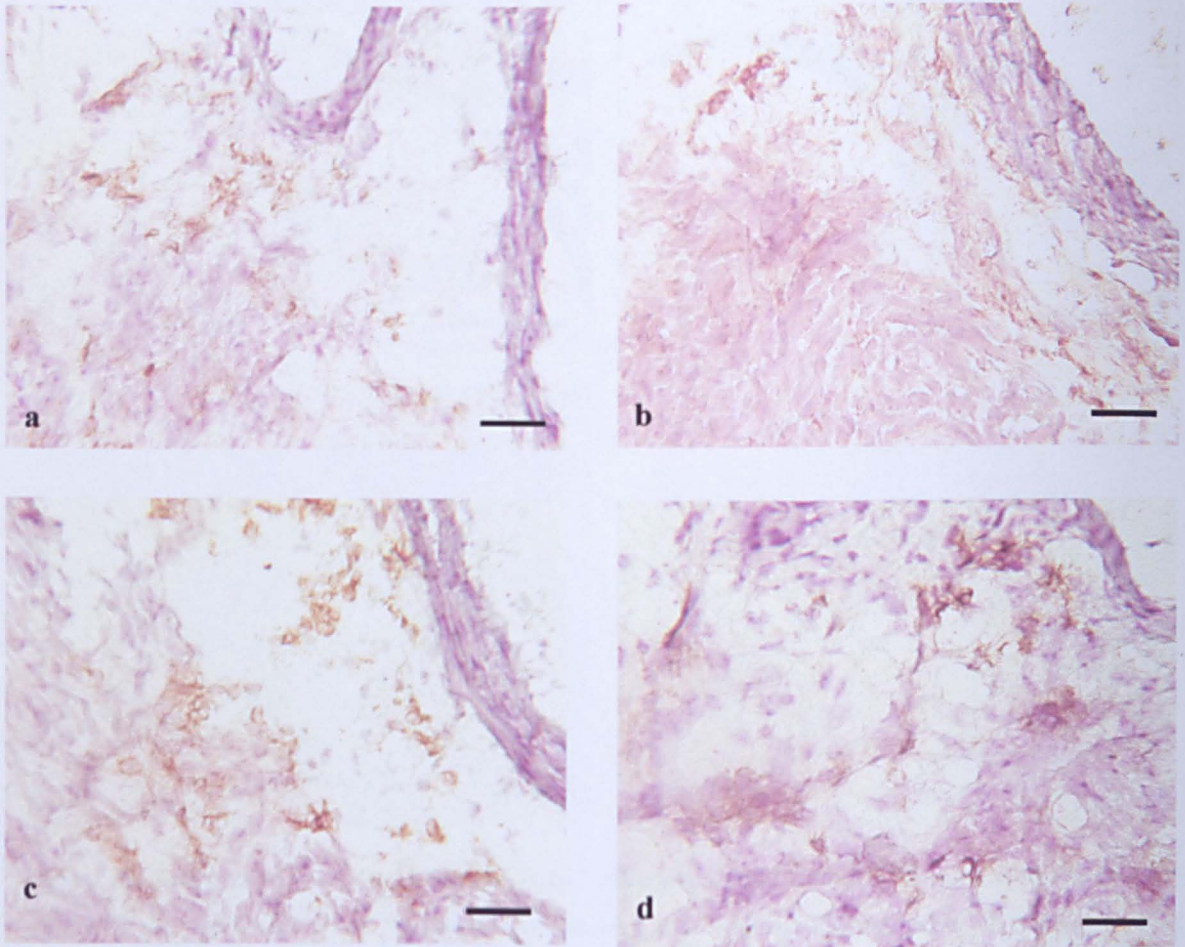


Figure 39: Activated F4/80⁺ cells (macrophages) and CD4⁺ T-cells in the aortic root lesion of a 56 day old male *Il1rn*^{-/-} mouse. In each, brown staining indicates a) F4/80⁺ cells, b) IL-1β⁺ cells, c) CD4⁺ cells, and d) IFNγ⁺ cells. This animal scored 1 for cellular infiltrate. Scale bar = 40 μm.

Figure 40: Lack of inflammatory markers, other than small numbers of activated F4/80⁺ and CD4⁺ cells, in aortic root lesions of 56-59 day old *Il1rn*^{-/-} mice.

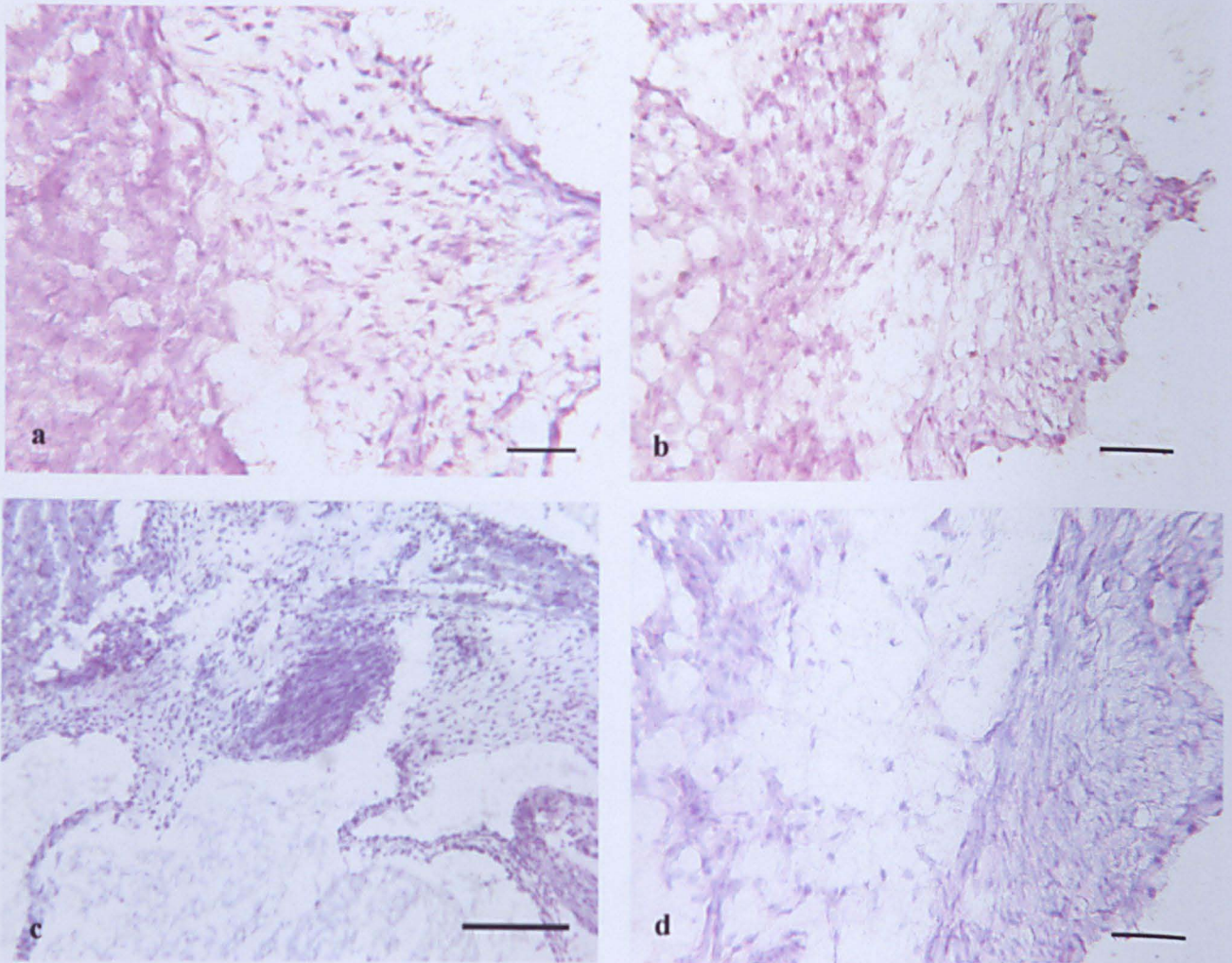


Figure 40: Other than a small number of activated CD4⁺ and F4/80⁺ cells (see figure 39), the aortic root lesions of 56-59 day old mice, scoring 1 for cellular infiltrate, contain few or no other inflammatory markers. a) aortic root lesion from a 56 day old male *Il1rn*^{-/-} mouse, stained for neutrophils. b) aortic root lesion from a second 56 day old male *Il1rn*^{-/-} mouse, stained for MCP-1. c) aortic root lesion from a 59 day old female *Il1rn*^{-/-} mouse, stained for DEC205⁺ cells (dendritic cells), d) aortic root lesion from a 56 day old *Il1rn*^{-/-} mouse stained for CD62e⁺ cells (E-selectin). Scale bar a, b, and d = 40 μ m. Scale bar in c = 200 μ m.

The course of arteritic lesion development

Within Set 1, the youngest group of animals (23-24 days old), a small inflammatory infiltrate was seen in 1 of 3 *Il1rn*^{-/-} animals, with a score of 1 (Figure 36). The infiltrate consisted of <50 CD4⁺ T-cells, of which <25% were producing IFN γ . There were also a small number of CD4⁺ T-cells and macrophages present throughout all of the sections examined, with roughly equal numbers in *Il1rn*^{+/+} and *Il1rn*^{-/-} mice. No elastin damage was seen in any animals (Figure 36). Aside from within the small infiltrate, there was no production of IFN γ , IL-1 β , IL-4 or IL-5 suggesting the macrophages and CD4⁺ T-cells present throughout the tissue were not activated (Figure 37). No neutrophils, dendritic cells, B-cells, or other inflammatory markers were seen in any sections from this age group (Figure 37).

In Set 2 (56-57 days old), there were small infiltrates (score 1, <50 cells) visible with haematoxylin and eosin in 4/4 *Il1rn*^{-/-} mice and 1/1 *Il1rn*^{+/+} mouse, but elastic Van Gieson staining showed that the elastic layers of the vessel walls were all intact apart from one *Il1rn*^{-/-} animal in which the elastin appeared to be completely degraded at one point (Figure 38). CD4⁺ T-cells within the adventitial layer of the vessels were activated since they were producing IFN γ (Figure 39). CD8⁺ T-cells were rare or absent (<5 cells/section). F4/80⁺ macrophages were localised in the same areas of the vessel wall as the CD4⁺ T-cells (Figure 39). The macrophages were also activated as judged by their production of IL-1 β (Figure 39). There appeared to be larger numbers of CD4⁺ T-cells present than macrophages within these early lesions. There did not appear to be any MCP-1 or E-selectin positive staining (Figure 40), and neutrophils and dendritic cells were also absent (Figure

Figure 41: Little IL-4 production in the aortic root lesion of a 59 day old *Il1rn*^{-/-} mouse

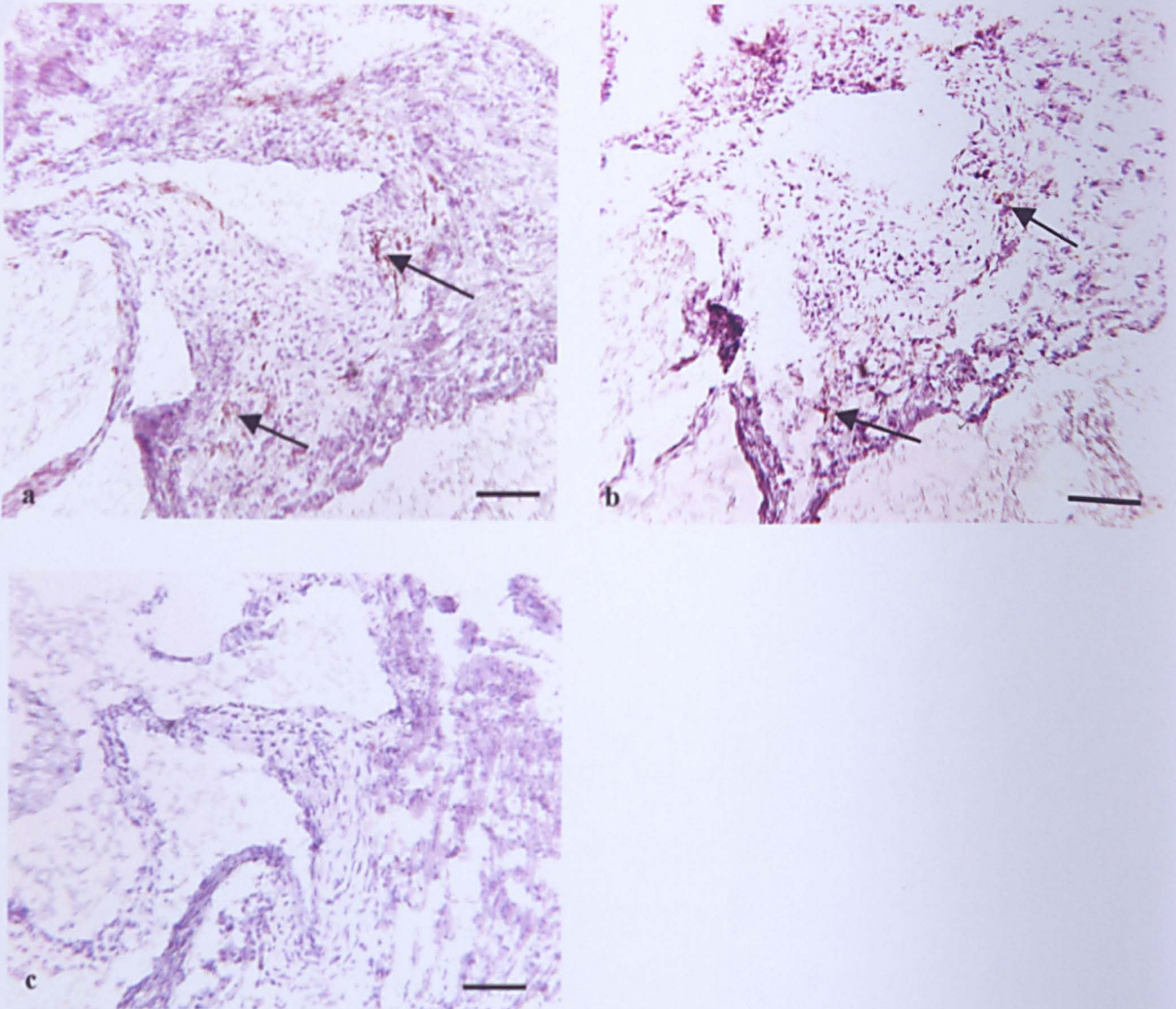


Figure 41: Serial sections from the aortic root lesion of a 59 day old female *Il1rn*^{-/-} mouse (cellular infiltrate score 1) stained for a) CD4⁺ cells, b) IFNγ⁺ cells, and c) IL-4⁺ cells. Brown staining indicates a positively stained cell, examples are indicated by arrows. In very early lesions, CD4⁺ T-cells are of a Th1 rather than Th2 type. Scale bar = 40 μm.

Figure 42: Aortic root lesions in 75-81 day old mice

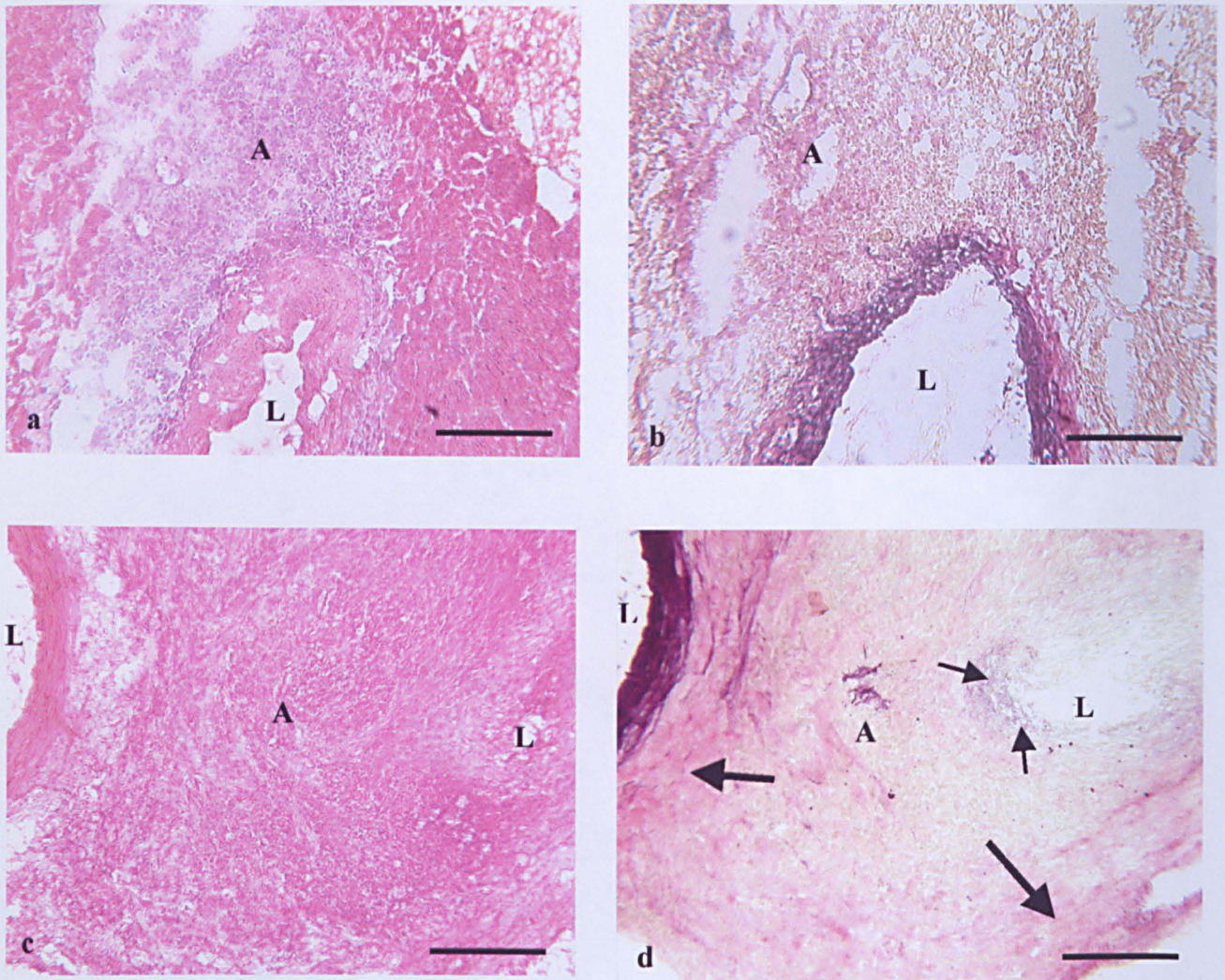


Figure 42: Sections of aortic root lesions from 75-81 day old mice stained with haematoxylin and eosin and for connective tissue. a) and b) aortic root lesion in a 75 day old female *Il1rn*^{-/-} mouse scoring 2 for cellular infiltrate and 1 for elastin damage. c) and d) aortic root lesion in an 81 day old male *Il1rn*^{-/-} mouse scoring 3 for both cellular infiltrate and elastin damage. In d, thin arrows indicate remaining fragments of elastin which has been mostly destroyed, thick arrows indicate collagen deposition. In all cases, L = vessel lumen, A = lesional area. Scale bar = 200 μ m.

Figure 43: Activated macrophages in aortic root lesions from 75-81 day old *Il1rn*^{-/-} mice

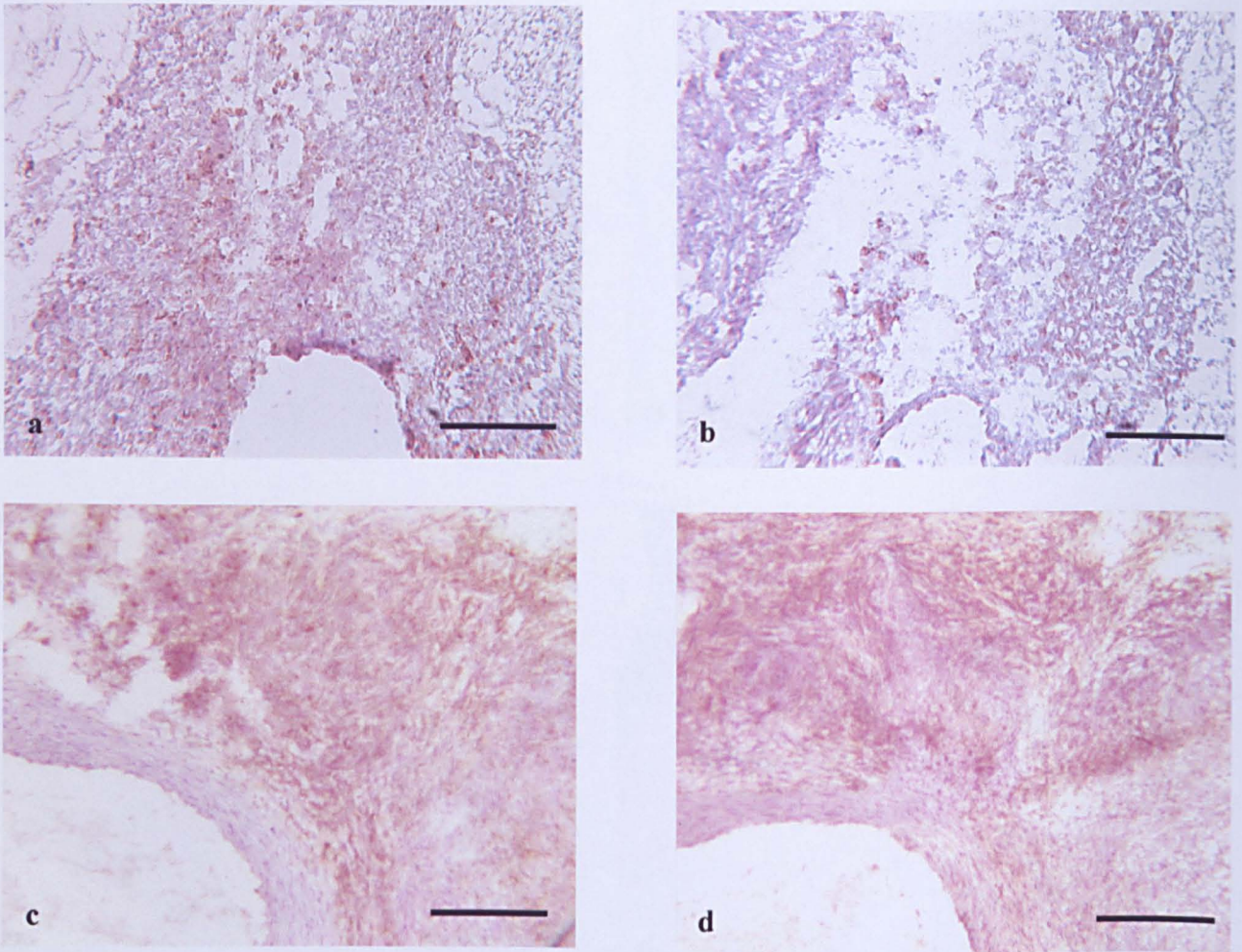


Figure 43: Activated macrophages in aortic root lesions of two 75-81 day old *Il1rn*^{-/-} mice. a) and b) show F4/80⁺ and IL-1β⁺ cells respectively stained in brown, in the aortic root lesion of a 75 day old female *Il1rn*^{-/-} mouse with a cellular infiltrate score of 2. c) and d) show F4/80⁺ and IL-1β⁺ cells respectively stained in brown, in a more advanced (score 3) aortic root lesion from an 81 day old male *Il1rn*^{-/-} mouse. Scale bar = 200 μm.

Figure 44: Activated CD4⁺ T-cells in aortic root lesions of 75-81 day old *Il1rn*^{-/-} mice

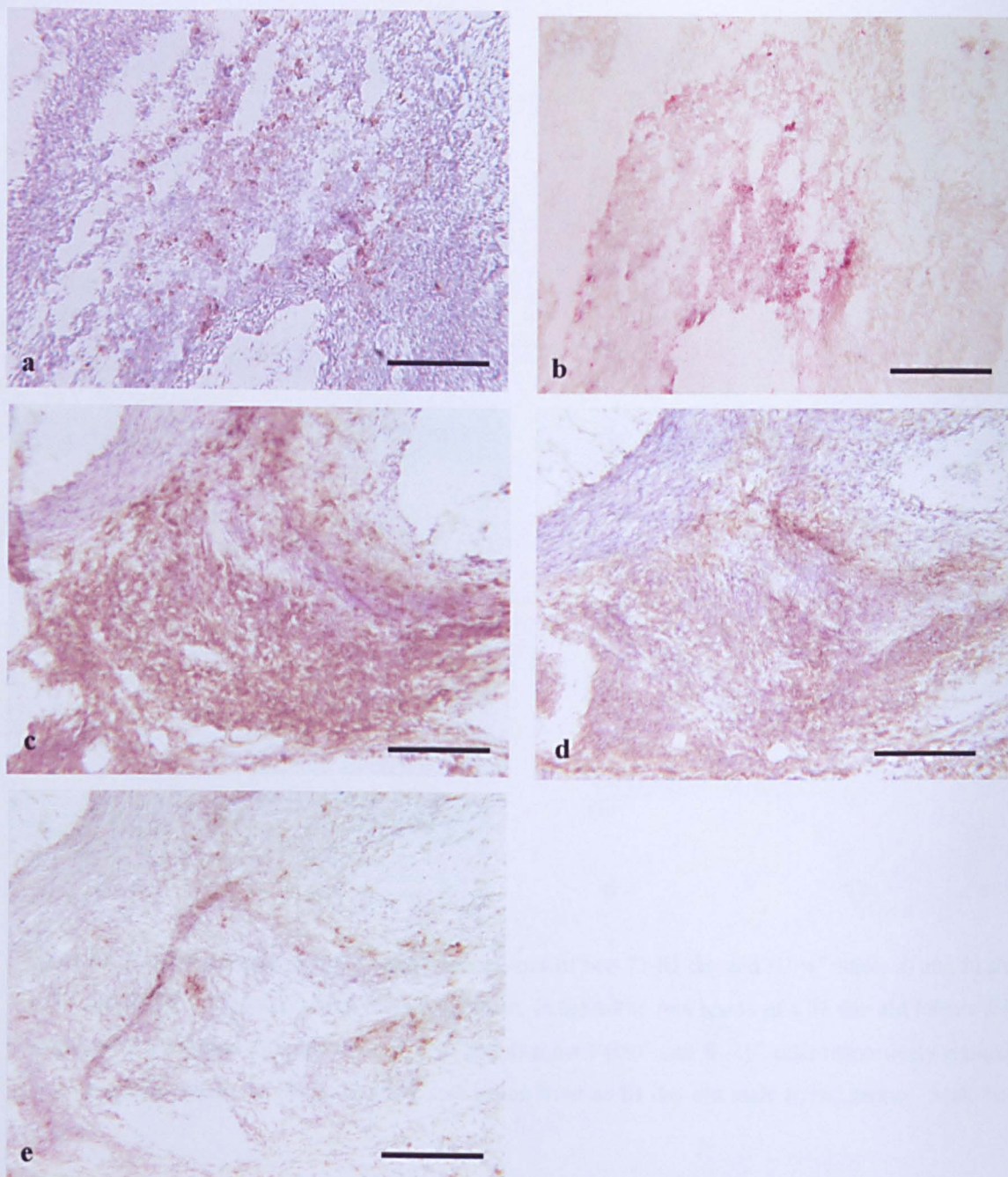


Figure 44: Activated CD4⁺ T-cells in aortic root lesions of two 75-81 day old *Il1rn*^{-/-} mice. a) shows CD4⁺ cells stained in brown, and b) is double stained, showing CD4⁺ and IFN γ ⁺ cells in black and red respectively. a and b are in the aortic root lesion of a 75 day old female *Il1rn*^{-/-} mouse with a cellular infiltrate score of 2. c) and d) show CD4⁺ and IFN γ ⁺ cells respectively stained in brown, in a more advanced (score 3) aortic root lesion from an 81 day old male *Il1rn*^{-/-} mouse. e) is a section from the same mouse as in c) and d), stained for CD8. Even in very inflamed aortic roots such as this, CD8⁺ T-cells remain relatively rare. Scale bar = 200 μ m.

Figure 45: Chemokine and adhesion molecule production and expression in the aortic root lesions of *Il1rn*^{-/-} mice aged 75-81 days

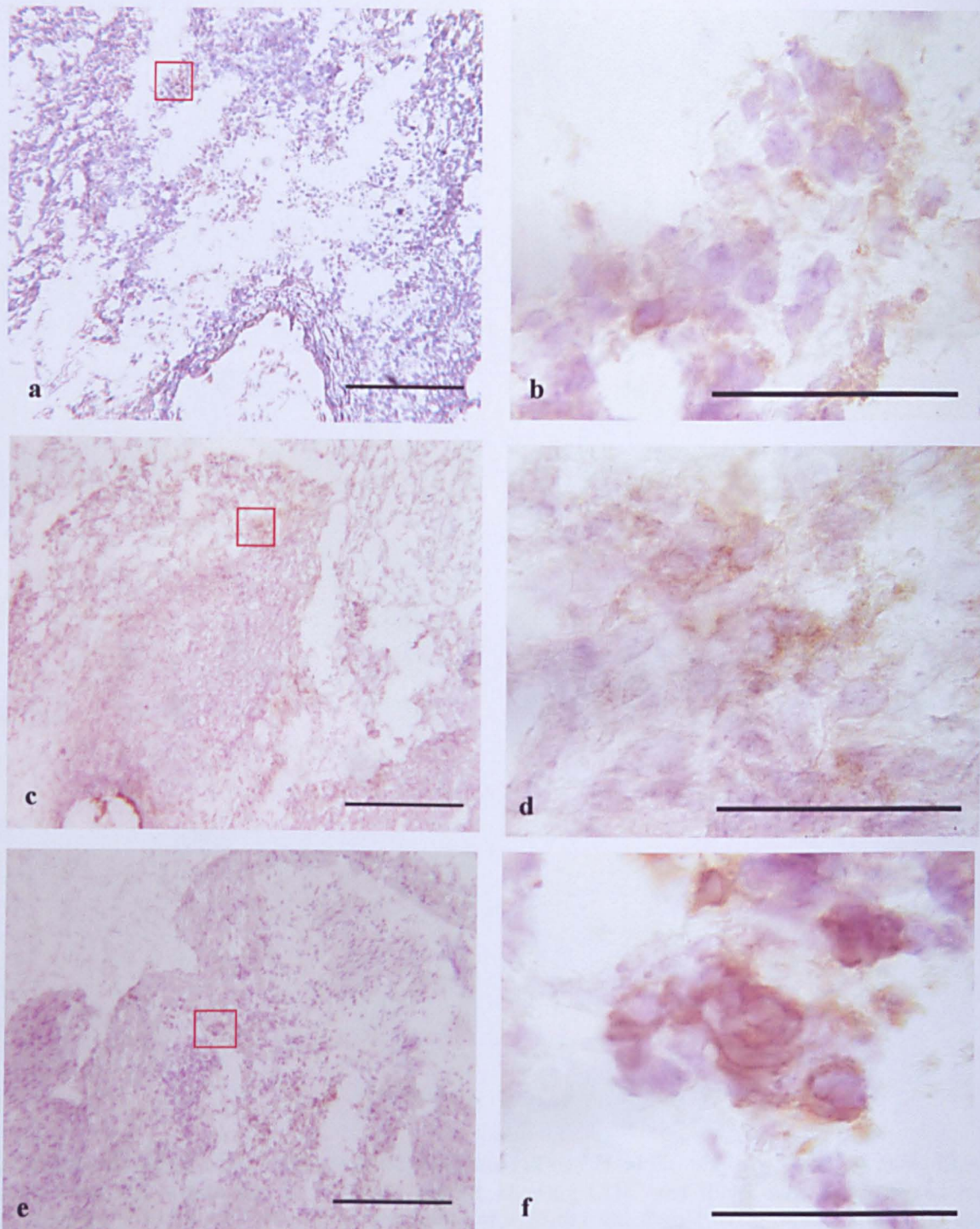


Figure 45: Chemokine (MCP-1) production and adhesion molecule (CD54, ICAM-1) expression in the aortic root lesions of *Il1rn*^{-/-} mice aged 75 days. a) shows MCP-1⁺ cells (in brown) in the aortic root lesion of a female *Il1rn*^{-/-} mouse, b) is a higher power magnification of the boxed area in (a). c) shows, in brown, ICAM-1⁺ cells in the same lesion, d) is a higher power magnification of the boxed area in (c). e) shows ICAM-1 expression in a second 75 day old female *Il1rn*^{-/-} mouse, f) is a higher power magnification of the boxed area in (e). Scale bar in a, c, e = 200 μm, in b, d, f = 40 μm.

Figure 46: Neutrophils and dendritic cells are present in the aortic root lesions of *Il1rn*^{-/-} mice aged 75-81 days

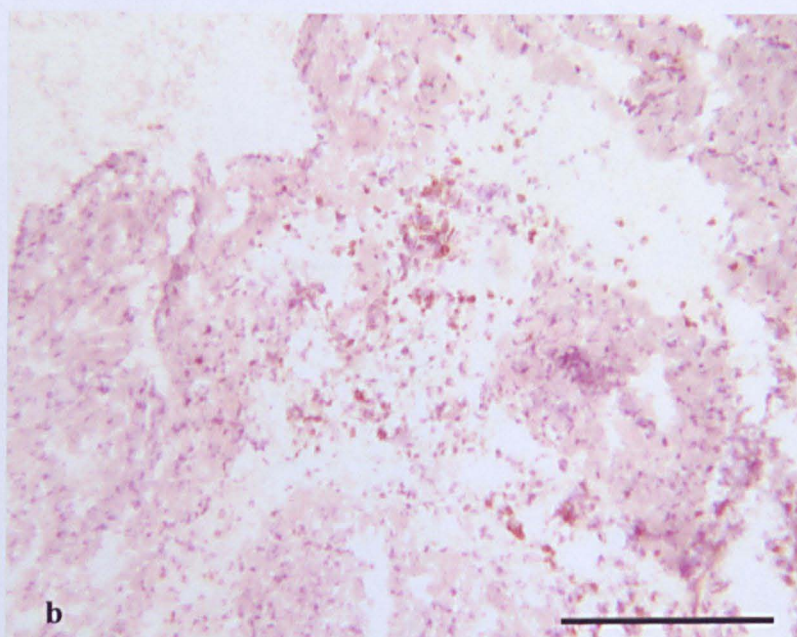
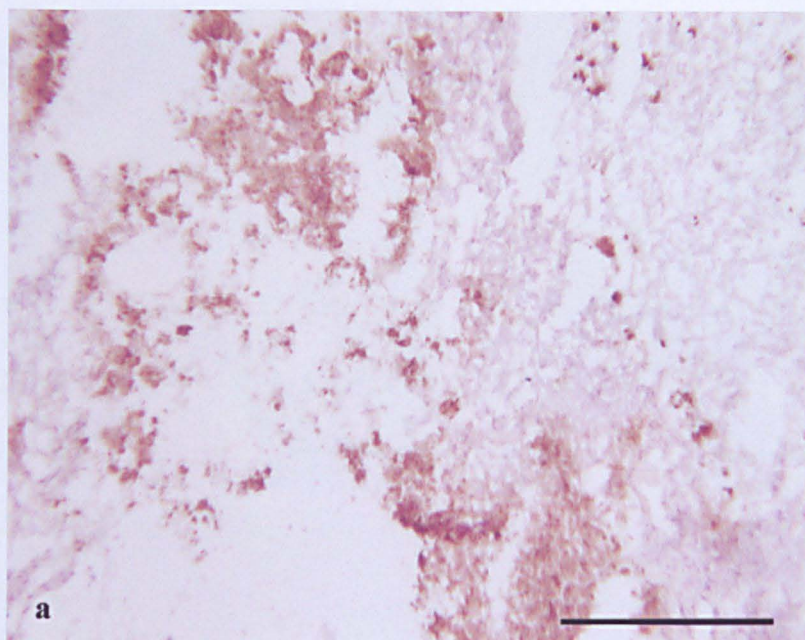


Figure 46: Neutrophils and dendritic cells are both found in the aortic root lesions of *Il1rn*^{-/-} mice aged 75-81 days. a) is the aortic root lesion from a 75 day old female mouse stained for neutrophils (brown), and b) is a section from the aortic root lesion of a second 75 day old female mouse stained for the dendritic cell marker DEC205 (DEC205⁺ cells in brown). Scale bar = 200 μ m.

40). Cells staining positive for IL-4 and IL-5 were also not in evidence (Figure 41).

By Set 3 (75-81 days old), the lesions had further developed in *Il1rn*^{-/-} mice, although there was a range of lesion severity within this group. One *Il1rn*^{-/-} mouse appeared unaffected (score 0), one was similar in appearance to *Il1rn*^{-/-} mice in set 2 (score 1), and two had further advanced lesions (scores 2 and 3). Of these two, the cellular infiltrates visible on haematoxylin and eosin staining were larger in size (>25% of the vessel area), and appeared to have an increase in density of the cells than lesions scoring 1 for cellular infiltrate (Figure 42). In the mouse that scored 2, the infiltrate was still localised to the outer layers of the vessel walls. In the mouse that scored 3, there was heavy infiltration of all layers of the vessel wall.

Elastic van Gieson staining showed that the animal with no cellular infiltrate also had no degradation of the elastin, whereas the mice that scored 1 and 2 both had some fragmentation of the outer layers. The animal scoring 3 for cellular infiltrate had advanced elastin damage, with complete degradation in parts and also evidence of repair (Figure 42).

In the inflammatory infiltrates of the mice scoring 2 and 3, there were abundant macrophages producing IL-1 β (Figure 43), large numbers of CD4⁺ T-cells, most of which were producing IFN γ (Figure 44), there was evidence of MCP-1 production, and ICAM-1 expression (Figure 45), and large numbers of neutrophils and dendritic cells (Figure 46). There was however little or no staining for IL-4 or

Figure 47: Few cells produce IL-4 or IL-5 in aortic root lesions of 75-81 day old *Il1rn*^{-/-} mice

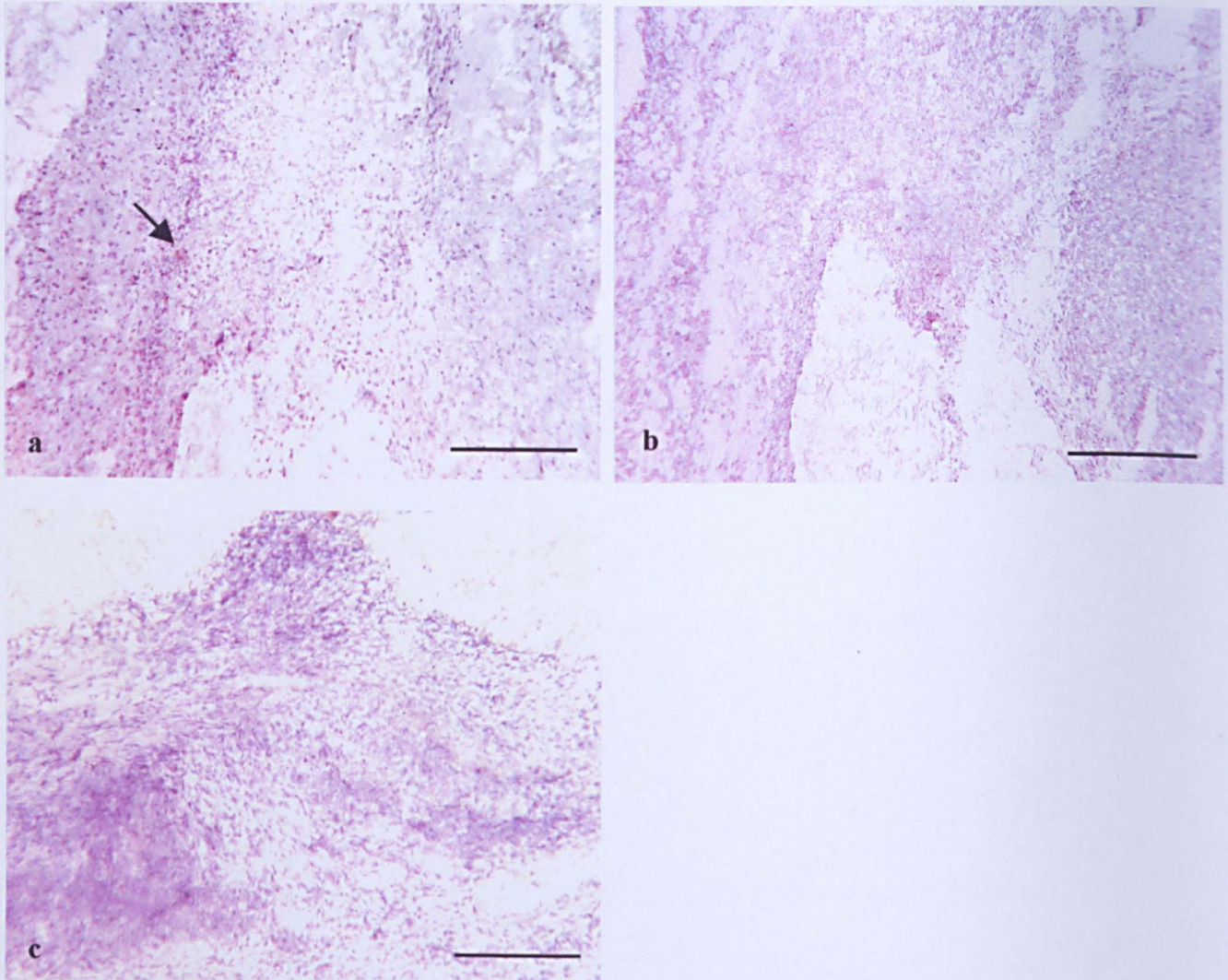


Figure 47: Few cells produce IL-4 or IL-5 in the aortic root lesions of 75-81 day old *Il1rn*^{-/-} mice. a) and b) are sections from the aortic root lesion of a 75 day old female mouse and are stained for a) IL-4 and b) IL-5. An example of a positive stain (in brown) is indicated by the arrow in (a). c) is a section from the aortic root lesion of a 81 day old male mouse with a cellular infiltrate score of 3, stained for IL-4. Scale bar = 200 μ m.

Figure 48: Activated endothelium in aortic root lesions from 75-81 day old mice

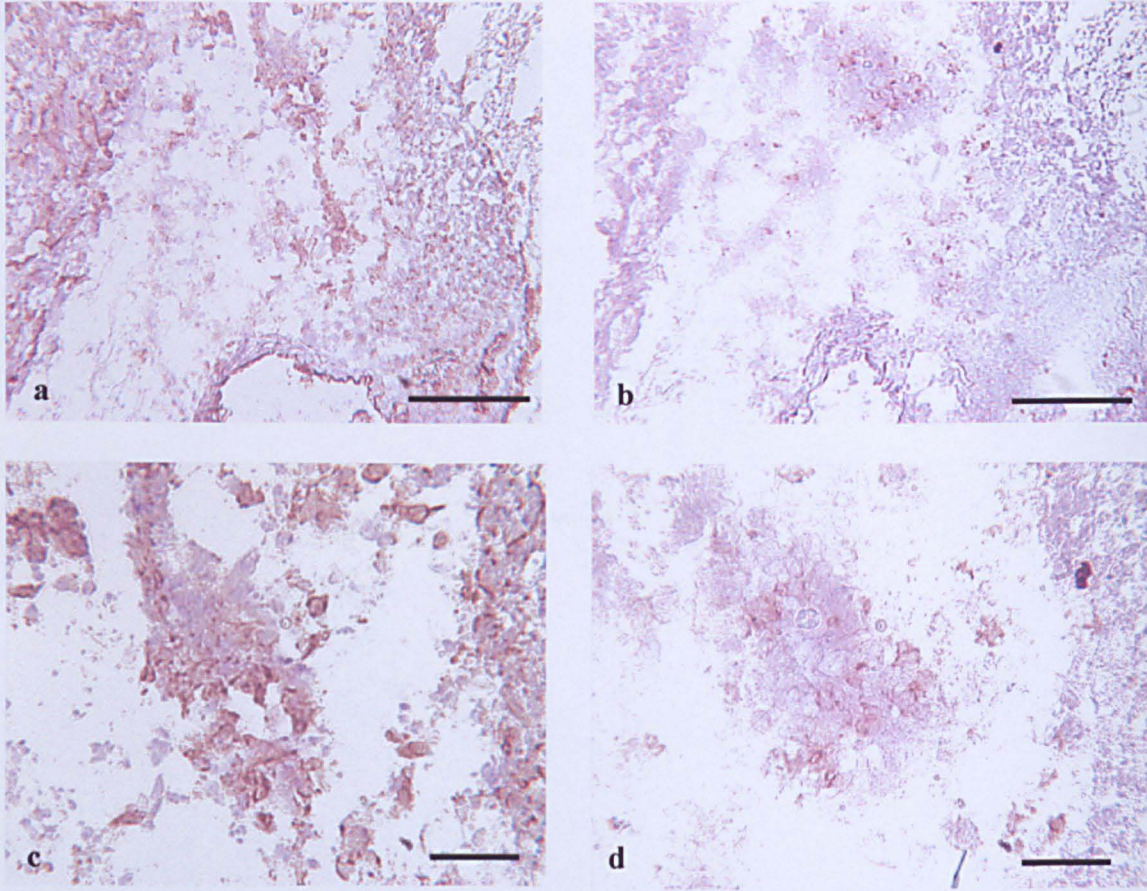


Figure 48: Sections from an aortic root lesion in a 75 day old female *Illrn*^{+/-} mouse are shown, stained with CD31 and CD62e. a) CD31⁺ cells, b) CD62e (E-selectin)⁺ cells, c) and d) higher power magnifications of boxed areas in a & b. The endothelium of the microvasculature is activated in this mouse, as judged by the expression of E-selectin. Scale bar a & b = 200 μ m, c & d = 40 μ m.

Figure 49: Damaged aortic roots in *Il1rn*^{-/-} mice aged 105-108 days

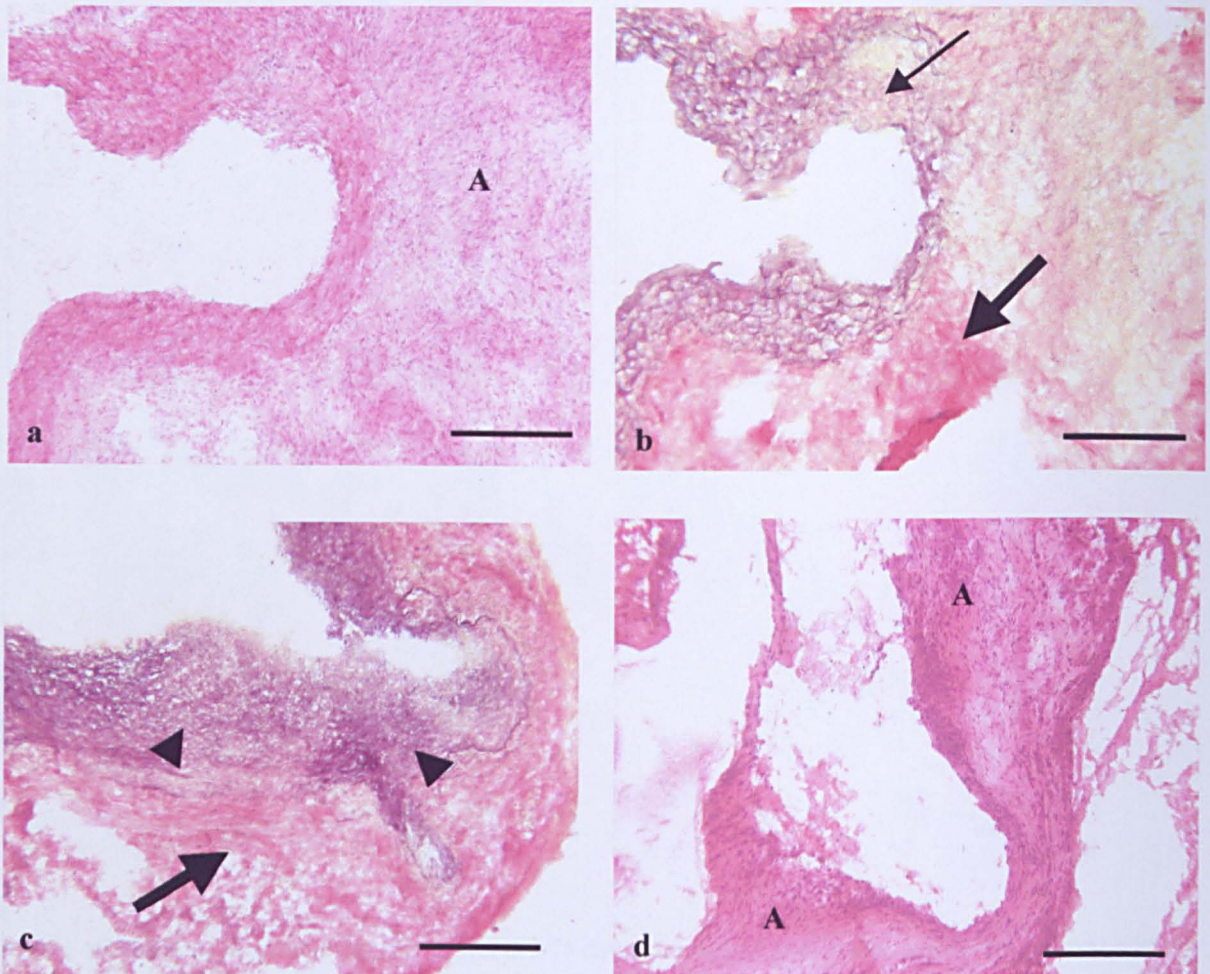


Figure 49: Advanced aortic root lesions in *Il1rn*^{-/-} mice aged 105-108 days. a, b and c are aortic root sections from a male *Il1rn*^{-/-} mouse aged 105 days. d is a section from a male *Il1rn*^{-/-} mouse aged 106 days. a and d are stained with haematoxylin and eosin (A = lesional area). b and c are stained for connective tissue. In b), the thin arrow indicates an area of complete elastin degradation, while the thick arrow indicates an area of collagen deposition (red colour). In c), the thick arrow again indicates an area of collagen deposition, and arrowheads indicate thickened and disorganised elastin layers. Scale bar = 200 μm .

Figure 50: Activated Th1 type CD4⁺ cells in the aortic root of a 105 day old *Il1rn*^{-/-} mouse

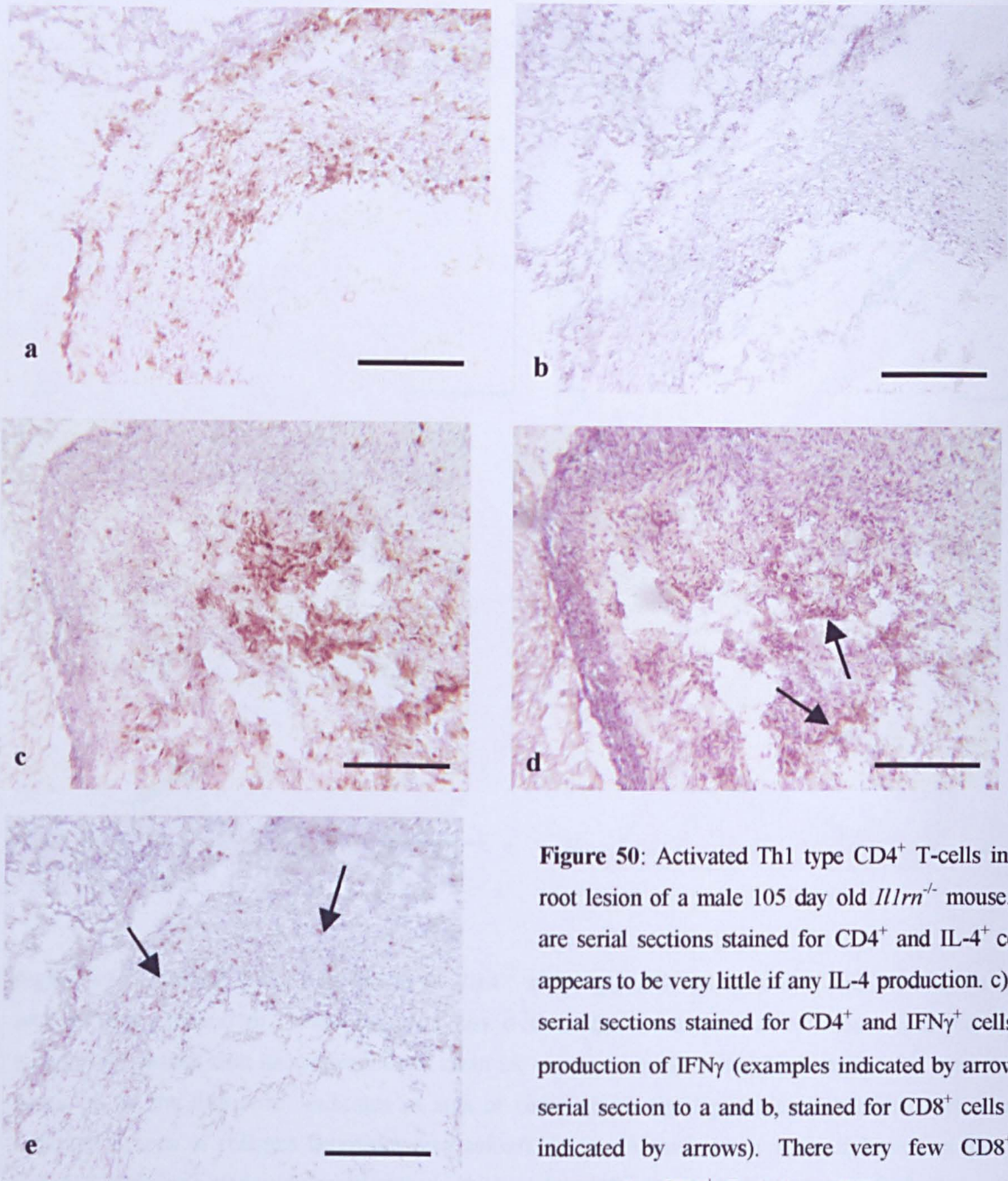


Figure 50: Activated Th1 type CD4⁺ T-cells in the aortic root lesion of a male 105 day old *Il1rn*^{-/-} mouse. a) and b) are serial sections stained for CD4⁺ and IL-4⁺ cells. There appears to be very little if any IL-4 production. c) and d) are serial sections stained for CD4⁺ and IFN γ ⁺ cells, showing production of IFN γ (examples indicated by arrows). e) is a serial section to a and b, stained for CD8⁺ cells (examples indicated by arrows). There very few CD8⁺ cells as compared to CD4⁺. Scale bar = 200 μ m.

Figure 51: Neutrophils and activated macrophages in the aortic root lesion of a 105 day old *Il1rn*^{-/-} mouse

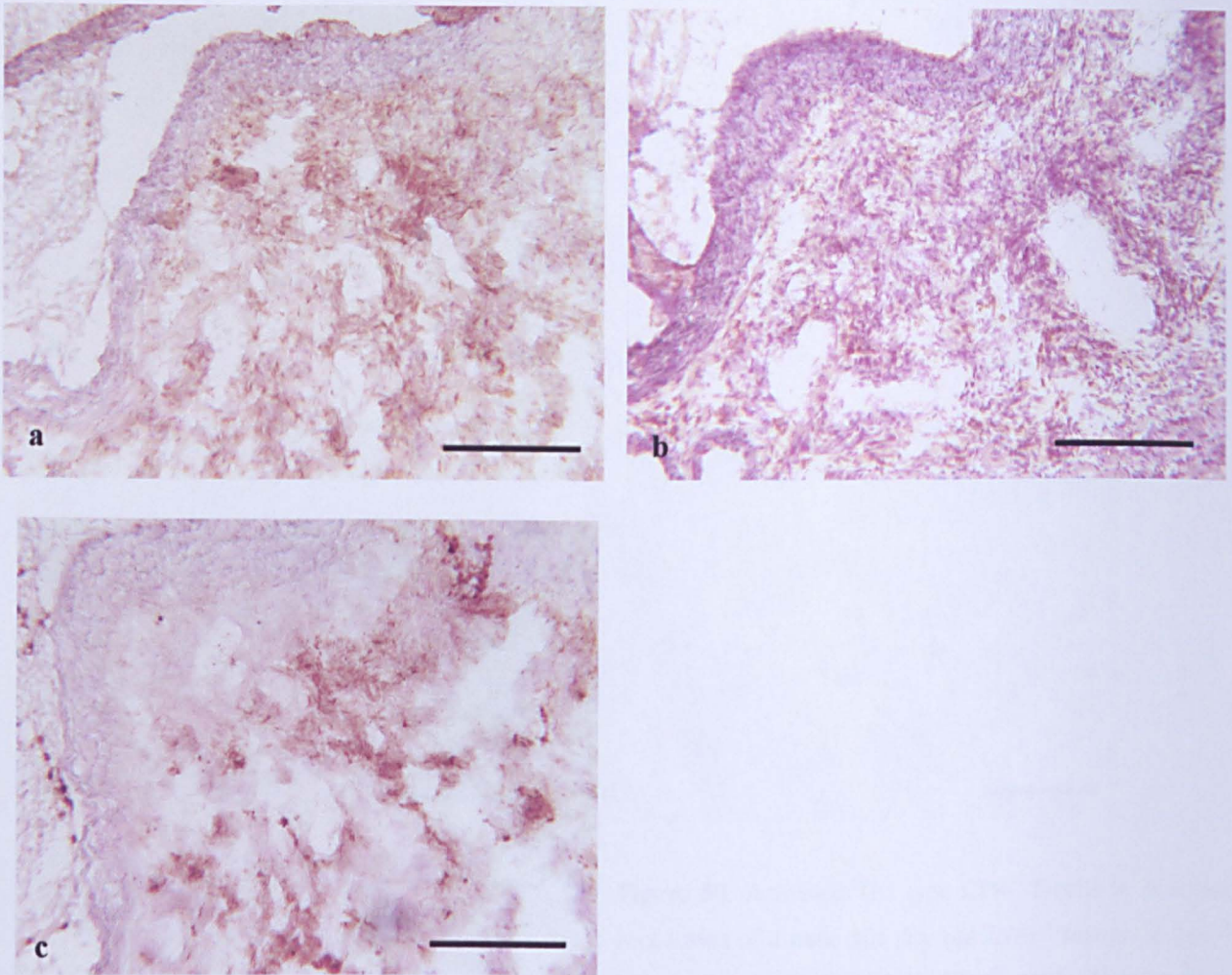


Figure 51: Sections stained for a) F4/80⁺ cells (macrophages) and b) IL-1β⁺ cells reveal activated macrophages in the aortic root lesion of a 105 day old *Il1rn*^{-/-} mouse. A section of aortic root lesion from the same mouse stained for neutrophils reveals their presence in large numbers (c). Scale bar = 200 μm.

Figure 52: Activated endothelium in the aortic root lesion of a 105 day old *Il1rn^{-/-}* mouse

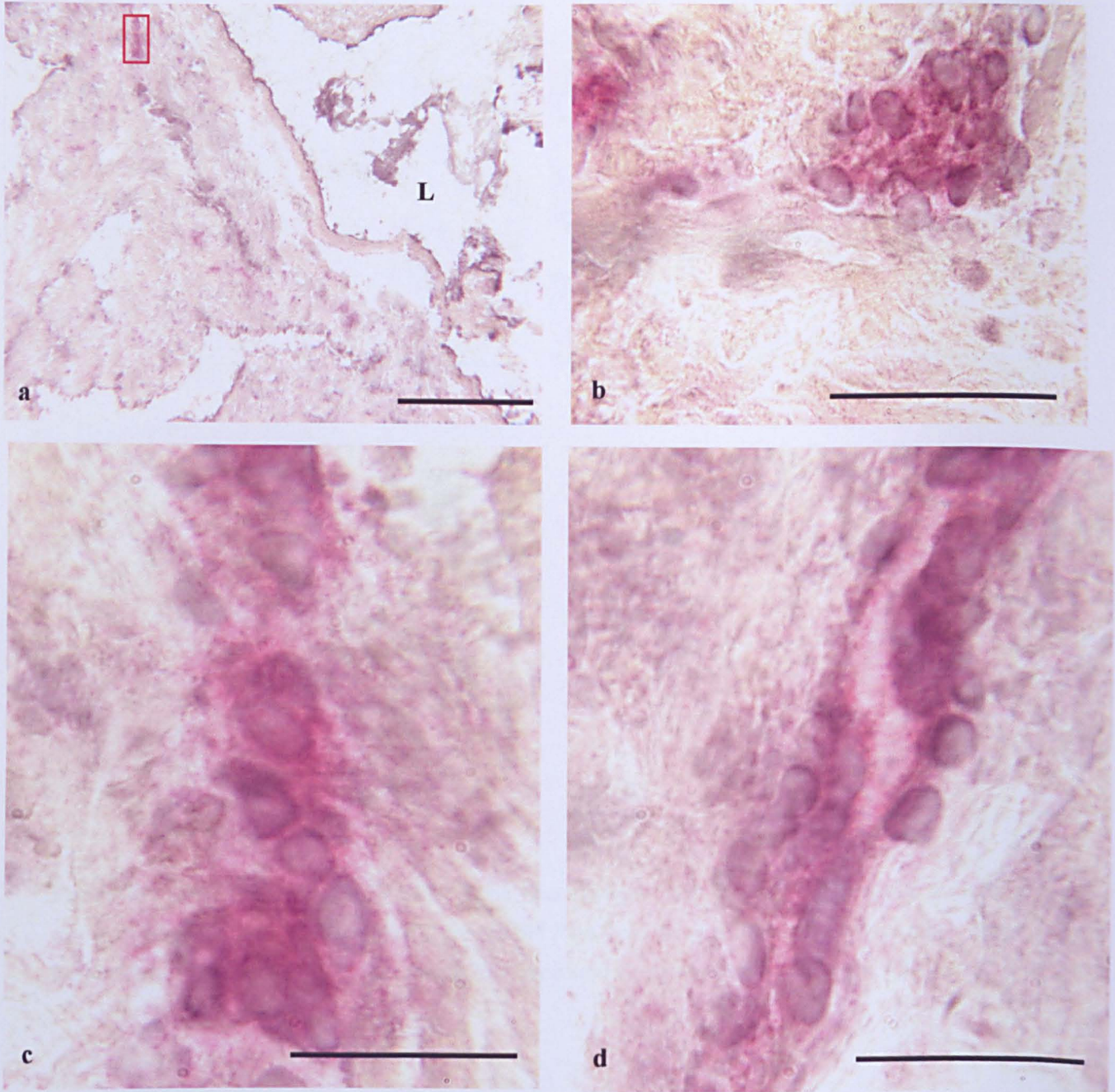


Figure 52: Lesional aortic root sections from a male 105 day old *Il1rn^{-/-}* mouse double stained for CD31 (endothelial cells, black) and CD62e (E-selectin, red). The double staining demonstrates the co-localisation of CD31 and CD62e to the same cells. c) is a higher power magnification of the boxed area in a. In this example, the microvasculature surrounding the main vessel (L = vessel lumen) is activated. Scale bar in a = 200 μm , scale bar b-d = 40 μm .

Figure 53: Cellular infiltrates and elastin damage in aortic roots of *Il1rn*^{-/-} mice aged >125 days

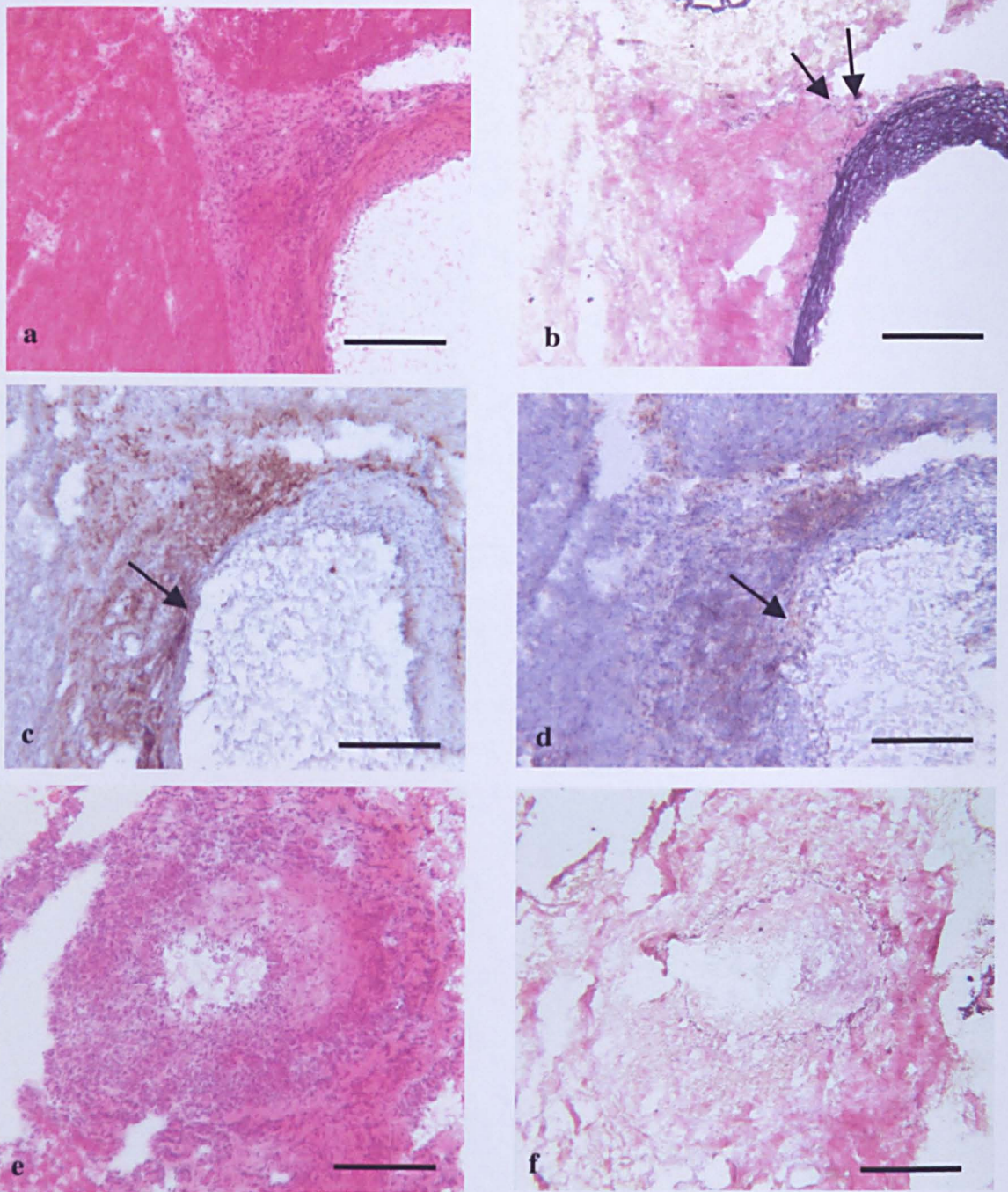


Figure 53: 7/8 *Il1rn*^{-/-} mice aged over 125 days had aortic root lesions with a cellular infiltrate score of 2 or 3, whilst 3/4 had elastin damage scores of 3. One mouse (shown in a-d) aged 125 days, had a cellular infiltrate score of 3, with inflammatory cells permeating all layers of the vessel wall, but an elastin damage score of only 1. a) haematoxylin and eosin stain, b) stained for connective tissue. Arrows indicate where the outer elastin layers are fragmented. c) and d) show aortic root sections of the same mouse stained for F4/80⁺ and IL-1β⁺ cells respectively. Activated macrophages can be seen in all layers of the vessel wall, including at the luminal surface (arrows). e) and f) are aortic root sections from a 125 day old *Il1rn*^{-/-} mouse with cellular infiltrate and elastin damage scores of 3, stained with haematoxylin and eosin and for connective tissue. Scale bar = 200 μm.

Figure 54: Undamaged aortic root in one 154 day old *Il1rn*^{-/-} mouse

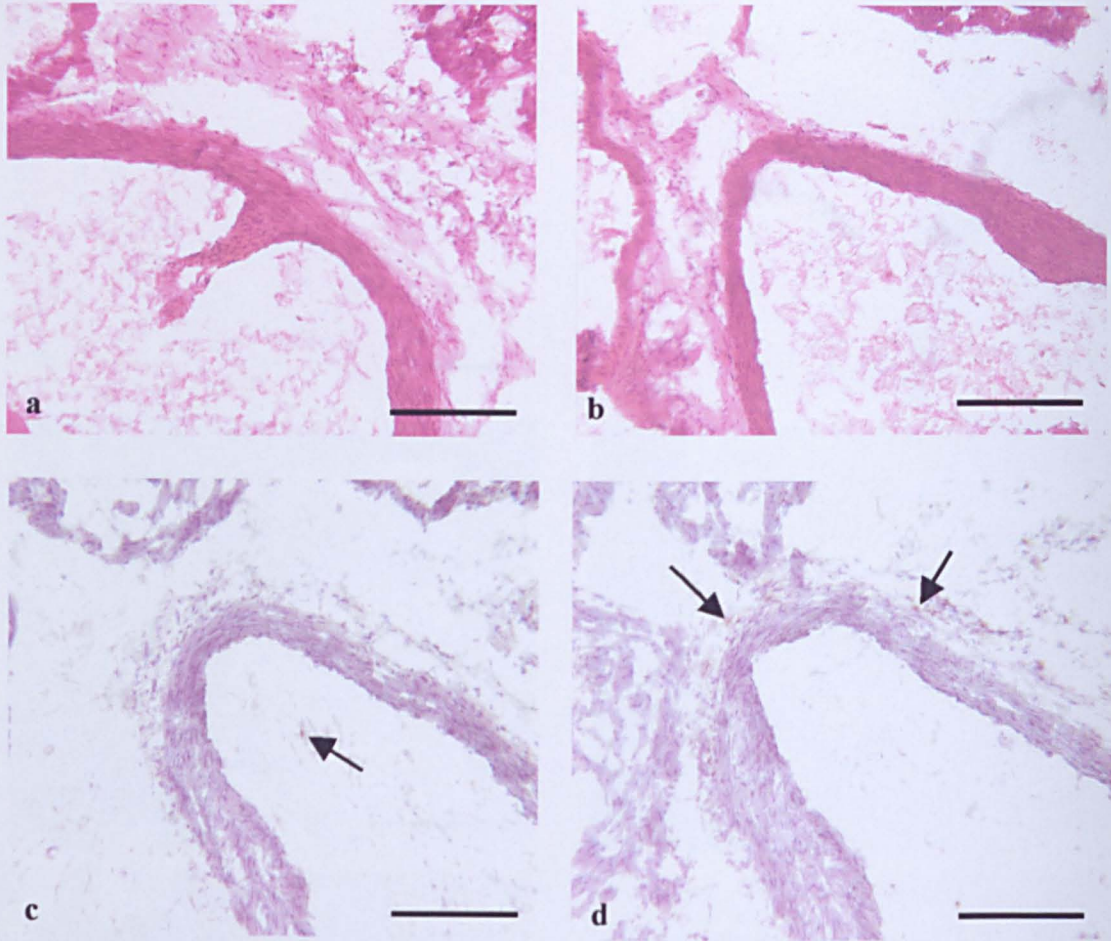


Figure 54: The aortic root from one male *Il1rn*^{-/-} mouse aged >125 days old (154 days old) appeared unaffected by arteritis. a) and b) haematoxylin and eosin stained sections of aortic root, with no visible cellular infiltrate. c) and d) aortic root from the same mouse stained for CD4⁺ and F4/80⁺ cells. Only similar numbers of bystander cells to those seen in wild-type mice stain positively (arrows). Scale bar = 200 μ m.

IL-5 (< 5 cells) (Figure 47). CD8⁺ T-cells, although present, were rare in comparison to CD4⁺ T-cells (<10% of the CD4⁺ T-cells) (Figure 44). E-selectin expression on CD31⁺ endothelial cells of the microvasculature was also visible at this stage of lesion development (Figure 48).

At 105-108 days old (Set 4), 2/4 *Il1rn*^{-/-} mice appeared unaffected, 1 mouse scored 2 for cellular infiltrate and 1 mouse scored 3 (Figure 49). 2/2 *Il1rn*^{+/+} mice were unaffected and 1/1 *Il1rn*^{+/-} mouse scored 1. The lesions appeared similar to those in previous sets with the same cellular infiltrate scores (Figures 50, 51 and 52). A full survey of the major arterial system was not undertaken, so it is possible that any of these mice had lesions away from the aortic root. Previous findings [Nicklin *et al.*, 2000] would indicate that in the older animals, this is likely to be the case.

In the oldest age group, >125 days old (Set 5), complete degradation of all elastic layers of the vessel wall could be seen at the most affected site in 3/4 *Il1rn*^{-/-} animals checked, with cellular infiltrate permeating all layers of the vessel wall at the areas of elastin destruction. One *Il1rn*^{-/-} animal had less severe damage to the elastin (score 1), although it had a severe inflammatory infiltrate (score 3) (Figure 53). A score of 0 for cellular infiltrate was given to 1 of the 8 *Il1rn*^{-/-} mice within this set (Figure 54), whilst 6 scored 3. In older animals of this age group there was also evidence of repair, with fibrosis, excess collagen and new and repaired elastin layers which were thickened and disorganised.

Figure 55: Activated CD4⁺ T-cells in aortic root lesions from *Il1rn*^{-/-} mice aged >125 days

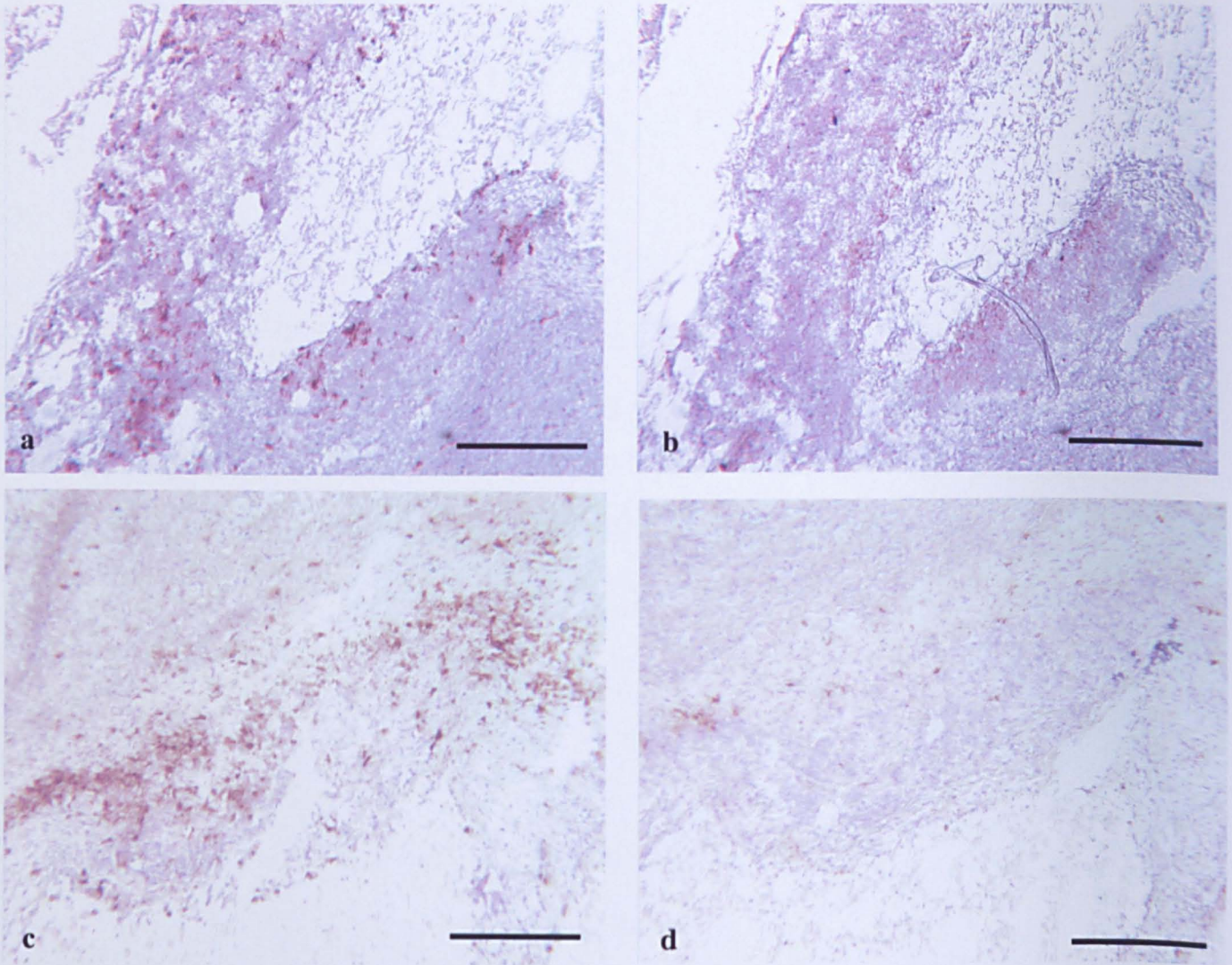


Figure 55: CD4⁺ T-cells in aortic root lesions of two male *Il1rn*^{-/-} mice aged 131 days. a) and c) are sections stained for CD4. b) is stained for IFN γ , and d) is stained for CD8. In all cases, brown staining indicates positively stained cells. The production of IFN γ suggests the CD4⁺ cells are of the Th1 type (a and b). CD8⁺ T-cells are relatively rare in comparison to CD4⁺ T-cells (c and d). Scale bar = 200 μ m.

Figure 56: Activated macrophages in the aortic root lesion of an *Il1rn*^{-/-} mouse aged >125 days

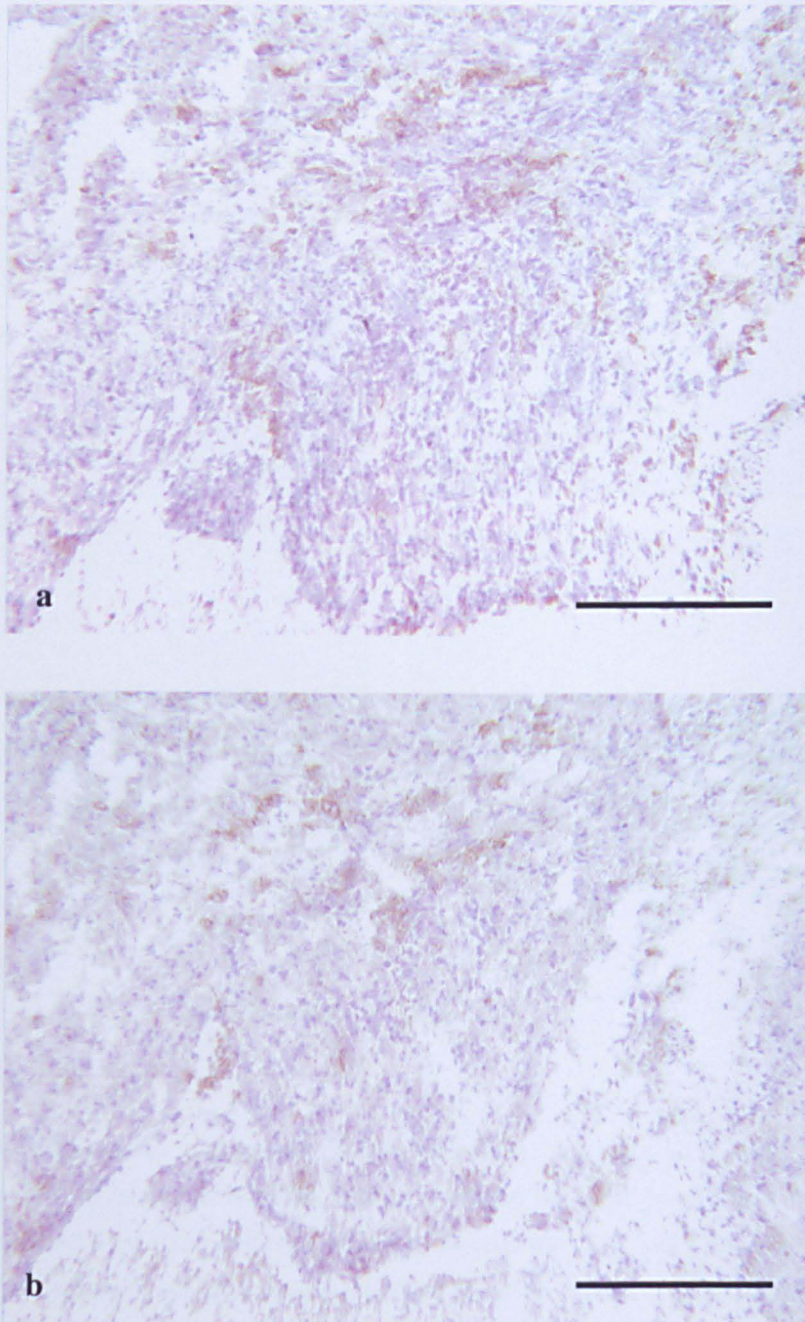


Figure 56: Activated macrophages secreting IL-1 β in the aortic root lesion of a male 131 day old *Il1rn*^{-/-} mouse. Sections are stained for a) F4/80 and b) IL-1 β . Brown staining indicates F4/80⁺ or IL-1 β ⁺ cells. Scale bar = 200 μ m.

Figure 57: Dendritic cells and abundant neutrophils in aortic root lesion of *Il1rn*^{-/-} mouse aged >125 days

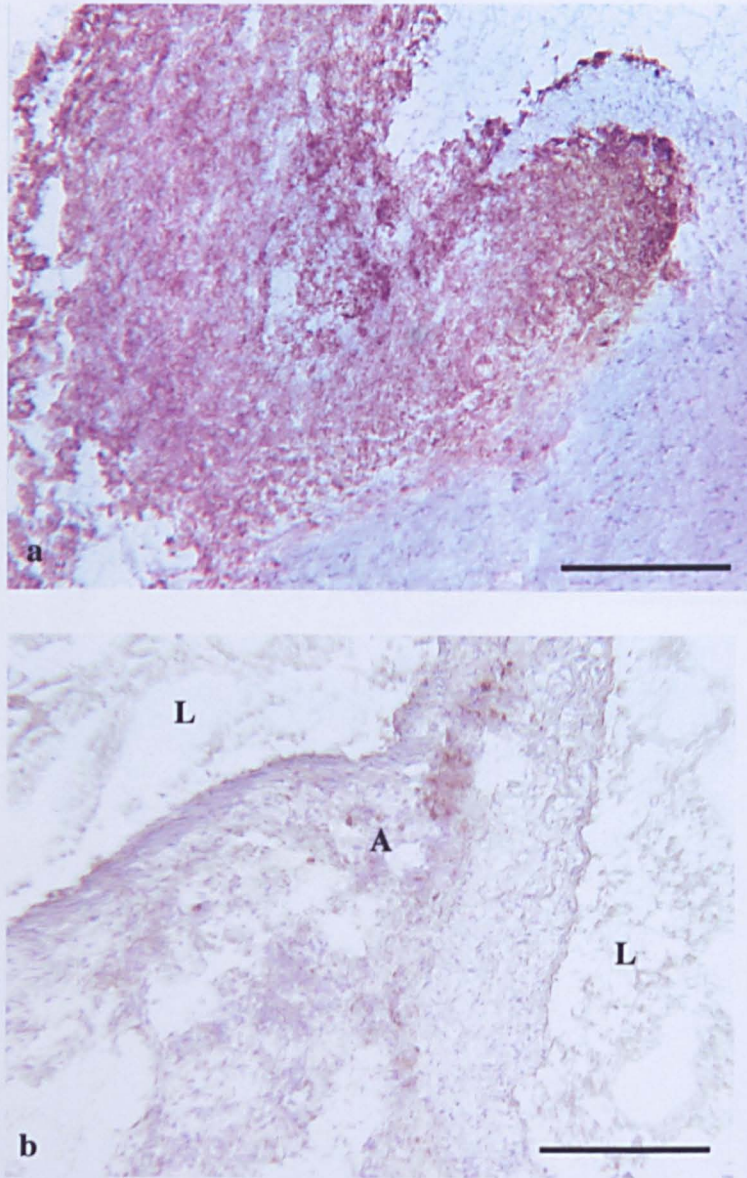


Figure 57: Aortic root lesion from a male 131 day old *Il1rn*^{-/-} mouse. a) brown staining indicates cells staining positively as neutrophils, which are abundant and found in all areas of the lesion. b) aortic root lesion from a 131 day old *Il1rn*^{-/-} mouse, stained for DEC205, a dendritic cell marker. Brown staining indicates DEC205⁺ cells. L = vessel lumen, A = lesional area. Scale bar = 200 μ m.

Figure 58: Activated endothelium in aortic root lesions from *Il1rn*^{-/-} mice aged >125 days

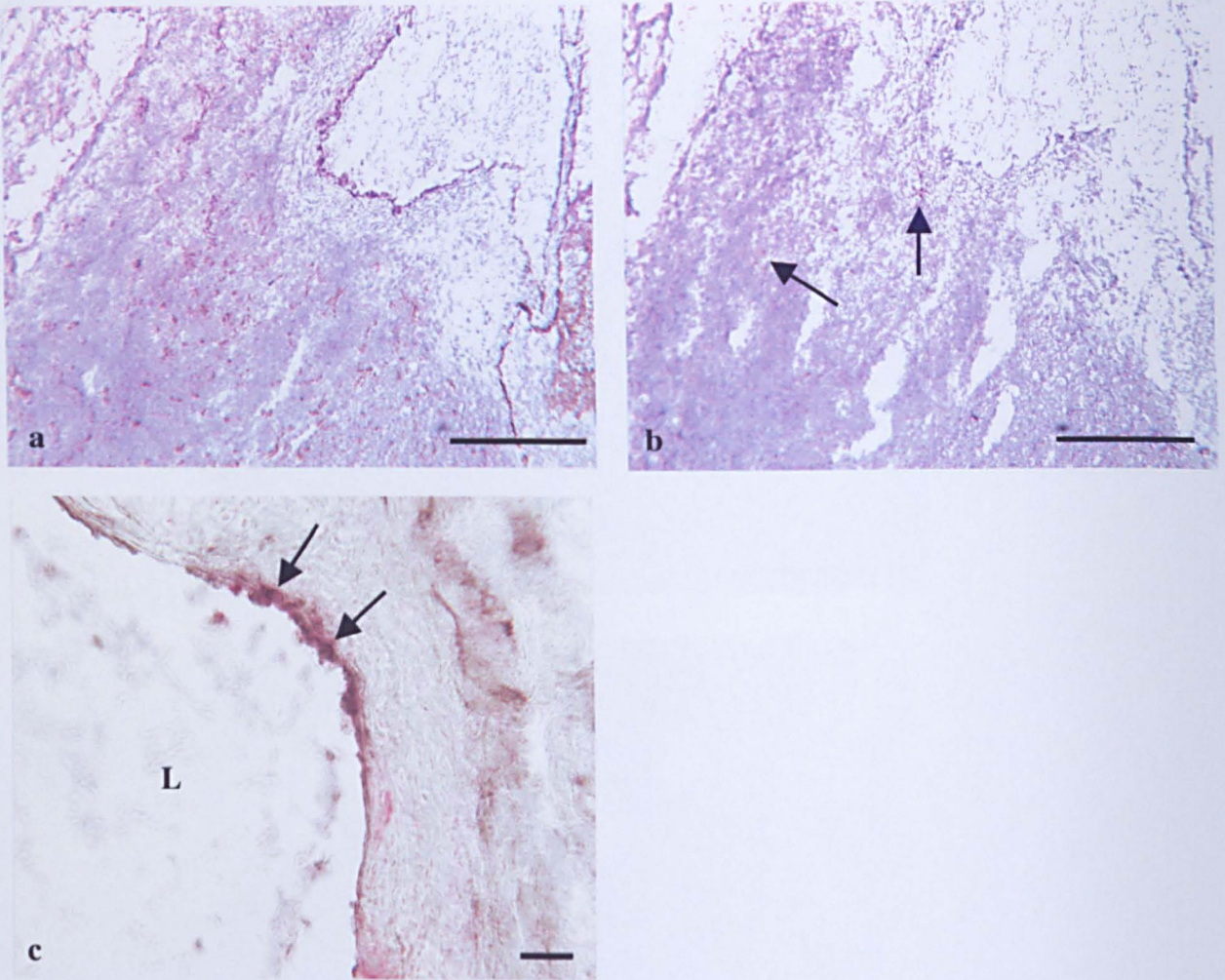


Figure 58: Activated endothelium in the aortic root lesions from two *Il1rn*^{-/-} mice aged >125 days. In a and b (male *Il1rn*^{-/-} mouse aged 131 days), brown staining indicates a) CD31⁺ (endothelial) cells, b) CD62e⁺ (E-selectin) cells. Examples of CD62e⁺ cells are indicated by arrows. c) aortic root lesion from a 125 day old *Il1rn*^{-/-} mouse, double stained for CD31 (brown/black) and CD62e (red). In this example, endothelial cells on the luminal surface of the vessel are activated and expressing E-selectin (arrows). L = vessel lumen. Scale bar in a & b = 200 μ m, c = 40 μ m.

Figure 59: ICAM-1 production in the aortic root lesion of an *Il1rn*^{-/-} mouse aged >131 days

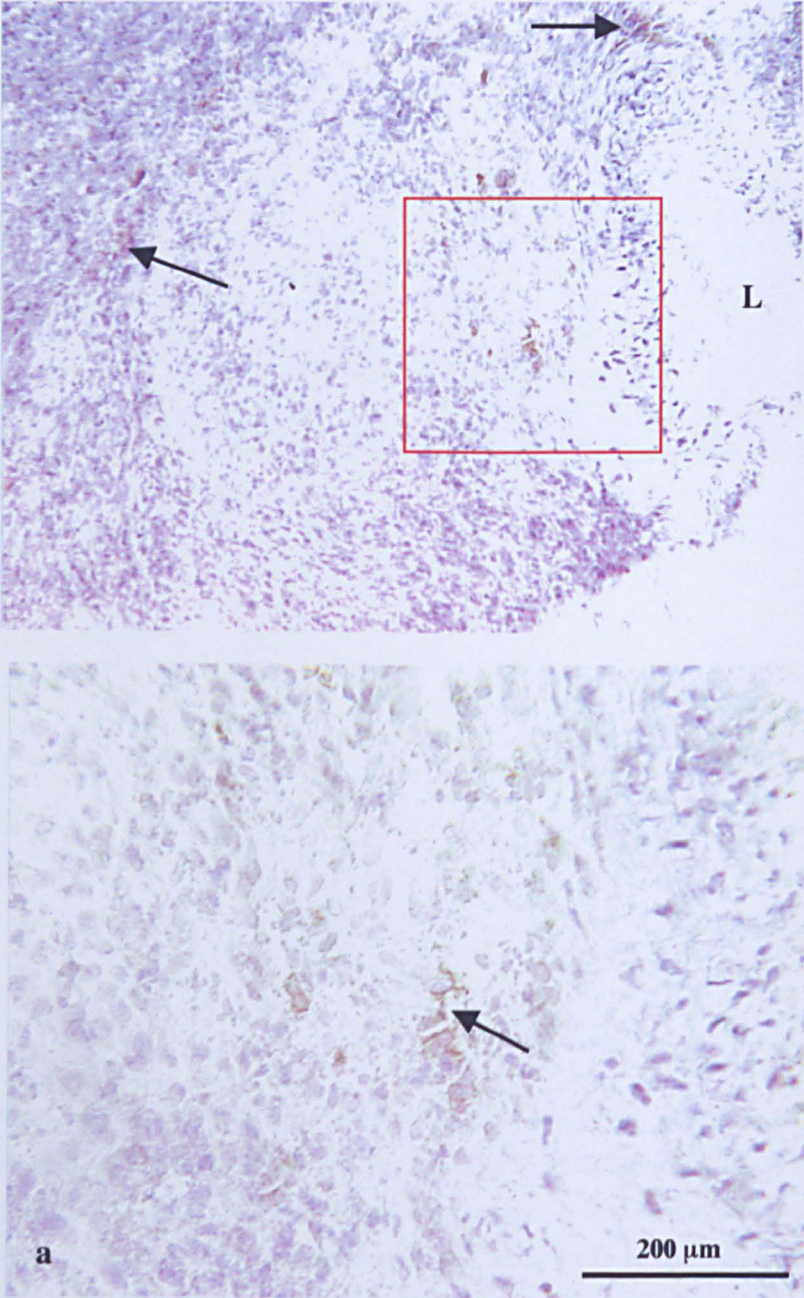


Figure 59: The adhesion molecule ICAM-1 is produced in the advanced arteritic lesions of *Il1rn*^{-/-} mice. The example above shows the aortic root lesion of a male *Il1rn*^{-/-} mouse aged 131 days. b) is a higher power magnification of the boxed area in a). Examples of CD54⁺ (ICAM-1) cells are indicated by arrows. L = vessel lumen.

Figure 60: Chemokine production in aortic root lesions of *Il1rn*^{-/-} mice aged >125

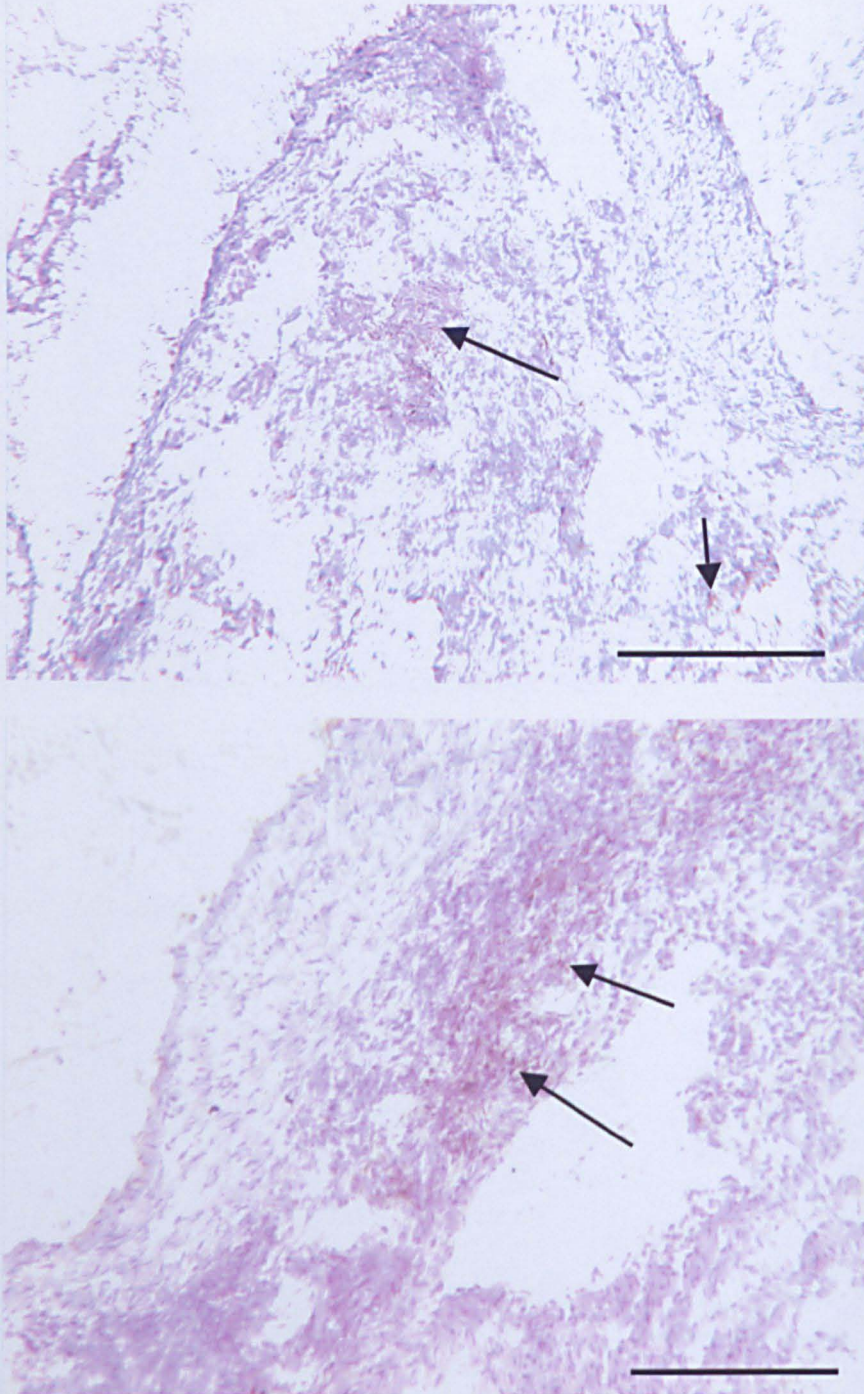


Figure 60: MCP-1 production in aortic root lesions from two male *Il1rn*^{-/-} mice, both aged 131 days. Examples of cells staining positively (brown) for MCP-1 are indicated by arrows. Scale bar = 200 μ m.

Aortic root lesions from this age group which scored 2 and 3 contained the same cell types and activation markers as lesions in younger mice (i.e. abundant CD4⁺ T-cells producing IFN γ (Figure 55), abundant macrophages producing IL-1 β (Figure 56), large numbers of neutrophils and dendritic cells (Figure 57), expression of E-selectin on endothelial cells (Figure 58), ICAM-1 expression (Figure 59), MCP-1 production (Figure 60), few CD8⁺ T-cells (Figure 55), few B-cells).

In all age sets, even at >150 days old, *Il1rn*^{+/+} mice appeared histologically normal. There was no cellular infiltrate and in all cases the elastin layers of the vessel walls were intact, unfragmented, and there was no evidence of any repair processes (see Figure 19). In each case there were a small number of circulating CD4⁺ T-cells and macrophages present, but they did not localise to the adventitial layers of the vessel walls, rather they were spread throughout the tissue (see Figure 33). These cells were not activated since there was no detectable production of IFN γ or IL-1 β , or any other inflammatory cells or markers (see Figure 34). We conclude that they are bystanders.

Il1rn^{+/-} appear to suffer from less severe arteritic lesions. 3/6 mice examined had lesions with a cellular infiltrate score of 1, whilst only 1/6 had a more severe infiltrate. In this animal, which was the oldest heterozygous animal examined, there was also a myocardial scar, indicative of a previous inflammatory event. This result is concurrent with previous observations [Nicklin *et al.*, 2000]. It appears that a single functional *Il1rn* allele is enough to provide a decreased

amount of IL-1ra production, but not to give complete protection from disease in the Sf3 background.

The inflammatory aortic root lesions found in *Il1rn*^{-/-} mice appear to progress from an initial small infiltrate of activated CD4⁺ T-cells (Th1 type) and macrophages, to a larger infiltrate composed of several different activated cell types and with the expression of chemokines and adhesion molecules. The infiltrates appeared to arise from the outer adventitial layers of the vessel walls, and progress towards the lumen of the vessel. Initially there was no visible damage to the elastin layers of the vessel walls, but as the lesions progressed and the infiltrates moved closer to the lumen the elastin became fragmented (from the outer layers inwards) and was eventually completely destroyed. In older lesions, the infiltrates, although remaining active, seemed smaller in comparison to lesions in younger mice, and the vessel walls had evidently undergone some repair processes, becoming fibrotic.

In all cases, aortic roots from *Il1rn*^{+/+} mice were unaffected, even at an advanced age.

The cell types and cytokine profiles present within the lesions, the advancing of the infiltrate from the outer layers of the vessel wall inwards, the elastin damage and the fact that older lesions were repaired and fibrotic, are all comparable to inflammatory arterial lesions found in the human.

3.3.5: Carriage of *H-2* haplotype in relation to sensitivity to arteritis

Two lines of *IIIrn^{-/-}* mice seemed to emerge in the early stages of inbreeding the colony, with differing and apparently heritable ages of onset of disease. One line appeared to be much more sensitive to the disease, and had a mean death age of 103 days. The other line seemed more resistant and survived for >1 yr, although at death, or culling at a late age, arterial inflammation was clearly present. It seemed plausible that the *H-2* haplotypes of the mice may be influencing their sensitivity to arteritis. In humans, the genetic basis for susceptibility to many diseases, including arteritis and RA, appears to lie within the MHC cluster, and several autoimmune mouse models such as NOD (non-obese diabetes), CIA and EAE (experimental autoimmune encephalitis) are highly *H-2* dependent. As the cellular components of the infiltrate resemble those involved in autoimmunity, and arteritis appears to be strain specific, it was postulated *H-2* haplotype may play a role in disease sensitivity. Due to the parentage of the colony, there were three possible alleles for *H-2* haplotype within the colony; one from the inbred 129/Ola parent of the ES cell carried in the chimaera (which is reported to be at least partly *H-2* haplotype *H2^b*) and two from the outbred Swiss mouse MF1. DNA from all individuals was not available, so their genotypes needed to be inferred retrospectively.

The aim was to deduce which *H-2* haplotypes were present within the colony, then investigate whether the animals' *H-2* haplotypes correlated with the age of onset of detectable illness as a result of arteritis. In this case, the end-point was always a report of malaise, noisy breathing (indicative of aortic stenosis), apparent organ infarction or sudden death.

Experimental procedure

PCR amplification was used to genotype five known polymorphisms across the *H-2*. The initial experiments were to genotype the mice at the *H2IEb* locus within the *H-2* Class II region where there is a polymorphic microsatellite that contains varying numbers of tandem repeats of the tetranucleotides TGGA and GGCA, according to *H-2* class II haplotype. By amplifying this region using PCR and sizing the products, it is possible to distinguish between several different *H-2* class II haplotypes.

Polymorphic markers in genes spread across the *H-2* were then tested in a similar manner, to deduce whether *H-2* class I genes exerted any influence over susceptibility to arteritis. These were in *H2K*, *H2Q4*, *Mog* and *H2M2*. *Mog*, which encodes myelin oligodendrocyte glycoprotein, is not a classic *H-2* class I gene but lies within the *H2M* cluster (see Figure 6).

The initial genotyping by amplification of the microsatellite within the *H2IEb* gene gave only two products, when three were possible. To test whether there was simply poor separation of two products which may be very close in size, secondary PCRs were performed with radiolabelled primers, using the primary PCR products as templates. The radiolabelled PCR products were run on 8% polyacrylamide gels, which were then placed on autoradiograph film to visualise the secondary PCR products.

Figure 61: Polyacrylamide gel electrophoresis of radiolabelled *H2IEb* PCR

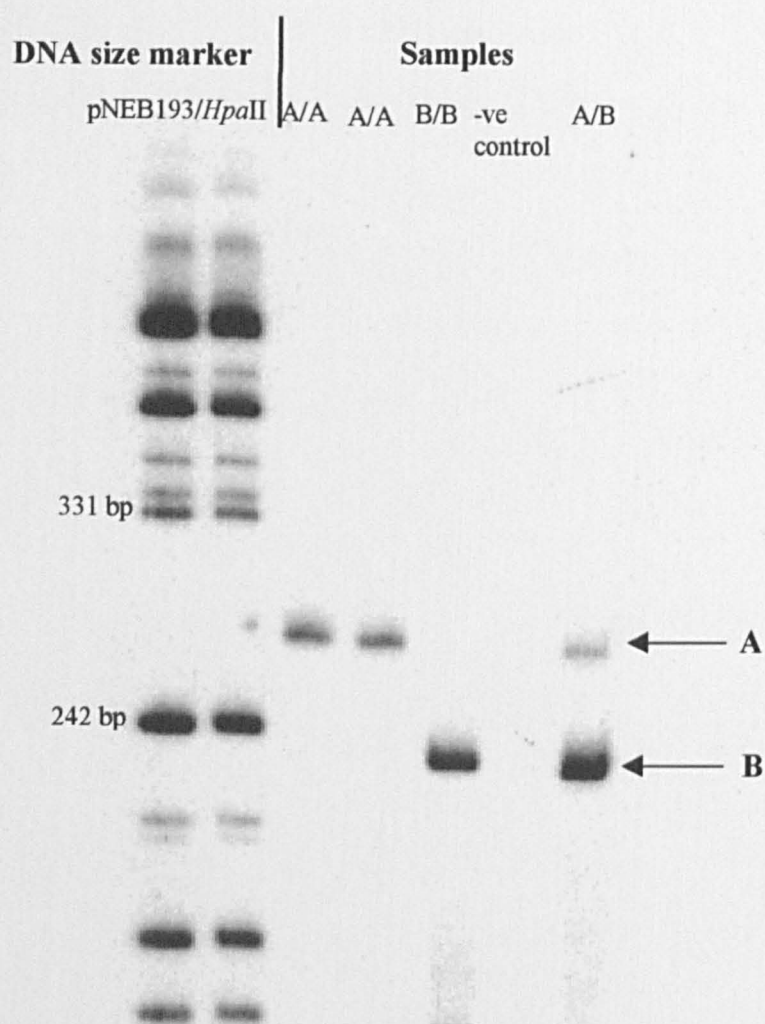


Figure 61: Polyacrylamide gel electrophoresis of radiolabelled PCR products from amplification of a microsatellite in *H2IEb* shows separation of only two products (A) and (B). Samples used appeared to be homozygous for the upper band A, the lower band B, or heterozygous after agarose gel electrophoresis of the primary PCR products.

Figure 62: Sequence of larger PCR product of H2IEb (haplotype H-2^u) microsatellite locus

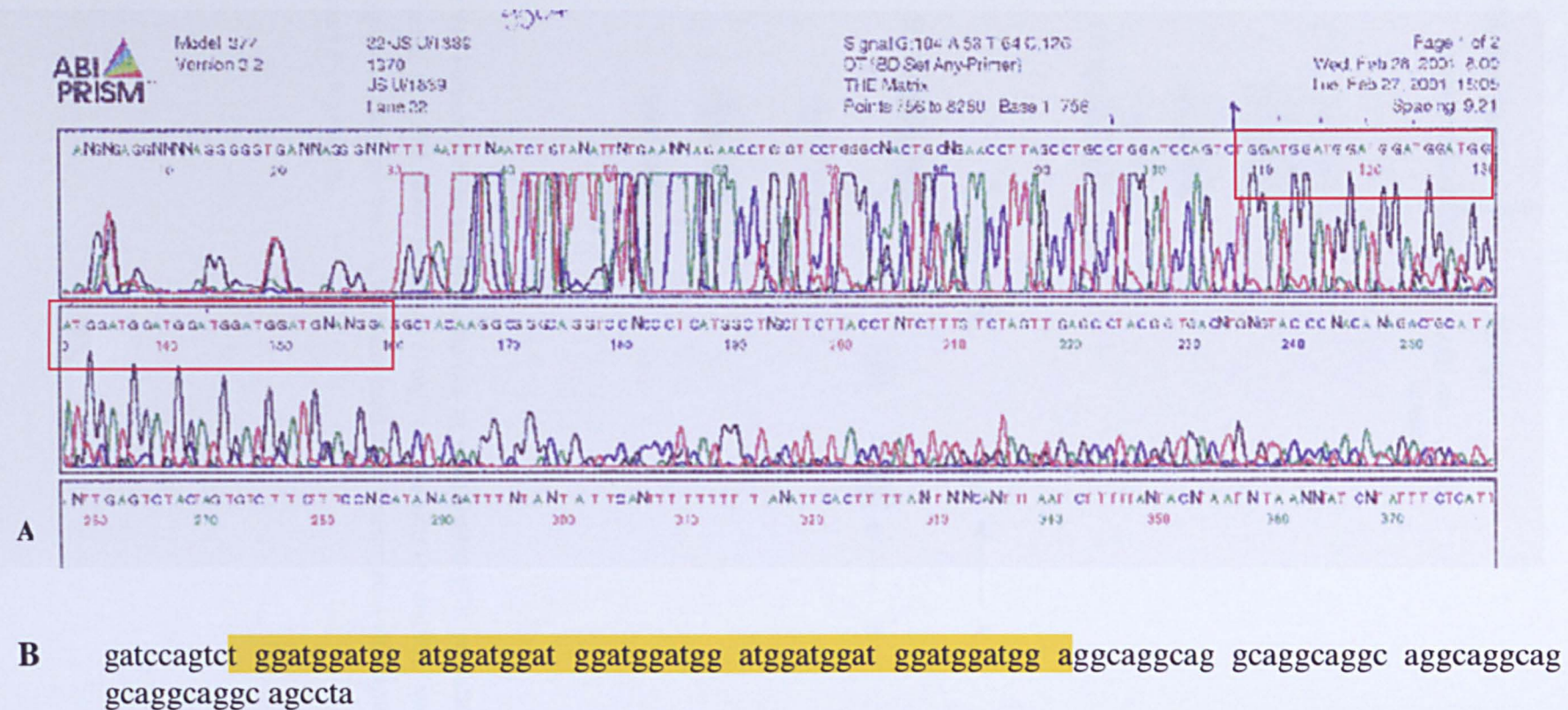
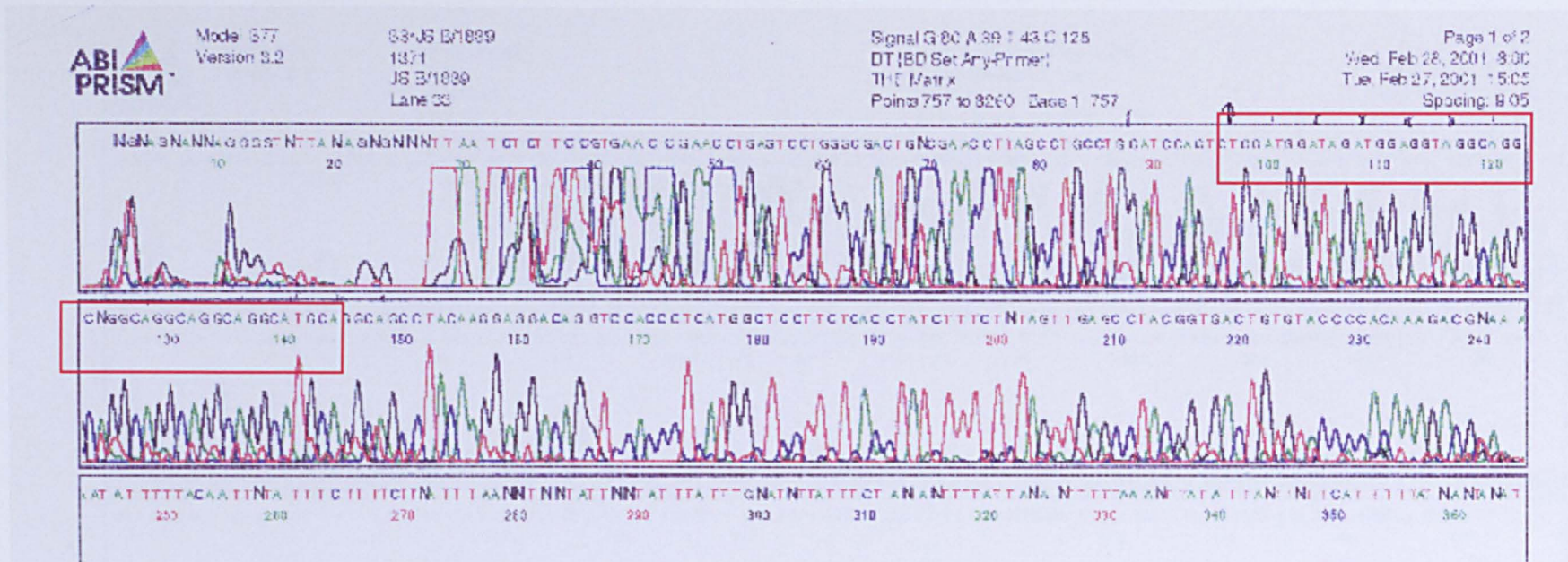


Figure 62: The sequence of the area highlighted in A corresponds to that highlighted in B. B is the microsatellite sequence for H2IEb^u, obtained from the nucleotide database at <http://www.ncbi.nlm.nih.gov>, accession no. U78804.

Figure 63: Sequence of smaller PCR product of *H2IEb* (haplotype H-2^b) microsatellite locus



B

2101 tgattctcc tgagagtgga gctgacagta aatttgaaa acagaacctg agtctctggc
 2161 gactgtagaa ccttagcctg cctggatcca gtctggatgg atagatggag gtaggcaggc
 2221 aggcaggcag gcaggcatgc aggcagccta caaggaggac agtccaccc tcattgctcc
 2281 ttctaccta tctttctcta gttgagccta cggtgactgt gtacccaca aagacacag

Figure 63: The sequence of the area highlighted in A corresponds to that highlighted in B. B is the microsatellite sequence for *H2IEb*^b, obtained from the nucleotide database at <http://www.ncbi.nlm.nih.gov>, accession no. M14236.

Figure 64: Comparison of PCR products from *H2IEb* microsatellite amplification between strains

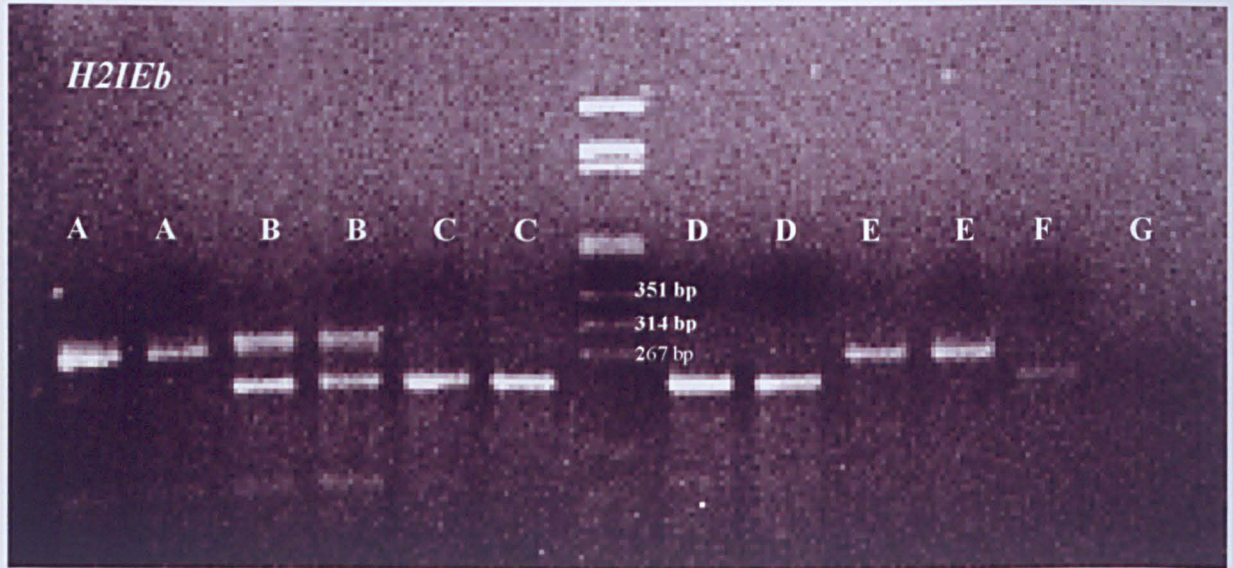


Figure 64: Comparison of PCR products from microsatellite amplification in the *H2IEb* gene between strains. A) Sf3 *H2IEb*^{w^u}, B) Sf3 *H2IEb*^{w^b}, C) Sf3 *H2IEb*^{b^b}, D) C57BL/6 *H2IEb*^{b^b}, E) Balb/c *H2IEb*^{d^d}, F) DBA/1 *H2IEb*^{q^q}, G) negative control. These results demonstrate that the b allele from Sf3 mice appears to be the same as the b allele from C57BL/6 mice, and that both the Sf3 b and u alleles are distinct from *H2IEb* d and q alleles.

Figure 65: *H-2* and Longevity

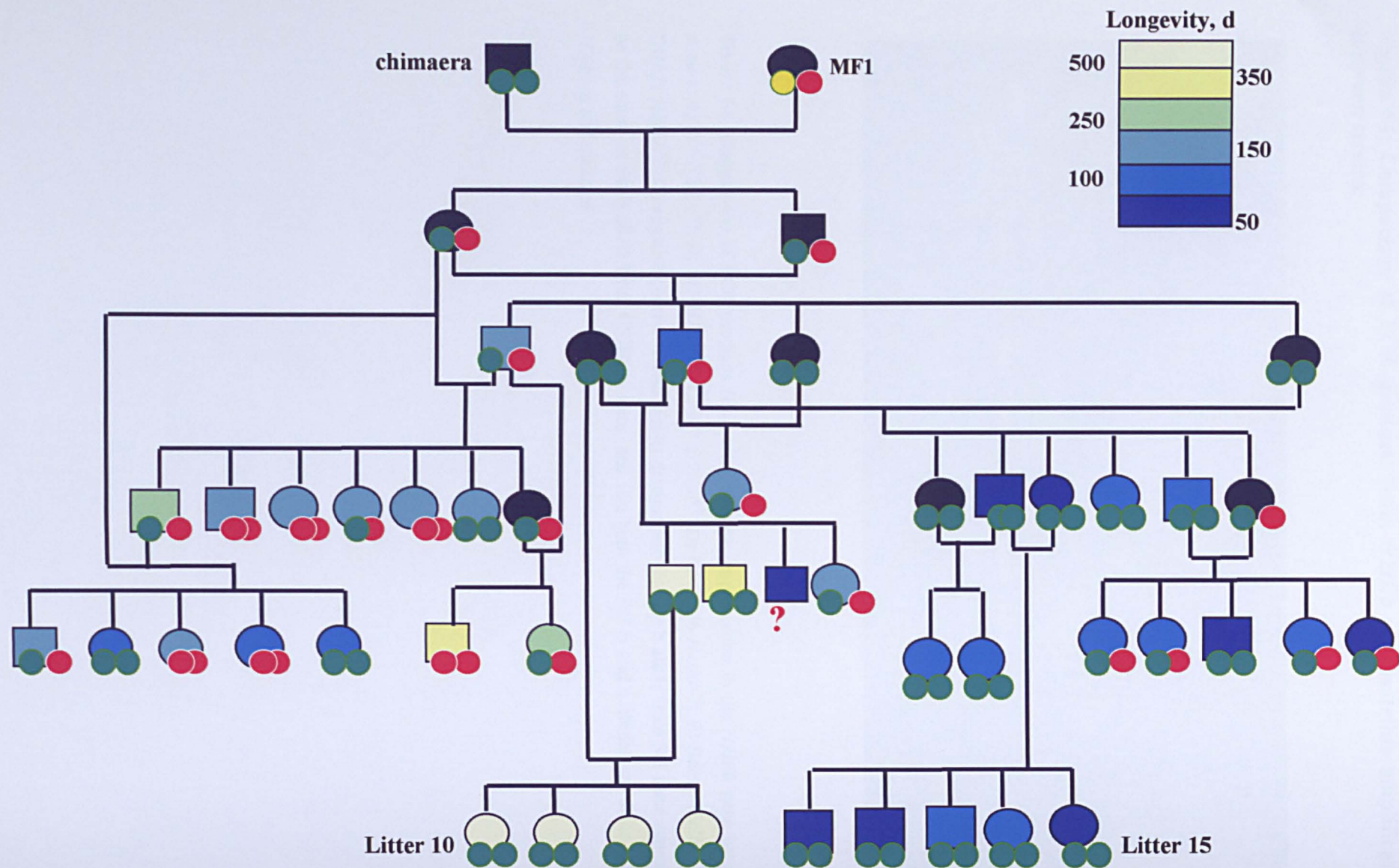


Figure 65: Carriage of H2IEb haplotypes in relation to longevity. Litters 10 and 15 (which were also genotyped for markers at H-2K, H-2Q4 and Mog) are labelled.

● Allele b (129) ● Allele b (MF1) ● Allele u

Figure 66: Radiolabelled PCR amplification of *H2IEb* microsatellite

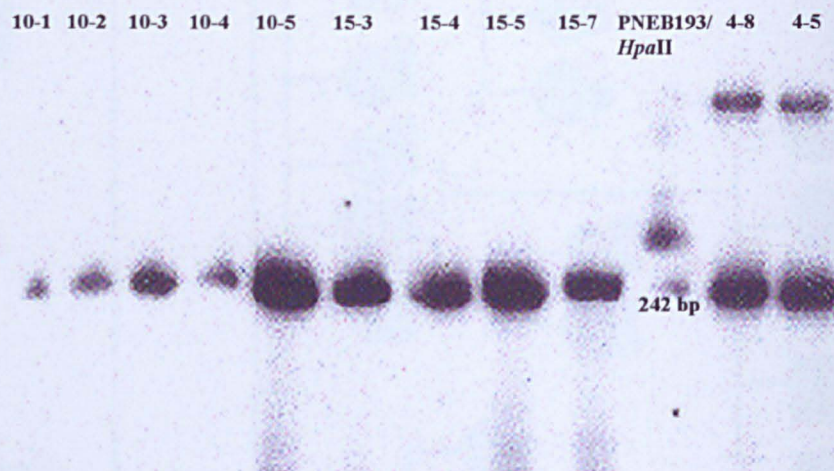


Figure 66: Radiolabelled PCR amplification of a microsatellite in the *H2IEb* gene shows that *Il1rn*^{-/-} animals from one sensitive (litter 10) and one non-sensitive (litter 15) litter are all of the same haplotype, *H2IEb*^{b/b} at this locus. Mice 4-8 and 4-5 were of haplotype *H2IEb*^{u/b}.

Figure 67: Amplification of microsatellite markers across *H-2* by PCR

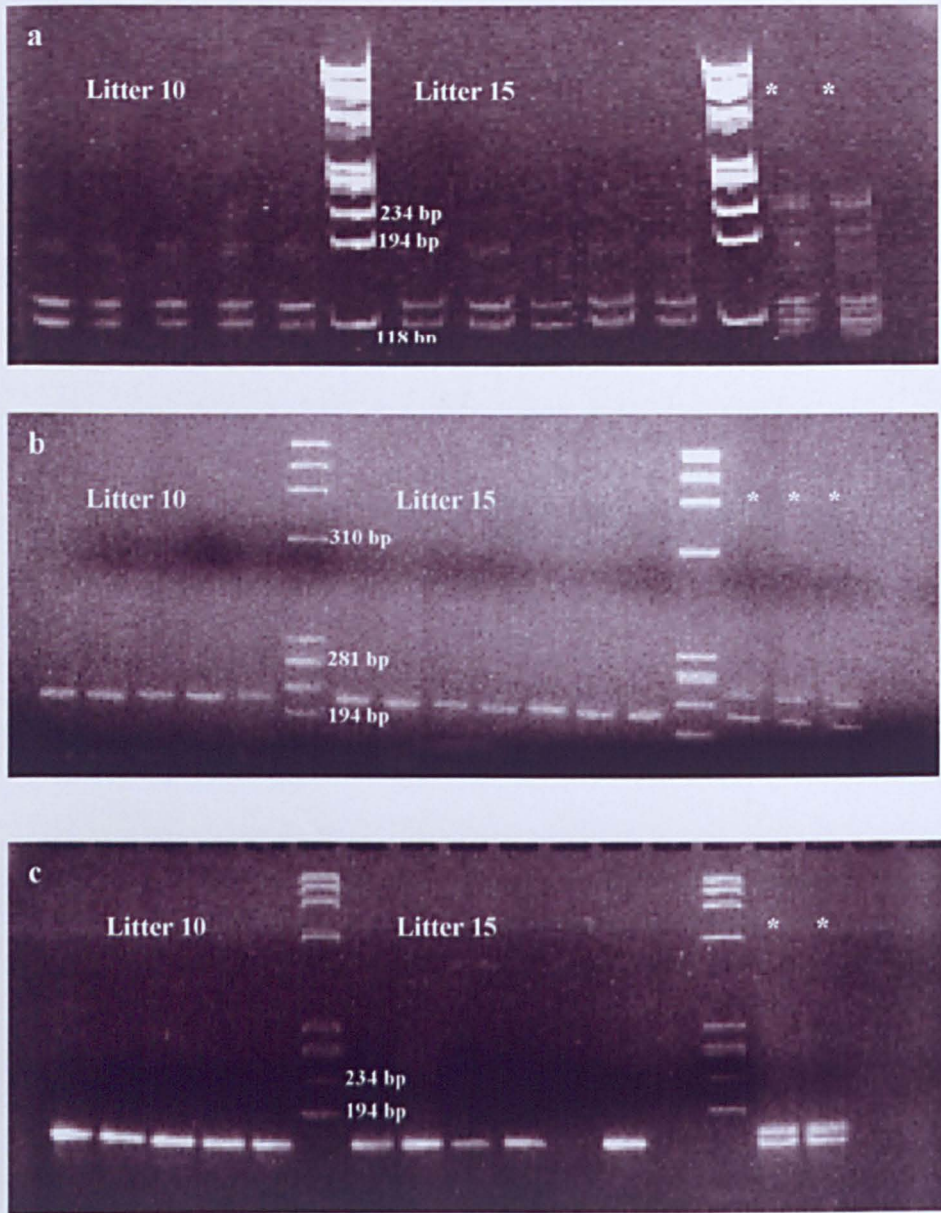


Figure 67: Amplification of microsatellite markers across *H-2* demonstrates that all animals from one sensitive (litter 10) and one non-sensitive (litter 15) litter are of the same genotypes at these loci. a) marker in *H-2K*, b) marker in *H-2Q4*, c) marker in *Mog*. * were animals which were heterozygous at *H2IEb*. The PCR products for *H-2K* are double bands (the heterozygotes have four bands).

Again, only two products were found (Figure 61). Since one of the alleles was known to be *b* from the 129 strain, it was concluded that the outbred MF1 mouse also carried the *b* allele and one other.

Sequence identification of H2IEb alleles

To confirm the presence of a band corresponding to the *H2IEb^b* allele, and to deduce the haplotype represented by the other PCR product, the bands were excised from TAE agarose gel, and the DNA purified and sequenced. The number of tetranucleotide repeats in each sequence were compared with those in *H2IEb* sequences from mice of different strains (Genbank (<http://www.ncbi.nlm.nih.gov>)), and the *H-2* class II haplotypes of the matching strains were then identified [Roderick & Guidi, 1990]. It was shown that the haplotypes were *H2IEb^b* (Figure 63) and *H2IEb^a* (Figure 62). *H2IEb^b* was also confirmed by genotyping alongside a C57BL/6(Harlan) mouse (a classic *H-2^b* strain) (Figure 64).

Animals from the first 18 litters, which had died spontaneously, and the founder MF1 mice were all genotyped at the *H2IEb* locus. This included 92 animals in total, 53 of which were *IIIrn^{-/-}*. All *IIIrn^{-/-}* mice from one sensitive and one non-sensitive litter were of the same haplotype, *H2^{b/b}* (Figure 65, Figure 66). Moreover, it could be deduced from the family tree that two of the most extreme litters had inherited both of their *H2^b* alleles from the founding chimaera. When *IIIrn^{-/-}* mice from these litters were then genotyped at *H2K*, *Mog* and *H2Q4*, it was again found that all animals were of the same haplotype (Figure 67). The *H2K* PCR gave double banded products for homozygotes, whilst heterozygotes

annealed to another site on the genome, however the important feature is that all mice from both litters were of the same haplotype at this locus. The polymorphism at *H2M2* was uninformative, in that it did not distinguish between the two known haplotypes. It was thus shown that there had been no recombination between the *H-2* markers tested.

Kruskall-Wallis test

To test statistically whether *H-2* haplotype at *H2IEb* contributes to age of death, a Kruskal-Wallis test (a one-way analysis of variance by ranks) was performed. This tests whether differences amongst samples signify population differences, or whether they represent normal variance found between samples from the same population.

The *H2IEb* genotypes for 53 *Il1rn^{-/-}* mice were tested. The ages of death were ranked from highest (1) to lowest (53), and these ranks were then placed in three groups (for *H2^{b/b}*, *H2^{u/b}* and *H2^{u/u}*). The mean rank of each group was then calculated.

n1 = 8	n2 = 15	n3 = 30
2	8	1
9	10	3
17	11	4
19	13	5
21	14	6
27	20	7
32	22	12
41	23	15
	24	16
	25	18
	28	26
	33	29
	38	30
	52	31
	53	34
		35
		36
		37
		39
		40
		42
		43
		44
		45
		46
		47
		48
		49
		50
		51
$\bar{R}_1 = 21$	$\bar{R}_2 = 24.9$	$\bar{R}_3 = 29.6$

$$\bar{R} = 25.2$$

N=53 (total number of samples)

k=3 (number of groups)

$H-2^{u/u}$ = group 1, $H-2^{u/b}$ = group 2, $H-2^{b/b}$ = group 3

n_j = number of animals in each group

$$n_j = n_1 = 8$$

$$n_2 = 15$$

$$n_3 = 30$$

\bar{R}_j = means in groups

$$\bar{R}_1 = 21$$

$$\bar{R}_2 = 24.9$$

$$\bar{R}_3 = 29.6$$

$$\bar{R} = 25.2$$

$$KW = \frac{12}{N(N+1)} \sum_{j=1}^k n_j (\bar{R}_j - \bar{R})^2$$

Where k = number of samples or groups

n_j = number of cases in the jth sample

N = number of cases in the combined sample (sum of n_j 's)

\bar{R}_j = sum of the ranks in jth or group

\bar{R}_j = average of ranks in the jth sample or group

\bar{R} = (N+1)/2 – the average of the ranks in the combined sample

In this case, KW = 2.35. Applied to the Chi-square table at 2 degrees of freedom (k-1), 2.35 is not significant at the 5% level ($p = 0.309$).

It can therefore be shown that the three haplotypes $H2IEb^{u/u}$, $H2IEb^{u/b}$ and $H2IEb^{b/b}$ are not significantly associated with age of death.

Only two *H-2* haplotypes were found ($H2^b$ and $H2^u$) rather than the expected three, therefore it is assumed that the outbred MF1 mouse was of haplotype $H2IEb^{b/u}$. From these results, it seems unlikely that *H-2* haplotype influences age of death from arteritis, since $Il1rn^{-/-}$ mice from sensitive and non-sensitive litters were all $H2IEb^{b/b}$. This is supported statistically by the results of the Kruskal-Wallis test. Moreover, $Il1rn^{-/-}$ mice on a C57BL/6 background do not appear to develop spontaneous arteritis [Nicklin *et al.*, 2000]. C57BL/6 mice are also *H-2* haplotype $H2IEb^b$. In addition, $Il1rn^{-/-}$ Balb/c mice, which are $H2IEb^d$, also develop arteritis. It is statistically likely that there is a single modifier gene involved in sensitivity in arteritis in IL-1ra null mice [M. Iles, personal communication] but from these results it does not appear to lie within the *H-2*.

3.3.6: *Helicobacter* infection in *Il1rn*^{-/-} mice

Bacterial infection in heart disease

Various studies suggest that *Chlamydia*, *H. pylori* and other micro-organisms may increase patient risk of development of inflammatory arterial disease [Muhlestein *et al.*, 1998; Folsom *et al.*, 1998]. Our colony of *Il1rn*^{-/-} mice, which suffer from arteritis, is housed under SPF conditions and have been shown to be free of infection by mouse *Chlamydia*. Murine *Helicobacter* infection however is not routinely assayed and is known to be widespread amongst laboratory mice.

In order to examine mice from our colony for evidence of infection by *Helicobacter* species, a PCR assay was performed which is designed to amplify a stretch of the 16S rRNA gene which is conserved across members of the genus *Helicobacter* [Riley *et al.*, 1996]. It is then possible to distinguish which species of *Helicobacter* is present by the use of restriction enzyme digests.

Genomic DNA from *Il1rn*^{-/-} and *Il1rn*^{+/+} mice from our Sf3 colony and from the C57BL/6 *Il1rn*^{-/-} colony in New York [Hirsch *et al.*], which are unaffected by arteritis, was assayed by PCR for evidence of infection by *Helicobacter* spp. All mice tested, both from our colony and from the Hirsch colony were infected with murine *Helicobacter*.

To determine which *Helicobacter* species was present in the colonies, restriction digest analysis was performed. From this result, it became clear that all mice

Figure 68: PCR amplification and restriction enzyme analysis of *Helicobacter* spp. rRNA

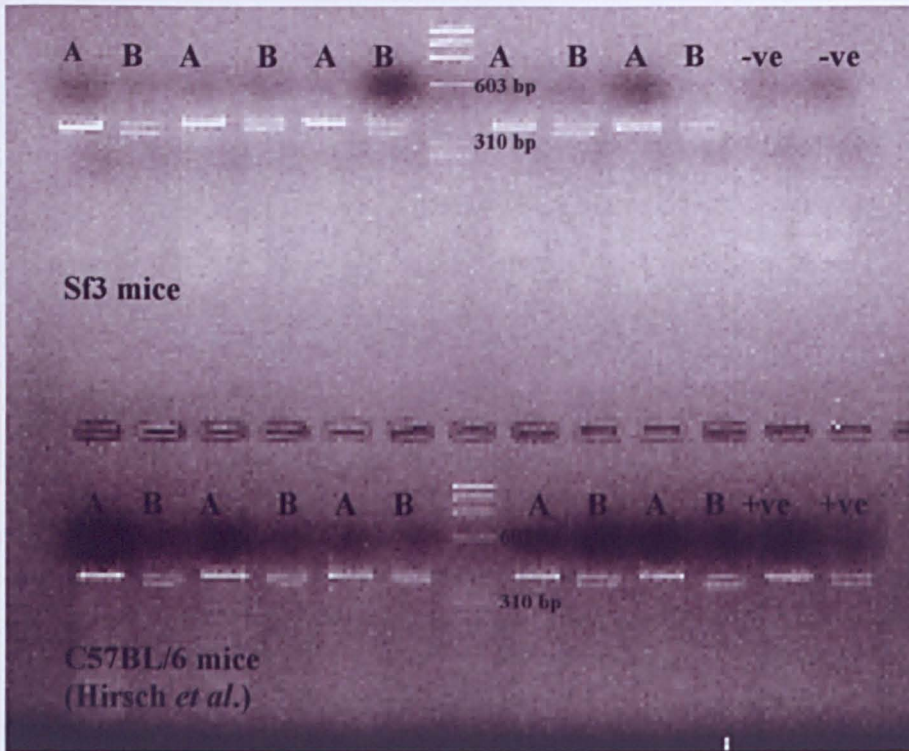


Figure 68: PCR amplification of *Helicobacter* rRNA demonstrated evidence of *Helicobacter* spp. infection in all animals tested, both from our colony and that of Hirsch et al. Which do not develop arteritis. A) PCR products B) PCR products digested with *Mbo*I, showing some undigested (375 bp) and digested (348 bp) product. This result indicates *Helicobacter hepaticus* infection. -ve) PCR negative controls, +ve) positive control for *H.hepaticus* rRNA supplied by L.Reily.

tested were positive for infection by the murine *Helicobacter hepaticus* (Figure 68).

Since all mice, even those which show no evidence of arteritis, were infected with *Helicobacter hepaticus*, it was concluded that *Helicobacter* infection does not play a causative role in the development of arteritis in *Il1rn^{-/-}* mice.

3.3.7: Measurement of the acute phase response in arteritis by measuring levels of SAA

Secretion of serum amyloid A is strongly enhanced (up to 1000-fold) during the acute phase response in the mouse [Kushner, 1982; Weinstein & Taylor, 1987; Meek *et al.*, 1989]. The gene responds to circulating IL-1 and IL-6 [Weinstein & Taylor, 1987]. It is increased non-specifically as a result of inflammatory stimuli (see section 1.1.5). In order to determine whether serum levels of SAA could be used as a diagnostic marker for the presence of arteritic disease in *Il1rn^{-/-}* mice, serum SAA levels were measured by ELISA in animals which were also examined histologically for arteritis.

Table 5: SAA levels in comparison to lesion development

Mouse I.D number	Age at death (days)	<i>Illrn</i> genotype	Cellular infiltrate	Elastin degradation	SAA ($\mu\text{g/ml}$)
134-08	23	-/-	0	0	15.8
137-03	24	-/-	1	0	12.7
150-01	56	-/-	1	0	12.9
150-05	56	-/-	1		13.1
144-05	75	-/-	1	1	16.3
151-01	81	-/-	0	0	12.8
151-02	81	-/-	3	3	35.1
133-02	105	-/-	3	3	24.8
133-08	105	-/-	0		35.1
149-01	106	-/-	2		12.9
149-03	106	-/-	0	1	15.4
140-01	154	-/-	3	2	35.4
140-02	154	-/-	0		14.6
154-02	163	-/-	2		13.1
150-06	56	+/-	1		13.5
149-04	106	+/-	1		14.0
137-01	24	+/+	0	0	13.3
137-02	24	+/+	0	0	13.9
148-03	108	+/+	0	0	14.0
148-06	108	+/+	0	0	14.3
145-02	151	+/+	0	0	22.4
145-03	151	+/+	0	1	13.8
153-06	193	+/+	0		14.0
151-09	220	+/+	0		14.3

SAA levels appear to rise detectably only in *Illrn*^{-/-} animals with advanced lesions (cellular infiltrate score of 3), although a slight increase was seen in 1 mouse which scored 1. In the oldest *Illrn*^{-/-} mouse tested, SAA levels were low, although the animal only had a cellular infiltrate score of 2. In all cases where the SAA level was raised, and the animals were found histologically to have advanced lesions, the animals did not appear outwardly ill and were apparently healthy when culled. Compared with reported levels of SAA activation [Kushner, 1982; Weinstein & Taylor, 1987] during inflammation, these elevations are small. SAA would appear to be of no value in investigating the onset of the disease.

3.4: Psoriatiform disease in Balb/c *Il1rn*^{-/-} mice

3.4.1: Introduction

As discussed in section 1.2.16, IL-1 potentially plays various roles in the development of psoriasis in humans. Sf3 *Il1rn*^{-/-} mice were backcrossed with Balb/c. After observing that a number of the Balb/c *Il1rn*^{-/-} mice, as early as F2, were suffering from reddened, scaly outer ears which appeared to be slightly thickened, a study was undertaken to investigate whether the mice were spontaneously developing a psoriasis-like disease.

3.4.2: Retrospective histological study of formaldehyde fixed ear skin sections

Experimental procedures

A retrospective study of the ears from Balb/c *Il1rn*^{-/-}, *Il1rn*^{+/-} and *Il1rn*^{+/+} mice, and some Sf3 *Il1rn*^{-/-} mice, which had been fixed in formaldehyde was undertaken. 7 Balb/c *Il1rn*^{-/-} mice were from an F2 of Balb/c and an *Il1rn*^{-/-} Sf3. A further 47 animals (31 *Il1rn*^{-/-}, 9 *Il1rn*^{+/-}, 7 *Il1rn*^{+/+}) were inbred (from N5 – N9 Balb/c *Il1rn*^{+/-} parents).

Outer ears were removed from formaldehyde fixed cadavers and were embedded in paraffin, sectioned and stained with haematoxylin and eosin to elucidate whether any of the signs of a psoriatiform disease (such as epidermal thickening, dermal infiltrate, acanthosis and the formation of epidermal rete pegs and Munro microabcesses) were present in ears which were reddened and scaly. Outwardly affected ear skin sections were compared immunohistologically with those from *Il1rn*^{-/-} mice which appeared unaffected, and with apparently unaffected ears from *Il1rn*^{+/-} and ^{+/+} mice. Formaldehyde fixed, paraffin embedded ear sections were

Figure 69: Psoriasiform features in inflamed ear skin sections from Balb/c *Il1rn*^{-/-} mice

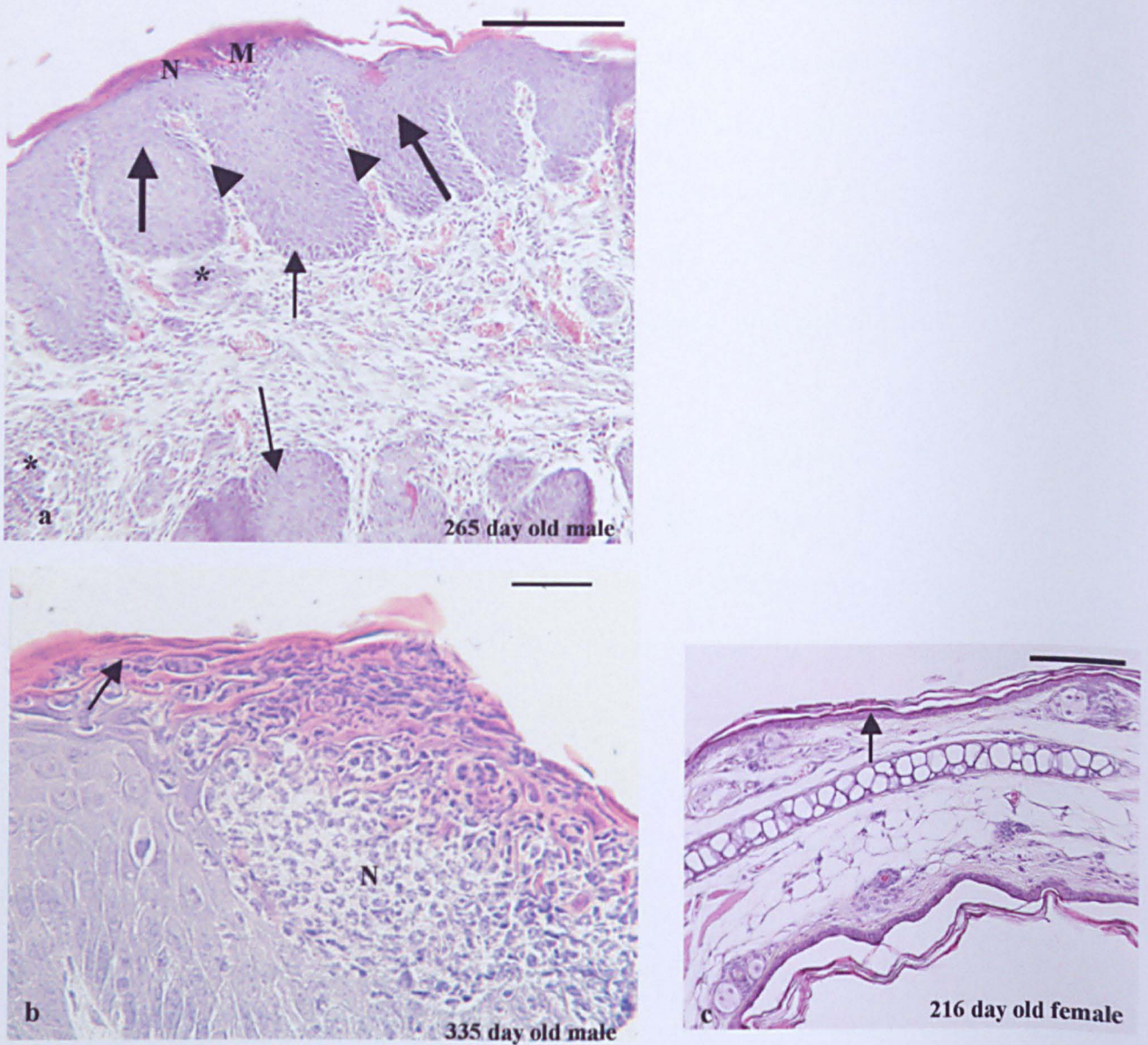
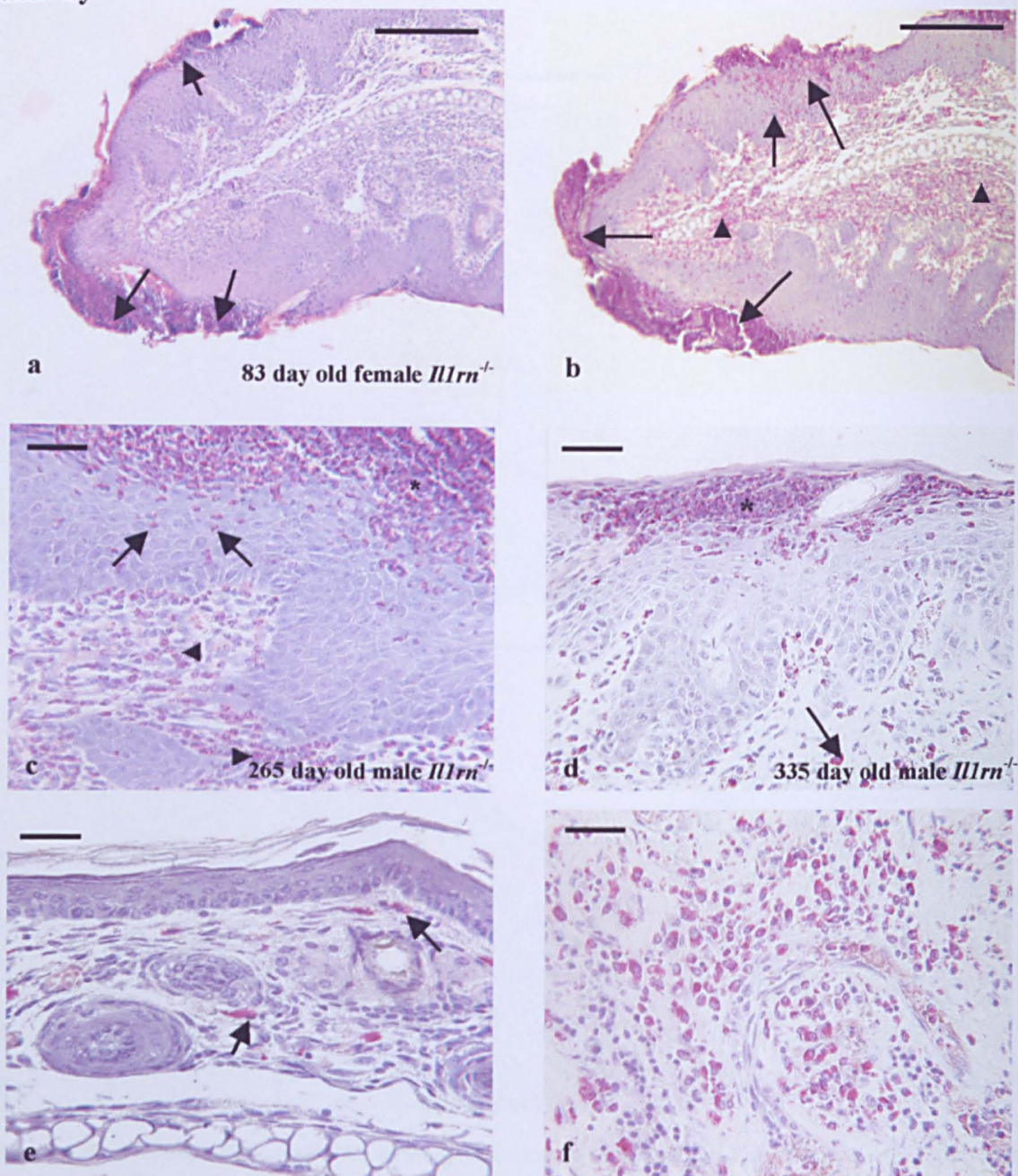


Figure 69: a) Haematoxylin and eosin staining of sections of inflamed ear from Balb/c *Il1rn*^{-/-} mice reveals several hallmarks of psoriasis, including acanthosis (thickened epidermis) (arrows), dermal cellular infiltrates (*), formation of epidermal rete pegs (thin arrows), elongation of dermal papillae (arrowheads), neutrophilic epidermal infiltrates (N), Munro microabscesses (M).

b) Higher power magnification of hematoxylin and eosin stained *Il1rn*^{-/-} epidermis showing neutrophil aggregation beneath the stratum corneum (N) and parakeratosis (retention of nuclei in stratum corneum) (arrow).

c) Hematoxylin and eosin stain of *Il1rn*^{+/+} ear section for comparison. Note lack of dermal infiltrate, rete peg formation, epidermal infiltrates or acanthosis (epidermis is normal, <5 cell s thick (arrow)). Scale bars in a & c = 200 μ m Scale bar in b = 40 μ m

Figure 70: Epidermal neutrophilic infiltrate as identified by chloroacetate esterase activity



- Haematoxylin and eosin stained inflamed ear tip, showing epidermal infiltrates (arrows)
- Same ear tip as in (a) stained for chloroacetate esterase activity (red staining). Note neutrophils within epidermis (arrows) and in dermal infiltrate (arrowheads).
- Higher power magnification of epidermal infiltrate. Note neutrophils visible within epidermis (arrows) and dermis (arrowheads) as well as underneath stratum corneum (*).
- As c). Also note mast cells within the dermis (arrow)
- Ear section from a wild-type animal. Note lack of neutrophils in dermis or epidermis, but some mast cells within dermis (arrows)
- Positive control for chloroacetate esterase staining – human bone marrow smear from leukaemia patient

Scale bars a & b = 200 μ m, c-f 40 μ m.

Figure 71: Haematoxylin and eosin scored ear skin sections

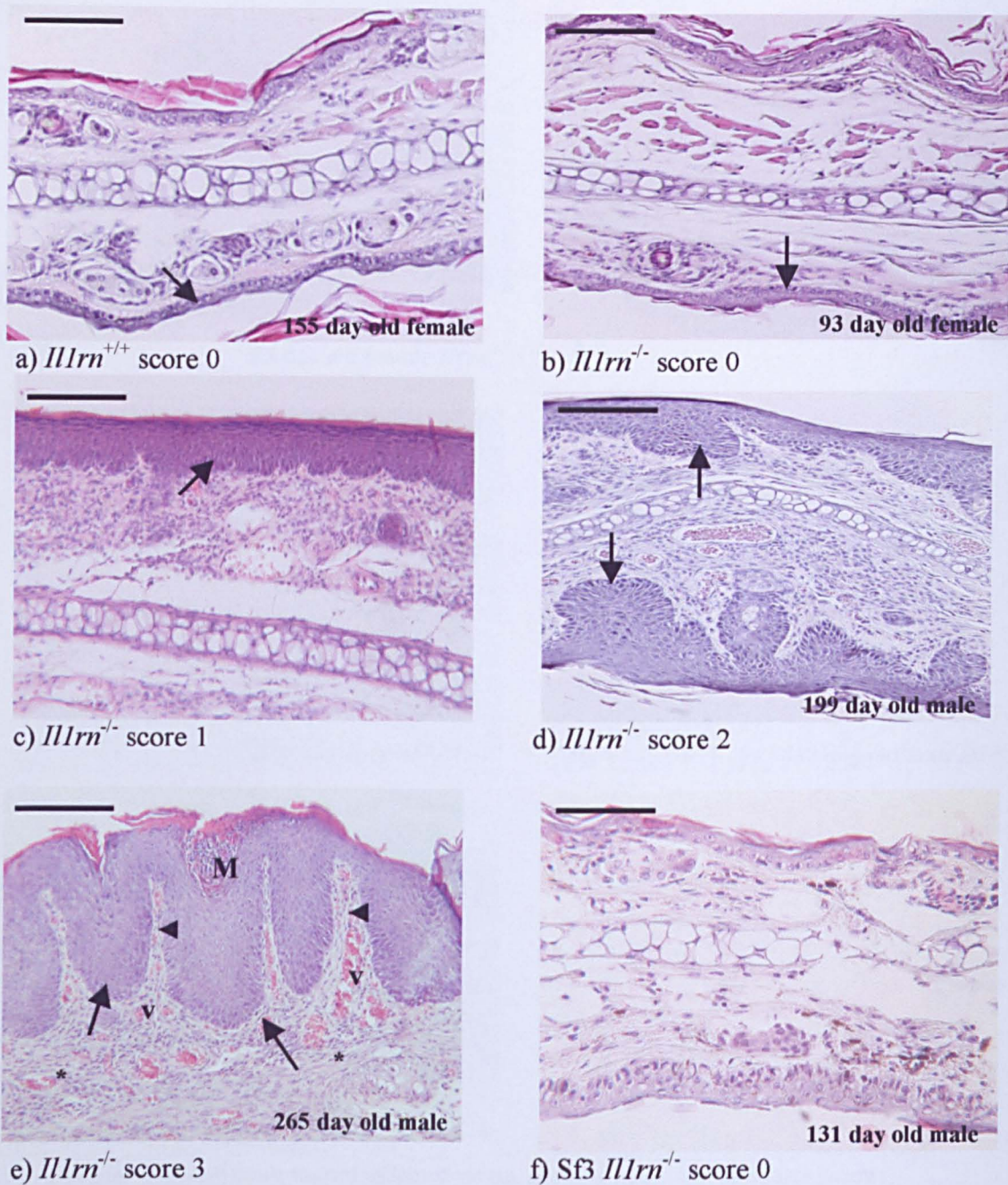


Figure 71: Examples of scored haematoxylin and eosin stained ear sections: a) and b) 0 for unaffected (epidermis < 5 cells thick) (arrow). c) 1 for a thickened epidermis of >5 cells thick (arrow). d) 2 for a thickened epidermis with the formation of epidermal rete pegs (arrows). e) 3 for the additional neutrophilic infiltration. In this example the extended rete pegs (arrows), the elongated dermal papillae (arrowheads), dermal infiltrate (*), increased number of small blood vessels (v) and the formation of a neutrophil-containing Munro microabscess underneath the stratum corneum (M) are all clearly visible. f) Sf3 *Illrn*^{-/-} ear, score 0. Scale bar = 200 μ m.

stained with toluidine blue to detect mast cells, since mast cell numbers are elevated in human psoriatic skin. They were also stained for chloroacetate esterase to detect neutrophils, since neutrophilic epidermal infiltrates and formation of neutrophil-containing Munro microabscesses are also a feature of human psoriatic skin.

Haematoxylin and eosin staining of formaldehyde fixed paraffin embedded ear sections revealed structural and cellular changes associated with psoriasis-affected skin in 6/7 *Il1rn*^{-/-} F2 and 24/31 N5-N9 Balb/c mice examined. These changes included dermal cellular infiltrates, acanthosis (thickening of the epidermis due to keratinocyte hyperproliferation), formation and elongation of epidermal rete pegs, elongation of the dermal papillae, neutrophilic epidermal infiltrates and the formation of Munro microabscesses as neutrophil aggregates beneath the stratum corneum, and an overall thickening of the ear (Figure 69).

The presence of large numbers of neutrophils was confirmed by staining formaldehyde fixed, paraffin-embedded sections for chloroacetate esterase. (Figure 70).

The extent to which the disease had affected the skin was noted by clinically scoring the haematoxylin and eosin stained paraffin embedded sections of ears. Scores were as follows: 0 for unaffected (epidermis < 5 cells thick), 1 for a thickened epidermis of >5 cells thick, 2 for a thickened epidermis with the formation of epidermal rete pegs, and 3 for the additional epidermal neutrophilic infiltration. (Figure 71). Of the 31 Balb/c *Il1rn*^{-/-} mice, 7 mice scored 0, 5 mice

scored 1, 3 mice scored 2 and 16 mice scored 3. 7/7 *Il1rn*^{+/+} mice scored 0, whilst 7/9 and 2/9 *Il1rn*^{+/-} mice scored 0 and 1 respectively. Of 5 Sf3 mice examined (3 *Il1rn*^{-/-}, 2 *Il1rn*^{+/-}), all scored 0. This number is relatively small, but more importantly, there is a lack of external signs of psoriatic disease throughout the Sf3 colony.

Table 6: Animals used in psoriasis study

Mouse I.D number	Sex	Back-ground	<i>Il1rn</i> genotype	Age at death (days)	Signs of illness	Ear score	Mast cells / mm ² (approx.)
123-03	M	Sf3	-/-	131		0	-
123-05	M	Sf3	-/-	131		0	-
135-02	F	Sf3	-/-	203		0	-
134-06	M	Sf3	+/-	203		0	-
135-05	F	Sf3	+/-	203		0	-
IB07-02	M	F2	-/-	117		1	81
IB05-03	M	F2	-/-	120		2	127
IB08-08	F	F2	-/-	211	BE	3	188
IB08-11	F	F2	-/-	211		3	110
IB04-02	M	F2	-/-	216	BE	2	247
IB06-07	M	F2	-/-	216		0	82
IB07-03	M	F2	-/-	220		3	72
IB5I3-05	M	N5-N9	-/-	103		2	85
IB8IA-01	M	N5-N9	-/-	71	BE	1	109
IB57-13	F	N5-N9	-/-	80	LF, BH	1	133
IB46-03	F	N5-N9	-/-	83	BE, BH	3	116
IB5I5-08	F	N5-N9	-/-	93		0	165
IB5I5-09	F	N5-N9	-/-	93	LH	0	119
IB67-05	M	N5-N9	-/-	93	LH	0	70
IB67-09	F	N5-N9	-/-	93	RH	0	143
IB5I3-01	M	N5-N9	-/-	103		3	156
IB6I0-09	F	N5-N9	-/-	108		3	89
IB8IC-01	M	N5-N9	-/-	115	BH	1	107
IB8IC-02	M	N5-N9	-/-	115	RE, LH	2	*
IB8IC-04	M	N5-N9	-/-	115		0	107
IB5I1-02	M	N5-N9	-/-	120	BE	3	115
IB8I1-04	F	N5-N9	-/-	130	BE, BH	3	255
IB6I3-04	F	N5-N9	-/-	132	BE, BH	3	171
IB5I1-06	F	N5-N9	-/-	147	RE	0	108
IB5I1-09	F	N5-N9	-/-	147		0	88
IB8IA-02	M	N5-N9	-/-	158	LE, BH	3	*
IB57-01	M	N5-N9	-/-	160		3	44

Figure 72: Toluidine blue staining of paraffin embedded ear skin sections

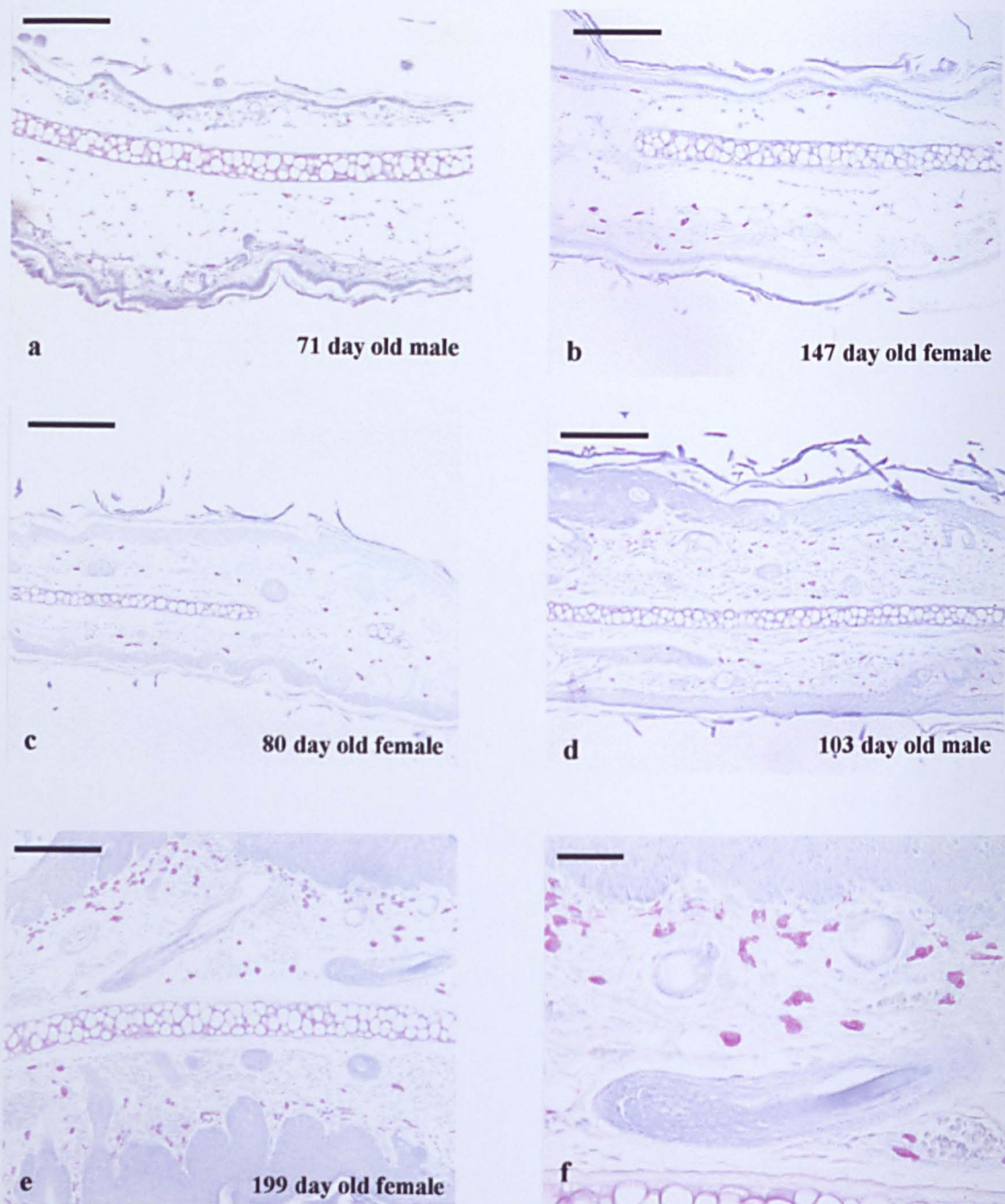


Figure 72: Toluidine blue stains mast cells and basophils violet, and background blue in paraffin embedded sections. a) *Illrn^{+/+}* ear, score 0. b) *Illrn^{-/-}* ear, score 0. c) *Illrn^{+/-}* ear, score 1. d) *Illrn^{-/-}* ear, score 2. e) *Illrn^{-/-}* ear, score 3. f) as e), higher power magnification. Mast cell numbers appear to increase with ear score. Scale bar a-e = 200 μ m, f = 40 μ m.

Mouse I.D number	Sex	Back-ground	<i>Illrn</i> genotype	Age at death (days)	Signs of illness	Ear score	Mast cells /mm ²
IB67-06	M	N5-N9	-/-	171	LE	1	173
IB6I1-04	M	N5-N9	-/-	172	BE	3	83
IB6I0-06	M	N5-N9	-/-	174	BE	3	144
IB6I0-07	F	N5-N9	-/-	174	BE, RH	3	266
IB57-09	F	N5-N9	-/-	187	BE, RH	3	101
IB5I5-03	M	N5-N9	-/-	199	BE, BH	3	112
IB5I5-11	F	N5-N9	-/-	199	BE, RH	3	173
IB8I9-01	M	N5-N9	-/-	216	RE, RH	1	117
IB8I9-07	F	N5-N9	-/-	216	LE	2	37
IB46-01	M	N5-N9	-/-	265	BE	3	129
IB57-04	M	N5-N9	-/-	335	BE	3	154
IB8IB-07	F	N5-N9	+/-	136		1	74
IB8IA-09	F	N5-N9	+/-	155		0	*
IB8I9-02	M	N5-N9	+/-	216	LE	0	96
IB8I9-03	M	N5-N9	+/-	216		0	78
IB8I9-04	M	N5-N9	+/-	216		1	61
IB8I9-05	M	N5-N9	+/-	216		0	112
IB8I9-06	F	N5-N9	+/-	216		0	78
IB8I9-08	F	N5-N9	+/-	216		0	89
IB8IA-04	M	N5-N9	+/-	224		0	107
IB8IA-10	F	N5-N9	+/+	155		0	78
IB8IA-11	F	N5-N9	+/+	155		0	73
IB8IA-12	F	N5-N9	+/+	155		0	57
IB8I8-02	M	N5-N9	+/+	171		0	79
IB8I8-04	M	N5-N9	+/+	171		0	*
IB8IB-08	F	N5-N9	+/+	191		0	75
IB8IB-09	F	N5-N9	+/+	191		0	72

*Mast cell count not taken as only frozen sections were available

LE = left ear appeared scaly

LH = left hind joint swollen

RE = right ear appeared scaly

RH = right hind joint swollen

BE = both ears appeared scaly

BH = both hind joints swollen

LF = left front joint swollen

Paraffin embedded sections were stained for mast cells using toluidine blue, to detect whether their numbers were elevated in psoriatic skin as compared to unaffected skin (as is the case in human psoriasis) (Figure 72). Initial observations suggested that mast cell numbers were increased in inflamed ear sections as opposed to uninflamed, and this observation was supported by counting the

numbers of mast cells under a light microscope (see table 6). The numbers of mast cells counted per mm² in the ear skin sections of N2-N5 mice scoring 0 were compared to those scoring 3 by using the Mann-Whitney test. The numbers of mast cells in ear skin sections scoring 3 were significantly greater than those scoring 0 at the 5% level ($p = 0.0014$).

3.4.3: Characterisation of psoriatic lesions by immunohistochemistry

Frozen sections from 4 Balb/c *Il1rn*^{+/+} and 5 *Il1rn*^{-/-} mice were examined immunohistochemically to detect the presence of CD4⁺ T-cells, CD8⁺ T-cells, B-cells, macrophages, dendritic cells and endothelial cells. This was done to compare the cell types present within the dermal and epidermal inflammatory infiltrates to those found in human psoriatic skin, and to compare vascularity of unaffected and affected sections (by identifying endothelial cells lining the small vessels). E-selectin staining was used to detect whether the endothelial cells were activated. IFN γ , IL-4 and IL-5 were detected to discover the activation status and Th1/Th2 polarity of the CD4⁺ T-cells, and IL-1 β was identified both to confirm the activation status of the macrophages and to test the hypothesis that the disease is caused by the action of unopposed IL-1. The adhesion molecule ICAM-1 and the chemokine MCP-1 were detected as their expression is upregulated during inflammation, and finally keratin 6 was identified as a marker for hyperproliferative keratinocytes, where it is expressed at high levels [Weiss *et al.*, 1984; Stoler *et al.*, 1988]. Keratin 6 mRNA is normally only expressed at low levels in normal epidermis without production of the proteins, except for around the outer root sheath of hair follicle, on the nail bed [Stoler *et al.*, 1988] and in the oral mucosa [Wong *et al.*, 2000] .

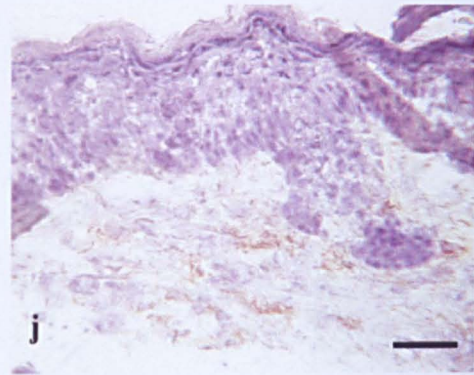
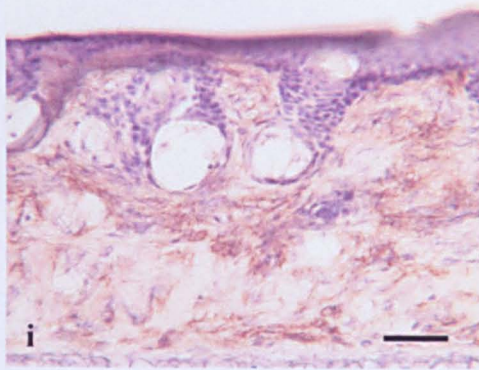


Figure 73: Immunohistochemical stains of inflamed ear sections from two separate Balb/c *Illrn*^{+/-} mice are shown (216 day old female and 158 day old male). In all cases brown staining indicates a positive reaction. All are counterstained with haematoxylin. a & b CD4⁺ cells (T-cells), c & d CD8a⁺ cells (T-cells), e & f) F4/80⁺ cells (macrophages), g & h) DEC-205⁺ cells (dendritic cells), i & j) CD19⁺ cells (B-cells). Scale bars = 40 μ m.

Figure 73: Psoriatiform Balb/c *IIIrn*^{-/-} ear sections contain a mixed dermal infiltrate

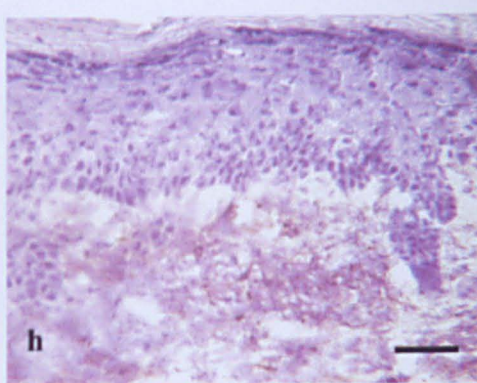
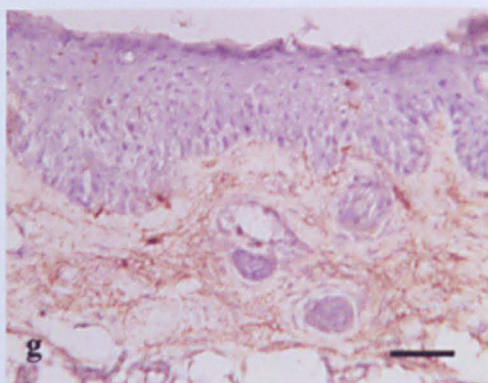
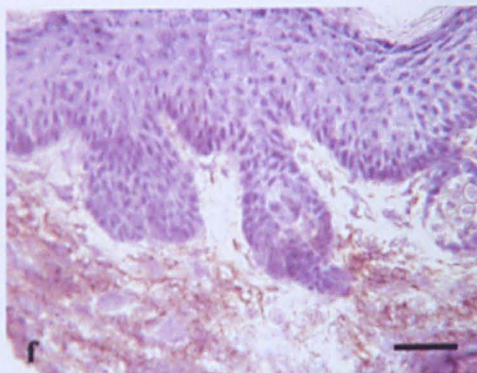
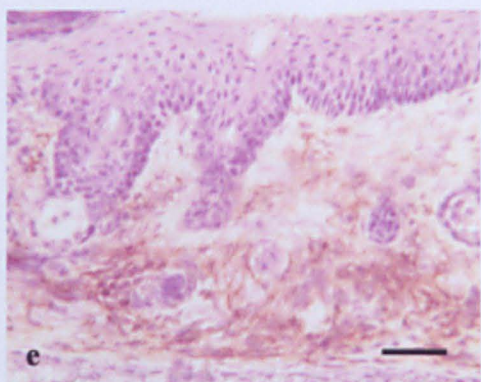
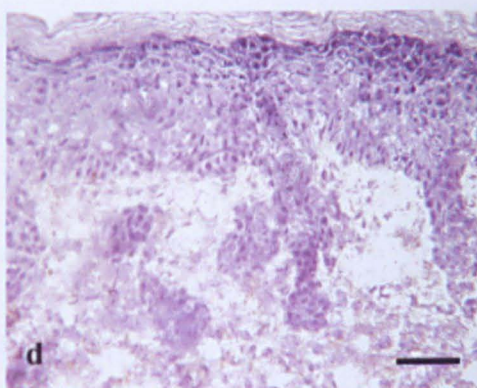
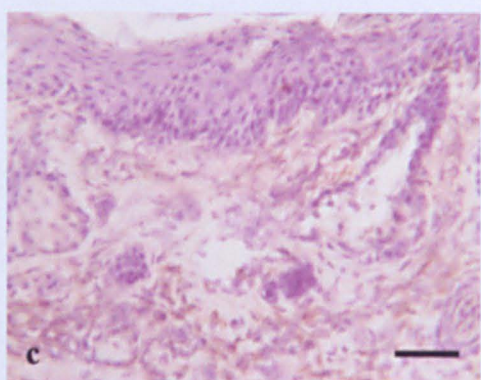
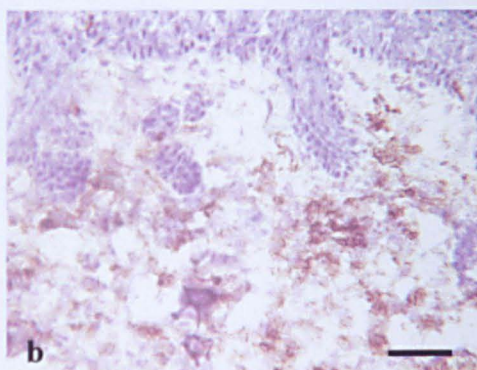
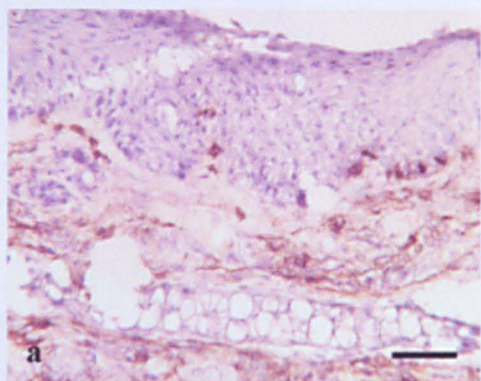


Figure 74: Mixed cytokine profile within dermal infiltrate of inflamed Balb/c ear skin sections

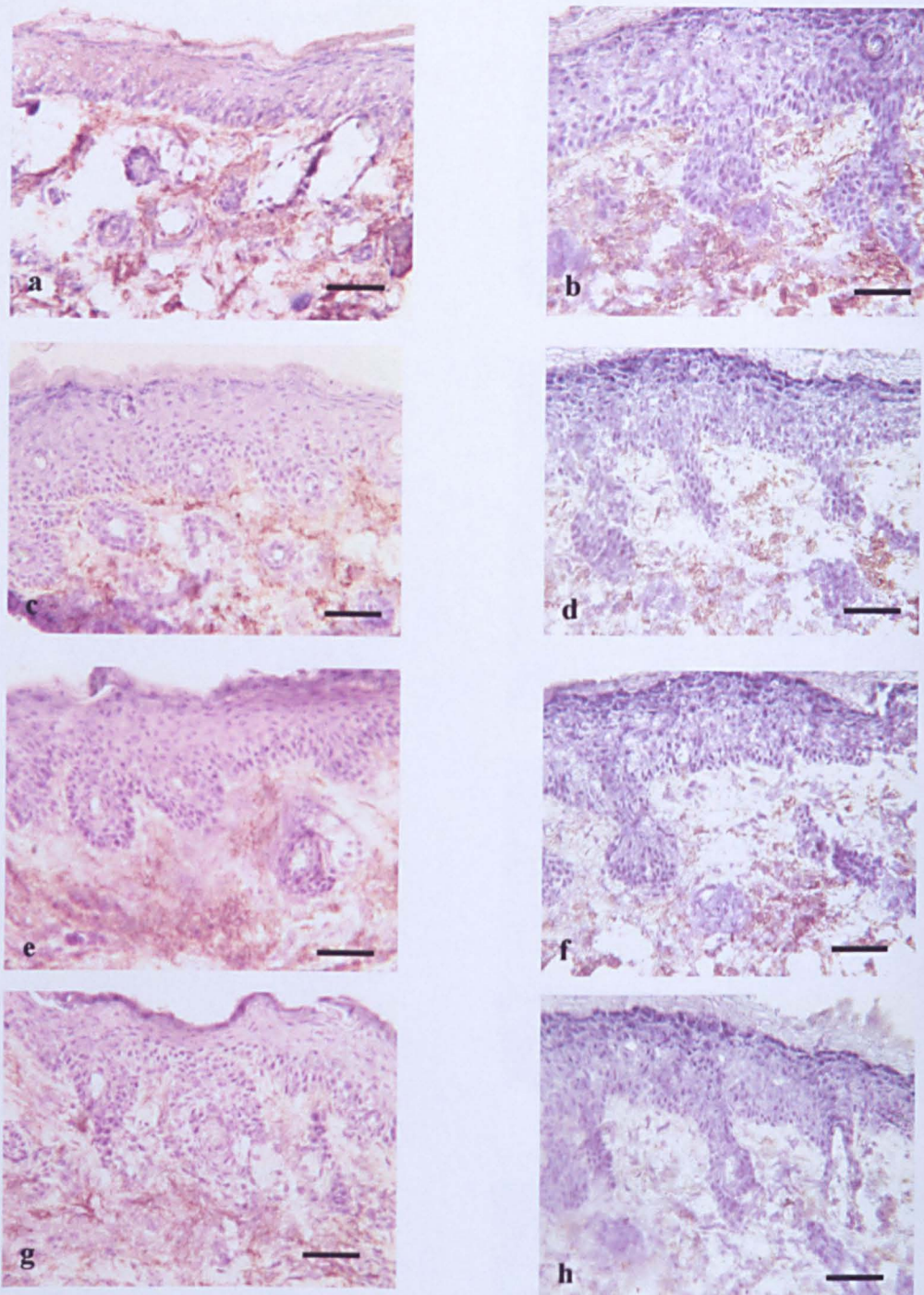


Figure 74: Immunohistochemical stains of inflamed ear sections from two separate Balb/c *Illrn*^{-/-} mice (216 day old female and 158 day old male) are shown. In all cases brown staining indicates a positive reaction. All are counterstained with haematoxylin. Sections are stained for cytokines as follows: a & b) IL-1 β , c & d) IFN γ , e & f) IL-4, g & h) IL-5. Scale bar = 40 μ m.

Figure 75: Chemokine and adhesion molecule expression in inflamed dermis of Balb/c *Il1rn*^{-/-} ear skin sections

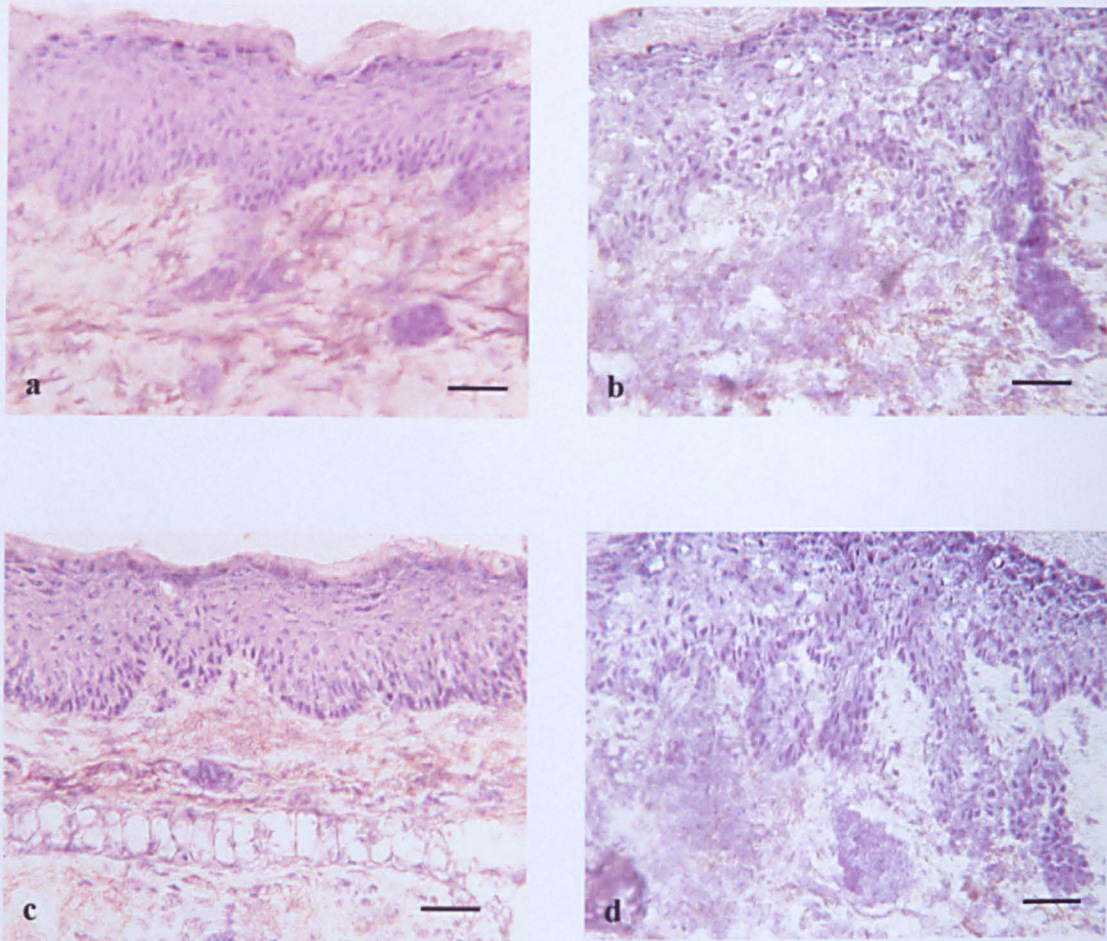


Figure 75: Immunohistochemical stains of inflamed ear sections from two separate Balb/c *Il1rn*^{-/-} mice (216 day old female and 158 day old male) are shown. In all cases brown staining indicates a positive reaction. All are counterstained with haematoxylin. Sections are stained for a & b) MCP-1⁺ cells, c & d) ICAM-1⁺ cells. Scale bars = 40 μm.

Figure 76: Increased vascularity and activation of endothelial cells within the dermis of inflamed Balb/c *Il1rn*^{-/-} ear sections as compared to *Il1rn*^{+/+}

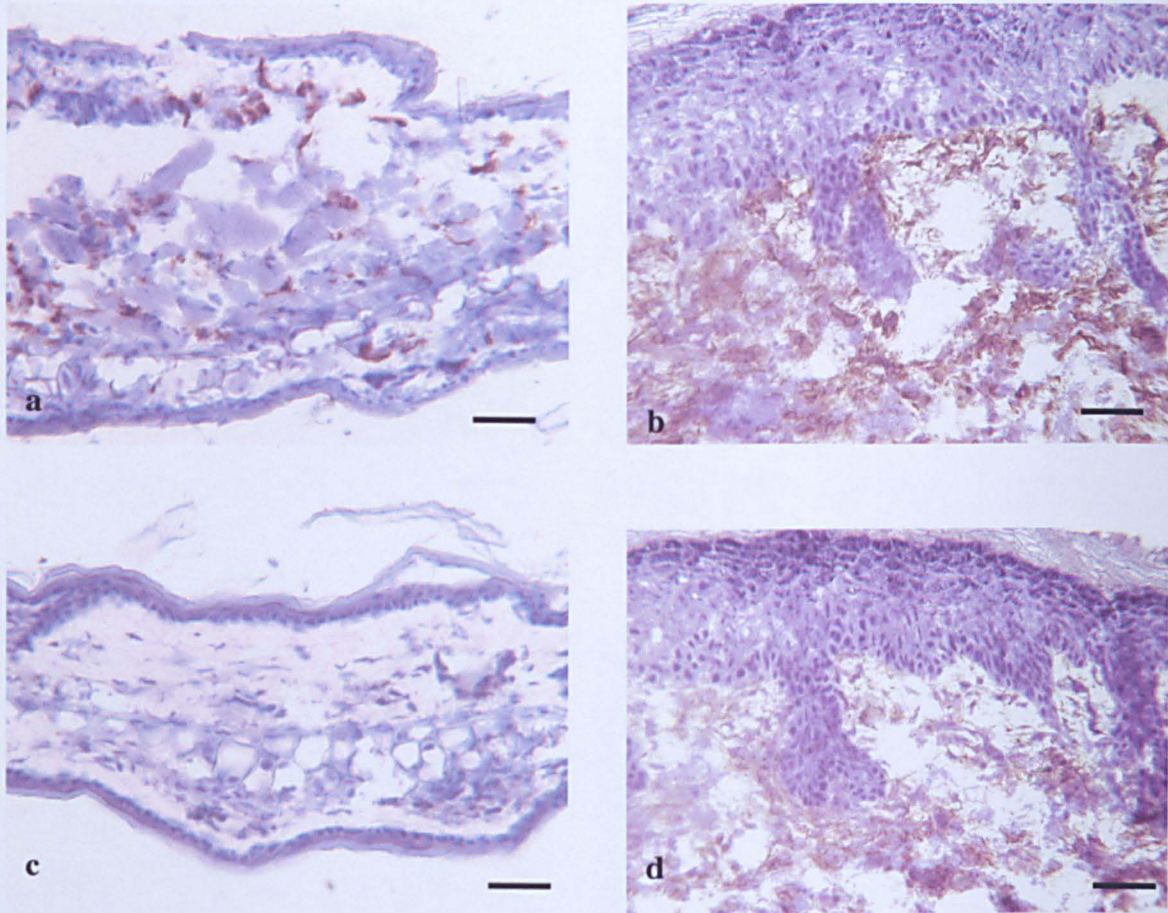


Figure 76: Immunohistochemical stains of inflamed ear sections from one Balb/c *Il1rn*^{-/-} (216 day old female) and one *Il1rn*^{+/+} (191 day old female) mouse are shown. In all cases brown staining indicates a positive reaction. All are counterstained with haematoxylin. a) *Il1rn*^{+/+} CD31⁺ cells (endothelial cells), b) *Il1rn*^{-/-} CD31⁺ cells, c) *Il1rn*^{+/+} CD62E⁺ cells (E-selectin), d) *Il1rn*^{-/-} CD62E⁺ cells. scale bars = 40 μ m.

Figure 77: CD4⁺ T-cells infiltrating into the epidermis of lesional skin in *Il1rn*^{-/-} Balb/c mice

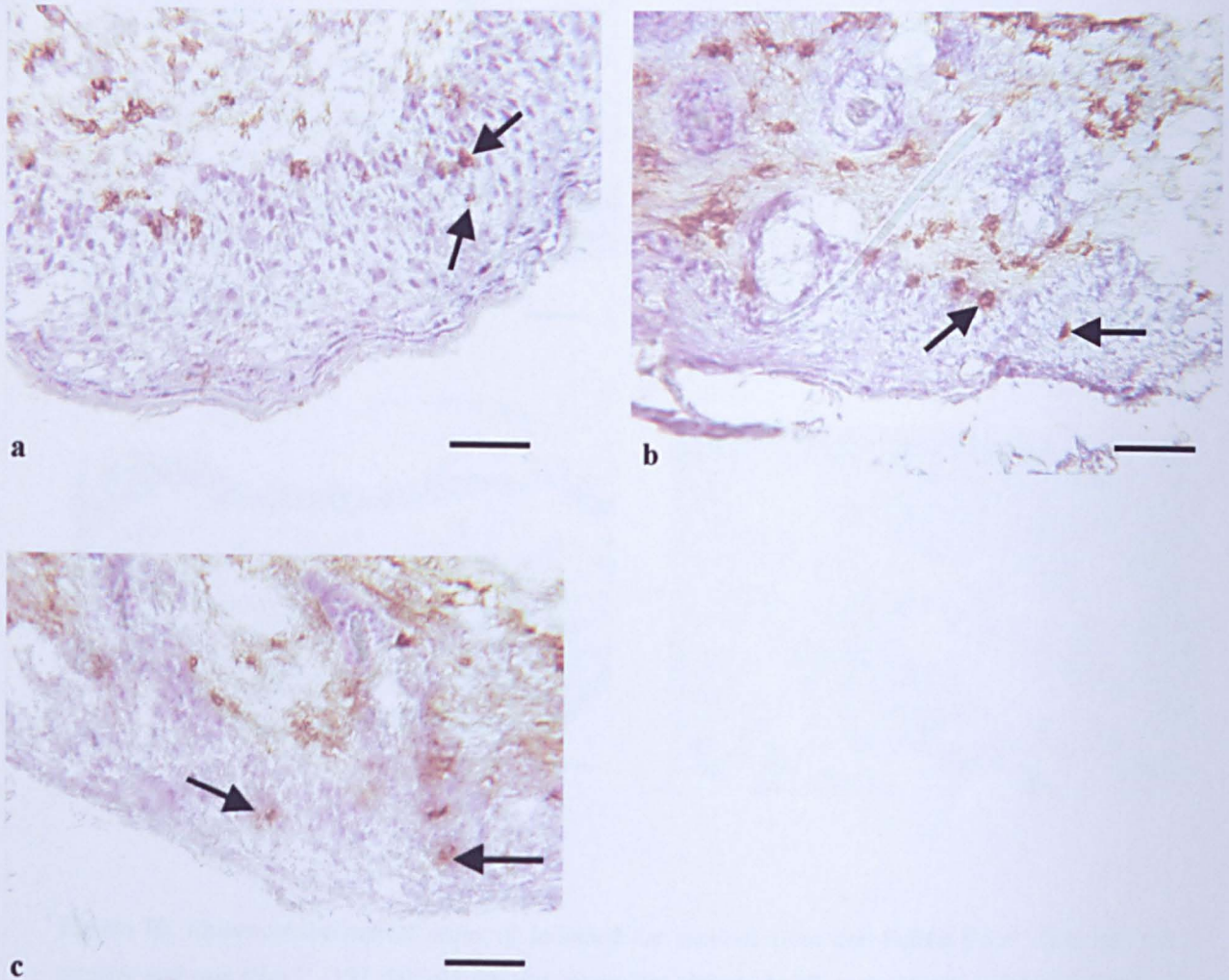


Figure 77: CD4⁺ cells (arrows) infiltrating into the epidermis of lesional skin from *Il1rn*^{-/-} Balb/c mice. Examples shown are from three different *Il1rn*^{-/-} animals, a) 216 day old female, b) 158 day old male, c) 115 day old male. Scale bar = 40 μ m.

Figure 78: Epidermal Langerhans' cells appear to be activated and more numerous in psoriatiform *Il1rn*^{-/-} Balb/c ear skin than in *Il1rn*^{+/+}

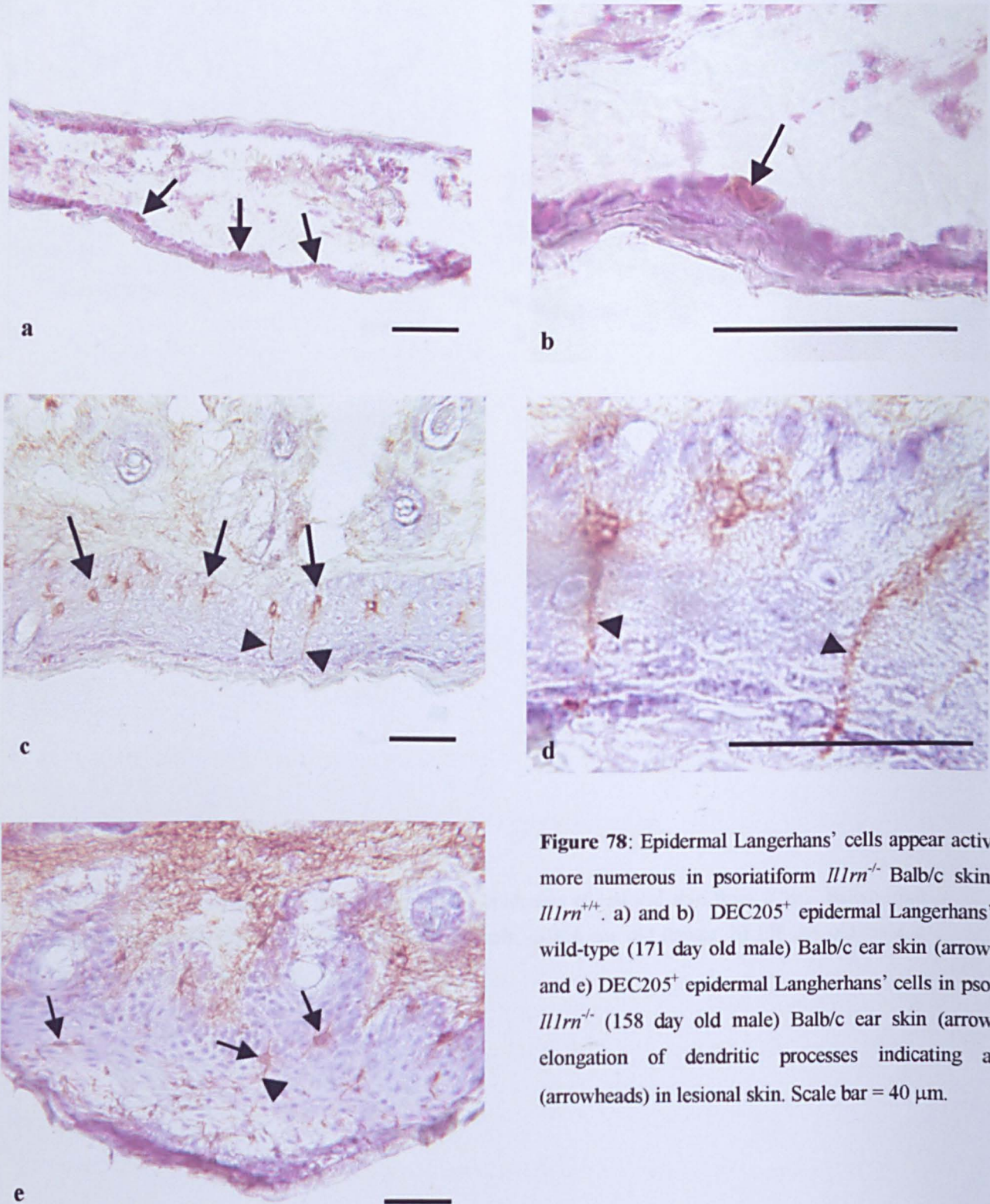


Figure 78: Epidermal Langerhans' cells appear activated and more numerous in psoriatiform *Il1rn*^{-/-} Balb/c skin than in *Il1rn*^{+/+}. a) and b) DEC205⁺ epidermal Langerhans' cells in wild-type (171 day old male) Balb/c ear skin (arrows). c), d) and e) DEC205⁺ epidermal Langerhans' cells in psoriatiform *Il1rn*^{-/-} (158 day old male) Balb/c ear skin (arrows). Note elongation of dendritic processes indicating activation (arrowheads) in lesional skin. Scale bar = 40 μ m.

Sections of ears from *Il1rn*^{-/-} mice which had outwardly appeared red and thickened were histologically confirmed as being inflamed. Dermal infiltrates were found to be composed of CD4⁺ T-cells, CD8⁺ T-cells, macrophages, dendritic cells, neutrophils and B-cells (Figure 73).

Within the dermal infiltrate, there was production of IL-1 β and IFN γ , and also IL-4 and IL-5 (Figure 74) (unlike in the inflammatory infiltrates of the arteritis in *Il1rn*^{-/-} mice), demonstrating a mixed Th1/Th2 type response. A comparison of figures 25 and 74 show infiltrates in the heart and ear of same animal, a 158 day old male Balb/c *Il1rn*^{-/-} mouse (IB8IA-02). In the aortic lesion infiltrate, there is very little positive staining for IL-4 or IL-5 whereas both are found within the inflamed dermis. In the same animal, there is also little or no positive staining for IL-4 (unlike IFN γ) within the pannus of a rheumatoid arthritis like disease which it had developed (Figure 85), as well as the arteritis and psoriatic disease.

MCP-1 production and ICAM-1 expression (Figure 75) were both enhanced within the inflamed dermis, further demonstrating the inflamed status of the skin. An increase in vascularity within the dermis, along with activation of endothelial cells as judged by abundant E-selectin expression (Figure 76) was also seen in these sections.

CD4⁺ T-cells and neutrophils were observed infiltrating into the epidermis (Figure 77). Numbers of dendritic cells within the epidermis (Langerhans' cells) also appeared increased in inflamed ear sections (Figure 78). Epidermal infiltrates and

Figure 79: Transverse epidermal skin sections of affected and unaffected mice stained for keratin 6

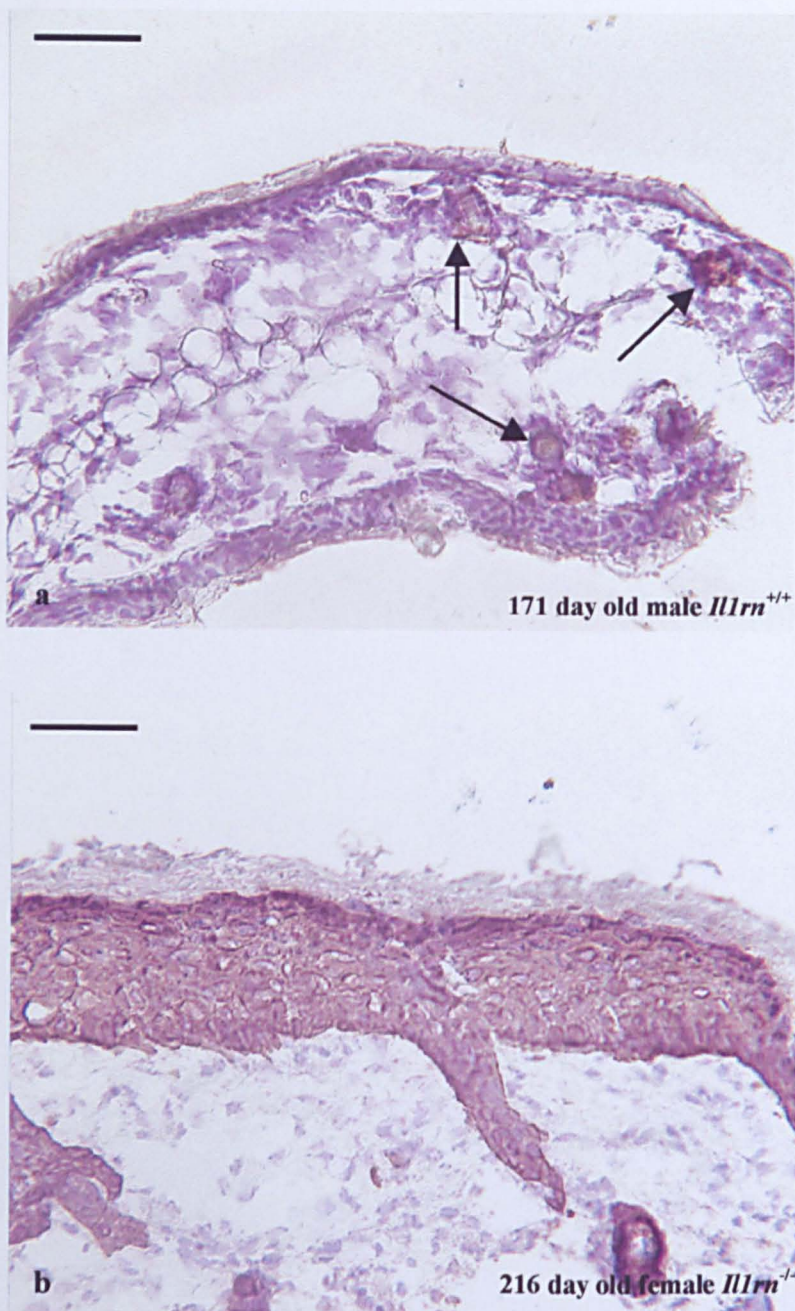


Figure 79: Immunohistochemical staining for keratin 6 in *Il1rn*^{+/+} (a) and *Il1rn*^{-/-} (b) mice. In the wild-type mouse, cells staining positively for keratin 6 are restricted to those surrounding hair follicles (arrows). In the IL-1ra deficient mice, keratinocytes in all layers of the epidermis express keratin 6, indicating a hyperproliferative state. Scale bar = 40 μ m.

Figure 80: *IL1rn^{+/+}* Balb/c mice have a low level of inflammation in the ears

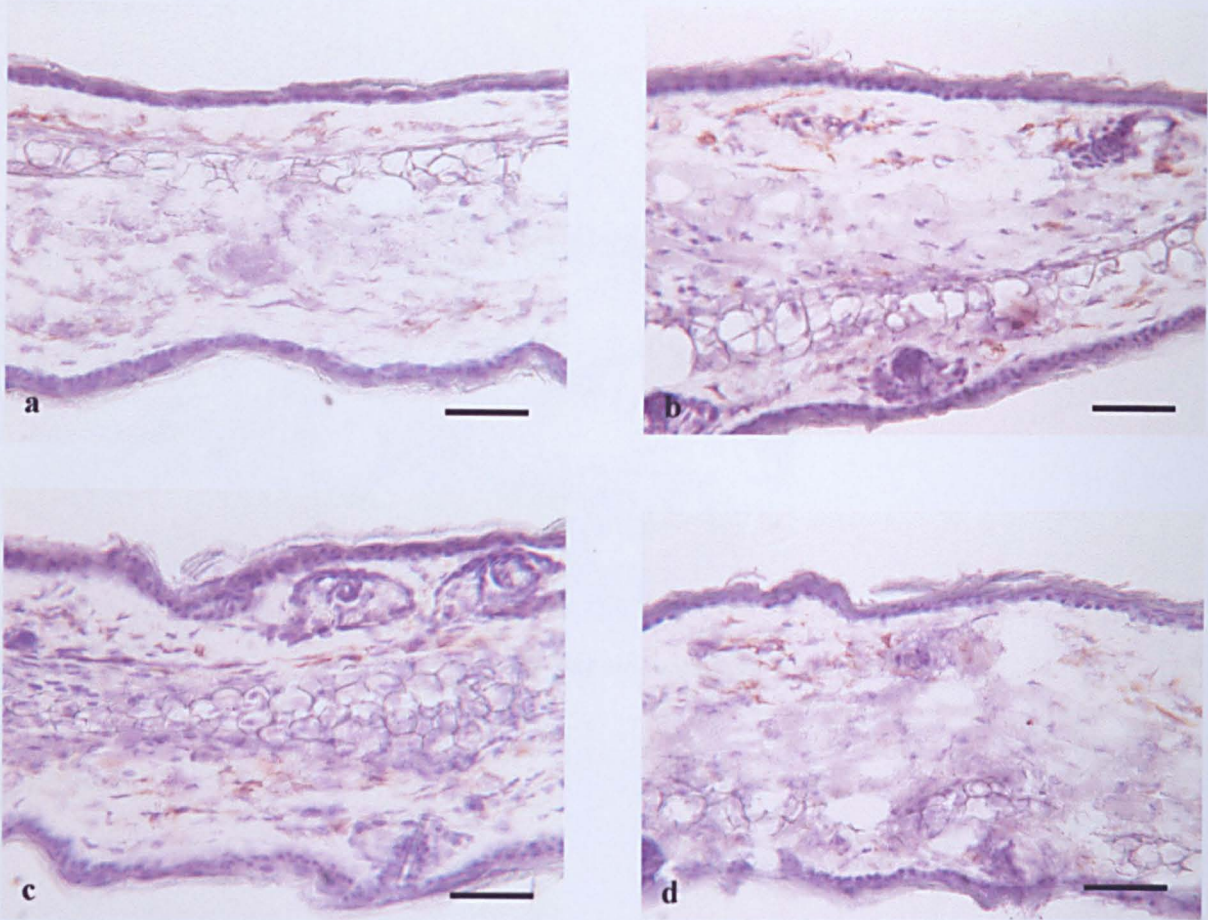


Figure 80: Immunohistochemical stains of inflamed ear sections from one Balb/c *IL1rn^{+/+}* (191 day old female) mouse are shown. In all cases brown staining indicates a positive reaction. All are counterstained with haematoxylin. Sections show a) F4/80⁺ cells, b) IL-1 β ⁺ cells, c) CD4⁺ cells, and d) IFN γ ⁺ cells. Activated F4/80⁺ and CD4⁺ cells are present in the dermis of the ears in *IL1rn^{+/+}* mice. Scale bar = 40 μ m.

Figure 81: *Il1rn*^{+/+} Balb/c mice have no IL-4 or IL-5 production within the ears

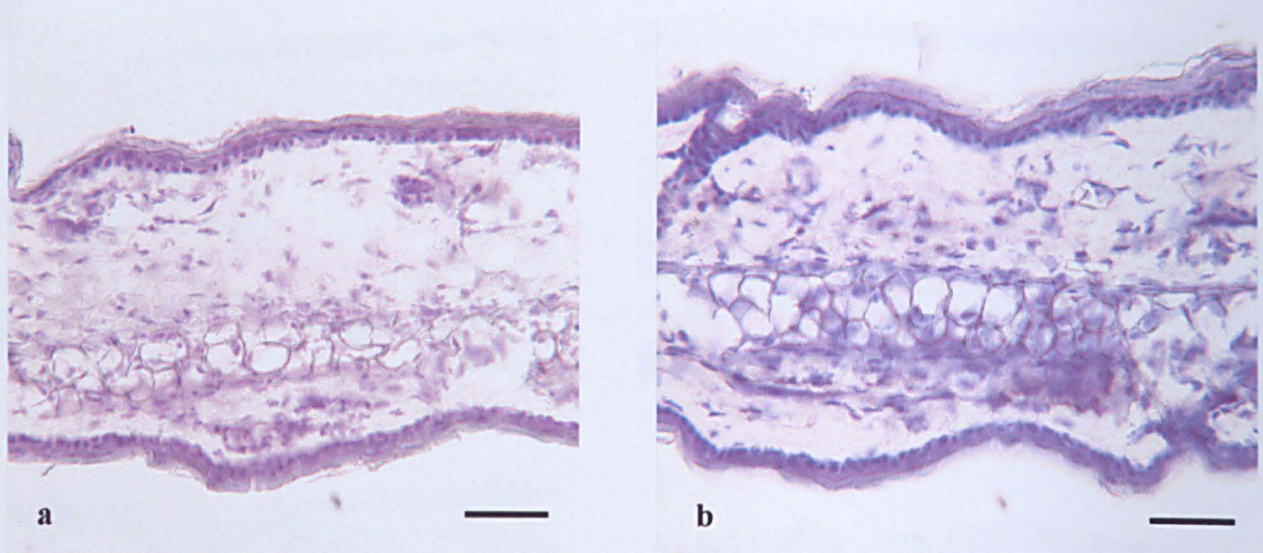


Figure 81: Immunohistochemical stains of inflamed ear sections from one Balb/c *Il1rn*^{+/+} mouse (191 day old female) are shown. In all cases brown staining indicates a positive reaction. All are counterstained with haematoxylin. a) stained for IL-4, b) stained for IL-5 . Scale bar = 40 μ m.

an increase in numbers and activation of Langerhans' cells are also observed in human psoriatic skin.

Keratin 6 expression was upregulated in inflamed ear sections (Figure 79). This protein was expressed in all layers of the inflamed epidermis. In unaffected sections, its expression was restricted to the basal keratinocyte layer, and surrounding hair follicles. This demonstrates the hyperproliferative state of the keratinocytes within the inflamed epidermis, possibly due to the action of IL-1.

Ear sections from wild-type Balb/c mice also showed positive staining for macrophages (F4/80), CD4⁺ T-cells, IL-1 β and IFN γ (Figure 80) within the dermis, but were negative for IL-4 and IL-5 (Figure 81), indicating that inflammatory processes in the ear were normal, but cells staining positively were fewer in number than in inflamed ears. A possible explanation for the presence of activated macrophages and T-cells in the dermis of wild-type ear skin is that the ear routinely undergoes mild physical trauma or routinely suffers the incursion of bacteria from the epidermis. A similar pattern was observed in Sf3 *Il1rn*^{+/+} mice which do not develop the disease, suggesting that the sensitivity of Balb/c *Il1rn*^{-/-} mice to the pathology is not the result of a weak epithelial barrier to incursion in Balb/c.

In addition, some cells within the epidermis of wild-type ear sections stained positively with the dendritic cell marker DEC205 as expected, due to the presence of Langerhans' cells in normal epidermis (see Figure 78).

Figure 82: Inflamed skin at the base of the tail in a Balb/c *Il1rn*^{-/-} mouse

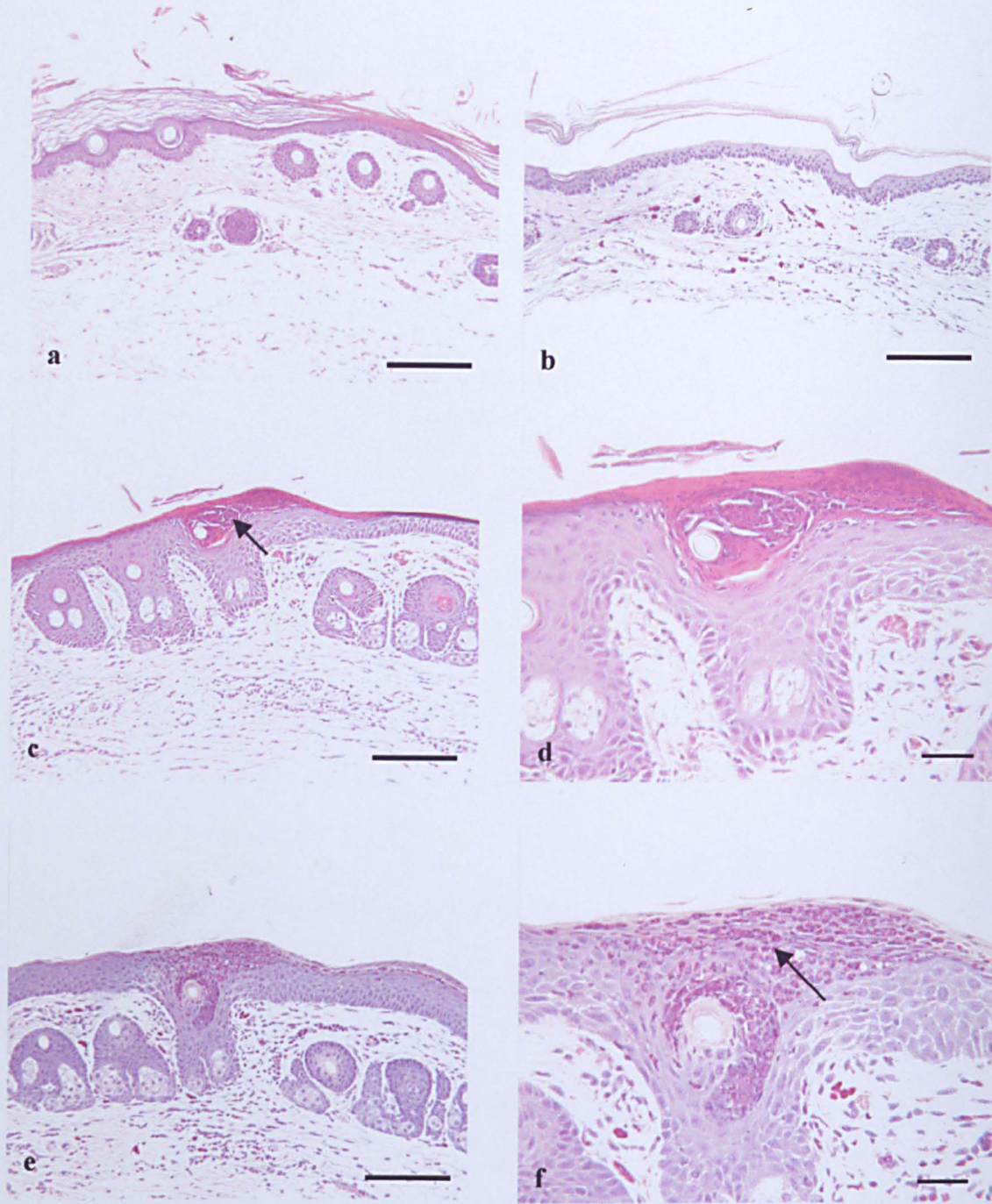


Figure 82: a) Haematoxylin and eosin stained tail skin, *Il1rn*^{+/+} mouse (191 day old female). b) tail skin stained for chloroacetate esterase, same *Il1rn*^{+/+} mouse. c) haematoxylin and eosin stained tail skin from *Il1rn*^{-/-} mouse (335 day old male, IB57-04). Note formation of Munro microabscess (arrow). d) as c, higher power magnification. e) section from same *Il1rn*^{-/-} tail, stained for chloroacetate esterase activity (neutrophils). f) as e, higher power magnification. Note red-staining neutrophils (arrow). Scale bars a, b, c, e = 200 μ m, d & f = 40 μ m.

Figure 83: Haematoxylin and eosin stained paraffin embedded skin sections from *Il1rn*^{-/-} and *Il1rn*^{+/+} Balb/c mice

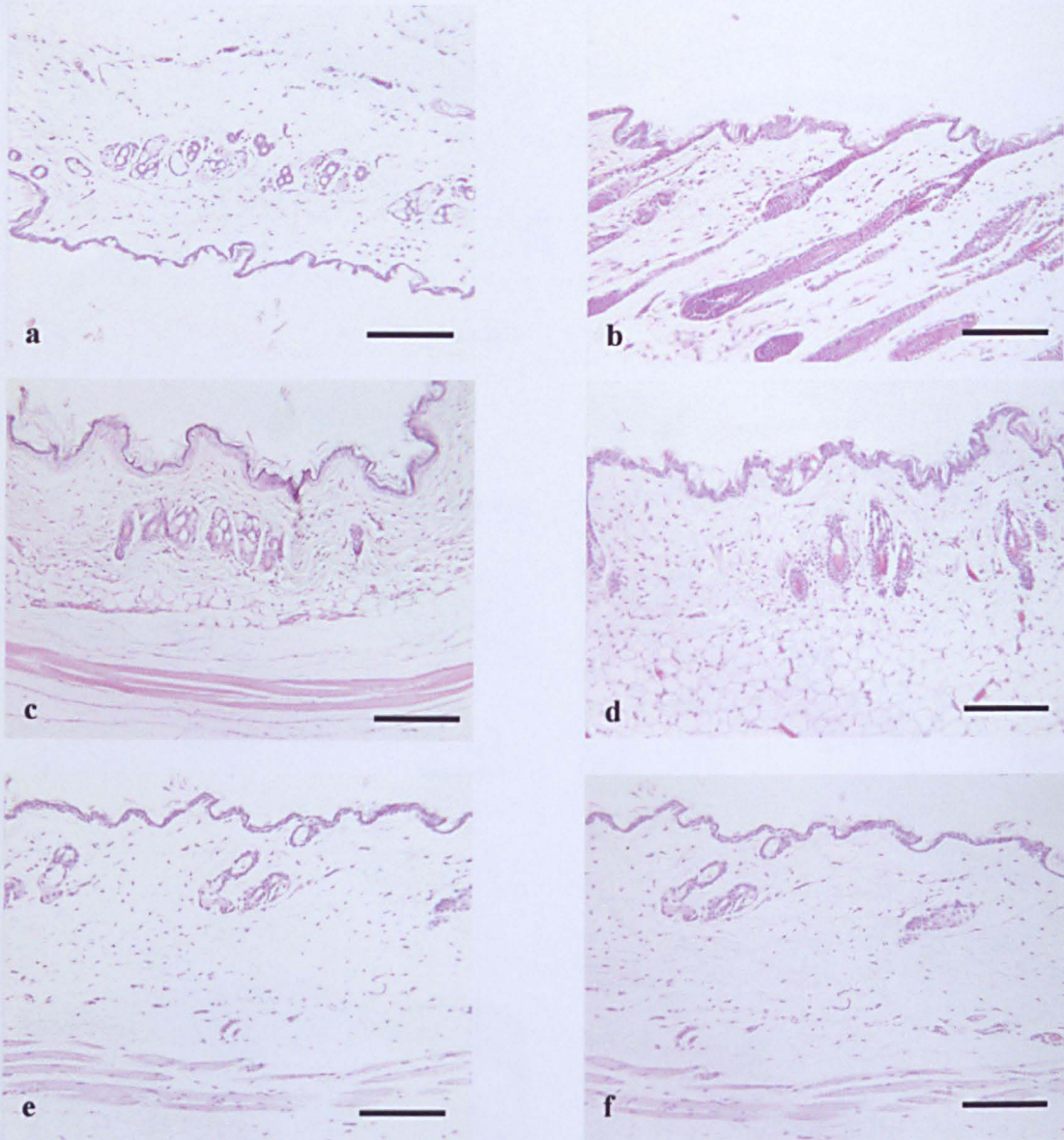


Figure 83: Haematoxylin and eosin staining of paraffin embedded sections of skin from the flexure of the elbow, the back (dorsal), and belly (ventral) revealed no lesions in the animals examined. a) & b) – elbow. c) & d) dorsal skin. e) & f) ventral skin. a, c & e are all from the same *Il1rn*^{-/-} mouse (IB57-04, 335 day old male), ear score 3. b, d, & f are from the same *Il1rn*^{+/+} mouse (IB8IB-09, 191 day old female), ear score 0. Scale bar = 200 μ m.

A proportion of Balb/c *Il1rn*^{-/-} mice spontaneously develop a psoriatiform disease which histologically and immunohistologically appears to be similar to human psoriasis. The disease appears only in *Il1rn*^{-/-} mice, but appears to be strain specific. Additionally, in 1/3 Balb/c *Il1rn*^{-/-} mice examined, psoriatiform lesions that were histologically similar to those found on the ears, were found at the base of the tail (Figure 82). In all 3 of these cases, as well as in skin sections from 4 *Il1rn*^{+/-} and 1 *Il1rn*^{+/+} mouse, no lesions were found elsewhere (either on dorsal skin, ventral skin or from the flexure of the elbow) (Figure 83).

3.5: *Il1rn*^{-/-} mice on a Balb/c background spontaneously develop a rheumatoid arthritis-like disease

3.5.1: Introduction

Il1rn^{-/-} mice deeply backcrossed onto a Balb/c background (but not C57BL/6 or Sf3 backgrounds, nor the F2 of an Sf3 x Balb/c cross) spontaneously develop an RA-like disease. This phenotype was previously observed in another colony of *Il1rn*^{-/-} mice on a Balb/cA background [Horai *et al.*, 2000], despite the fact that the structure of the null alleles differs between the two laboratories, and strains used are slightly different (see section 1.1.13). The age of onset of disease differs between the two colonies. The colony established by Horai *et al* begin to show signs of the disease at 30 days old, whereas age of onset in our colony is later, with animals beginning to develop swollen joints at around 70 days. This difference may result from allelic differences, but more likely results from uncontrolled environmental differences or from differences in genetic background (our background is Balb/c(Harlan), Horai *et al* use Balb/cA).

3.5.2: Clinical signs of arthropathy

Il1rn^{-/-} mice on all backgrounds were routinely checked for swollen limbs or unusual gait. The ratio of males to females suffering from the disease was noted, since in the human RA affects women/men in the ratio 2.5:1 [Lawrence *et al.*, 1998].

Outwardly, Balb/c *Il1rn*^{-/-} animals suffering from the RA-like disease had swollen hind ankles (either one ankle or both) in comparison to unaffected joints. The swollen joints were reddened in colour in the live animals. Gait was affected in animals with swollen joints – in advanced cases the mice limped or dragged the affected limb(s) which appeared to be stiff and immobile. The forelimbs appeared to be less affected.

No *Il1rn*^{-/-} mice from the Sf3 background, from a total of over 400 mice bred over 5 years, outwardly appeared affected by the disease, even at an advanced age. There is also no evidence of the disease in *Il1rn*^{-/-} mice bred onto a C57BL/6 background, in agreement with Horai *et al.*

3.5.3: Histological analysis of decalcified joint sections

In order to establish whether the arthropathy observed in our Balb/c *Il1rn*^{-/-} animals histologically resembles human RA and the RA-like disease found in other Balb/c *Il1rn*^{-/-} mice [Horai *et al.*, 2000], histological analysis of 5 joints was performed. Two were ankle joints from Balb/c *Il1rn*^{-/-} mice which had been recorded as appearing swollen, 1 was an outwardly normal ankle joint from a

Figure 84: Haematoxylin and eosin stained decalcified, paraffin embedded joint sections

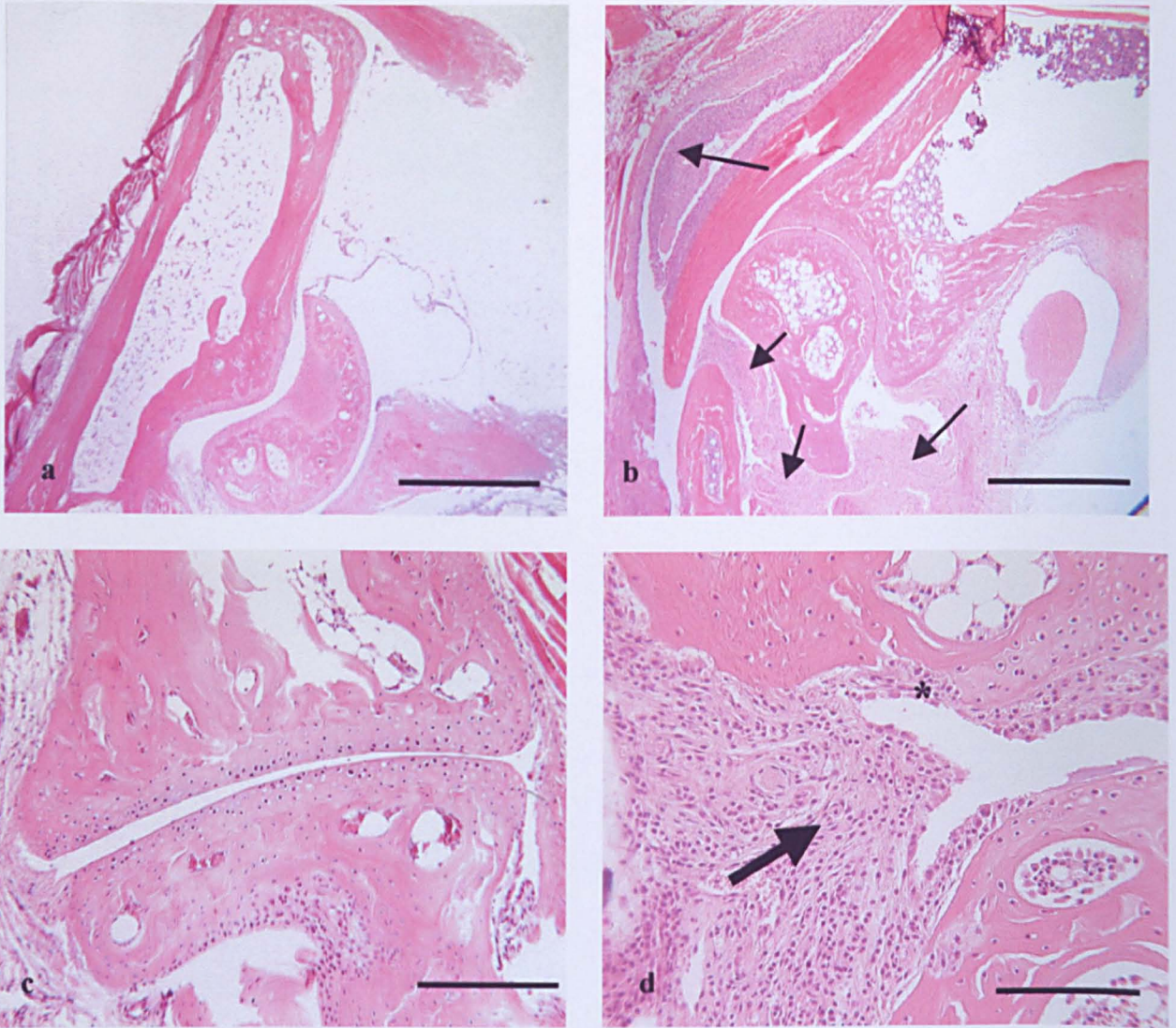


Figure 84: Haematoxylin and eosin staining of decalcified Balb/c joints (ankles). a & c) *Illrn*^{+/+} animal (155 day old female). b & d) arthritic *Illrn*^{-/-} animal (132 day old female). Note inflammatory infiltrates (arrows), pannus invading the synovial joint space (thick arrow), and destruction of chondrocytes at the joint (*). Scale bars a and b = 500 μ m, c and d = 200 μ m.

Balb/c *Il1rn*^{+/+} animal, one was an outwardly normal ankle joint from an *Il1rn*^{-/-} Sf3 mouse, and one was an apparently unaffected wrist joint from an *Il1rn*^{-/-} Balb/c mouse with swollen ankles. Decalcified joints were formaldehyde fixed, paraffin embedded and sectioned, and used for haematoxylin and eosin staining to observe any structural or cellular changes which may be similar to human RA, such as destruction of cartilage and pannus formation.

In one of the ankle joints from the affected *Il1rn*^{-/-} Balb/c mice, there was an inflammatory infiltrate (pannus) around the ankle joint, which in parts infiltrated almost all of the tissue across the joint. There was visible destruction of the cartilage and bone within the joint (Figure 84). The other ankle joint from an *Il1rn*^{-/-} animal appeared histologically normal. The ankle joints from the Balb/c wild-type animal and the *Il1rn*^{-/-} Sf3 mouse appeared histologically unaffected by the arthropathy. There was no inflammatory infiltrate and the cartilage and bones appeared healthy, with no visible erosion (Figure 84). This was also the case with the wrist joint from the affected Balb/c *Il1rn*^{-/-} mouse.

3.5.4: Immunohistochemical analysis of undecalcified joints

Undecalcified frozen joints from 6 animals were sectioned and immunohistochemically stained to identify T-cells (CD4⁺ and CD8⁺) and macrophages (F4/80⁺), and their products IFN γ , IL-4 and IL-1 β to determine whether they were activated and whether the CD4⁺ T-cells were of a Th1 or Th2 type. In addition, it was expected that IL-1 β would be present in the affected joints, if the disease is a result of the action of unopposed IL-1. The six joints were from the hind limbs (ankles) of four *Il1rn*^{-/-} and two *Il1rn*^{+/+} mice, all Balb/c. Of the

Figure 85: Pannus in arthritic Balb/c *Il1rn*^{-/-} mouse joint

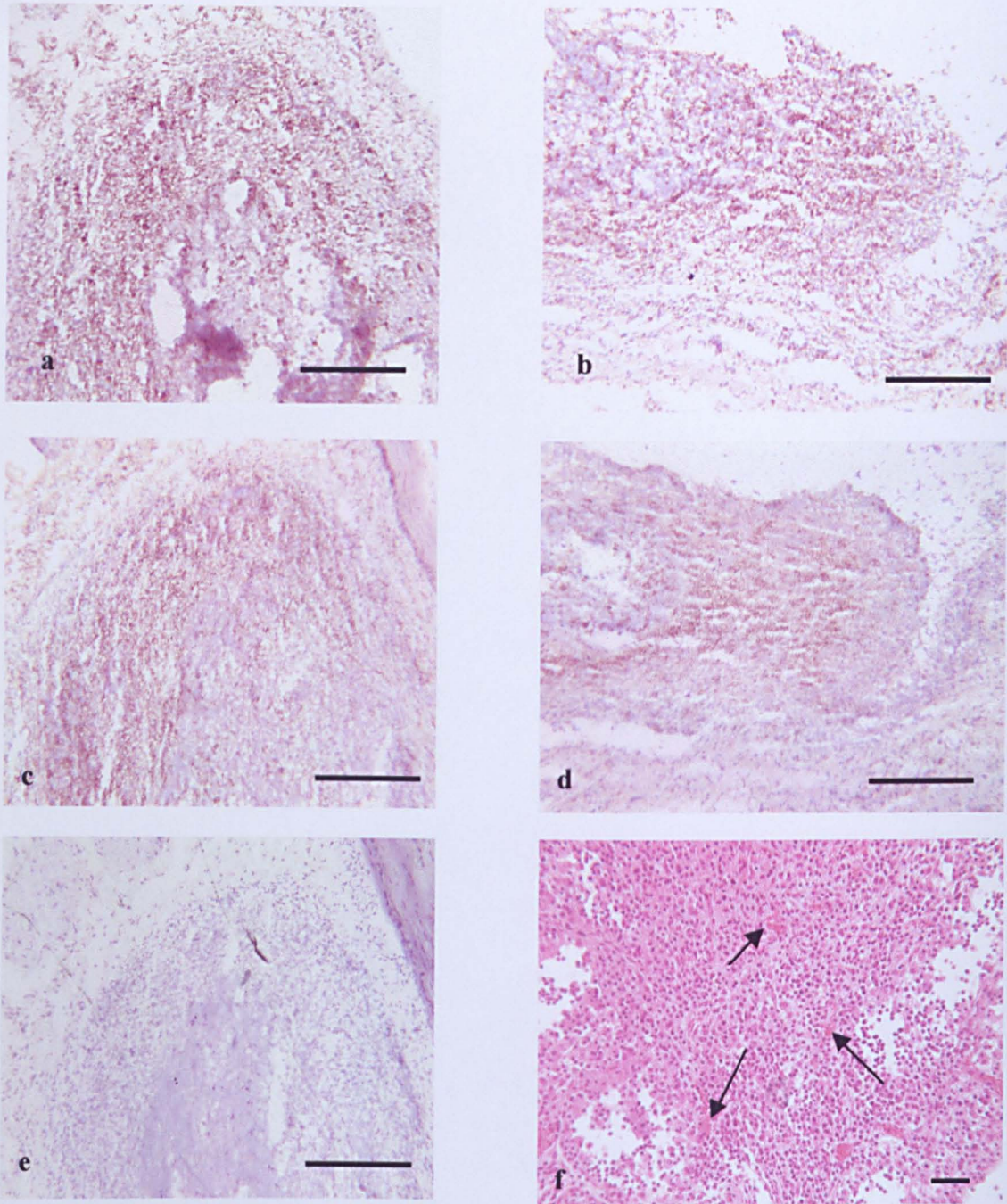


Figure 85: Immunohistochemical staining of pannus formed in joints of a Balb/c *Il1rn*^{-/-} mouse (158 day old male). a) CD4⁺ cells, b) F4/80⁺ cells (macrophages), c) IFNγ⁺ cells, d) IL-1β⁺ cells, e) IL-4, rare +ve cells. f) haematoxylin and eosin stained pannus from a decalcified joint (132 day old female). Note vascularity within the pannus (arrows). Scale bars a – e = 200 μm, f = 40 μm.

Figure 86: Activated macrophages in inflammatory infiltrate of a Balb/c *Il1rn*^{-/-} joint

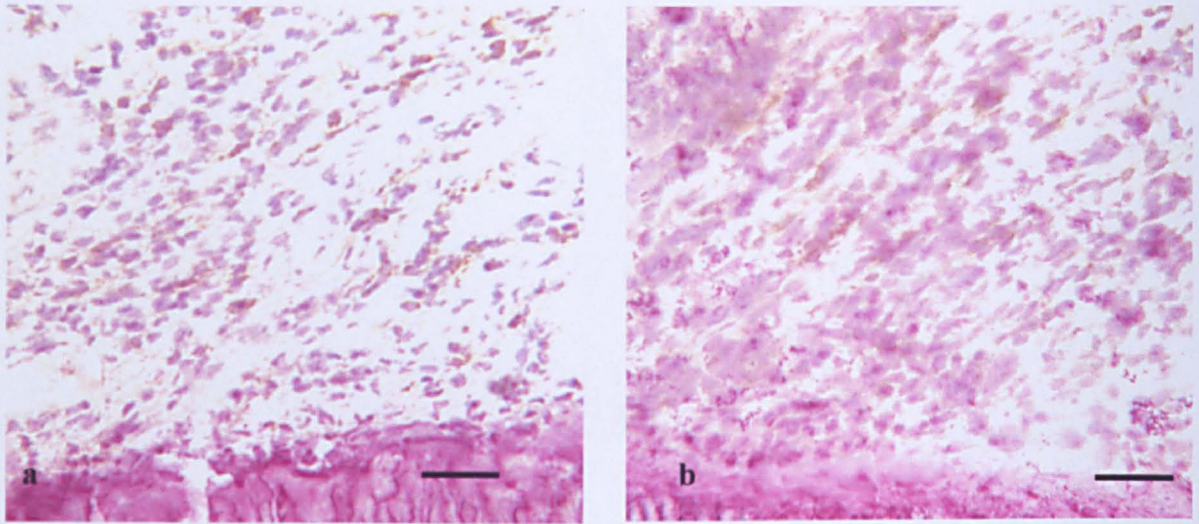


Figure 86: Undecalcified joint sections from a 158 day old male *Il1rn*^{-/-} mouse stained for a) F4/80⁺ cells (macrophages), and b) IL-1β⁺ cells. Scale bar = 40 μm.

Figure 87: Th1 type CD4⁺ T-cells within infiltrate of an arthritic Balb/c *Il1rn*^{-/-} joint

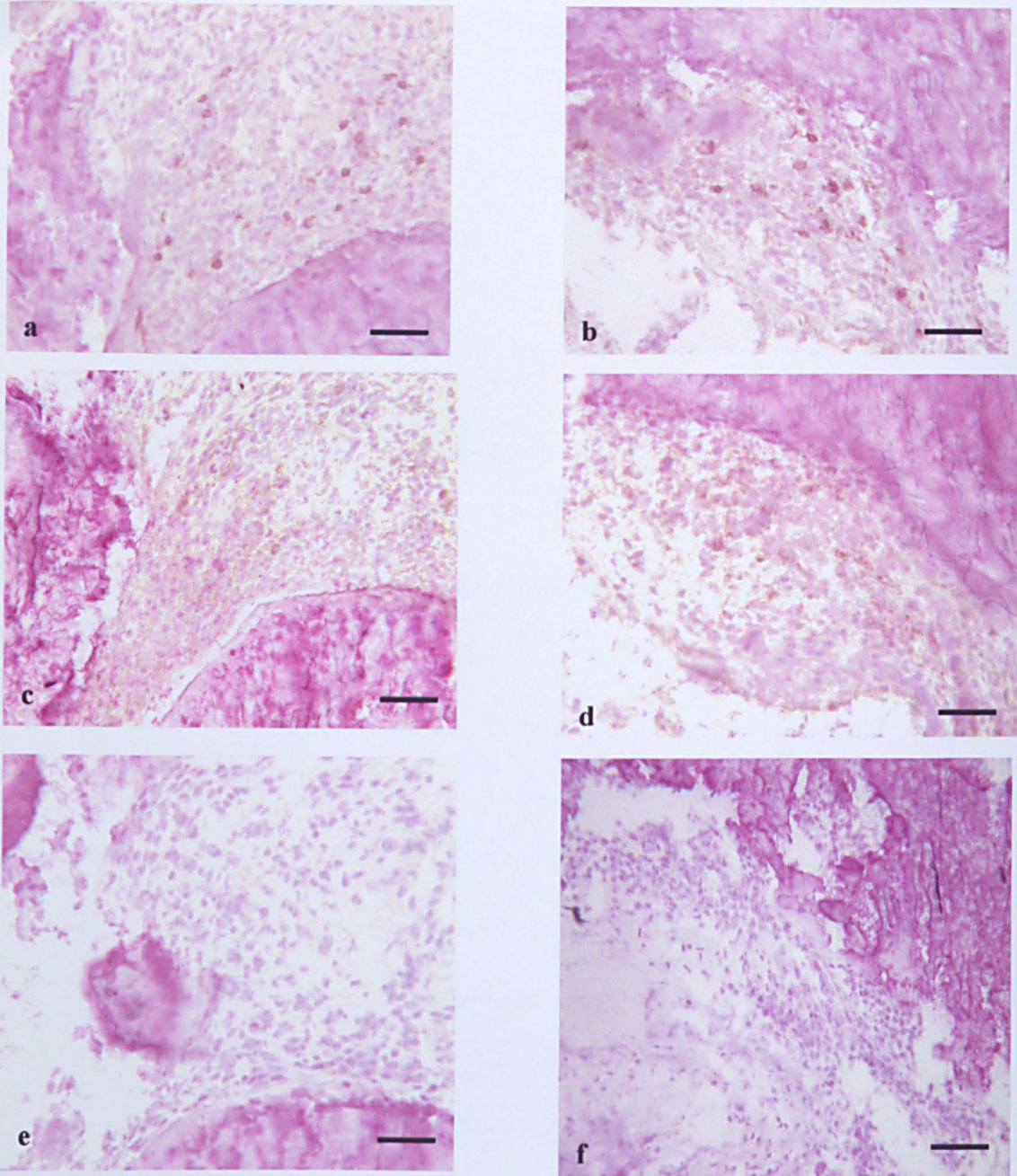


Figure 87: Undecalcified joint sections from a 158 day old *Il1rn*^{-/-} mouse. a & b) CD4⁺ cells within the inflammatory infiltrate of the arthritic joint. c & d) IFN γ ⁺ cells in same areas as CD4⁺ cells. e & f) lack of IL-4⁺ cells. Scale bar = 40 μ m.

Il1rn^{-/-} mice, one joint was severely swollen, and three were slightly swollen. Neither wild-type mouse outwardly appeared affected.

Immunohistochemical staining of undecalcified joints revealed the presence of large numbers of F4/80⁺ macrophages within the pannus (Figure 85) and abundant IL-1 β production (Figure 85, Figure 86) in the most severely affected joint. The presence of large numbers of macrophages within the infiltrate is consistent with the pannus seen in human RA joints. The production of IL-1 β is also consistent with human RA where biologically active IL-1 β is abundant in synovial fluid from the inflamed joints [Wood *et al.*, 1983; Hopkins *et al.*, 1988].

CD4⁺ T-cells, although numerous, were less abundant than macrophages (Figure 85) in the most affected joint. Although there was a visible production of IFN γ within the infiltrate, IL-4 production was rare in the very swollen *Il1rn*^{-/-} joint, and absent in all other joints tested (Figure 85, Figure 87). Therefore, the majority of the CD4⁺ T-cells present were of a Th1 type. In human RA, T-cells within the pannus also display a Th1-type cytokine profile [Simon *et al.*, 1994]. CD8⁺ T-cells, although present within the inflammatory infiltrate of the most affected joint, were far fewer in number than either CD4⁺ T-cells or macrophages. The slightly swollen joints from the three other *Il1rn*^{-/-} mice appeared histologically normal.

In *Il1rn*^{+/+} mice, there was no visible pannus formation, and immunohistochemical stains for IL-1 β , IFN γ and IL-4 were all negative. A very small number of T-cells

Figure 88: Immunohistochemical staining of a Balb/c *Il1rn*^{+/+} joint

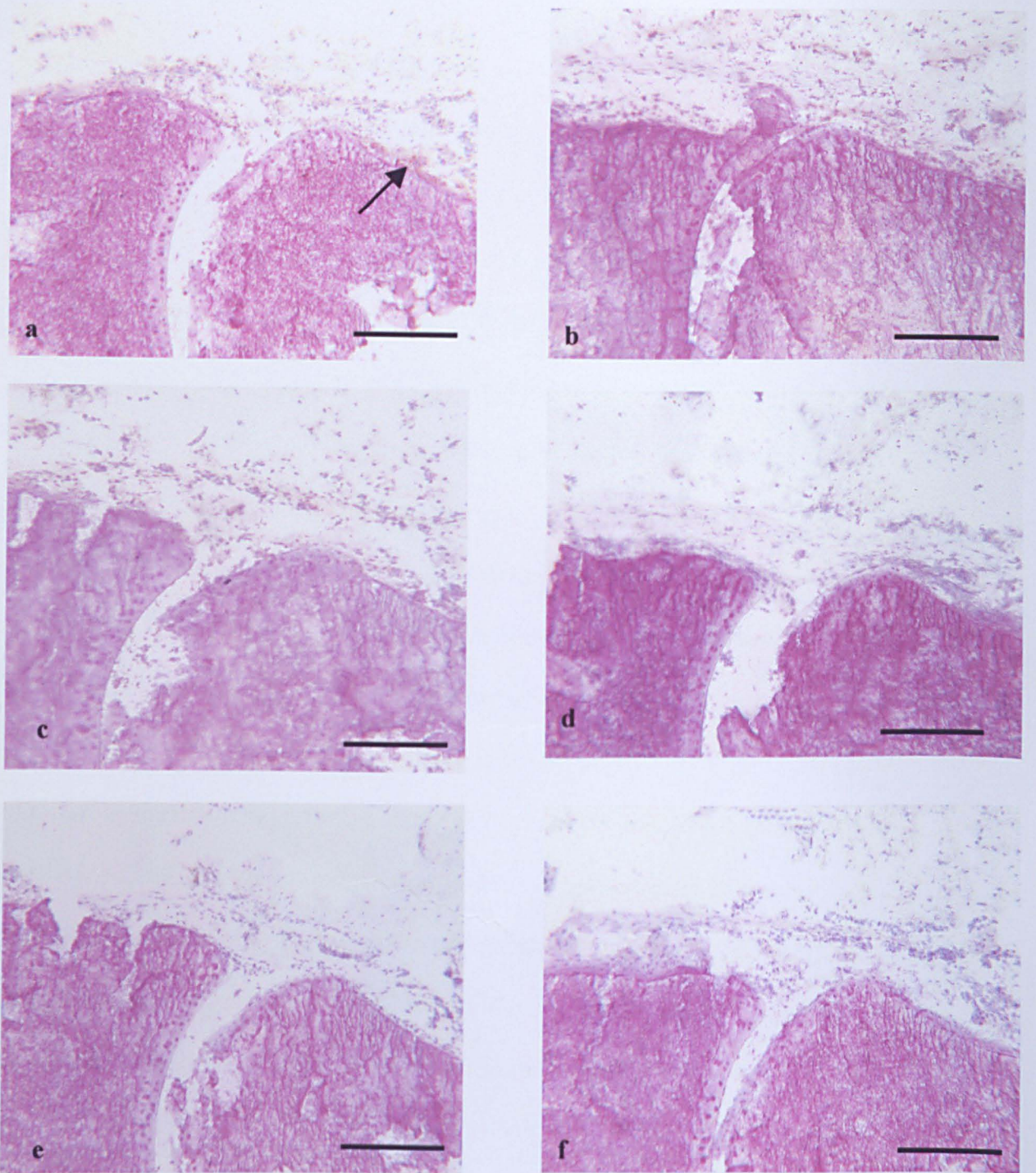


Figure 88: Immunohistochemical staining of *Il1rn*^{+/+} joint (155 day old female). a) F4/80 staining. Note macrophage-like synovial cells which are F4/80⁺ (arrow). b) IL-1 β , c) CD4⁺, d) IFN γ ⁺, e) IL-4, f) negative control. Scale bar = 200 μ m.

and macrophages were detected throughout the joint, and macrophage-like synovial lining cells were also detected with the F4/80 antibody (Figure 88).

These results are preliminary, and further undecalcified frozen joints will be immunohistochemically stained to ascertain whether these results can be supported.

3.6: *Il1rn*^{-/-} mice on a Balb/c background can develop arteritis, a psoriatic disease and an RA-like disease simultaneously

Il1rn^{-/-} mice on a Balb/c background can suffer from arteritis, a psoriasis-like disease and an RA-like disease, either independently or as a combination of two or three of the diseases. On the other hand, *Il1rn*^{-/-} mice on the Sf3 background suffer from arteritis but not the psoriatic or RA-like diseases. C57BL/6 appear not to suffer from any of these diseases [Nicklin *et al.* 2000; Horai *et al.*, 2000].

Of 20 Balb/c *Il1rn*^{-/-} mice examined for arteritis, 9/20 were suffering from all three diseases if arthritis was judged by an external examination, 10/20 were suffering from the psoriatic disease and arteritis, and 1/20 had the psoriatic disease but neither RA nor arteritis. In these cases however presence or absence of the RA-like disease was only confirmed histologically in 3 animals (out of 4 examined). The others were judged as having the RA-like disease if their limbs were reddened and swollen, and/or their gait was affected.

Although it is unclear whether the animals are suffering from psoriatic arthritis or psoriatic disease and arthropathy concurrently, it seems more likely to be the

latter case. Whereas the psoriatic disease is seen as early as F2 in these animals, with the same incidence as in deeply backcrossed animals, the arthropathy only occurs in the deep backcross. Moreover, some animals develop the psoriatic disease but not the arthropathy, and vice versa. The arteritis appears in all generations. It is postulated that the *Il1rn*^{-/-} mice actually have three distinct inflammatory diseases with a genetic component which makes them strain specific.

Section 4: Discussion

4.1: Mice lacking IL-1ra spontaneously develop inflammatory diseases

Mice which lack interleukin-1 receptor antagonist, whose only known function is to oppose the activity of the pro-inflammatory cytokine IL-1, spontaneously develop at least three chronic inflammatory diseases with high penetrance. These include an inflammatory disease of the major arteries, a psoriatic disease of the exposed skin on the ears (as first shown in this work), and a rheumatoid arthritis-like disease of the joints. Of the three, the psoriatic and RA-like diseases are seen in animals on a Balb/c background, and not in Sf3 animals. In addition, C57BL/6 *Il1rn*^{-/-} mice do not appear to develop any of the three diseases. The lack of obvious exogenous antigens suggests that these are autoimmune diseases with genetic influences on susceptibility, but we would not discount the possibility of a strain-specific exogenous trigger.

4.2: Arteritis

4.2.1: Inflammatory artery disease in *Il1rn*^{-/-} mice

Characterisation of the inflammatory arterial lesions which spontaneously develop in mice lacking IL-1ra demonstrated their similarity to inflammatory arterial lesions in human giant cell arteritis (GCA) and Takayasu's arteritis (TA) in the following respects. The murine lesions localise to the same areas of turbulent blood flow in the major elastic arteries as those in the human [Hunder *et al.*, 1985; Numano *et al.*, 2000]. Immunohistologically, the similarities to GCA and TA include the presence of a large inflammatory cellular infiltrate surrounding the affected vessel, which consists of large numbers of activated macrophages, activated Th1-type CD4⁺ T-cells, neutrophils and dendritic cells [Banks *et al.*,

1983; Wagner *et al.*, 1994; Weyand *et al.*, 1996; Inder *et al.*, 2000]. Multinucleated giant cells have not been observed thus far in the lesions of our *Il1rn*^{-/-} mice, but giant cells have been seen in the heart lesions of other murine diseases, such as experimentally induced autoimmune myocarditis [Afanasyeva *et al.*, 2001]. Examination of larger numbers of paraffin embedded sections may demonstrate the presence of giant cells in the future.

The infiltrate, as in GCA and TA [Wagner *et al.*, 1994; Weyand *et al.*, 1996] appears to arrive at the lesional area via the vasa vasorum, the microvasculature deep within the adventitial layer, rather than via the main vessel. Evidence for this arises from the observations that inflammatory infiltrates are apparent before elastin degradation (see Figure 17), and in earlier lesions the infiltrate is observed only within the outer layers of the vessel walls, progressing towards the lumen of the large vessel as the lesion develops (see Figure 21). The elastic layers of the vessel wall become damaged and fragmented, but there is also evidence of repair. The repair process is also seen in TA lesions where younger inflammatory lesions can be found near to older, fibrotic ones [Hotchi, 1992]. The lesions are also specific to the large elastic arteries (as are GCA and TA); neighbouring veins and small arteries are unaffected. It appears that *Il1rn*^{-/-} mice may make an appropriate animal model for the study of human arteritides such as GCA and TA, whose causes and aetiologies are currently unknown. Presently, the only animal models for the study of GCA are xenotransplantation models, where temporal biopsies from GCA patients are engrafted onto NOD-SCID mice [Brack *et al.*, 1997a, 1997b], or infection-induced arteritides [Blessing *et al.*, 2000; reviewed in Dal Canto & Virgin, 2000]. Our *Il1rn*^{-/-} mice develop a GCA/TA-like disease

spontaneously and with a high penetrance. They may provide a more useful model than xenografts or infection based disease, since the initiating factors (other than bacterial or viral infection) in disease development could be studied.

From the initial study presented here, it seems that serum amyloid A levels are not useful as a marker for the presence of destructive arterial lesions. Although levels were raised in animals with destructive arteritic lesions, the levels were not as high as expected. For example, 2 days after experimental injection of mice with 10 µg of LPS, plasma SAA levels rise from a mean of 470 µg/ml to a mean of 300 mg/ml [Yamada *et al.*, 1999]. The baseline levels of SAA in this study are high in comparison to another in which SAA levels rise from a baseline of < 5 µg/ml to ~ 170 µg/ml 49 hours post injection of CpG-DNA [Schmidt *et al.*, 1999]. In another study which involved monitoring SAA mRNA levels in mice following intraperitoneal injection of IL-1β, SAA mRNA levels were increased in a dose-responsive manner by up to 16-fold [Weinstein & Taylor, 1987]. The peak level of SAA measured in our animals was only 35 µg/ml, which is physiologically insignificant, and represents only a 2-fold increase from the baseline.

4.2.2: Initiating factors in development of arteritis

Although the initiating factors are still unclear, it can be seen that the lesions develop rapidly. From 56-57 to 75-81 days in the time course study, in which there was a maximum of 25 days age difference, there was a development in the size and inflammatory capacity of the lesions. Therefore, large lesions can clearly be seen in young adults. During the 75-81 day age group there was also the first positive staining for the chemokine MCP-1 and E-selectin (indicating activated

endothelial cells). Although it may be expected that E-selectin expression on endothelial cells would precede the larger infiltrate, it could be that this was in fact the case and was missed by having a 25 day gap between age groups. Alternatively, it is possible that E-selectin was being expressed at the early lesional sites in the younger *Il1rn*^{-/-} animals but was at too low a level, or at too few sites, to be detected by this technique.

From the immunohistochemical staining performed, it appears CD4⁺ T-cells are possibly the first to arrive at the lesional sites of turbulent blood flow, since in the earliest detectable lesions they appeared in larger numbers than the activated macrophages. This could indicate an interaction between activated CD4⁺ T-cells and mature dendritic cells within the lymph nodes. It is possible that IL-1 produced in response to turbulent blood flow in the absence of IL-1ra causes the inappropriate maturation of dendritic cells, which migrate to the lymph nodes and present autoantigen to T-cells which are then directed to the vascular wall. Possible dendritic cell involvement is discussed further in section 4.6.

Lesions localise to areas of turbulent blood flow such as around valves, and in early lesions activated CD4⁺ T-cells and macrophages can be seen accumulating at these sites. Therefore, it seems likely that turbulent blood flow, which creates low, fluctuating shear stresses may be the causative factor in arterial lesion development in *Il1rn*^{-/-} mice. At these same sites, there may be the deposition of both endogenous and exogenous debris. In wild-type mice, the balance of IL-1 and IL-1ra available to the receptors remains undisturbed. Both IL-1 and IL-1ra are produced simultaneously, and compete for the type 1 receptor. However, with

the removal of IL-1ra from the balance, there is no competition and all IL-1R1 present within the area is available for binding by IL-1. In wild-type mice, the mild damage occurring as a result of turbulent blood flow may cause the recruitment of macrophages and dendritic cells to the area. However, any possible autoantigens processed by the DCs would not be presented, since they would not frequently be matured and thus would not often migrate to the lymph nodes to activate CD4⁺ T-cells with autoantigen. If this was the case, a small number of activated macrophages would be expected at the sites of turbulent blood flow in *Il1rn*^{+/+} animals as well as *Il1rn*^{-/-}. Again it is possible that this occurs at an undetectable level, or it may be that the action of IL-1ra is rapid and prolonged, and any initial activation of macrophages has been missed in this study.

With the removal of IL-1ra from the system however, a rapid sequence of inflammatory events could occur via the action of unopposed IL-1. These may include the inappropriate maturation of dendritic cells which could present vascular autoantigens to T-cells following their migration to the lymph nodes (see section 4.6), upregulation of adhesion molecules, production of chemokines inducing further recruitment of leukocytes to the area, and self-upregulation. Therefore, it is proposed that arterial lesions in *Il1rn*^{-/-} mice initially develop as a result of chaotic shear stresses caused by turbulent blood flow, and steadily and rapidly increase in size and destructive capacity due to the unopposed action of IL-1.

4.2.3: Bacterial infection in heart disease

Various studies suggest that *Chlamydia*, *H. pylori* and other micro-organisms may increase patient risk of development of inflammatory arterial disease [Muhlstein, 1998; Folsom *et al.*, 1998]. Our colony of *Il1rn*^{-/-} mice, which suffer from arteritis, is housed under SPF conditions and have been shown to be free of infection by mouse *Chlamydia*, and a set of other pathogens (see section 2.1.2). Murine *Helicobacter* infection however is not routinely assayed and is known to be widespread amongst laboratory mice.

This investigation revealed evidence of infection by *Helicobacter hepaticus* in mice of all genotypes, both from our laboratory and from the colony of Hirsch *et al.*

Since the C57BL/6 *Il1rn*^{-/-} mice of Hirsch *et al.* do not develop arteritis, it appears that infection by *H. hepaticus* alone is not enough to induce the formation of inflammatory arterial lesions in *Il1rn*^{-/-} mice. However, the possibility that it may be insufficient but required for multifactorial disease development cannot be excluded. Future work to eliminate the possibility of pathogens as causative agents will involve sterile rederivation of *Il1rn*^{-/-} mice (collaborative study with Leo Joosten and Wim Van den Berg, University of Nijmegen, the Netherlands). From the model for arterial lesion development in *Il1rn*^{-/-} mice proposed here, rederivation of *Il1rn*^{-/-} mice into a sterile environment should not affect the incidence of arteritis.

4.2.4: The influence of *H-2* haplotype on lethality of arteritis

Il1rn^{-/-} Sf3 mice appeared to segregate into two lines, one of which suffered from an increased lethality of the arteritis. The lines had apparently heritable ages of signs of disease onset [Nicklin *et al.*, 2000]. Mice from the non-sensitive line, although still developing arteritis as confirmed by histology, all had a death age of >350 days whereas the sensitive line had a mean death age of 103 days. It seemed likely that MHC haplotype may influence sensitivity to the disease, however genotyping of *Il1rn*^{-/-} mice from both lines at 4 points across the murine MHC (*H-2*) revealed that they shared the same *H-2* haplotypes. In addition, the haplotype, *H2*^b, is shared by C57BL/6 mice, which do not develop arteritis. Although it remains statistically likely that a single modifier gene confers sensitivity to arteritis, this study does not suggest that the *H-2* haplotypes *H2*^u and *H2*^b give differential susceptibility, nor that *H2*^b is a susceptibility factor.

4.3: Psoriasis

4.3.1: Balb/c mice lacking *IL-1ra* suffer from a psoriasis-like disease

All of the histological hallmarks of human psoriasis investigated were present in inflamed *Il1rn*^{-/-} ear sections. These included a mixed dermal inflammatory infiltrate, acanthosis (a thickening of the epidermis) and expression of keratin 6, indicating keratinocyte hyperproliferation, the formation and elongation of epidermal rete pegs, the elongation of the dermal papillae between the rete pegs, neutrophilic epidermal infiltrates and the formation of Munro microabscesses with neutrophil aggregation beneath the stratum corneum, an increase in vascularity, upregulation of adhesion molecules (ICAM-1) and E-selectin expression, and the presence of a large number of dermal mast cells.

One difference from the inflammatory infiltrate seen in arteritic lesions was the presence of the Th2 type cytokines IL-4 and IL-5 as well as IFN γ and IL-1 β . IL-4 and IL-5 are generally not found in arteritic lesions of *Il1rn*^{-/-} mice, even in the same animals. This is not in disagreement with data on human psoriatic lesions, where analysis of T-cell clones derived from psoriatic plaques revealed the presence of Th0, Th1 and Th2 T-cell subsets [Barna *et al.*, 1994]. In another study, the production of IL-5 in T-cell clones derived from lesional psoriatic skin has been detected. This profile was observed in T-cell clones whose supernatants were capable of acting as mitogens for keratinocytes *in vitro*, indicating a possible novel subset of T-cells in the pathology of psoriatic lesions [Vollmer *et al.*, 1994].

Il1rn^{-/-} mice on an Sf3 background, housed in the same laboratory as the Balb/c mice, only exceptionally rarely appear to develop the disease. This suggests a genetic influence on disease susceptibility. Human psoriasis is multifactorial in origin, but also shows a genetic contribution to disease development. It shows a strong association with, for example, the MHC gene HLA-CW6. Balb/c mice have an overall MHC genotype of *H-2*^d, unlike the Sf3 and C57BL/6 mice, which may in part play a role in the development of psoriasis and arthritis in Balb/c mice. Further experiments are currently in progress to identify genetically predisposing factors, involving the crossing of C57BL/6 *Il1rn*^{-/-} mice with Balb/c *Il1rn*^{-/-} mice and correlating the progress of the inflammatory diseases in the F2 with carriage of *H-2* alleles, and later with a whole genome search. This should reveal whether the *H-2*^d haplotype has a major role in determining sensitivity to arthritis, arteritis, and psoriasis in *Il1rn*^{-/-} mice.

Various other animal models for psoriasis exist (see section 1.2.17). However, despite collectively displaying all of the hallmarks of human psoriatic disease, none of these examples seem to be complete models of human psoriasis. For example, T-cells do not appear to play a role in the development of the flaky skin phenotype, which is otherwise a good model [Schon, 1999]. The psoriatiform disease which spontaneously arises in our Balb/c *Il1rn*^{-/-} mice compares very favourably to other models, and all the key features of human psoriasis examined so far have been present. More detailed studies, such as the effect of treatment with cyclosporin A, or adoptive T-cell transfer into SCID mice, may offer further support to the value of IL-1ra deficient mice on a Balb/c background being a useful animal model in the study of human psoriasis.

4.4: Rheumatoid arthritis

4.4.1: Rheumatoid arthritis in Balb/c *Il1rn*^{-/-} mice

Initial experiments suggest that the arthropathy which develops spontaneously in Balb/c *Il1rn*^{-/-} mice is an erosive arthritis similar to human RA. Both involve destruction of the bone and cartilage by an inflammatory pannus which contains predominantly activated macrophages producing IL-1 β . CD4⁺ displaying a Th-1 type cytokine profile are also abundantly present within the inflamed area. The disease appears to be strain specific to *Il1rn*^{-/-} mice on a Balb/c background, suggesting a strong genetic contribution to susceptibility to the disease.

4.4.2: Comparison to RA in another colony of Balb/c *Il1rn*^{-/-} mice

Horai *et al.* describe a chronic erosive arthropathy in their Balb/c *Il1rn*^{-/-} mice [Horai *et al.*, 2000]. They showed, by histology, synovitis and articular erosion with the formation of a lymphocyte- and neutrophil-containing pannus. They also described other features similar to human RA such as the proliferation of synovial lining cells and activation of osteoclasts. Histologically, arthritic joints from our Balb/c *Il1rn*^{-/-} mice are similar in appearance. Pannus formation, degradation of bone and cartilage, and activated inflammatory cells are all evident.

ELISA determination of serum autoantibody levels by Horai *et al.* revealed increased levels of anti-IgG, anti-type II collagen and anti-DS DNA in the affected mice, although autoantibody levels did not correlate with disease severity. No antinuclear antibodies were found in the sera from three SF3 *Il1rn*^{-/-} mice in our colony [Nicklin *et al.*, 2000] although autoantibody levels in our Balb/c *Il1rn*^{-/-} mice have not been measured.

Horai *et al.* also showed, by densitometric analysis of Northern blots, augmented mRNA levels of IL-1 β , IL-6 and TNF- α in the affected joints, although TNF- α levels were only increased 1.2-1.5-fold compared to *Il1rn*^{+/+} mice. These results are not surprising, since the large increase in mRNA levels were seen at 112 days old, when the arthropathy was well established. The Balb/c *Il1rn*^{-/-} mice of Horai *et al.* begin to develop the disease by 35 days of age, with 100% of the animals being affected by 91 days of age. Our Balb/c *Il1rn*^{-/-} mice tend to develop the disease at a later age. This is the only difference detected thus far between the two colonies, since the Balb/c *Il1rn*^{-/-} mice of Horai *et al.* also develop arteritis, as

confirmed by examining cadavers kindly supplied by Y. Iwakura, and their ears also appear scaly (personal communication). The difference in age of onset may be due to the slight differences in genetic background. Horai *et al.* used a Balb/cA background whereas our mice are on a Balb/c(Harlan) background. There is also the possibility of environmental factors, such as differing microbial flora within the two facilities.

Another explanation for the phenotypic differences might be that the construction of the null allele may influence phenotype. Whereas in our colony only parts of exons 3 and 4 are deleted, the entire coding region was deleted by Horai *et al.* Overall however, the two colonies appear to have the same inflammatory phenotypes (apart from a later age of onset of arthritis in our colony). Whether the two arthropathies are similar in cell type and cytokine composition remains to be seen, since the immunohistochemical analysis of arthritic joints from Balb/c *Il1rn*^{-/-} mice presented in this study is unique. Further immunohistochemical analysis of the cell types and their products present within the arthritic lesions should give additional indications of similarities to human RA.

4.5: Psoriatic arthropathy or psoriasis and arthritis?

There is only one reported case of a human with psoriatic arthritis (PsA) and Takayasu's arteritis (TA) concurrently [Fukuhara *et al.*, 1998], whereas in the Balb/c *Il1rn*^{-/-} mice of our colony we have seen 8/9 of the cases with overt arthropathy examined for psoriasis and arteritis having the three diseases simultaneously. In addition, some features of the arthropathy observed in our animals may not necessarily agree with a diagnosis of PsA; for example the spine

does not appear to be affected, and the destruction of the joint seems more complete than may be expected in PsA where there is a lower cartilage turnover than in RA [Mansson *et al.*, 2001]. Further tests, such as measurement of rheumatoid factor (generally absent in PsA) and examination of the microvasculature of the synovium (which appears more tortuous in PsA arthropathy) [Reece *et al.*, 1999] may help to elucidate whether the mice suffer from PsA, or psoriatic and RA like diseases separately. The distinction however is often unclear even in human patients, and the clinical significance of making such a distinction in terms of treatment seems low.

An additional argument against a diagnosis of PsA in our mice is that *Il1rn*^{-/-} mice on a Balb/c background develop the psoriatic disease as early as the F2, where the arthritis is not observed. This suggests that the two diseases are under separate genetic controls, implying separate diseases.

4.6: Aetiology of inflammatory diseases in *Il1rn*^{-/-} mice – a possible central role for dendritic cells

Sources of IL-1

It is assumed that for the three diseases, in each case an initial source of biologically active IL-1 is required to begin the inflammatory cycle. In arteritis, it is proposed that low, chaotic shear stresses induce the release of IL-1 from vascular smooth muscle (SMC) and endothelial (EC) cells. IL-1 could be upregulated by low shear induced nuclear translocation of the transcription factor NF-κB (which acts on the *IL1A* and *IL1B* genes) [Nagel *et al.*, 1999], as a result of low amounts of regulatory nitric oxide (NO production by endothelial nitric oxide

synthase is induced by high shear stress) [Peng *et al.*, 1995], or by the deposition of inflammatory debris at the sites of low blood flow.

In the skin, IL-1 α is produced constitutively in epidermal keratinocytes [Ansel *et al.*, 1988; Partridge *et al.*, 1991]. In addition, in our animals *Il1rn*^{+/+} mice on Balb/c and Sf3 backgrounds showed the presence of CD4⁺ and F4/80⁺ cells within the dermis, with detectable IL-1 β and IFN γ production, without any further disease development. This indicates a constant, low level of inflammation within the exposed skin of the ears, possibly due to continual mild physical trauma. In the wild-type mice, this low level of inflammation is presumably kept in check by the action of IL-1ra. However, with the removal of IL-1ra, IL-1 is more potent and may initiate further IL-1 release from keratinocytes and other cells, thus beginning the inflammatory cascade.

Low levels of expression of both IL-1 α and IL-1 β mRNA can be measured in the joints of *Il1rn*^{+/+} mice [Horai *et al.*, 2000]. This expression may be due to mechanical stresses. Again, it is proposed that in wild-type mice, an IL-1/IL-1ra balance is maintained which does not favour the progression of an inflammatory response. The removal of IL-1ra from the system allows the constitutively produced IL-1 to commence an inflammatory cycle.

Experiments involving the breeding of animals lacking both IL-1ra and IL-1R1 are currently underway. Since the hypothesis is that the inflammatory diseases are due to the unopposed action of IL-1, then mice lacking the type 1 receptor as well

as IL-1ra should not suffer from the inflammatory diseases observed in *Il1rn*^{-/-} mice.

The action of IL-1 on dendritic and other cells

Extensive studies using dendritic cells (DC) in recent years have proved them to be key players in the immune response, with co-stimulatory and cytokine/chemokine producing functions as well as antigen processing and presentation. IL-1 has been shown to have several effects on DCs which would be relevant in these disease models.

DC activation in the skin will be considered first, since the epidermis contains a specific subset of DC. A critical first step in cutaneous inflammation is the migration of activated epidermal DC (Langerhans' cells, LC) to the draining lymph nodes where they encounter and prime naïve T-cells. IL-1 has been demonstrated to trigger the maturation and migration of LC in various studies. In a model using LC-like DC expanded from murine skin, IL-1 induced their dissociation from keratinocytes and increased the expression of MHC class II molecules, CD40 and CD86 (a co-stimulatory molecule) on the DC surfaces. It was shown that IL-1 enabled the DC to dissociate from the epidermal keratinocytes by causing a decrease in the expression of E-cadherin, a DC adhesion molecule [Jakob & Udey, 1998]. Intradermal injections of IL-1 cause a decrease in the number of LC in the epidermis and an increase in their numbers found in draining lymph nodes [Cumberbatch *et al.*, 1997], and in ICE and IL-1 β null mice, LC are not activated and do not migrate to the draining lymph nodes following the application of contact allergens [Antonopoulos *et al.*, 2001;

Shornick *et al.*, 2001]. IL-1 β produced by LC following their activation provides signalling for activation and migration of further LC [Cumberbatch *et al.*, 2001].

In the skin, IL-1 also has various effects on keratinocytes, such as inducing the expression of the hyperproliferative markers keratin 6 and keratin 16 [Weiss *et al.*, 1984; Stoler *et al.*, 1988], upregulating expression of ICAM-1 [Groves *et al.*, 1992], and the induction of production of the chemokine CCL27 (CTACK) [Homey *et al.*, 2002]. The receptor for CCL27, CCR10, is found on circulating skin-homing CLA⁺ (cutaneous lymphocyte-associated antigen) T-cells, dermal microvascular endothelial cells and fibroblasts. *In vivo* intracutaneous CCL27 attracts lymphocytes to the injection site [Homey *et al.*, 2002].

As well as its effects on LC specifically, the action of IL-1 on DC (including LC) has several outcomes. DC express CD40 on the cell surface, and ligation of CD40 by its ligand CD40L, in conjunction with IL-1 β , induces activation of both immature and mature DC causing them to release IL-12 [Wesa & Galy 2001]. IL-12 in turn induces CD4⁺ T-cells to produce a Th1 type cytokine profile, including the production of IFN γ [Manetti *et al.*, 1993]. IL-1 β /CD40L (CD40L is expressed on the surface of activated T-cells) can then synergise with IFN γ to induce a higher rate of IL-12 production from DC [Wesa & Galy 2001]. IFN γ also increases the expression of CD40 and E-selectin on human dermal microvascular endothelial cells, increasing lymphocyte trafficking into the area of inflammation within the skin [Singh *et al.*, 2001].

Figure 89: Model of proposed involvement of dendritic cells

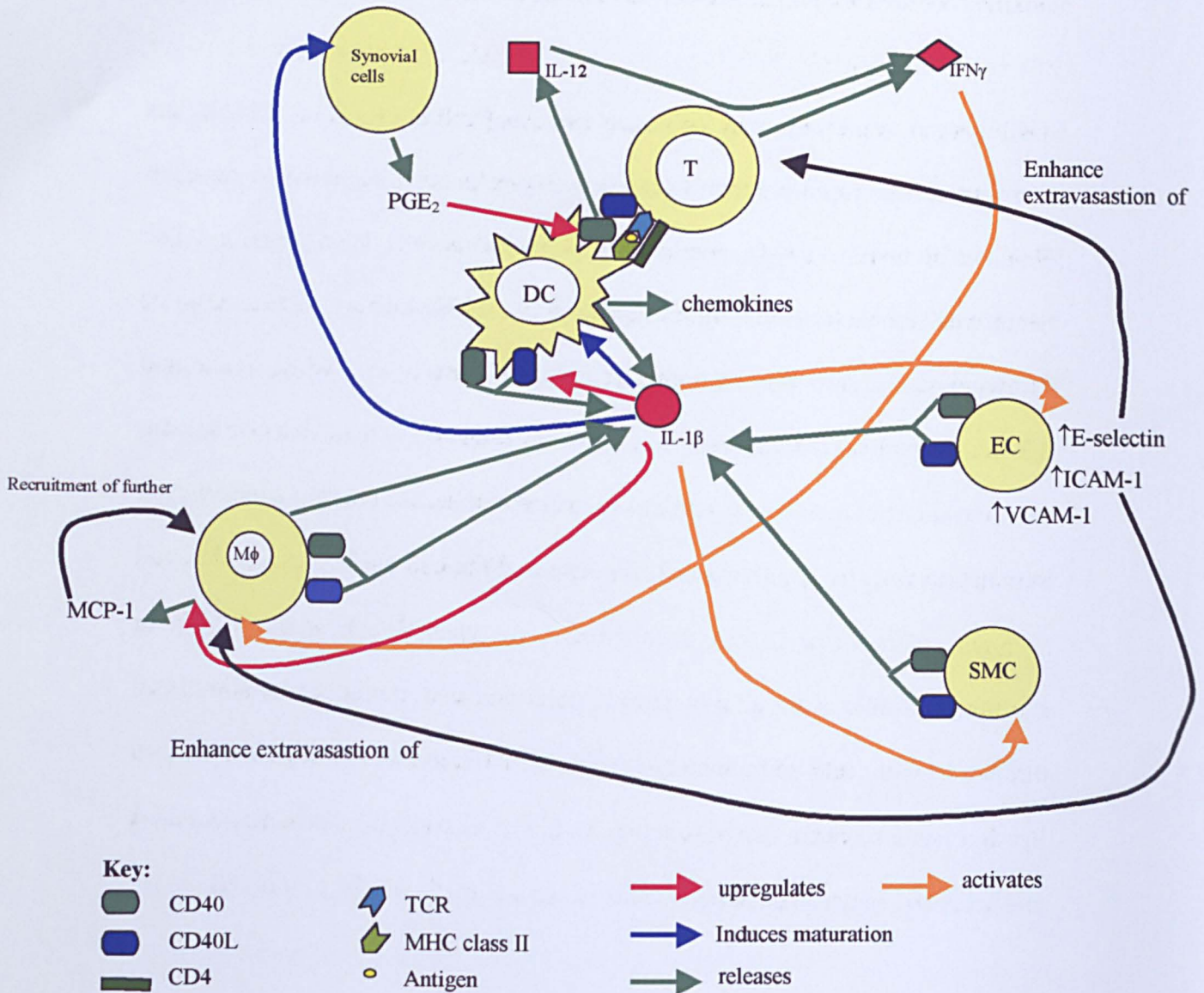


Figure 89: Ligation of CD40 on the DC cell surface by CD40L in conjunction with IL-1 β induces DC to release IL-12. IL-12 induces the release of IFN γ from T-cells which synergises with IL-1/CD40L to induce further production of IL-12 from DC. IL-1 induces the maturation of DC, and it may be in the case of IL-1ra deficient mice that unopposed IL-1 causes an inappropriate maturation of DC, causing them to present self-antigens to T-cells, thereby activating them, via MHC class II.

In a T-cell independent system, IL-1 β can increase the expression and de novo synthesis of CD40L on DC, vascular smooth muscle cells, macrophages and endothelial cells which all also express CD40. DC, vascular SMC and EC can release further IL-1 β following CD40 ligation, and on EC, it can also lead to augmented expression of E-selectin, ICAM-1 and VCAM-1 (as well as these molecules being upregulated directly by IL-1 β). PGE $_2$ released from synovial cells following stimulation with IL-1 β can cause DC to release IL-1 β and upregulates expression of CD40. Activated DC also release chemokines, as do activated macrophages, resulting in an increase in leukocyte extravasation into the inflamed area.

In a recent study, Luft *et al.* showed that IL-1 β enhanced the CD40L mediated cytokine secretion by DC in a T-cell independent manner, since no T-cells or T-cell cytokines, originally thought to be essential for DC cytokine release following CD40 ligation, were present in their assay systems [Luft *et al.*, 2002]. CD40L has been found to be rapidly upregulated on non-T-cells such as activated platelets [Henn *et al* Nature 1998], eosinophils [Gauchat *et al.*, 1995], and on DC themselves [Pinchuk *et al.*, 1996; Salgado *et al.*, 1999] during inflammation or following stress. Importantly, from the point of view of this work, functional CD40L, co-expressed with CD40, has also been found on human vascular smooth muscle cells, endothelial cells and macrophages in atherosclerotic plaques *in situ*. Stimulation with IL-1 β , TNF α or IFN γ increased the cell surface expression and de novo synthesis of CD40L in all three cell types [Mach *et al.*, 1997]. In addition, vascular wall smooth muscle cells and endothelial cells, stimulated through CD40L, release biologically active IL-1 [Schonbeck *et al.*, 1997]. CD40 ligation has also been shown to augment the expression of E-selectin, ICAM-1 and VCAM-1 in aortic endothelial cells [Karmann *et al.*, 1995] (Figure 89).

These initial T-cell independent activation and cytokine secretion mechanisms, particularly for DC, may explain in part why antigens or autoantigens cannot be detected in some inflammatory diseases, since antigen specific T-cells are not required for these pathways of cytokine release. However, IFN γ released from T-cells certainly appears to augment many of these processes, and production of IFN γ is seen in all three inflammatory diseases in our *Il1rn*^{-/-} mice.

On the other hand, maturation of DC involves a change from being efficient at capturing and processing antigen, to having immunostimulatory capabilities. Inappropriate maturation of DC by IL-1 or by IL-1 upregulated by CD40L-CD40 interactions with T-cells or non T-cells, may cause the DC to present autoantigens to naïve T-cells in the lymph nodes in the absence of any maturation/migration induced by exogenous antigen uptake. Moreover, in humans the association of certain MHC haplotypes with RA, GCA, TA and psoriasis does point to the importance of antigen presentation in disease development. As DC are “professional” antigen presenting cells, this supports the hypothesis that they play a central role.

Experiments which may be useful to study the role of T-cells in the development of the inflammatory diseases in our *Il1rn*^{-/-} mice would include crossing the SCID mutation into the colony, crossing *Il1rn*^{-/-} with CD40L (CD154) null mice, and using complement fixing antibodies against CD4⁺ T-cells. Use of the SCID mutation would eliminate functional B-cells as well as T-cells, thereby enabling study into the effects of removing both humoral and cell-mediated immune reactions from the IL-1ra null mice. Unless there is as yet identified autoantibody production in our IL-1ra deficient mice, the effects of crossing in the SCID mutation may be similar to those achieved by using antibodies against CD4⁺ T-cells, or even by performing neonatal thymectomies on the *Il1rn*^{-/-} mice (which would prevent the development of all mature T-cells). Crossing *Il1rn*^{-/-} with CD40L deficient mice may have a far more generalised effect, since several cell types have CD40L on the cell surface. Comparison of these animals to *Il1rn*^{-/-} mice treated with anti-CD4 antibodies may help to elucidate the importance of T-

cell derived CD40L interactions with CD40, in comparison to other CD40L-bearing cells, in the mechanism of disease development.

Further release of IL-1 β by DC, as well as an increase in cell surface CD40 and MHC class II molecules and release of IL-6, TNF- α and IL-12, follows stimulation of DC with prostaglandins, especially PGE₂ [Steinbrink *et al.*, 2000]. PGE₂ production is induced by IL-1 in human synovial cells [Mizel *et al.*, 1981; Dayer *et al.*, 1986] and fibroblasts [Postlethwaite *et al.*, 1988]. This may have importance in the arthritic disease; IL-1 could stimulate PGE₂ production from synovial cells, which could act, along with IL-1 β , on DC to increase cell surface CD40 allowing increased interactions with CD40L on T- and other cells, and to increase the production of further IL-1 β and TNF- α , which has been proved to be a major cytokine involved in RA. Both DC progenitors and myeloid DC growth factors can be detected in RA synovial fluid, which may act as a reservoir for active DC [Santiago-Schwarz *et al.*, 2001].

Therefore, it is proposed that from an initial release of IL-1 by, for example, stressed endothelial cells, which would be kept in balance by IL-1ra in a wild-type mouse, an inflammatory cascade occurs which involves DC in a central role. Initial maturation of DC by IL-1 could lead to chemokine and pro-inflammatory cytokine release by DC, chemokine and IL-1 up-regulated adhesion molecule and selectin mediated recruitment of macrophages (providing the bulk of IL-1 β secretion) and IFN γ producing T-cells. The further secretion of IL-1 β by macrophages and IFN γ production in T-cells would augment the inflammatory processes, including macrophage activation and increased DC maturation by IL-1,

and IL-1 acting in conjunction with CD40L. DC maturation would in turn lead to increased cytokine and chemokine release, and stimulation of further T-cells to proliferate and polarise to a Th1 phenotype by DC production of IL-12.

Meanwhile, chemokines (for example, MCP-1 as seen in this study) may also be released by other cells including macrophages, monocytes, fibroblasts and keratinocytes, which would act as chemoattractants for further macrophages, neutrophils and T-cells. Neutrophils are observed in abundance in the inflammatory diseases in *Il1rn*^{-/-} mice (Figure 89).

In the psoriatic disease, the overproduction of IL-1 may lead to dysregulation of keratinocyte proliferation, causing them to hyperproliferate resulting in the characteristic psoriatic epidermis. In the arteritis and RA-like disease, destruction of the tissues, bone and cartilage is presumably due to the release of matrix metalloproteinases from activated macrophages. Further studies on the release of MMPs at these sites should increase our understanding of precise damage mechanisms. Analysis of lesional and non-lesional tissue by quantitative real-time reverse transcriptase PCR could be used to study the comparative levels of MMP mRNA within the tissues, and also to identify the major proteinases present within lesions.

These complex and destructive processes may all stem from a low level of IL-1 initially produced, which in a system lacking IL-1ra, is a high effective level.

4.7: Conclusions

Since the three inflammatory diseases found in our *Il1rn*^{-/-} mice histologically and immunohistochemically resemble human diseases including giant cell arteritis, Takayasu's arteritis, psoriasis and rheumatoid arthritis, it is proposed that they may make appropriate models for the study of these diseases.

It would appear that the inflammatory diseases which develop in *Il1rn*^{-/-} mice are indeed a direct result of the unopposed action of IL-1, although other factors, such as genetic background, also play a role in specific disease development. It is possible to propose mechanisms by which an imbalance in the IL-1/IL-1ra dynamic would cause the development of each specific inflammatory response, although direct evidence to support these models is still required. Further experiments, such as rederivation into a sterile environment, crossing *Il1rn*^{-/-} animals with, for example, CD154 null mice, correlating disease phenotype with the carriage of H2^d and H2^b alleles in C57BL/6 x Balb/c crosses, and examining the phenotypes of *Il1rn*^{-/-}/*Il1r1*^{-/-} mice should provide further evidence in support of the proposed models. The exact mechanisms of how joint or organ specific inflammatory responses arise in an animal that systemically lacks IL-1ra remain to be elucidated, but these animal models provide a starting point for solving these and other problems.

The presence of a variety of striking inflammatory diseases in mice which lack functional IL-1ra reinforces the importance of the maintenance of a systemic balance between pro- and anti-inflammatory cytokines.

Section 5: References

Afanasyeva, M., Wang, Y., Kaya, Z., Park, S., Zilliox, M.J., Schofield, B.H., Hill, S.L., and Rose, N.R. (2001). Experimental autoimmune myocarditis in A/J mice is an interleukin-4-dependent disease with a Th2 phenotype. *Am J Pathol.* **159**: 193-203

Akahoshi, T., Wada, C., Endo, H., Hirota, K., Hosaka, S., Takagishi, K., Kondo, H., Kashiwazaki, S., and Matsushima, K. (1993). Expression of monocyte chemotactic and activating factor in rheumatoid arthritis. Regulation of its production in synovial cells by interleukin-1 and tumour necrosis factor. *Arthritis Rheum.* **36**: 762-771.

Akira, S., Takeda, K., and Kaisho, T. (2001). Toll-like receptors: critical proteins linking innate and acquired immunity. *Nature Immunol.* **2**: 675-680.

Allen, M.H., Veal, C., Faassen, A., Powis, S.H., Vaughan, R.W., Trembath, R.C., and Barker, J.N.W.N. (1999). A non-HLA gene within the MHC in psoriasis. *Lancet* **353**: 1589-1590.

Andersson, J., Bjork, L., Dinarello, C.A., Towbin, H., and Andersson, U. (1992). Lipopolysaccharide induces human interleukin-1 receptor antagonist and interleukin-1 production in the same cell. *Eur. J. Immunol.* **22**: 2617-2623.

Ansel, J.C., Luger, T.A., Lowry, D., Perry, P., Roop, D.R., and Mountz, J.D. (1988). The expression and modulation of IL-1 alpha in murine keratinocytes. *J. Immunol.* **140**: 2274-2278.

Antonopoulos, C., Cumberbatch, M., Dearman, R.J., Daniel, R.J., Kimber, I., and Groves, R.W. (2001). Functional caspase-1 is required for Langerhans cell migration and optimal contact sensitisation in mice. *J. Immunol.* **166**: 3672-3677.

Arend, W.P., Michel, B.A., Bloch, D.A., Hunder, G.G., Calabrese, L.H., Edworthy, S.M., Fauci, A.S., Leavitt, R.Y., Lie, J.T., Lightfoot, R.W., Masi, A.T., McShane, D.J., Mills, J.A., Stevens, M.B., Wallace, S.L., and Zvaifler, N.J. (1990). The American college of rheumatology 1990 criteria for the classification of Takayasu arteritis. *Arthritis Rheum.* **33**: 1129-1134.

Arend, W.P., Smith, M.F., Janson, R.W., and Joslin, F.G. (1991). IL-1 receptor antagonist and IL-1 β production in human monocytes are regulated differently. *J. Immunol.* **147**: 1530-1536.

Arenzana-Seisdedos, F., Virelizier, J., and Fiers, W. (1985). Interferons as macrophage-activating factors III. Preferential effects of interferon- γ on the interleukin-1 secretory potential of fresh or aged human monocytes. *J. Immunol.* **134**: 2444-2448.

Auron, P.E. and Webb, A.C. (1994). Interleukin-1: A gene expression system regulated at multiple levels. *Eur. Cytokine Netw.* **5**: 573-592.

- Auron, P.E., Webb, A.C., Rosenwasser, L.J., Mucci, S.F., Rich, A., Wolff, S.M., and Dinarello, C.A. (1984) Nucleotide sequence of human monocyte interleukin 1 precursor cDNA. *Proc Natl Acad Sci U S A*. **81**: 7907-7911.
- Austrup, F., Vestweber, D., Borges, E., Lohning, M., Brauer, R., Herz, U., Renz, H., Hallmann, R., Scheffold, A., Radbruch, A., and Hamann, A. (1997). P- and E-selectin mediate recruitment of T-helper-1 but not T-helper-2 cells into inflamed tissues. *Nature* **385**: 81-83.
- Baden, H.P. (1984). Biology of the epidermis and pathophysiology of psoriasis and certain ichthyosiform dermatoses. In: *Pathophysiology of dermatologic diseases* (Eds. Soter, N.A., and Baden, H.P.). McGraw-Hill. pp. 101-127.
- Baker, B.S., Swain, A.F., Fry, L., and Valdimarsson, H. (1984). Epidermal T lymphocytes and HLA-DR expression in psoriasis. *Br. J. Dermatol.* **110**: 555-564.
- Balavoine, J., de Rochemonteix, B., Williamson, K., Seckinger, P., Cruchaud, A., and Dayer, M. (1986). Prostaglandin E₂ and collagenase production by fibroblasts and synovial cells is regulated by urine-derived human interleukin-1 and inhibitor(s). *J. Clin. Invest.* **78**: 1120-1124.
- Baltazares, M., Mendoza, F., Dabague, J., and Reyes, P.A. (1998). Antiaorta antibodies and Takayasu arteritis. *Int. J. Cardiol.* **66**: S183-S187.
- Banks, P.M., Cohen, M.D., Ginsburg, W.W., and Humnder, G.G. (1983). Immunohistologic and cytochemical studies of temporal arteritis. *Arthritis Rheum.* **26**: 1201-1207.
- Barker, J. N.W. N. (1991) The pathophysiology of psoriasis. *Lancet* **338**: 227-230
- Barna, M., Snijedewint, F.G., van der Heijden, F.L., Bos, J.D., and Kapsenberg, M.L. (1994). Characterisation of lesional psoriatic skin T lymphocyte clones. *Acta Derm. Venereol. Suppl. (Stockh)* **186**: 9-11.
- Baumhueter, S., Dybdal, N., Kyle, C., and Lasky, L.A. (1994). Global vascular expression of murine CD34, a sialomucin-like endothelial ligand for L-selectin. *Blood* **84**: 2554-2565.
- Beasley, D., and Cooper, A.L. (1999). Constitutive expression of interleukin-1 α precursor promotes human vascular smooth muscle cell proliferation. *Am. J. Physiol.* **276**: H901-H912.

- Beg, A.A., Finco, T.S., Nantermet, P.V., and Baldwin, A.S. (1993). Tumour necrosis factor and interleukin 1 lead to phosphorylation and loss of I κ B α : a mechanism for NF- κ B activation. *Mol. Cell. Biol.* **13**: 3301-3310.
- Berliner, J.A., Navab, M., Fogelman, A.M., Frank, J.S., Demer, L.L., Edwards, P.A., Watson, A.D., and Lusis, A.J. (1995). Atherosclerosis: basic mechanisms: oxidation, inflammation and genetics. *Circulation* **91**: 2488-2496.
- Bertolini, D.R., Nedwin, G.E., Bringman, T.S., Smith, D.D., and Mundy, G.R. (1986). Stimulation of bone resorption and inhibition of bone formation in vitro by human tumour necrosis factors. *Nature* **319**: 516-518.
- Besedovsky, H., Del Rey, A., Sorkin, E., and Dinarello, C.A. (1986). Immunoregulatory feedback between interleukin-1 and glucocorticoid hormones. *Science* **233**: 652-654.
- Bevilacqua, M.P., Pober, J.S., Wheeler, M.E., Cotran, R.S., and Gimbrone, M.A. (1985). Interleukin-1 acts on cultured human vascular endothelium to increase the adhesion of polymorphonuclear leukocytes, monocytes, and related leukocyte cell lines. *J. Clin. Invest.* **76**: 2003-2011.
- Bjerke, J.R., Krogh, H, and Matre, R. (1978). Characterisation of mononuclear cell infiltrates in psoriatic lesions. *J. Invest. Dermatol* **71**: 340-343.
- Black, R.A., Kronheim, S.R., and Sleath, P.R. (1989). Activation of interleukin-1 beta by a co-induced protease. *FEBS Lett.* **247**: 386-390.
- Blakemore, A.I., Watson, P.F., Weetman, A.P., and Duff, G.W. (1995). Association of Graves' disease with an allele of the interleukin-1 receptor antagonist gene. *J Clin Endocrinol Metab.* **80**: 111-115.
- Blakemore, A.I.F., Tarlow, J.K., Cork, M.J., Gordon, C., Emery, P., and Duff, G.W. (1994). Interleukin-1 receptor antagonist gene polymorphism as a disease severity factor in systemic lupus erythmatosus. *Arthritis Rheum.* **37**: 1380-1385.
- Blank, M., Krause, I., Goldkorn, T., Praprotnik, S., Livneh, A., Langevitz, P., Kaganobsky, E., Morgenstern, S., Cohen, S., Braak, V., Eldor, A., Weksler, B., Shoenfeld, Y. (1999). Monoclonal anti-endothelial cell antibodies from a patient with Takayasu arteritis activate endothelial cells from large vessels. *Arthritis Rheum.* **42**: 1421-1432.

- Blessing, E., Lin, T., Campbell, L.A., Rosenfeld, M.E., Lloyd, D., and Kuo, C. (2000). Chlamydia pneumoniae induces inflammatory changes in the heart and aorta of normocholesterolemic C57BL/6J mice. *Infect. Immun.* **68**: 4765-4768.
- Bochner, B.S., Luscinskas, F.W., Gimbrone, M.A., Newman, W., Sterbinsky, S.A., Derse-Anthony, C.P., Klunk, D., and Schleimer, R.P. (1991). Adhesion of human basophils, eosinophils, and neutrophils to interleukin-1 activated human vascular endothelial cells: contributions of endothelial cell adhesion molecules. *J. Exp. Med.* **173**: 1553-1556.
- Bocker, U., Damiao, A., Holt, L., Han, D.S., Jobin, C., Panja, A., Mayer, L., and Sartor, R.B. (1998). Differential expression of interleukin 1 receptor antagonist isoforms in human intestinal epithelial cells. *Gastroenterology* **115**: 1426-1438.
- Bodolay, E., Bojan, F., Szegedi, G., Stenszky, V., Farid, N.R. (1989). Cytotoxic endothelial cell antibodies in mixed connective tissue disease. *Immunol Lett.* **20**: 163-167.
- Boiardi, L., Salvarani, C., Timms, J.M., Silvestri, T., Macchioni, P.L., and di Giovine, F.S. (2000). Interleukin-1 cluster and tumor necrosis factor-alpha gene polymorphisms in polymyalgia rheumatica. *Clin. Exp Rheumatol.* **18**: 675-681.
- Bomsztyk, K., Sims, J.E., Stanton, T.H., Slack, J., McMahan, C.J., Valentine, M.A., and Dower, S.K. (1989). Evidence for different interleukin-1 receptors in murine B- and T-cell lines. *Proc. Natl. Acad. Sci. USA.* **86**: 8034-8038.
- Borges, E., Tietz, W., Steegmaier, M., Moll, T., Hallmann, R., Hamann, A., Vestweber, D. (1997). P-selectin glycoprotein ligand-1 (PSGL-1) on T helper 1 but not on T helper 2 cells binds to P-selectin and supports migration into inflamed skin. *J. Exp. Med.* **185**: 573-578.
- Bornstein, D.L. (1982). Leukocytic pyrogen: a major mediator of the acute phase reaction. *Ann. N.Y. Acad. Sci.* **389**: 323-337.
- Brack, A., Rittner, H.L., Younge, B.R., Kaltschmidt, C., Weyand, C.M., and Goronzy, J.J. (1997a). Glucocorticoid-mediated repression of cytokine gene transcription in human arteritis-SCID chimeras. *J Clin Invest.* **99**: 2842-2850.
- Brack, A., Geisler, A., Martinez-Taboada, V.M., Younge, B.R., Goronzy, J.J., and Weyand, C.M. (1997b). Giant cell vasculitis is a T cell-dependent disease. *Mol Med.* **3**: 530-453.
- Breedveld, F.C. (1998). New insights in the pathogenesis of rheumatoid arthritis. *J. Rheumatol.* **25 Suppl. 53**: 3-7.

- Brennan, F.M., Chantry, D., Jackson, A., Maini, R., and Feldmann, M. (1989). Inhibitory effect of TNF α antibodies on synovial cell interleukin-1 production in rheumatoid arthritis. *Lancet* **2(8657)**: 244-247.
- Bresnihan, B. (1999). Pathogenesis of joint damage in rheumatoid arthritis. *J. Rheumatol.* **26**: 717-719.
- Bresnihan, B., Alvaro-Gracia, J.M., Cobby, M., Doherty, M., Domljan, Z., Emery, P., Nuki, G., Pavelka, K., Rau, R., Rozman, B., Watt, I., Williams, B., Aithison, R., McCabe, D., and Musikic, P. (1998). Treatment of rheumatoid arthritis with recombinant human interleukin-1 receptor antagonist. *Arthritis Rheum.* **41**: 2196-2204.
- Brew, K., Dinakarpanian, D., and Nagase, H. (2000). Tissue inhibitors of metalloproteinases: evolution, structure and function. *Biochim. Biophys. Acta.* **1477(1-2)**: 267-283.
- Bromley, M., Fisher, W.D., and Wooley, D.E. (1984). Mast cells at sites of cartilage erosion in the rheumatoid joint. *Ann. Rheum. Dis.* **43**: 76-79.
- Brooks, J.W., and Mizel, S.B. (1994). Interleukin-1 signal transduction. *Eur. Cytokine Netw.* **5**: 547-561.
- Buchan, G., Barrett, K., Turner, M., Chantry, D., Maini, R.N., and Feldmann, M. (1988). Interleukin-1 and tumour necrosis factor mRNA expression in rheumatoid arthritis: prolonged production of IL-1 α . *Clin. Exp. Immunol.* **73**: 449-455.
- Butcher, C., Steinkasserer, A., Tejura, S., and Lennard, A.C. (1994). Comparison of two promoters controlling expression of secreted or intracellular IL-1 receptor antagonist. *J. Immunol.* **153**: 701-711.
- Byrne, J.A., Cotton, J.M., and Thomas, M. (2001). Bilateral ostial coronary artery stenosis: an important presentation of Takayasu's arteritis. *Heart* **85**: 555.
- Cairns, J.A., and Walls, A.F. (1996). Mast cell tryptase is a mitogen for epithelial cells. Stimulation of IL-8 production and intercellular adhesion molecule-1 expression. *J Immunol.* **156**: 275-283.
- Cairns, J.A., and Walls, A.F. (1997). Mast cell tryptase stimulates the synthesis of type I collagen in human lung fibroblasts. *J Clin Invest.* **99**: 1313-1321.

- Cantagrel, A., Navaux, F., Loubet-Lescoulie, P., Nourhashemi, F., Enault, G., Abbal, M., Constantin, A., Laroche, M., and Mazieres, B. (1999). Interleukin-1 beta, Interleukin-1 receptor antagonist, interleukin-4 and interleukin-10 gene polymorphisms: relationship to occurrence and severity of rheumatoid arthritis. *Arthritis. Rheum.* **42**: 1093-1100.
- Cao, Z., Henzel, W.J., and Gao, X. (1996). IRAK: a kinase associated with the interleukin-1 receptor. *Science* **271**: 1128-1131.
- Caron, G., Delneste, Y., Roelandts, E., Duez, C., Herbault, N., Magistrelli, G., Bonnefoy, J., Pestel, J., and Jeannin, P. (2001). Histamine induces CD86 expression and chemokine production by human immature dendritic cells. *J. Immunol.* **166**: 6000-6006.
- Cartmell, T., Poole, S., Turnbull, A.V, Rothwell, A.J., and Luhesi, G. (2000). Circulating interleukin-6 mediates the febrile response to localised inflammation in rats. *J. Physiol.* **526**: 653-661.
- Cerretti, D.P., Kozlosky, C.J., Mosley, B., Nelson, N., Van Ness, K., Greenstreet, T.A., March, C.J., Kronheim, S.R., Druck, T., Cannizzaro, L.A, Huebner, K., and Black, R.A. (1992). Molecular cloning of the interleukin-1 beta converting enzyme. *Science* **256**: 97-100.
- Chai, Z., Gatti, S., Toniatti, C., Poli, V., and Bartfai, T. (1996). Interleukin (IL)-6 gene expression in the central nervous system is necessary for fever response to lipopolysaccharide or IL-1beta: a study on IL-6 deficient mice. *J. Exp. Med.* **183**: 311-316.
- Charoenwongse, P., Kangwaanshiratada, O., Boonnam, R., and Hoomsindhu, U. (1998). The association between the HLA antigens and Takayasu's arteritis in Thai patients. *Int. J. Cardiol.* **66**: S117-S120.
- Cheng, L., Zhang, S.Z., Xiao, C.Y., Hou, Y.P., Li, L., Luo, H.C., Jiang, H.Y., and Zuo, W.Q. (2000). The A5.1 allele of the major histocompatibility complex class I chain-related gene A is associated with psoriasis vulgaris in Chinese. *Br. J. Dermatol.* **143**: 324-329.
- Chizzolini, C., Chicheportiche, R., Burger, D., and Dayer, J. (1997). Human Th1 cells preferentially induce interleukin (IL)-1 β while Th2 cells induce interleukin-1 receptor antagonist production upon cell/cell contact with monocytes. *Eur. J. Immunol* **27**: 171-177.
- Chizzonite, R., Truitt, T., Kilian, P.L., Stern, A.S., Nunes, P., Parker, K.P., Kaffka, K.L., Chua, A.O., Lugg, D.K., and Gubler, U. (1989). Two high affinity interleukin 1 receptors represent separate gene products. *Proc. Natl. Acad. Sci. USA.* **86**: 8029-8033.

- Chow, J.C., Young, D.W., Golenbock, D.T., Christ, W.J., and Gusovsky, F. (1999). Toll-like receptor-4 mediates lipopolysaccharide-induced signal transduction. *J Biol Chem.* **274**: 10689-10692
- Clark, B.D., Collins, K.L., Gandy, M.S., Webb, A.C., and Auron, P.E. (1986) Genomic sequence for human prointerleukin 1 beta: possible evolution from a reverse transcribed prointerleukin 1 alpha gene. *Nucleic Acids Res.* **14**: 7897-7914.
- Clay, F.E., Tarlow, J.K., Cork, M.J., Cox, A., Nicklin, M.J.H., and Duff, G.W. (1996). Novel interleukin-1 receptor antagonist exon polymorphisms and their use in allele-specific mRNA assessment. *Hum. Genet.* **97**: 723-726.
- Compton, S.J., Cairns, J.A., Holgate, S.T., and Walls, A.F. (1998). The role of mast cell tryptase in regulating endothelial cell proliferation, cytokine release, and adhesion molecule expression: Tryptase induces expression of mRNA for IL-1 β and IL-8 and stimulates the selective release of IL-8 from human umbilical vein endothelial cells. *J. Immunol.* **161**: 1939-1946.
- Courtenay, J.S., Dallman, M.J., Dayan, A.D., Martin, A., and Mosedale, B. (1980). Immunisation against heterologous type II collagen induces arthritis in mice. *Nature* **283**: 666-668.
- Courtenay, J.S., Dallman, M.J., Dayan, A.D., Martin, A., and Mosedale, B. (1980). Immunisation against heterologous type II collagen induces arthritis in mice. *Nature* **283**: 666-668.
- Cox, A., Camp, N.J., Cannings, C., Di Giovine, F.S., Dale, M., Worthington, J., John, S., Ollier, W.E.R., Silman, A.J., and Duff, G.W. (1999). Combined sib-TDT and TDT provide evidence for linkage of the interleukin-1 cluster to erosive rheumatoid arthritis. *Hum. Mol. Gen.* **8**: 1707-1713.
- Cullinan, E.B., Kwee, L., Nunes, P., Shuster, D.J., Ju, G., McIntyre, K.W., Chizzonite, R.W., and Labow, M.A. (1998). Il-1 receptor accessory protein is an essential component of the IL-1 receptor. *J. Immunol.* **161**: 5614-5620.
- Cumberbatch, M., Dearman, R.J., and Kimber, I. (1997). Interleukin 1 beta and the stimulation of Langerhans cell migration: comparisons with tumour necrosis factor alpha. *Arch. Dermatol. Res.* **289**: 277-284.
- Cumberbatch, M., Dearman, R.J., Antonopoulos, C., Groves, R.W., and Kimber, L. (2001). Interleukin (IL)-18 induces Langerhans cell migration by a tumour necrosis factor and IL-1beta-dependent mechanism. *Immunology* **102**: 323-330.

Cunnane, G., Madigan, A., Murphy, E., FitzGerald, O., and Bresnihan, B. (2001). The effects of treatment with interleukin-1 receptor antagonist on the inflamed synovial membrane in rheumatoid arthritis. *Rheumatology* 40: 62-69.

Dahlen, G.H., Boman, J., Birgander, L.S., and Lindblom, B. (1995). LP(a) lipoprotein, IgG, IgA, and IgM antibodies to *Chlamydia pneumoniae* and HLA class II genotype in early coronary artery disease. *Atherosclerosis* 114: 165-174.

Dal Canto, A.J., and Virgin, H.W. (2000). Animal models of infection-mediated vasculitis: implications for human disease. *Int. J. Cardiol.* 75: S37-S45.

Dalton, B.J., Connor, J.R., and Johnson, W.J. (1989). Interleukin-1 induces interleukin-1 alpha and interleukin-1 beta gene expression in synovial fibroblasts and peripheral blood monocytes. *Arthritis Rheum.* 32: 279-287.

Danis, V.A., Millington, M., Hyland, V.J., and Grennan, D. (1995). Cytokine production by normal human monocytes: inter-subject variation and relationship to an IL-1 receptor antagonist (IL-1Ra) gene polymorphism. *Clin. Exp. Immunol.* 99: 303-310.

Dascombe, M.J., Rothwell, N.J., Sagay, B.O., and Stock, M.J. (1989). Pyrogenic and thermogenic effects of interleukin 1 β in the rat. *Am. J. Physiol* 256: E7-E11.

Dayer, J., de Rochemonteix, B., Burrus, B., Demczuk, S., and Dinarello, C.A. (1986). Human recombinant interleukin 1 stimulates collagenase and prostaglandin E₂ production by human synovial cells. *J. Clin. Invest.* 77: 645-648.

Dayer, J.M., Beutler, B., and Cerami, A. (1985). Cachectin/tumor necrosis factor stimulates collagenase and prostaglandin E₂ production by human synovial cells and dermal fibroblasts. *J Exp Med.* 162: 2163-2168.

DeChiara, T.M., Young, D., Semionow, R., Stern, A.S., Batula-Bernado C., Fiedler-Nagy C., Kaffka K.L., Kilian, P.L., Yamazaki, S., Mizel, S.B., and Lomedico, P.T. (1986). Structure-function analysis of murine interleukin-1: Biologically active polypeptides are at least 127 amino acids long and are derived from the carboxyl terminus of a 270-amino acid precursor. *Proc. Natl. Acad. Sci. USA* 83: 8303-8307.

Deighton, C.M., Walker, D.J., Griffiths, I.D., and Roberts, D.F. (1989). The contribution of HLA to rheumatoid arthritis. *Clin. Genet.* 36: 178-182.

- Del Junco, D.J., Luthra, H.S., Annegers, J.F., Worthington, J.W., and Kurland, L.T. (1984). The familial aggregation of rheumatoid arthritis and its relationship to the HLA-DR4 association. *Am. J. Epidemiology*. **119**: 813-829.
- Del Papa, N., Guidali, L., Sironi, M., Shoenfeld, Y., Mantovani, A., Tincani, A., Balestrieri, G., Radice, A., Sinico, R.A., and Meroni, P.L. (1996). Anti-endothelial cell IgG antibodies from patients with Wegener's granulomatosis bind to human endothelial cells in vitro and induce adhesion molecule expression and cytokine secretion. *Arthritis Rheum*. **39**: 758-776.
- Dewberry, R., Holden, H., Crossman, D., and Francis, S.E. (2000). Interleukin-1 receptor antagonist expression in human endothelial cells and atherosclerosis. *Art. Thromb. Vasc. Biol*. **20**: 2394-2400.
- Dhingra, R., Chopra, P., Talwar, K.K., and Kumar, R. (1998). Enzyme-linked immunosorbent assay and immunoblot study in Takayasu's arteritis patients. *Indian Heart J*. **50**: 428-432.
- DiDonato, J.A., Hayakawa, M., Rothwarf, D.M., Zandi, E., and Karin, M. (1997). A cytokine-responsive I κ B kinase that activates the transcription factor NF- κ B. *Nature* **388**: 548-554.
- Dinarello, C.A., and Wolff, S.M. (1982). Molecular basis of fever in humans. *Am. J. Med*. **72**: 799-819.
- Dinarello, C.A., Ikejima, T., Warner, S.J., Orencole, S.F., Lonnemann, G., Cannon, J.G., and Libby, P. (1987). Interleukin 1 induces interleukin 1. I. Induction of circulating interleukin 1 in rabbits in vivo and in human mononuclear cells in vitro. *J. Immunol*. **139**: 1902-1910.
- Ding, A.H., Nathan, C.F., and Stuehr, D.J. (1988). Release of reactive nitrogen intermediates and reactive oxygen intermediates from mouse peritoneal macrophages. Comparison of activating cytokines and evidence for independent production. *J. Immunol*. **141**: 2407-2412.
- Dingle, J.T., Thomas, D.P.P., King, B., and Bard, D.R. (1987). In vivo studies of articular tissue damage mediated by catabolin/interleukin 1. *Ann. Rheum. Dis*. **46**: 527-533.
- Dower, S.K., Kronheim, S.R., Hopp, T.P., Cantrell, M., Deeley, M., Gillis, S., Henney, C.S., and Urdal, D.L. (1986). The cell surface receptors for interleukin-1 alpha and interleukin-1 beta are identical. *Nature* **324**: 266-268.
- Dustin, M.L., Rothlein, R., Bhan, A.K., Dinarello, C.A., and Springer, T.A. (1986). Induction by IL-1 and interferon- γ : tissue distribution, biochemistry, and function of a natural adherence molecule (ICAM-1). *J. Immunol*. **137**: 245-254.

- Eastgate, J.A., Symons, J.A., Wood, N.C., Grinlinton, F.M., Di Giovine, F.S., and Duff, G.W. (1988). Correlation of plasma interleukin 1 levels with disease activity in rheumatoid arthritis. *Lancet* **2**(8613): 706-709.
- Eichorn, J., Sima, D., Thiele, B., Lindschau, C., Turowski, A., Schmidt, H., Schneider, W., Haller, H., and Luft, F. (1996). Myocardial ischaemia/infarction/arteritis: anti-endothelial cell antibodies in Takayasu arteritis. *Circulation* **94**: 2396-2401.
- Eisenberg, S.P., Evans, R.J., Arend, W.P., Verderber, E., Brewer, M.T., Hannum, C.H., and thompson, R.C. (1990). Primary structure and functional expression from complementary DNA of a human interleukin-1 receptor antagonist. *Nature* **343**: 341-346.
- Elling, P., Olsson, A.T., and Elling, H. (1996). Synchronous variations of the incidence of temporal arteritis and polymyalgia rheumatica in different regions of Denmark; association with epidemics of *Mycoplasma pneumoniae* infection. *J Rheumatol.* **23**: 112-9.
- Ellingsen, T., Elling, P., Olson, A., Elling, H., Baandrup, U., Matshshima, K., Deleuran, B., and Stengaard-Pedersen, K. (2000). Monocyte chemoattractant protein 1 (MCP-1) in temporal arteritis and polymyalgia rheumatica. *Ann. Rheum. Dis.* **59**: 775-780.
- Elliot, M.J., Maini, R.N., Feldmann, M., Kalden, J.R., Antoni, C., Smolen, J.S., Leeb, B., Breedveld, F.C., Macfarlane, J.D., Bijl, H., and Woody, J.N. (1994). *Lancet* **344**: 1105-1110.
- Ertepinar, H., Suzen, B., Ozoran, A., Ozoran, Y., Ceylan, S., Teginoglu, G., and Uremek, G. (1990). Effects of drag reducing polymer on atherosclerosis. *Biorheology* **27**: 631-644.
- Fantuzzi, G., Zheng, H., Faggioni, R., Benigni, F., Ghezzi, P., Sipe, J.D., Shaw, A.R., and Dinarello, C.A. (1996). Effect of endotoxin in IL-1 β -deficient mice. *J. Immunol.* **157**: 291-296.
- Farber, E.M., Nall, M.L., and Watson, W. (1974). Natural history of psoriasis in 61 twin pairs. *Arch. Dermatol.* **109**: 207-211.
- Faruqui, F.I., Otten, M.D., and Polimeni, P.I. (1987). Protection against atherogenesis with the polymer drag-reducing agent Separan AP-30. *Circulation* **75**: 627-635.
- Feldmann, M., Brennan, F.M., and Maini, R.N. (1996). Rheumatoid arthritis. *Cell* **85**: 307-310.

Ferraro, G., Meroni, P.L., Tincani, A., Sinico, A., Barcellini, W., Radice, A., Gregorini, G., Froidi, M., Borghi, M.O., and Balestrieri, G. (1990). Anti-endothelial cell antibodies in patients with Wegener's granulomatosis and micropolyarteritis. *Clin. Exp. Immunol.* **79**: 47-53.

Finzel, B.C., Clancy, L.L., Holland, D.R., Muchmore, S.W., Watenpaugh, K.D., and Einsphar, H.M. (1989). Crystal structure of recombinant human interleukin-1 beta at 2.0 Å resolution. *J. Mol. Biol.* **209**: 779-791.

Fitzgerald, K.A., Palsson-McDermott, E., Bowie, A.G., Jefferies, C.A., Mansell, A.S., Brady, G., Brint, E., Dunne, A., Gray, P., Harte, M.T., McMurray, D., Smith, D.E., Sims, J.E., Bird, T.A., and O'Neill, L.A.J. (2001). Mal (Myd88-adaptor-like) is required for Toll-like receptor-4 signal transduction. *Nature* **413**: 78-83.

Folsom, A.R., Niet, F.J., Sorlie, P., Chambless, L.E., and Graham, D.Y. (1998). Helicobacter pylori seropositivity and coronary heart disease incidence. *Circulation* **98**: 845-850.

Fontana, A., Kristensen, F., Dubs, R., Gemsa, D., and Weber, E. (1982). Production of prostaglandin E and interleukin-1 like factor by cultured astrocytes and C6 glioma cells. *J. Immunol* **129**: 2413-2419.

Francis, S.E., Camp, N.J., Dewberry, R.M., Gunn, J., Syrris, P., Carter, N.D., Jeffery, S., Kaski, J.C., Cumberland, D.C., Duff, G.W., and Crossman, D.C. (1999). Interleukin-1 receptor antagonist gene polymorphism and coronary artery disease. *Circulation* **99**: 861-866.

Freedberg, I.M., Tomic-Canic, M., Komine, M., and Blumenberg, M. (2001). Keratins and the keratinocyte activation cycle. *J. Invest. Dermatol.* **116**: 633-640.

FtENCH, J.F., Lambert, L.E., and Dage, R.C. (1991). Nitric oxide synthase inhibitors inhibit interleukin-1 β induced depression of vascular smooth muscle. *J. Pharmacol. Exp. Therapeut.* **259**: 260-264.

Fukuhara, K., Urano, Y., Akaike, M., Ahsan, K., and Arase, S. (1998) Psoriatic arthritis associated with dilated cardiomyopathy and Takayasu's arteritis. *Br. J. Dermatol* **138**: 329-333.

Furutani, Y., Notake, M., Fukui, T., Ohue, M., Nomura, H., Yamada, M., and Nakamura, S. (1986). Complete nucleotide sequence of the gene for human interleukin 1 alpha. *Nucleic Acids Res.* **14**: 3167-3179.

Gabay, C., Porter, B., Guenette, D., Billir, B., and Arend, W.P. (1999). Interleukin-4 (IL-4) and IL-13 enhance the effect of IL-1beta on production of IL-1 receptor antagonist by primary human hepatocytes and hepatoma HepG2 cells: differential effect on C-reactive protein production. *Blood* **93**: 1299-1307.

Gabriel, S.E., Espy, M., Erdman, D.D., jornsson, J., Smith, T., and Hunder, G.G. (1999). The role of parvovirus B19 in the pathogenesis of giant cell arteritis. *Arthritis Rheum.* **42**: 1255-1258.

Galindo, R.L., Edwards, D.N., Gillespie, S.K., and Wasserman, S.A. (1995). Interaction of the pelle kinase with the membrane-associated protein tube is required for transduction of the dorsoventral signal in *Drosophila* embryos. *Development.* **121**: 2209-2218.

Gao, X., Olsen, N.J., Pincus, T., and Stastny, P. (1990). HLA-DR alleles with naturally occurring amino acid substitutions and risk for developmebt of rheumatoid arthritis. *Arthritis Rheum.* **33**: 939-946.

Gauchat, J.F., Henchoz, S., Fattah, D., Mazzei, G., Aubry, J.P., Jomotte, T., Dash, L., Page, K., Solari, R., Aldebert, D., Capron, M., Dahinden, C., and Bonnefoy, Y. (1995). CD40 ligand is functionally expressed on human eosinophils. *Eur J Immunol.* **25**: 863-865.

Gay, N.J., and Keith, F.J. (1991). *Drosophila* Toll and IL-1 receptor. *Nature* **351**: 355-356.

Geisler, R., Bergmann, A., Hiromi, Y., and Nusslein-Volhard, C. (1992). *cactus*, a gene involved in dorsoventral pattern formation of *Drosophila*, is related to the I kappa B gene family of vertebrates. *Cell.* **71**: 613-621.

Geller, D.A., De Vera, M.E., Russell, D.A., Shapiro, R.A., Nussler, A.K., Simmons, R.L., and Billiar, T.R. (1995). A central role for Il-1 β in the in vitro and in vivo regulation of hepatic inducible nitric oxide synthase. Il-1 β induces hepatic nitric oxide synthesis. *J. Immunol.* **155**: 4890-4898.

Gerszten, R.E., Garcia-Zepeda, E.A., Lim, Y.C., Yoshida, M., Ding, H.A., Gimbrone, M.A., Luster, A.D., Luscinskas, F.W., and Rosenzweig, A. (1999). MCP-1 and IL-8 trigger firm adhesion of monocytes to vascular endothelium under flow conditions. *Nature* **398**: 718-723.

Gery, I., and Waksman, B.H. (1972). Potentiation of the T-lymphocyte response to mitogens II: The cellular source of potentiating mediator(s). *J. Exp. Med.* **136**: 143-155.

Gillis, S., and Mizel, S.B. (1981). T-cell lymphoma model for the analysis of interleukin 1-mediated T-cell activation. *Proc. Natl. Acad. Sci. USA.* **78**: 1133-1137.

- Gitter, B.D., Labus, J.M., Lees, S.L., and Scheetz, M.E. (1989). Characteristics of human synovial fibroblast activation by IL-1 β and TNF α . *Immunology* **66**: 196-200.
- Glaccum, M.B., Stocking, K.L., Charrier, K., Smith, J.L., Willis, C.R., Maliszewski, C., Livingston, D.J., Peschon, J.J., and Morrissey, P.J. (1997). Phenotypic and functional characterisation of mice that lack the type I receptor for IL-1. *J. Immunol.* **159**: 3364-3371.
- Gladman, D.D., and Brockbank, J. (2000). Psoriatic arthritis. *Expert Opin. Investig. Drugs* **9**: 1511-1522.
- Godambe, S.A., Chaplin, D.D., Takova, T., and Bellone, C.J. (1994). Upstream NFIL-6-like site located within a Dnase I hypersensitivity region mediates LPS-induced transcription of the murine interleukin-1 β gene. *J. Immunol.* **153**: 143-152.
- Gonzalez-Gay, M.A., Garcia-Porrua, C., Salvarani, C., and Hunder, G.G. (1999). Diagnostic approach in a patient presenting with polymyalgia rheumatica. *Clin. Exp. Rheumatol.* **17**: 276-278.
- Gordon, J., and MacLean, L.D. (1965). A lymphocyte-stimulating factor produced *in vitro*. *Nature* **208**: 795-796.
- Gowen, M., Wood, D.D., Ihrie, E.J., McGuire, M.K.B., and Russell, R.G.C. (1983). An interleukin 1 like factor stimulates bone resorption *in vitro*. *Nature* **306**: 378-380.
- Grabovsky, V., Feigelson, S., Chen, C., Bleijs, D.A., Peled, A., Cinamon, G., Baleux, F., Arenzana-Seisodos, F., Lapidot, T., Van Kooyk, Y., Lobb, R.R., and Alon, R. (2000). Subsecond induction of α 4 integrin clustering by immobilised chemokines stimulates leukocyte tethering and rolling on endothelial vascular cell adhesion molecule 1 under flow conditions. *J. Exp. Med.* **192**: 495-505.
- Gravallese, E.M., Darling, J.M., Ladd, A.M., Katz, J.N., and Glichmer, L.H. (1991). In situ hybridisation studies of stromelysin and collagenase messenger RNA expression in rheumatoid synovium. *Arthritis Rheum.* **34**: 1076-1084.
- Graves, B.J., Hatada, M.H., Hendrickson, W.A., Miller, J.K., Madison, V.S., and Satow, Y. (1990). Structure of interleukin-1 α at 2.7 \AA resolution. *Biochemistry* **29**: 2679-2684.
- Gray, P.W., Glaister, D., Chen, E., Goeddel, D.V., and Pennica, D. (1986). Two interleukin 1 genes in the mouse: cloning and expression of the cDNA for murine interleukin 1 beta. *J Immunol.* **137**: 3644-3648.

Greenfeder, S.A., Nunes, P., Kwee, L., Labow, M., Chizzonite, R.A., Ju, G. (1995). Molecular cloning and characterisation of a second subunit of the interleukin-1 receptor complex. *J. Biol. Chem.* **270**: 13757-13765.

Gregerson, P.K., Silver, J., and Winchester, R.J. (1987). The shared epitope hypothesis. An approach to understanding the molecular genetics of susceptibility to rheumatoid arthritis. *Arthritis Rheum.* **30**: 1205-1213.

Grehan, S., Herbert, J., and Whitehead, A.S. (1997). Down-regulation of the major circulating precursors of proteins deposited in secondary amyloidosis by a recombinant mouse interleukin-1 receptor antagonist. *Eur. J. Immunol.* **27**: 2593-2599.

Griffiths, C.E., Powles, A.V., McFadden, J., Baker, B.S., Valdimarsson, H., and Fry, L. (1989). Long-term cyclosporin for psoriasis. *Br J Dermatol.* **120**: 253-260.

Groh, V., Steinle, A., Bauer, S., and Spies, T. (1998). Recognition of stress-induced MHC molecules by intestinal epithelial $\gamma\delta$ T cells. *Science* **279**: 1737-1740.

Groves, R.W., Mizutani, H., Kieffer, J.D., and Kupper, T.S. (1995). Inflammatory skin disease in transgenic mice that express high levels of interleukin 1 alpha in basal epidermis. *Proc. Natl. Acad. Sci. USA.* **92**: 11874-11878.

Groves, R.W., Rauschmayr, T., Nakamura, K., Sarkar, S., Williams, I.R., and Kupper, T.S. (1996). Inflammatory and hyperproliferative skin disease in mice that express elevated levels of the IL-1 receptor (type 1) on epidermal keratinocytes. Evidence that IL-1-inducible secondary cytokines produced by keratinocytes in vivo can cause skin disease. *J. Clin. Invest.* **98**: 336-344.

Groves, R.W., Ross, E., Barker, J.N., Ross, J.S., Camp, R.D.R., and MacDonald, D. (1992). Effect of in vivo interleukin-1 on adhesion molecule expression in normal human skin. *J. Invest. Dermatol.* **98**: 384-387.

Gruber, B.L., Kew, R.R., Jelaska, A., Marchese, M.J., Garlick, J., Ren, S., Schwartz, L.B., and Korm, J.H. (1997). Human mast cells activate fibroblasts. Trypsin is a fibrogenic factor stimulating collagen messenger ribonucleic acid synthesis and fibroblast chemotaxis. *J. Immunol.* **158**: 2310-2317.

Gu, Y., Kuida, K., Tsutsui, H., Ku, G., Hsiao, K., Fleming, M.A., Hayashi, N., Higashino, K., Okamura, H., Nakanishi, K., Kurimoto, M., Tanimoto, T., Flavell, R.A., Sato, V., Harding, M.W.,

- Livingston, D.J., and Su, M.S. (1997). Activation of interferon-gamma inducing factor mediated by interleukin-1beta converting enzyme. *Science* **275**: 206-209.
- Gunther, C., Rollinghoff, M., and Beuscher, H.U. (1989). Proteolysis of the native murine IL 1 beta precursor is required to generate IL 1 beta bioactivity. *Immunobiology* **178**: 436-48.
- Hancock, G.E., Kaplan, G., and Cohn, Z.A. (1988). Keratinocyte growth regulation by the products of immune cells. *J. Exp. Med.* **168**: 1395-1402.
- Hannum, C.H., Wilcox, C.J., Arend, W.P., Joslin, F.G., Dripps, D.J., Heimdal, P.L., Arme, L.G., Sommer, A., Eisenberg, S.P., and Thompson, R.C. (1990). Interleukin-1 receptor antagonist activity of a human interleukin-1 inhibitor. *Nature* **343**: 336-340.
- Haregewoin, A., Soman, G., Hom, R.C., and Finberg, R.W. (1989). Human $\gamma\delta^+$ T cells respond to mycobacterial heat-shock protein. *Nature* **340**: 309-312.
- Hashimoto, C., Hudson, K.L., and Anderson, K.V. (1988). The Toll gene of *Drosophila*, required for dorsal-ventral embryonic polarity, appears to encode a transmembrane protein. *Cell* **52**: 269-279.
- Haskill, S., Martin, G., Van Le, L., Morris, J., Peace, A., Bigler, C.F., Jaffe, G.J., Hammerberg, C., Sporn, S.A., Fong, S, Arend, W.P., and Ralph, P. (1991). CDNA cloning of an intracellular form of the human interleukin 1 receptor antagonist associated with epithelium. *Proc. Natl. Acad. Sci. USA* **88**: 3681-3685.
- Hazuda, D.J., Lee, J.C., and Young, P.R. (1988). The kinetics of interleukin 1 secretion from activated monocytes. Differences between interleukin 1 alpha and interleukin 1 beta. *J Biol Chem.* **263**: 8473-9.
- He, S. and Walls, A.F. (1997). Human mast cell tryptase: a stimulus of microvascular leakage and mast cell activation. *Eur. J. Pharmacol.* **328**: 89-97.
- He, S., Peng, Q., and Walls, A.F. (1997). Potent induction of a neutrophil and eosinophil-rich infiltrate in vivo by human mast cell tryptase: selective enhancement of eosinophil recruitment by histamine. *J Immunol.* **159**: 6216-6225.
- Helle, M., Brakenhoff, J.P.J., De Groot, E., and Aarden, L.A. (1988). Interleukin 6 is involved in interleukin-1 induced activities. *Eur. J. Immunol.* **18**: 957-959.

Henn, V., Slupsky, J.R., Grafe, M., Anagnostopoulos, I., Forster, R., Muller-Berghaus, G., and Kroczeck, R.A. (1998). CD40 ligand on activated platelets triggers an inflammatory reaction of endothelial cells. *Nature*. **391**: 591-594.

Henseler, T. (1997). The genetics of psoriasis. *J Am Acad Dermatol*. **37**: S1-S11.

Henseler, T., and Christophers, E. (1985). Psoriasis of early and late onset: characterization of two types of psoriasis vulgaris. *J Am Acad Dermatol*. **13**: 450-456.

Henserson, B., Revell, P.A., and Edwards, J.C.W. (1988). Synovial lining cell hyperplasia in rheumatoid arthritis: dogma and fact. *Ann. Rheum. Dis*. **47**: 348-349.

Heufler, C, Koch, F., and Schuler, G. (1988). Granulocyte/macrophage colony-stimulating factor and interleukin 1 mediate the maturation of murine epidermal Langerhans' cells into potent immunostimulatory dendritic cells. *J. Exp. Med*. **167**: 700-705.

Hirsch, E., Irikura, V.M., Paul, S.M., and Hirsh, D. (1996). Functions of interleukin 1 receptor knockout and overproducing mice. *Proc. Natl. Acad. Sci. USA*. **93**: 11008-11013.

Hofmeister, R., Wiegmann, K., Korherr, C., Bernardo, K., Kronke, M., and Falk, W. (1997). Activation of acid sphingomyelinase by interleukin-1 (IL-1) requires the IL-1 receptor accessory protein. *J. Biol. Chem*. **272**: 27730-27736.

Hom, J.T., Bendele, A.M., and Carlson, D.G. (1988). In vivo administration with IL-1 accelerates the development of collagen-induced arthritis in mice. *J. Immunol*. **141**: 834-841.

Homey, B., Alenius, H., Muller, A., Soto, H., Bowman, E.P., Yuan, W., McEvoy, L., Lauerma, M., Assmann, T., Bunemann, E., Lehto, M., Wolff, H., Yen, D., Marxhausen, H., To, W., Sedgewick, J., Ruzicka, T., Lehmann, P., and Zlotnick, A. (2002). CCL27-CCR10 interactions regulate T cell-mediated skin inflammation. *Nature Med*. **8**: 157-165.

Homey, B., Dieu-Nosjean, M.C., Wiesenborn, A., Massacrier, C., Pin, J.J., Oldham, E., Catron, D., Buchanan, M.E., Muller, A., deWaal Malefyt, R., Deng, G., Orozco, R., Ruzicka, T., Lehmann, P., Lebecque, S., Caux, C., and Zlotnick, A. (2000). Up-regulation of macrophage inflammatory protein-3 alpha/CCL20 and CC chemokine receptor 6 in psoriasis. *J. Immunol*. **164**: 6621-6632.

Hopkins, S.J., Humphreys, M., and Jayson, M.I.V. (1988). Cytokines in synovial fluid. I. The presence of biologically active and immunoreactive IL-1. *Clin. Exp. Immunol*. **72**: 422-427.

Horai, R., Asano, M., Sudo, K., Kanuka, H., Suzuki, M., Nishihara, M., Takahashi, M., and Iwakura, Y. (1998). Production of mice deficient in genes for interleukin (IL)-1 α , IL-1 β , IL-1 α/β and IL-1 receptor antagonist shows that IL-1 β is crucial in turpentine-induced fever development and glucocorticoid secretion. *J. Exp. Med.* **187**: 1463-1475.

Hotchi, M. (1992). Pathological studies on Takayasu arteritis. *Heart Vessels Suppl.* **7**: 11-17.

Huang, J.J., Newton, R.C., Rutledge, S.J., Horuk, R., Matthew, J.B., Covington, M., and Lin, Y. (1988). Characterization of murine IL-1 beta. Isolation, expression, and purification. *J Immunol.* **140** :3838-3843.

Hunder, G.G., and Michet, C.J. (1985). Giant cell arteritis and polymyalgia rheumatica. *Clin Rheum Dis.* **11**: 471-483.

Hunder, G.G., Bloch, D.A., Michel, B.A., Stevens, M.B., Arend, W.P., Calabrese, L.H., Edworthy, S.M., Fauci, A.S., Leavitt, R.Y., Lie, J.T., Lightfoot, R.W., Masi, A.T., McShane, D.J., Mills, J.a., Wallace, S.L., and Zvaifler, N.J. (1990). The american college of rheumatology 1990 criteria for the classification of giant cell arteritis. *Arthritis Rheum.* **33**: 1122-1128.

Hurme, M., and Santtial, S. (1998). IL-1 receptor antagonist (IL-1Ra) plasma levels are coordinatley regulated by both IL-1Ra and IL-1beta genes. *Eur. J. Immunol.* **28**: 2598-2602.

Huston, K.A., Hunder, G.G., Lie, J.T., Kennedy, R.H., and Elveback, L.R. (1978). Temporal arteritis: a 25-year epidemiologic, clinical, and pathologic study. *Ann. Intern. Med.* **88**: 162-167.

Iguchi, T., and Ziff, M. (1986). Electron microscopic study of rheumatoid synovial vasculature. Intimate relationship between tall endothelium and lymphoid aggregation. *J. Clin. Invest.* **77**: 35-361.

Ikeda, U., Ikeda, M., Oohara, T., Kano, S., and Yaginuma, T. (1990). Mitogenic action of interleukin-1 alpha on vascular smooth muscle cells mediated by PDGF. *Atherosclerosis* **84**: 183-188.

Inder, S.J., Bobryshev, Y.U., Cherian, S.M., Wang, A.Y., Lord, R.S., Masuda, K., and Yutani, C. (2000). Immunophenotypic analysis of the aortic wall in Takayasu's arteritis: involvement of lymphocytes, dendritic cells and granulocytes in immuno-inflammatory reactions. *Cardiovasc. Surg.* **8**: 141-148.

Irikura, V.M., Hirsch, E., and Hirsh, D.. (1999). Effects of interleukin-1 receptor antagonist overexpression on infection by *Listeria monocytogenes*. *Infect Immun.* **67**: 1901-1909.

Jakob, T., and Udey, M.C. (1998). Regulation of E-cadherin mediated adhesion in Langerhans cell-like dendritic cells by inflammatory mediators that mobilise Langerhans cells in vivo. *J. Immunol.* **160**: 4067-4073.

Jasin, H.E. (1985). Autoantibody specificities of immune complexes sequestered in articular cartilage of patients with rheumatoid arthritis and osteoarthritis. *Arthritis Rheum.* **28**: 241-248.

Jawien, A., Bowen-Pope, D.F., Lindner, V., Schwartz, S.M., and Clowes, A.W. (1992). Platelet-derived growth factor promotes smooth muscle migration and intimal thickening in a rat model of balloon angioplasty. *J. Clin. Invest.* **89**: 507-511.

Jenisch, S., Kock, S., Henseler, T., Nair, R.P., Elder, J.T., Watts, C.E., Westphal, E., Voorhees, J.J., Christophers, E., and Kronke, M. (1999). Corneodesmosin gene polymorphism demonstrates strong linkage disequilibrium with HLA and association with psoriasis vulgaris. *Tissue Antigens* **54**: 439-449.

Jiang, Y., Beller, D.I., Frenzl, G., and Graves, D.T. (1992). Monocyte chemoattractant protein-1 regulates adhesion molecule expression and cytokine production in human monocytes. *J. Immunol.* **148**: 2423-2428.

Jiang, Y., Genant, H.K., Watt, I., Cobby, M., Bresnihan, B., Aitchison, R., and McCabe, D. (2000). A multicenter, double-blind, dose-ranging, randomised, placebo-controlled study of recombinant human interleukin-1 receptor antagonist in patients with rheumatoid arthritis. *Arthritis Rheum.* **43**: 1001-1009.

Jiang, Y., Kohara, K., and Hiwada, K. (1999). Low wall shear stress contributes to atherosclerosis of the carotid artery in hypertensive patients. *Hypertens. Res.* **22**: 203-207.

Joosten, L.A., Helsen, M.M., Saxne, T., van De Loo, F.A., Heinegard, D., and van Den Berg, W.B. (1999). IL-1 alpha beta blockade prevents cartilage and bone destruction in murine type II collagen-induced arthritis, whereas TNF-alpha blockade only ameliorates joint inflammation. *J Immunol.* **163**: 5049-5055.

Joosten, L.A.B., Helsen, M.M.A., Saxne, T., Van de Loo, F.A.J., Heinegard, D., and Van den Berg, W.B. (1999). IL-1 α β blockade prevents cartilage and bone destruction in murine type II collagen-induced arthritis, whereas TNF- α blockade only ameliorates joint inflammation. *J. Immunol.* **163**: 5049-5055.

Joosten, L.A.B., Helsen, M.M.A., Van de Loo, F.A.J., and Van den Berg, W. (1996). Anticytokine treatment of established type II collagen-induced arthritis in DBA/1 mice. *Arthritis Rheum.* **39**: 797-809.

Jouvenne, P., Chaudhary, A., Buchs, N., Di Giovine, F.S., Duff, G.W., and Miossec, P. (1999). Possible genetic association between interleukin-1 α gene polymorphism and the severity of chronic polyarthritis. *Eur. Cytokine. Netw.* **10**: 33-36.

Kaiser, M., Weyand, C.M., Bjornsson, J., and Gorozny, J.J. (1998). Platelet-derived growth factor, intimal hyperplasia, and ischaemic complications in giant cell arteritis. *Arthritis Rheum.* **41**: 623-633.

Kaiser, M., Younge, B., Bjornsson, J., Gorozny, J.J., and Weyand, C.M. (1999). Formation of new vasa vasorum in vasculitis. Production of angiogenic cytokines by multinucleated giant cells. *Am. J. Pathol.* **155**: 765-774.

Kampschmidt, R.F., Pulliam, L.A., and Upchurch, H.F. (1980). The activity of partially purified leukocytic endogenous mediator in endotoxin-resistant C3H/HeJ mice. *J. Lab. Clin. Med.* **95**: 616-623.

Kapur, V., Majesky, M.W., Li, L., Black, R.A., and Musser, J.M. (1993). Cleavage of interleukin-1 β precursor to produce active IL-1 β by a conserved extracellular cysteine protease from *Streptococcus pyogenes*. *Proc. Natl. Acad. Sci. USA* **90**: 7676-7680.

Karmann, K., Hughes, C.C., Schechner, J., Fanslow, W.C., and Pober, J.S. (1995). CD40 on human endothelial cells: inducibility by cytokines and functional regulation of adhesion molecule expression. *Proc Natl Acad Sci US A.* **92**: 4342-4346.

Keffer, J., Probert, L., Cazlaris, H., Georgopoulos, S., Kaslari, E., Kioussis, D., and Kollias, G. (1991). Transgenic mice expressing human tumour necrosis factor: a predictive genetic model of arthritis. *EMBO J.* **10**: 4025-4031.

Kerr, G.S., Hallahan, C.W., Giordano, J., Leavitt, R.Y., Fauci, A.S., Rottem, M., and Hoffman, G.S. (1994). Takayasu arteritis. *Ann. Intern. Med.* **120**: 919-929.

Kerr, G.S., Hallahan, C.W., Giordano, J., Leavitt, R.Y., Fauci, A.S., Rottem, M., and Hoffman, G.S. (1994). Takayasu arteritis. *Ann. Intern. Med.* **120**: 919-929.

Kilian, P.L., Kaffka, K.L., Stern, A.S., Woehle, D., Benjamin, W.R., Dechiara, T.M., Gubler, U., Farrar, J.J., Mizel, S.B., and Lomedico, P.T. (1986). Interleukin 1 alpha and interleukin 1 beta bind to the same receptor on T cells. *J. Immunol.* **136**: 4509-4514.

Kim, Y.S., Han, S.J., Ryu, J.H., Choi, K.H., Hong, Y.S., Chung, Y.H., Perrot, S., Raibaud, A., Brey, P.T., and Lee, W.J. (2000). Lipopolysaccharide-activated kinase, an essential component for the induction of the antimicrobial peptide genes in *Drosophila melanogaster* cells. *J Biol Chem.* **275**: 2071-2079.

Kimura, A., Kitamura, H., Date, Y., and Numano, F. (1996). Comprehensive analysis of HLA genes in Takayasu arteritis in Japan. *Int. J. Cardiol.* **54**: S61-S69.

Kimura, A., Kobayashi, Y., Takahashi, M., Ohbuchi, N., Kitamura, H., Nakamura, T., Satoh, M., Sasaoka, T., Hiroi, S., Arimura, T., Akai, J., Aerbajinai, W., Yasukochi, Y., and Nomano, F. (1998). MICA gene polymorphism in Takayasu's arteritis and Buerger's disease. *Int. J. Cardiol.* **66**: S107-S113.

Kitamura, H., Kobayashi, Y., Kimura, A., and Numano, F. (1998). Association of clinical manifestations with HLA-B alleles in Takayasu arteritis. *Int. J. Cardiol.* **66**: S121-S126.

Kobayashi, Y., Yamamoto, K., Saido, T., Kawasaki, H., Oppenheim, J.J., and Matsushima, K. (1990). Identification of calcium-activated neutral protease as a processing enzyme of human interleukin-1 α . *Proc. Natl. Acad. Sci. USA.* **87**: 5548-5552.

Kominato, Y., Galson, D.L., Waterman, W.R., Webb, A.C., and Auron, P.E. (1995). Monocyte expression of the human proinflammatory 1 β gene (*IL1B*) is dependent on promoter sequences which bind the haematopoietic transcription factor Spi-1/PU.1. *Mol. Cell Biol.* **15**: 58-68.

Komine, M., Rao, L.S., Freedberg, I.M., Simon, M., Milisavljevic, V., and Blumenberg, M. (2001). Interleukin-1 induces transcription of keratin K6 in human epidermal keratinocytes. *J. Invest. Dermatol.* **116**: 330-338.

Konine, M., Rao, L.S., Kaneko, T., Tomic-Canic, M., Tamaki, K., Freedberg, I.M., and Blumenberg, M. (2000). Inflammatory versus proliferative processes in epidermis. *J. Biol. Chem.* **275**: 32077-32088.

Konttinen, Y.T., Ainola, M., Valleala, H., Ma, J., Ida, H., Mandelin, J., Kinne, R.W., Santavirta, S., Sorsa, T., Lopez-Ortin, C., and Tkagi, M. (1999). Analysis of 16 different matrix metalloproteinases (MMP-1 to MMP-20) in the synovial membrane: different profiles in trauma and rheumatoid arthritis. *Ann. Rheum. Dis.* **58**: 691-697.

Kopp, E.B., and Ghosh, S. (1995). NF- κ B and rel proteins in innate immunity. *Adv. Immunol.* **58**: 1-27.

Korganow, A., Ji, H., Mangialaio, S., Duchatelle, V., Pelanda, R., Martin, T., Degott, C., Kikutani, H., Rajewsky, K., Pasquali, J., Benoist, C., and Mathis, D. (1999). From systemic T cell self-reactivity to organ-specific autoimmune disease via immunoglobulins. *Immunity* **10**: 451-461.

Korherr, C., Hofmeister, R., Wesche, H., and Falk, W. (1997). A critical role for interleukin-1 receptor accessory protein in interleukin-1 signalling. *Eur. J. Immunol.* **27**: 262-267.

Kostura, M.J., Tocci, M.J., Limjoco, G., Chin, J., Cameron, P., Hillman, A.G., Chartrain, N.A., and Schmidt, J.A. (1989). Identification of a monocyte specific pre-interleukin 1 β convertase activity. *Proc. Natl. Acad. Sci. USA.* **86**: 5227-5231.

Kouskoff, V., Korganow, A., Duchatelle, V., Degott, C., Benoist, C., and Mathis, D. (1996). Organ-specific disease provoked by systemic autoimmunity. *Cell* **87**: 811-822.

Krutmann, J., and Grewe, M. (1995). Involvement of cytokines, DNA damage, and reactive oxygen intermediates in ultraviolet radiation-induced modulation of intercellular adhesion molecule-1 expression. *J Invest Dermatol.* **105**: 67S-70S.

Kuida, K., Lippke, J.A., Ku, G., Harding, M.W., Livingston, D.J., Su, M.S., and Flavell, R.A. (1995). Altered cytokine export and apoptosis in mice deficient in interleukin-1 beta converting enzyme. *Science* **267**: 2000-2003.

Kupper, T.S., and Groves, R.W. (1995). The interleukin-1 axis and cutaneous inflammation. *J. Invest. Dermatol.* **105**: 62S-66S.

Kupper, T.S., Chua, A.O., Flood, P., McGuire, J., and Gubler, U. (1987). Interleukin-1 gene expression in cultured human keratinocytes is augmented by ultraviolet irradiation. *J. Clin. Invest* **80**: 430-436.

Kushner, I.(1982). The phenomenon of the acute phase response. *Ann N Y Acad Sci.* **389**: 39-48.

La, E., and Fischer, S.M. (2001). Transcriptional regulation of intracellular IL-1 receptor antagonist gene by IL-1 α in primary mouse keratinocytes. *J. Immunol.* **166**: 6149-6155.

- Labow, M., Shuster, D., Zetterstrom, M., Nunes, P., Terry, R., Cullinan, E.B., Bartfai, T., Solorzano, C., Moldawer, L.L., Chizzonite, R.W., and McIntyre, K.W. (1997). Absence of IL-1 signalling and reduced inflammatory response in IL-1 type I receptor-deficient mice. *J. Immunol.* **159**: 2452-2461.
- Labriola-Tompkins, E., Chandran, C., Varnell, T.A., Madison, V.S., and Ju, G. (1993). Structure-function analysis of human IL-1 alpha: identification of residues required for binding to the human type I IL-1 receptor. *Protein Eng.* **6**: 535-539.
- Lawrence, R.C., Helmick, C.G., Arnett, F.C., Deyo, R.A., Felson, D.T., Giannini, E.H., Heyse, S.P., Hirsch, R., Hochberg, M.C., Hunder, G.G., Liang, M.H., Pillemer, S.R., Steen, V.D., and Wolfe, F. (1998). Estimates of the prevalence of arthritis and selected musculoskeletal disorders in the United States. *Arthritis Rheum.* **41**: 778-799.
- Lemaitre, B., Nicolas, E., Michaut, L., Reichhart, J., and Hoffmann, J.A. (1996). The dorsoventral regulatory gene cassette *spatzle/Toll/cactus* controls the potent antifungal responses in *Drosophila* adults. *Cell* **86**: 973-983.
- Li, C.Y., Lam, K.W., and Yam, L.T. (1973). Esterases in human leukocytes. *J Histochem Cytochem.* **21**: 1-12.
- Li, P., Allen, H., Banerjee, S., Franklin, S., Herzog, L., Johnston, C., McDowell, J., Paskind, M., Rodman, L., Salfeld, J., Towne, E., Tracey, D., Wardwell, S., Wei, F., Wong, W., Kamen, R., and Seshadri, T. (1995). Mice deficient in IL-1 β -converting enzyme are defective in production of mature IL-1 β and resistant to endotoxic shock. *Cell* **80**: 401-411.
- Li, P., Allen, H., Banerjee, S., Franklin, S., Herzog, L., Johnston, C., McDowell, J., Paskind, M., Rodman, L., and Salfeld, J. (1995). Mice deficient in IL-1 beta-converting enzyme are defective in production of mature IL-1 beta and resistant to endotoxic shock. *Cell* **80**: 401-411.
- Libby, P., Warner, S.J., and Friedman, G.B. (1988). Interleukin 1: a mitogen for human vascular smooth muscle cells that induces the release of growth-inhibitory prostanooids. *J Clin Invest.* **81**: 487-498.
- Lichtig, C., Haim, S., Hammel, I., and Friedman-Birnbaum, R. (1980). The quantification and significance of mast cells in lesions of Behcets' disease. *Br. J. Dermatol.* **102**: 255-259.
- Lie, J.T. (1998). Pathology of isolated nonclassical and catastrophic manifestations of takayasu arteritis. *Int. J. Cardiol.* **66**: S11-S21.

- Lie, J.T. Illustrated histopathologic classification criteria for selected vasculitis syndromes. *Arthritis Rheum.* **33**: 1074-1087.
- Lipsky, P.E., Thompson, P.A., Rosenwasser, L.J., and Dinarello, C.A. (1983). The role of interleukin 1 in human B cell activation: inhibition of B cell proliferation and the generation of immunoglobulin-secreting cells by an antibody against human leukocytic pyrogen. *J. Immunol.* **130**: 2708-2714.
- Liu, C., Young, L., and Youngm J.D. (1996). Mechanisms of disease: lymphocyte-mediated cytolysis and disease. *N. Engl. J. Med.* **335**: 1651-1659.
- Loddick, S.A., Wong, M., Bongirno, P.B., Gold, P.W., Licinio, J., and Rothwell, N.J. (1997). Endogenous interleukin-1 receptor antagonist is neuroprotective. *Biochem. Biophys. Res. Comm.* **234**: 211-215.
- Lomedico, P.T., Gubler, U., Hellmann, C.P., Dukovich, M., Giri, J.G., Pan, Y.C., Collier, K., Semionow, R., Chua, A.O., and Mizel, S.B. (1984). Cloning and expression of murine interleukin-1 cDNA in *Escherichia coli*. *Nature* **312**: 458-462.
- Londei, M., Savill, C.M., Verhoef, A., Brennan, F., Leech, Z.A., Duance, V., Maini, R.N., and Feldmann, M. (1989). Persistence of collagen type II-specific T-cell clones in the synovial membrane of a patient with rheumatoid arthritis. *Proc. Natl. Acad. Sci. USA* **86**: 636-640.
- Luft, T., Jefford, M., Luetjens, P., Hochrein, H., Masterman, K., Maliszewski C., Shortman K., Cebon, J., and Maraskovsky, E. (2002) *J. Immunol* **168**: 713-722.
- Lundqvist, E.N., and Egelrud, T. (1997). Biologically active, alternatively processed interleukin-1 beta in psoriatic scales. *Eur J Immunol.* **27**: 2165-2171.
- Ma, Y., Thornton, S., Boivin, G.P., Hirsh, D., Hirsch, R., and Hirsch, E. (1998). Altered susceptibility to collagen-induced arthritis in transgenic mice with abberant expression of interleukin-1 receptor antagonist. *Arthritis Rheum.* **41**: 1798-1805.
- Mach, F., Schonbeck, U., Sukhova, G., Bourcier, T., Bonnefoy, J., Pober, J.S., and Libby, P. (1997). Functional CD40 ligand is expressed on human vascular endothelial cells, smooth muscle cells, and macrophages: implications for CD40-CD40 ligand signalling in atherosclerosis. *Proc. Natl. Acad. Sci. USA.* **94**: 1931-1936.

MacNaul, K.L., Chartrain, N., Lark, M., Tocci, M.J., and Hutchinson, N.I. (1990). Discoordinate expression of stromelysin, collagenase, and tissue inhibitor of metalloproteinases-1 in rheumatoid human synovial fibroblasts. Synergistic effects of interleukin-1 and tumour necrosis factor-alpha on stromelysin expression. *J. Biol. Chem.* **265**: 17238-17245.

Magilavy, D. (1999). Immunopharmacologic effects of Amevive™ (LFA3TIP) in chronic plaque psoriasis: selectivity for peripheral memory-effector (CD45RO⁺) over naïve (CD45RA⁺) T cells. *Br. J. Dermatol.* **141**: 990.

Malyak, M., Guthridge, J. M., Hance, K.R., Dower, S.K., Freed, J.H., and Arend, W.P. (1998a) Characterisation of a low molecular weight isoform of IL-1 receptor antagonist. *J. Immunol* **161**: 1997-2003.

Malyak, M., Smith, M.F., Abel, A.A., Hance, K.R., and Arend, W.P. (1998b). The differential production of three forms of IL-1 receptor antagonist by human neutrophils and monocytes. *J. Immunol* **161**: 2004-2010.

Manetti, R., Parronchi, P., Giudizi, M.G., Piccinni, M.P., Maggi, E., Trinchieri, G., and Romagnani, S. (1993). Natural killer cell stimulatory factor (interleukin 12 [IL-12]) induces T helper type 1 (Th1)-specific immune responses and inhibits the development of IL-4-producing Th cells. *J Exp Med.* **177**: 1199-1120.

Manetti, R., Parronchi, P., Giudizi, M.G., Piccinni, M.P., Maggi, E., Trinchieri, G., and Romagnani, S. (1993). Natural killer cell stimulatory factor (interleukin 12 [IL-12]) induces T helper type 1 (Th1)-specific immune responses and inhibits the development of IL-4-producing Th cells. *J Exp Med.* **177**: 1199-1204.

Mansson, B., Gulfe, A., Geborek, P., Heinegard, D., and Saxne, T. (2001). Release of cartilage and bone macromolecules into synovial fluid: differences between psoriatic arthritis and rheumatoid arthritis. *Ann. Rheum. Dis.* **60**: 27-31.

March, C.J., Mosley, B., Larsen, A., Cerretti, D.P., Braedt, G., Price, V., Gillis, S., Henney, C.S., and Kronheim, S.R. (1985). Cloning, sequence and expression of two distinct human interleukin-1 complementary DNAs. *Nature* **315**: 641-647.

Marie, C., Pitton, C., Fitting, C., and Cavaillon, J.M. (1996). IL-10 and IL-4 synergise with TNF-alpha to induce IL-1ra production by human neutrophils. *Cytokine* **8**: 147-151.

Matsukawa, A., Ohkawara, S., Maeda, T., Takagi, K., and Yoshinaga, M. (1993). Production of IL-1 and IL-1 receptor antagonist and the pathological significance in lipopolysaccharide-induced arthritis in rabbits. *Clin. Exp. Immunol.* **93**: 206-211.

McCaffrey, T.A., Pomerantz, K.B., Sanborn, T.A., Spokojny, A.M., Du, B., Park, M, Folk, J.E., Lamberg, A., Kivirikko, K.I., Falcone, D.J., Mehta, S.B., and Hanauske-Abel, H.H. (1995). Specific inhibition of eIF-5a and collagen hydroxylation by a single agent. Antiproliferative and fibrosuppressive effects on smooth muscle cells from human coronary arteries. *J. Clin. Invest.* **95**: 446-455.

McMahan, C.J., Slack, J.L., Mosley, B., Cosman, D., Lupton, S.D., Brunton, L.L., Grubin, C.E., Wignall, J.M., Jenkins, N.A., Brannan, C.I., Copeland, N.G., Huebner, K., Croce, C.M., Cannizzarro, L.A., Bejamin, D., Dower, S.K., Spriggs, M.K., and Sims, J.E. (1991). A novel, IL-1 receptor, cloned from B-cells by mammalian expression, is expressed in many cell types. *EMBO J.* **10**: 2821-2832.

Means, T.K., Golenbock, D.T., and Fenton, M.J. (2000). The biology of Toll-like receptors. *Cytokine Growth Factor Rev.* **11**: 219-232.

Medzhitov, R., and Janeway, C. (2000). Innate immune recognition: mechanisms and pathways. *Immunol Rev.* **173**: 89-97.

Meek, R.L., Eriksen, N., Benditt, E.P. (1989). Serum amyloid A in the mouse. Sites of uptake and mRNA expression. *Am J Pathol.* **135**: 411-419.

Mehra, N.K., Jaini, R., Balamurugan, A., Kanga, U., Prabhakaran, D., Jain, S., Talwar, K.K., and Sharma, B.K. (1998). Immunogenetic analysis of Takayasu arteritis in Indian patients. *Int. J. Cardiol.* **66**: S127-S132.

Mehra, N.K., Rajalingam, R., Sagar, S., Jain, S., and Sharma, B.K. (1996). Direct role of HLA-B5 in influencing susceptibility to Takayasu aortoarteritis. *Int. J. Cardiol.* **54**: S71-S79.

Mercurio, F., Zhu, H., Murray, B.W., Shevchenko, A., Bennett, B.L., Li, J.W., Young, D.B., Barbosa, M., Mann, M., Manning, A., and Rao, A. (1997). IKK-1 and IKK-2: cytokine-activated I κ B kinases essential for NF- κ B activation. *Science* **278**: 860-866.

Miller, D.K., Ayala, J.M., Eggert, L.A., Raju, S.M., Yamin, T., Ding, G.J.F., Gaffney, E.P., Howard, A.D., Palyha, O.C., Rolando, A.M., Salley, J.P., Thornberry, N.A., Weidner, J.R., Williams, J.H., Chapman, K.T., Jackson, J., Kostura, M.J., Limjuco, G., Molineaux, S.M., Mumford, R.A., and Calaycay, J.R. (1993). Purification and characterisation of active human interleukin-1 β -converting enzyme from THP.1 monocytic cells. *J. Biol. Chem.* **268**: 18062-18069.

Mino, T., Sugiyama, E., Taki, H., Kuroda, A., Yamashita, N., Maruyama, M., and Kobayashi, M. (1998). Interleukin-1 α and tumour necrosis factor α synergistically stimulate prostaglandin E₂-dependent production of interleukin-11 in rheumatoid synovial fibroblasts. *Arthritis Rheum.* **41**: 2004-2013.

Miossec, P. and Ziff, M. (1986). Immune interferon enhances the production of interleukin-1 by human endothelial cells stimulated with lipopolysaccharide. *J. Immunol* **137**: 2848-2852.

Miossec, P., Cavender, D., and Ziff, M. (1986). Production of interleukin-1 by human endothelial cells. *J. Immunol* **136**: 2486-2491.

Miossec, P., Dinarello, C.A., and Ziff, M. (1986). Interleukin-1 lymphocyte chemotactic activity in rheumatoid arthritis synovial fluid. *Arthritis Rheum.* **29**: 461-470.

Miyasaka, N., Sato, K., Goto, M., Sasano, M., Natsuyama, M., Inoue, K., and Nishioka, K. (1988). Augmented interleukin-1 production and HLA-DR expression in the synovium of rheumatoid arthritis patients. Possible involvement in joint destruction. *Arthritis Rheum.* **31**: 480-486.

Mizel, S.B., and Mizel, D.J. (1981) Purification to apparent homogeneity of murine interleukin 1. *J. Immunol.* **126**: 834-837.

Mizel, S.B., Dayer, J., Krane, S.M., and Mergenhagen, S.E. (1981). Stimulation of rheumatoid synovial cell collagenase and prostaglandin production by partially purified lymphocyte-activating factor (interleukin 1). *Proc. Natl. Acad. Sci. USA.* **78**: 2474-2477.

Mizutani, H., Black, R., and Kupper, T.S. (1991a). Human keratinocytes produce but do not process pro-interleukin-1 (IL-1) beta. Different strategies of IL-1 production and processing in monocytes and keratinocytes. *J. Clin. Invest.* **87**: 1066-1071.

Mizutani, H., Schlechter, N., Lazarus, G., Black, R.A., and Kupper, T.S. (1991b). Rapid and specific conversion of precursor interleukin 1 β (IL-1 β) to an active IL-1 species by human mast cell chymase. *J. Exp. Med.* **174**: 821-825.

Mohr, W., Beneke, G., and Mohing, W. (1975). Proliferation of synovial lining cells and fibroblasts. *Ann. Rheum. Dis.* **34**: 219-224.

Morales-Ducret, J., Wayner, E., Elices, M.J., Alvaro-Gracia, J.M., Zvaifler, N.J., and Firestein, G.S. (1992). α_4/β_1 integrin (VLA-4) ligands in Arthritis. Vascular cell adhesion molecule-1 expression in synovium and on fibroblast-like synoviocytes. *J. Immunol.* **149**: 1424-1431.

Morisato, D., and Anderson, K.V. (1994). The spatzle gene encodes a component of the extracellular signaling pathway establishing the dorsal-ventral pattern of the *Drosophila* embryo. *Cell.* **76**: 677-688.

Morita, K., Hogan, M.E., Nanney, L.B., King, L.E., Manabe, M., Sun, T.T., and Sundberg, J.P. (1995). Cutaneous ultrastructural features of the flaky skin (fsn) mouse mutation. *J. Dermatol.* **22**: 385-395.

Mosley, B., Urdal, D.L., Prickett, K.S., Larsen, A., Cosman, D., Conlon, P.J., Gillis, S., and Dower, S.K. (1987). The interleukin-1 receptor binds the human interleukin-1 α precursor but not the interleukin-1 β precursor. *J. Biol. Chem* **262**: 2941-2944.

Muhlestein, J.B. (1998). Bacterial infections and atherosclerosis. *J. Invest. Med* **46**: 396-402.

Muller, W.A., and Randolph, G.J. (1999). Migration of leukocytes across endothelium and beyond: molecules involved in the transmigration and fate of monocytes. *J. Leukoc. Biol.* **66**: 698-704.

Murphy, J.E., Robert, C., and Kupper, T.S. (2000). Interleukin-1 and cutaneous inflammation: a crucial link between innate and acquired immunity. *J. Invest. Dermatol.* **114**: 602-608.

Muzio, M., Ni, J., Feng, P., and Dixit, V.M. (1997). IRAK (Pelle) family member IRAK-2 and MyD88 as proximal mediators of IL-1 signalling. *Science* **278**: 1612-1615.

Muzio, M., Polentarutti, N., Sironi, M., Poli, G., De Gioia, L., Introna, M., Mantovani, A., and Colotta, F. (1995). Cloning and characterisation of a new isoform of the interleukin-1 receptor antagonist. *J. Exp. Med.* **182**: 623-628.

Nagel, T., Resnick, N., Dewey, C.F., and Gimbrone, M.A. (1999). Vascular endothelial cells respond to spatioal gradients in fluid shear stress by enhanced activation of transcription factors. *Arterioscl. Thromb. Vasc. Biol.* **19**: 1825-1834.

Nakae, S., Asano, M., Horai, R., Sakaguchi, N., and Iwakura, Y. (2001). IL-1 enhances T cell-dependent antibody production through induction of CD40 ligand and OX40 on T cells. *J. Immunol.* **167**: 90-97.

Nakae, S., Naruse-Nakajima, C., Sudo, K., Horai, R., Asano, M., and Iwakura, Y. (2001). IL-1 alpha, but not IL-1 beta, is required for contact-allergen-specific T cell activation during the sensitization phase in contact hypersensitivity. *Int Immunol.* **13**: 1471-1478.

Nakata, M., Smyth, M.J., Norihisa, Y., Kawasaki, A., Shinkai, Y., Okumura, K., and Yagita, H. (1990). Constitutive expression of pore-forming protein in peripheral blood γ/δ T-cells: Implication for their cytotoxic role in vivo. *J. Exp. Med.* **172**: 1877-1880.

Nawroth, P.P., Bank, I., Handley, D., Cassimeris, J., Chess, L., and Stern, D. (1986). Tumour necrosis factor/cachetin interacts with endothelial cell receptors to induce release of interleukin-1. *J. Exp. Med.* **163**: 1363-1375.

Nicklin, M.J., Hughes, D.E., Barton, J.L., Ure, J.M., and Duff, G.W. (2000). Arterial inflammation in mice lacking the interleukin 1 receptor antagonist gene. *J Exp Med.* **191**: 303-312.

Nickoloff, B.J., and Turka, L.A. (1993). Keratinocytes: key immunocytes of the integument. *Am. J. Pathol.* **143**: 325-331.

Nickoloff, B.J., Kunkei, S.L., Burdick, M., and Strieter, R.M. (1995). Severe combined immunodeficiency mouse and human psoriatic skin chimeras. Validation of a new animal model. *Am. J. Pathol.* **146**: 580-588.

Niki, Y., Yamada, H., Seki, S., Kikuchi, T., Takaishi, H., Toyama, Y., Fujikawa, K., and Tada, N. (2001). Macrophage- and neutrophil-dominant arthritis in human IL-1 α transgenic mice. *J. Clin. Invest.* **107**: 127-1135.

Nikkari, S.Y., Hoyhtya, M., Isola, J. and Nikkari, T. (1996). Macrophages contain 92-kd gelatinase (MMP-9) at the site of degenerated internal elastic lamina in temporal arteritis. *Am. J. Pathol.* **149**: 1427-1433.

Ninomiya-Tsuji, J., Kishimoto, K., Hiyama, A., Inoue, J., Cao, Z., and Matsumoto, K. (1999). The kinase TAK-1 can activate the NIK-I κ B as well as the MAP kinase cascade in the IL-1 signalling pathway. *Nature* **398**: 252-256.

- Nityanand, S., Mishra, K., Shrivastava, S., Holm, G., and Lefvert, A.K. (1997). Autantibodies against cardiolipin and endothelial cells in Takayasu's arteritis: prevalence and isotype distribution. *Br. J. Rheumatol.* **36**: 923-924.
- Nouri, A.M.E., Panayi, G.S., and Goodman, S.M. (1984). Cytokines and the chronic inflammation of rheumatic disease. I. The presence of interleukin-1 in synovial fluids. *Clin. Exp. Immunol.* **55**: 295-302.
- Numano, F., Okawara, M., Inomata, H., and Kobayashi, Y. (2000), Takayasu's arteritis. *Lancet* **356**: 1023-1025.
- O'Neill, L.A., and Greene, C. (1998). Signal transduction pathways activated by the IL-1 receptor family: ancient signalling machinery in mammals, insects, and plants. *J. Leukoc. Biol.* **63**: 650-657.
- Obermeier F., Gross, V., Scholmerich, J., and Falk, W. (1999). Interleukin-1 production by mouse macrophages is regulated in a feedback fashion by nitric oxide. *J. Leukoc. Biol.* **66**: 829-836.
- Ollier, W., Venebales, P.J.W., Mumford, P.A., Mini, R.N., Awad, J., Jaraquemada, D., D'Amaro, J., and Festenstein, H. (1984). HLA antigen associations with extra-articular rheumatoid arthritis. *Tissue Antigens* **24**: 279-291.
- O'Neill, T., and Silman, A.J. (1994). Psoriatic arthritis. Historical background and epidemiology. *Baillieres Clin Rheumatol* **8**: 245-261.
- Ong, G., Thomas, B.J., Mansfield, A.O., Davidson, B.R., and Taylor-Robinson, D. (1996). Detection and widespread distribution of *Chlamydia pneumoniae* in the vascular system and its possible implications. *J. Clin. Pathol* **49**: 102-106.
- Ortonne, J.P. (1999). Recent developments in the understanding of the pathogenesis of psoriasis. *Br. J. Dermatol.* **140 suppl. 54**: 1-7.
- Pakianathan, D.R. (1995). Extracellular matrix proteins and leukocyte function. *J Leukoc Biol.* **57**: 699-702.
- Paleolog, E.M. (1996). Angiogenesis: a critical process in the pathogenesis of RA – a role for VEGF? *Br. J. Rheumatol.* **35**: 917-920.

- Pan, R.Y., Chen, S.L., Xiao, X., Liu, D.W., Peng, H.J., and Tsao, Y.P. (2000). Therapy and prevention of arthritis by recombinant adeno-associated virus vector with delivery of interleukin-1 receptor antagonist. *Arthritis Rheum.* **43**: 289-297.
- Partridge, M., Chantry, D., Turner, M., and Feldmann, M. (1991). Production of interleukin-1 and interleukin-6 by human keratinocytes and squamous cell carcinoma cell lines. *J. Invest. Dermatol.* **96**: 771-776.
- Patel, S., Veale, D., FitzGerald, O., McHugh, N.J. (2001). Psoriatic arthritis – emerging concepts. *Rheumatology* **40**: 243-246.
- Peng, H., Libby, P., and Liao, J.K. (1995). Induction and stabilisation of I κ B α by nitric oxide mediates inhibition of NF- κ B. *J. Biol. Chem.* **270**: 14214-14219.
- Perlstein, R.S., Whitnall, M.H., Abrams, J.S., Mougey, E.H., and Neta, R. (1993). Synergistic roles of interleukin-6, interleukin-1, and tumour necrosis factor in the adrenocorticotropin response to bacterial lipopolysaccharide *in vivo*. *Endocrinology* **132**: 946-952.
- Pettipher, E.P., Higgs, G.A., and Henderson, B. (1986). Interleukin 1 induces leukocyte infiltration and cartilage proteoglycan degradation in the synovial joint. *Proc. Natl. Acad. Sci. USA.* **83**: 8749-8753.
- Pinchuk, L.M., Klaus, S.J., Magaletti, D.M., Pinchuk, G.V., Norsen, J.P., and Clark, E.A. (1996). Functional CD40 ligand expressed by human blood dendritic cells is up-regulated by CD40 ligation. *J Immunol.* **157**: 4363-4670.
- Pitzalis, C. Skin and joint disease in psoriatic arthritis: what is the line? (1998). *Br. J. Rheumatol.* **37**: 480-483.
- Pitzalis, C., Kingsley, G., Lanchbury, J.S., Murphy, J., and Panayi, G.S. (1987). Expression of HLA-DR, DQ and DP antigens and interleukin-2 receptor on synovial fluid T lymphocyte subsets in rheumatoid arthritis: evidence for "frustrated" activation. *J Rheumatol.* **14**: 662-666.
- Postlethwaite, A.E., Raghow, R., Stricklin, G.P., Poppleton, H., Seyer, J., and Kang, A.H. (1988). Modulation of fibroblast functions by interleukin 1: increased steady-state accumulation of type I procollagen messenger RNAs and stimulation of other functions but not chemotaxis by human recombinant interleukin 1 α and β . *J. Cell. Biol.* **106**: 311-318.

- Poutsika, D.D., Clark, B.D., Vannier, E., and Dinarello, C.A. (1991). Production of interleukin-1 receptor antagonist and interleukin-1 β by peripheral blood mononuclear cells is differentially regulated. *Blood* **78**: 1275-1281.
- Priestle, J.P., Schar, H.P., and Grutter, M.G. (1988). Crystal structure of the cytokine interleukin-1 beta. *EMBO J.* **7**: 339-343.
- Priestle, J.P., Schar, H.P., and Grutter, M.G. Crystallographic refinement of interleukin 1 beta at 2.0 A resolution. (1989). *Proc Natl Acad Sci U S A.* **86**: 9667-9971.
- Probert, L., Plows, D., Kontogeorgos, G., and Kollias, G. (1995). The type 1 interleukin-1 receptor acts in series with tumour necrosis factor (TNF) to induce arthritis in TNF-transgenic mice. *Eur. J. Immunol.* **25**: 1794-1797.
- Pugin, J., Ulevitch, R.J., and Tobias, P.J. (1993). A critical role for monocytes and CD14 in endotoxin-induced endothelial cell activation. *J. Exp. Med.* **178**: 2193-2200.
- Raines, E.W., Dower, S.K., and Ross, R. (1989). Interleukin-1 mitogenic activity for fibroblasts and smooth muscle cells is due to PDGF-AA. *Science.* **243**: 393-396.
- Rajavashisth, T.B., Liao, J.K., Galis, Z.S., Tripathi, S., Laufs, U., Tripathi, J., Chai, N., Xu, X., Jovinge, S., Shah, P.K., and Libby, P. (1999). Inflammatory cytokines and oxidised low density lipoproteins increase endothelial cell expression of membrane type 1-matrix metalloproteinase. *J. Biol. Chem.* **274**: 11924-11929.
- Ramadori, G., Sipe, J.D., Dinarello, C.A., Mizel, S.B., and Colten, H.R. (1985). Pretranslational modulation of acute phase hepatic protein synthesis by murine recombinant interleukin-1 (IL-1) and purified human IL-1. *J. Exp. Med.* **162**: 930-942.
- Re, F., Sironi, M., Muzio, M., Matteucci, C., Introna, M., Orlando, S., Penton-Rol, G., Dower, S.K., Sims, J.E., Colotta, F., and Mantovani, A. (1996). Inhibition of interleukin-1 responsiveness by type II receptor gene transfer: a surface "receptor" with anti-interleukin-1 function. *J. Exp. Med.* **183**: 1841-1850.
- Rectenwald JE, Moldawer LL, Huber TS, Seeger JM, Ozaki CK. (2000). Direct evidence for cytokine involvement in neointimal hyperplasia. *Circulation.* **102**: 1697-1702.
- Reece, R.J., Canete, J.D., Parsons, W.J., Emery, P., and Veale, J.D. (1999). Distinct patterns of early synovitis in psoriatic, reactive, and rheumatoid arthritis. *Arthritis Rheum.* **42**: 1481-1484.

- Regnier, C.H., Song, H.Y., Bao, X., Goeddel, D.V., Cao, Z., and Rothe, M. (1997). Identification and characterisation of an I κ B kinase. *Cell* 90: 373-383.
- Relton, J.K., Martin, D., Thompson, R.C., and Russell, D.A. (1996). Peripheral administration of interleukin-1 receptor antagonist inhibits brain damage after focal cerebral ischemia in the rat. *Exp. Neurol.* 138: 206-213.
- Rhodin, J., Thomas, T., Bryant, M., Clark, L., and Sutton, E.T. (1999). Animal model of vascular inflammation. *J. Submicrosc. Cytol. Pathol.* 31: 305-311.
- Riley, L.K., Frankloin, C.L., Hook, R.R., and Besch-Williford, C. (1996). Identification of murine helicobacters by PCR and restriction enzyme analysis. *J. Clin. Lab. Micro.* 34: 942-946.
- Roderick, T.H., and Guidi, J.N. (1990). Strain distribution of polymorphic variants. In: *Genetic strains and variants of the laboratory mouse, 2nd edition* (Eds: Lyon, M.F., and Searle, A.G.), Oxford University Press. pp 663-772.
- Rosales, C., and Juliano, R.L. (1995). Signal transduction by cell adhesion receptors in leukocytes. *J Leukoc Biol.* 57:189-198.
- Rosenbaum, J., Pottinger, B.E., Woo, P., Black, C.M., Loizou, S., Byron, M.A., and Pearson, J.D. (1988). Measurement and characterisation of circulating anti-endothelial cell IgG in connective tissue diseases. *Clin. Exp. Immunol.* 72: 450-456.
- Ross, R. (1999). Mechanisms of disease: atherosclerosis – an inflammatory disease. *N. Engl. J. Med.* 340: 115-126.
- Ross, R., Raines, E.W., and Bowen-Pope, D.F. (1986). The biology of platelet-derived growth factor. *Cell* 46: 155-169.
- Rothermel, C.D., Schachter, J., Lavrich, P., Lipsitz, E.C., and Francus, T. (1989). *Chlamydia trachomatis*-induced production of interleukin-1 by human monocytes. *Infect. Immun.* 57: 2705-2711.
- Saha, B.K., Shields, J.J., Miller, R.D., Hansen, T.H., and Schreffler, D.C. (1993). A highly polymorphic microsatellite in the class II *Eb* gene allows tracing of major histocompatibility complex evolution in mouse. *Proc. Natl. Acad. Sci. USA.* 90: 5312-5316.
- Saklatvala, J. (1986). Tumour necrosis factor alpha stimulates resorption and inhibits synthesis of proteoglycan in cartilage. *Nature* 322: 547-549.

Sako, D., Chang, X., Barone, K.M., Vachino, G., White, H.M., Shaw, G., Veldman, G.M., Bean, K.M., Ahern, T.J., Furie, B., Cumming, D.A., and Larsen, G.A. (1993). Expression cloning of a functional glycoprotein ligand for P-selectin. *Cell* **75**: 1179-1186.

Salgado, C.G., Nakamura, K., Sugaya, M., Tada, Y., Asahina, A., Koyama, Y., Irie, S., and Tamaki, K. (1999). Functional CD40 ligand is expressed on epidermal Langerhans cells. *J Leukoc Biol.* **66**: 281-285.

Salmon, M., and Gaston, J.S.H. (1995). The role of T-lymphocytes in rheumatoid arthritis. *Br. Med. Bull.* **51**: 332-345.

Salvarani, C., Sherine, E.G., O'Fallon, W.M., and Hunder, G.G. (1995). The incidence of giant cell arteritis in Olmstead county, Minnesota: apparent fluctuations in a cyclic pattern. *Ann. Intern. Med.* **123**: 192-194.

Sansonetti, P.J., Phalipon, A., Arondel, J., Thirumalai, K., Banerjee, S., Akira, S., Takeda, K., and Zychlinsky, A. (2000). Caspase-1 activation of IL-1beta and IL-18 are essential for Shigella flexneri-induced inflammation. *Immunity.* **12**: 581-590.

Santiago-Schwartz, F., Anand, P., Liu, S., and Carsons, S.F. (2001). Dendritic cells (DCs) in rheumatoid arthritis (RA): progenitor cells and soluble factors contained in RA synovial fluid yield a subset of myeloid DCs that preferentially activate Th1 inflammatory-type responses. *J. Immunol.* **167**: 1758-1768.

Santtila, S., Savinainen, K., and Hurme, M. (1998). Presence of the IL-1RA allele 2 (IL1RN*2) is associated with enhanced IL-1 β production *in vitro*. *Scand. J. Immunol.* **47**: 195-198.

Satoskar, A.R., Okano, M., Connaughton, S., Raisanen-Sokolwski, A., David, J.R., and Labow, M. Enhanced Th2-like responses in Il-1 type 1 receptor-deficient mice. *Eur. J. Immunol.* **28**: 2066-2074.

Savage, C.O.S., Harper, L., and Adu, D. (1997). Primary systemic vasculitis. *Lancet* **349**: 553-557.

Savage, C.O.S., Harper, L., Cockwell, P., Adu, D., and Howie, A.J. (2000). Vasculitis. *British Medical J.* **320**: 1325-1328.

Sawchuck, A.P., Unthank, J.L. and Dalsing, M.C. (1999). Drag reducing polymers may decrease atherosclerosis by increasing shear in areas normally exposed to low shear stress. *J. Vasc. Surg.* **30**: 761-764.

- Schaller, M., Burton, D.R., and Ditzel, H.J. (2001). Autoantibodies to GPI in rheumatoid arthritis: linkage between an animal model and human disease. *Nat Immunol.* **2**: 746-753.
- Schiff, B., Mizrachi, Y., Orgad, S., Yaron, M., and Gazit, E. (1982). Association of HLA-Aw31 and HLA-DR1 with adult rheumatoid arthritis. *Ann. Rheum. Dis.* **41**: 403-404.
- Schiff, M.H. (2000). Role of interleukin 1 and interleukin 1 receptor antagonist in the mediation of rheumatoid arthritis. *Ann. Rheum. Dis.* **59**: i103-i108.
- Schiffer, R., Klein, B., Klosterhalfen, B., and Zwadlo-Klarwasser, G. (1999). The contact of human macrophages with extracellular matrix proteins selectively induces expression of pro-inflammatory cytokines. *Pathobiology* **67**: 233-235.
- Schlaak, J.F., Buslau, M., Jochum, W., Hermann, E., Girndt, M., Gallati, H., Meyer zum Buschenfelde, K, and Fleischer, B. (1994). T cells involved in psoriasis vulgaris belong to the Th1 subset. *J. Invest. Dermatol.* **102**: 145-149.
- Schmidt, U., Wagner, H., and Miethke, T. (1999). CpG-DNA upregulates the major acute-phase proteins SAA and SAP. *Cell. Microbiol.* **1**: 61-67.
- Schmidt, H.H., and Walter, U. (1994). NO at work. *Cell.* **78**: 919-925.
- Schmitt-Egenolf, M., Boehncke, W., Stander, M., Eiermann, T.H., and Sterry, W. (1993). Oligonucleotide typing reveals association of type I psoriasis with the HLA-DRB*0701/2, -DQA1*0201, -DQB1*303 extended haplotype. *J. Invest. Dermatol.* **100**: 749-752.
- Schon, M., Behmenburg, C., Denzer, D., and Schon, M.P. (2001). Pathogenic function of IL-1 β in psoriasiform skin lesions of flaky skin (*fsn/fsn*) mice. *Clin. Exp. Immunol* **123**: 505-510.
- Schon, M., Denzer, D., Kubitza, R.C., Ruzicka, T., and Schon, M.P. (2000). Critical role of neutrophils for the generation of psoriasiform skin lesions in flaky skin mice. *J. Invest. Dermatol.* **114**: 976-983.
- Schon, M.P. (1999). Animal models of psoriasis – what can we learn from them? *J. Invest. Dermatol.* **112**: 405-410.
- Schon, M.P., Detmar, M., and Parker, C.M. (1997). Murine psoriasis-like disorder induced by naïve CD4⁺ T-cells. *Nature Med.* **3**: 183-188.

- Schonbeck, U., Mach, F., and Libby, P. (1998). Generation of biologically active IL-1 β by matrix metalloproteinases: a novel caspase-1 independent pathway of IL-1 β processing. *J. Immunol.* **161**: 3340-3346.
- Schonbeck, U., Mach, F., Bonnefoy, J., Loppnow, H., Flad, H., and Libby, P. (1997). Ligation of CD40 activates interleukin 1 β converting enzyme (caspase-1) activity in vascular smooth muscle and endothelial cells and promotes elaboration of active interleukin 1 β . *J. Biol. Chem.* **272**: 19569-19574.
- Scott, B.B., Weisbrot, L.M., Greenwood, J.D., Bogoch, E.R., Paige, C.J., and Keystone, E.C. (1997). Rheumatoid arthritis synovial fibroblast and U937 macrophage/monocyte cell line interaction in cartilage degradation. *Arthritis Rheum.* **40**: 490-498.
- Seckinger, P., Lowenthal, J.W., Williamson, K., Dayer, J., and McDonald, H.R. (1987b). A urine inhibitor of interleukin 1 activity that blocks ligand binding. *J. Immunol.* **139**: 1546-1549.
- Seckinger, P., Williamson, K., Balavoine, J., Mach, B., Mazzei, G., Shaw, A., and Dayer, J. (1987a). A urine inhibitor of interleukin 1 activity affects both interleukin 1 α and interleukin 1 β but not tumour necrosis factor α . *J. Immunol.* **139**: 1541-1545.
- Seko, Y., Minota, S., Kawasaki, A., Shinkai, Y., Maeda, K., Yagita, H., Okumura, K., Osamu, T., Atsuhiko, T., and Yazaki, Y. (1994). Perforin-secreting killer cell infiltration and expression of a 65-kD heat-shock protein in aortic tissue of patients with Takayasu's arteritis. *J. Clin. Invest.* **93**: 750-758.
- Seko, Y., Sato, O., Takagi, A., Tada, Y., Matsuo, H., Yagita, H., Okumura, K., and Yazaki, Y. Restricted usage of T-cell receptor V alpha-V beta genes in infiltrating cells in aortic tissue of patients with Takayasu's arteritis. *Circulation* **93**: 1788-1790.
- Seo, S.M., McIntyre, L.V., and Smith, C.W. (2001). Effects of IL-8, Gro- α , and LTB4 on the adhesive kinetics of LFA-1 and Mac-1 on human neutrophils. *Am. J. Physiol. Cell. Physiol.* **281**: C1568-C1578.
- Sharma, B.K., Jain, S., Suri, S., and Numano, F. (1996). Diagnostic criteria for Takayasu arteritis. *Int. J. Cardiol.* **54**: S127-S133.
- Shimuzu, Y., and Shaw, S. (1993). Mucins in the mainstream. *Nature* **366**: 630-631.

Shiozawa, S., Shiozawa, K., and Fujita, T. (1983). Morphologic observations in the early phase of the cartilage-pannus junction. Light and electron microscopic studies of active cellular pannus. *Arthritis Rheum.* **26**: 472-478.

Shornick, L.P., Bisarya, A.K., and Chaplin, D.D. (2001). IL-1beta is essential for langerhans cell activation and antigen delivery to the lymph nodes during contact sensitisation: evidence for a dermal source of IL-1beta. *Cell. Immunol.* **211**: 105-112.

Sica, A., Wang, J.M., Colotta, F., Dejana, E., Mantovani, A., Oppenheim, J.J., Larsen, C.G., Zachariae, C.O.C., and Matsushima, K. (1990). Monocyte chemotactic and activating factor gene expression induced in endothelial cells by IL-1 and tumour necrosis factor. *J. Immunol.* **144**: 3034-3038.

Sima, D., Thiele, B., Turowski, A., Wilke, K., Hiepe, F., Volk, D., and Sonnichsen, N. (1994). Anti-endothelial cells in Takayasu arteritis. *Arthritis Rheum.* **37**: 441-443.

Simon, A.K., Seipelt, E., and Sieper, J. (1994). Divergent T-cell cytokine patterns in inflammatory arthritis. *Proc. Natl. Acad. Sci. USA* **91**: 8562-8566.

Sims, J.E. (2002). Il-1 and IL-18 receptors, and their extended family. *Curr. Opin. Immunol.* **14**: 117-122.

Sims, J.E., Acres, R.B., Grubin, C.E., McMahan, C.J., Wignall, J.M., March, C.J., and Dower, S.K. (1989). Cloning the interleukin 1 receptor from human T-cells. *Proc. Natl. Acad. Sci. USA.* **86**: 8946-8950.

Sims, J.E., Gayle, M.A., Slack, J.L., Alderson, M.R., Bird, T.A., Giri, J.G., Colotta, F., Re, F., Mantovani, A., Shanebeck, K., Grabstein, K.H., and Dower, S.K. (1993). Interleukin-1 signalling occurs exclusively via the type 1 receptor. *Proc. Natl. Acad. Sci. USA.* **90**: 6155-6159.

Sims, J.E., March, C.J., Cosman, D., Widmer, M.B., MacDonald, H.R., McMahan, C.J., Grubin, C.E., Wignall, J.M., Jackson, J.L., Call, S.M., Friend, D., Alpert, A.R., Gillis, S., Urdal, D.L. and Dower, S.K. (1988). cDNA expression cloning of the IL-1 receptor, a member of the immunoglobulin superfamily. *Science* **241**: 585-589.

Sims, J.E., Painter, S.L., and Gow, I.R. (1995). Genomic organisation of the type I and type II IL-1 receptors. *Cytokine* **7**: 1-8.

Singh, S.R., Casper, K., Summers, S., and Swerlick, R.A. (2001). CD40 expression and function on human dermal microvascular endothelial cells: role in cutaneous inflammation. *Clin Exp Dermatol.* **26**: 434-440.

Sleath, P.R., Hendrickson, R.C., Kronheim, S.R., March, C.J., and Black, R.A. (1990). Substrate specificity of the protease that processes human interleukin-1 beta. *J. Biol. Chem.* **265**: 14526-14528.

Smith, C., Andreakos, E., Crawley, J.B., Brennan, F.M., Feldmann, M., and Foxwell, B.M.. (2001). NF-kappaB-inducing kinase is dispensable for activation of NF-kappaB in inflammatory settings but essential for lymphotoxin beta receptor activation of NF-kappaB in primary human fibroblasts. *J Immunol.* **167**: 5895-5903.

Snyder, D.S., and Unanue, E.R. (1982). Corticosteroids inhibit murine macrophage Ia expression and interleukin 1 production. *J. Immunol.* **129**: 1803-1805.

Son, K., Tomita, Y., Shimizu, T., Nishinarita, S., Sawada, S., and Horie, T. (2000). Abnormal IL-1 receptor antagonist production in patients with polymyositis and dermatomyositis. *Intern. Med.* **39**: 128-135.

Soter, N.A. (1976). Clinical presentations and mechanisms of necrotising angitis of the skin. *J. Invest. Dermatol.* **67**: 354-359.

Steinbrink, K., Paragnik, L., Jonuleit, H., Tuting, T., Knop, J., and Enk, J.H. (2000). Induction of dendritic cell maturation and modulation of dendritic cell-induced immune responses by prostaglandins. *Arch. Dermatol. Res.* **292**: 437-445.

Steiner, G., Tohidast-Akrad, M., Witzmann, G., Vesely, M., Studnicka-Benke, A., Gal, A., Kunaver, M., Zenz, P., and Smolen, J.S. (1999). Cytokine production by synovial T-cells in rheumatoid arthritis. *Rheumatology* **38**: 202-213.

Sterpetti, A.V., Cucina, A., D'Angelo, L.S., Cardillo, B., and Cavallaro, A. (1993). Shear stress modulates the proliferation rate, protein synthesis, and mitogenic activity of arterial smooth muscle cells. *Surgery* **113**: 691-699.

Stoler, A., Kopan, R., Duvic, M., and Fruchs, E. (1988). Use of monospecific antisera and cRNA probes to localise the major changes in keratin expression during normal and abnormal epidermal differentiation. *J. Cell Biol.* **107**: 427-446.

Stylianou, E., O'Neill, L.A.J., Rawlinson, L., Edbrooke, M.R., Woo, P., and Saklatvala, J. (1992). Interleukin 1 induces NF- κ B through its type 1 but not its type II receptor in lymphocytes. *J. Biol. Chem.* **267**: 15836-15841.

Sztein, M.B., Vogel, S.N., Sipe, J.D., Murphy, P.A., Mixel, S.B., Oppenheim, J.J., and Rosenstreich, D.L. (1981). The role of macrophages in the acute-phase response: SAA inducer is closely related to lymphocyte activating factor and endogenous pyrogen. *Cell. Immunol.* **63**: 164-176.

Tak, P.P., Smeets, T.J.M., Daha, M.R., Kluin, P.M., Meijers, K.A.E., Brand, R., Meinders, A.E., and Breedveld, F.C. (1997). Analysis of the synovial cell infiltrate in early rheumatoid synovial tissue in relation to local disease activity. *Arthritis Rheum.* **40**: 217-255.

Tarkowski, A., Klareskog, L., Carlsten, H., Herberts, P., and Koopman, W.J. (1989). Secretion of antibodies to types I and II collagen by synovial tissue cells in patients with rheumatoid arthritis. *Arthritis Rheum.* **32**: 1087-1092.

Tarlow, J.K., Clay, F.E., Cork, M.J., Blakemore, A.I.F., McDonagh, A.J.G., Messenger, A.G., and Duff, G.W. (1994). Severity of alopecia areata is associated with a polymorphism in the interleukin-1 receptor antagonist gene. *J. Invest. Dermatol.* **103**: 387-390.

Tarlow, J.K., Cork, M.J., Clay, F.E., Scmitt-Egenolf, M., Crane, A.M., Stierle, C., Boehncke, W., Eiermann, T.H., Blakemore, A.I.F., Bleehen, S.S., Sterry, W., and Duff, G.W. (1997). Association between interleukin-1 receptor antagonist (IL-1ra) gene polymorphism and early and late-onset psoriasis. *Br. J. Dermatol.* **136**: 147-148.

Tazi Ahnini, R., Camp, N.J., Cork, M.J., Mee, J.B., Keohane, S.G., Duff, G.W., and Di Giovine, F.S. (1999a). Novel genetic association between the corneodesmosin (MHC S) gene and susceptibility to psoriasis. *Hum. Mol. Genet.* **8**: 1135-1140.

Tazi Ahnini, R., Di Giovine, F.S., Cox, A., Keohane, S.G., and Cork, M.J. (1999b). Corneodesmosin (MHC S) gene in guttate psoriasis. *Lancet* **354**: 597.

Telford, J.L., Macchia, G., Massone, A., Carinci, V., Palla, E., and Melli, M. (1986). The murine interleukin-1 β gene: structure and evolution. *Nucleic Acids Research* **14**: 9955-9963.

Thompson, A.G., Pettit, A., Padmanabha, J., Mansfield, H., Frazer, I.H., Strutton, G.M., and Thomas, R. (2002). Nuclear RelB⁺ cells are found in normallymphoid organs and in peripheral tissue in the context of inflammation, but not under normal resting conditions. *Immunol Cell Biol.* **80**: 164-169.

Thornberry, N.A., Bull, H.G., Calaycay, J.R., Chapman, K.T., Howard, A.D., Kostura, M.J., Miller, D.K., Molineaux, S.M., Weidner, J.R., Aunins, J., Elliston, K.O., Ayala, J.M., Casano, F.J., Chin, J., Ding, G.J., Egger, L.A., Gaffney, E.P., Limjuco, G., Palyha, O.C., Raju, S.M., Rolando, A.M., Salley, J.P., Yamin, T., Lee, T.D., Shively, J.E., MacCross, M., Mumford, R.M., Schmidt, J.A., and Tocci, M.J. (1992). A novel heterodimeric cysteine protease is required for interleukin-1 beta processing in monocytes. *Nature* **356**: 768-774.

Tjernstrom, F., Hellmer, G., Nived, O., Truedsson, L., and Sturfelt, G. Synergetic effect between interleukin-1 receptor antagonist allele (IL1RN*2) and MHC class II (DR17, DQ2) in determining susceptibility to systemic lupus erythmatosus. *Lupus* **8**: 103-108.

Topper, J.N., and Gimbrone, M.A. (1999). Blood flow and vascular gene expression: fluid shear stress as a modulator of endothelial phenotype. *Mol Med Today*. **5**: 40-46.

Trentham, D.E., Townes, A.S., and Kang, A.H. (1977). Autoimmunity to type II collagen: an experimental model of arthritis. *J. Exp. Med.* **146**: 857-868.

Tsukada, J., Saito, K., Waterman, W.R., Webb, A.C., and Auron, P.E. (1994). Transcription factors NF-IL6 and CREB recognise a common essential site in the human prointerleukin 1 β gene. *Mol. Cell Biol.* **14**: 7285-7297.

Uria, J.A., Stahl-Backdahl, M., Seiki, M., Fueyo, A., and Lopez-Otin, C. (1997). Regulation of collagenase-3 expression in human breast carcinomas is mediated by stromal-epithelial cell interactions. *Cancer Res.* **57**: 4882-4888.

Uyemura, K., Yamamura, M., Fivenson, D.F., Modlin, R.L., and Nickoloff, B.J. (1993). The cytokine network in lesional and lesion-free psoriatic skin is characterised by a T-helper type 1 cell-mediated response. *J. Invest. Dermatol* **101**: 701-705.

Van de Loo, A.A.J., and Van den Berg, W.B. (1990). Effects of murine recombinant interleukin 1 on synovial joints in mice: measurement of patellar cartilage metabolism and joint inflammation. *Ann. Rheum. Dis.* **49**: 238-245.

Van den Berg, W., Joosten, L.A., Helsen, M., and Van der Loo, J. (1994). Amelioration of established murine collagen-induced arthritis with anti-IL-1 treatment. *Clin. Exp. Immunol.* **95**: 237-243.

Van Oostrum, J., Prestle, J.P., Grutter, M.G., and Schmitz, A. (1991). The structure of murine interleukin-1 β at 2.8 Å resolution. *J. Struct. Biol* **107**: 189-195.

Van Voorhis, W.C., Valinsky, J., Hoffman, E., Luban, J., Hair, L.S., and Steinman, R.M. (1983). Relative efficacy of human monocytes and dendritic cells as accessory cells for T cell replication. *J. Exp. Med.* **158**: 174-191.

Vannier, E., and Dinarello, C.A. (1993). Histamine enhances interleukin (IL)-1-induced IL-1 gene expression and protein synthesis via H2 receptors in peripheral blood mononuclear cells. Comparison with IL-1 receptor antagonist. *J Clin Invest.* **92**: 281-287.

Vargas-Alarcon, G., Flores-Dominguez, C., Hernandez-Pachecho, G., Zuniga, J., Gamboa, R., Soto, M.E., Granados, J., and Reyes, P.A. (2001). Immunogenetics and clinical aspects of Takayasu's arteritis patients in a mexican Mestizo population. *Clin. Exp. Rheumatol.* **19**: 439-443.

Veerapandian, B., Gilliland, G.L., Raag, R., Svensson, A.L., Masui, Y., Hirai, Y., and Poulos, T.L. (1992). Functional implications of interleukin-1 β based on the three-dimensional structure. *Proteins* **12**: 10-23.

Verheijden, G.F.M., Rijnders, A.W.M., Bos, E., Coenen de Roo, C.J.J., Van Staveren, C.J., Milterburg, A.M.M., Meijerink, J.H., Elewaut, D., De Keyser, F., Veys, E., and Boots, A.M.H. (1997). Human cartilage glycoprotein-39 as a candidate autoantigen in rheumatoid arthritis. *Arthritis Rheum.* **40**: 1115-1125.

Vollmer, S., Menssen, A., Trommler, P., Schendel, D., and Prinz, J.C. (1994). T lymphocytes derived from skin lesions of patients with psoriasis vulgaris express a novel cytokine pattern that is distinct from T helper type 1 and T helper type 2 cells. *Eur. J. Immunol* **24**: 2377-2382.

Wagner, A.B., Gerard, H.C., Freseman, T., Schmidt, W.A., Gromnica-Ihle, E., Hudson, A.P., and Zeidler, H. (2000). Detection of Chlamydia pneumoniae in giant cell vasculitis and correlation with the topographic arrangement of tissue-infiltrating dendritic cells. *Arthritis Rheum.* **43**: 1543-1551.

Wagner, A.D., Bjornsson, J., Bartley, G.B., Gorozny, J.J., and Weyand, C.M. (1996). Interferon- γ -producing T-cells in giant cell vasculitis represent a minority of tissue-infiltrating cells and are located distant from the site of pathology. *Am. J. Pathol.* **148**: 1925-1933.

Wagner, A.D., Gorozny, J.J., and Weyand, C.M. (1994). Functional profile of tissue-infiltrating and circulating CD68⁺ cells in giant cell arteritis. Evidence for two components of the disease. *J. Clin. Invest.* **94**: 1134-1140.

- Warner, S.J., Auger, K.R., and Libby, P. (1987). Human interleukin 1 induces interleukin 1 gene expression in human vascular smooth muscle cells. *J Exp Med.* **165**: 1316-1331.
- Watanabe, N., and Kobayashi, Y. (1994). Selective release of a processed form of interleukin 1 alpha. *Cytokine.* **6**: 597-601.
- Waterhouse, C.C.M., and Stadnyk, A.W. (1999). Rapid expression of IL-1 β by intestinal epithelial cells *in vitro*. *Cell. Immunol.* **193**: 1-8.
- Watson, J., Gillis, S., Marbrook, J., Mochizuki, D., and Smith, K.A. (1979). Biochemical and biological characterisation of lymphocyte regulatory molecules. I. Purification of a class of murine lymphokines. *J. Exp. Med.* **150**: 849-861.
- Weber, K.S.C., von Hundelshausen, P., Clark-Lewis, I., Weber, P.C., and Weber, C. (1999). Differential immobilisation and hierarchical involvement of chemokines in monocyte arrest and transmigration in inflamed endothelium in shear flow. *Eur. J. Immunol.* **29**: 700-712.
- Wei, L., Debets, R., Hegmans, J.J., Benner, R., and Prens, E.P. (1999). IL-1 β and IFN γ induce the regenerative epidermal phenotype of psoriasis in the transwell skin organ culture system. IFN γ up-regulates the expression of keratin 17 and keratinocyte transglutaminase via endogenous IL-1 production. *J. Pathol.* **187**: 358-364.
- Weinstein, J.A., and Taylor, J.M. (1987). Interleukin-1 and the acute-phase response: induction of mouse liver serum amyloid A mRNA by murine recombinant interleukin-1. *J. Trauma* **27**: 1227-1232.
- Weiss, R.A., Eichner, R., and Sun, T. (1984). Monoclonal antibody analysis of keratin expression in epidermal diseases: a 48- and 56-kdalton keratin as molecular markers for hyperproliferative keratinocytes. *J. Cell. Biol.* **98**: 1397-1406.
- Weller, A., Isenmann, S., and Vestweber, D. (1992). Cloning of the mouse endothelial selectins. *J. Biol. Chem.* **267**: 15176-15183.
- Werner, S., and Smola, H. (2001). Paracrine regulation of keratinocyte proliferation and differentiation. *Trends Cell. Biol.* **11**: 143-146.
- Wesa, A.K., and Galy, A. (2001). IL-1 beta induces dendritic cells to produce IL-12. *Int. Immunol.* **13**: 1053-1061.

Wesche, H., Henzel, W.J., Shillinglaw, W., Li, S., and Cao, Z. (1997). Myd88: an adapter that recruits IRAK to the IL-1 receptor complex. *Immunity* **7**: 837-847.

Wesche, H., Neumann, D., Resch, K., and Martin, M.U. (1996). Co-expression of mRNA for type I and type II interleukin-1 receptors and the IL-1 receptor accessory protein correlates to IL-1 responsiveness. *FEBS Lett.* **391**: 104-108.

Wesche, H., Resch, K., and Martin, M.U. (1998). Effects of IL-1 receptor accessory protein on IL-1 binding. *FEBS Lett.* **429**: 303-306.

Wewers, M.D., Dare, H.A., Winnard, A.V., Parker, J.M., and Miller, D.K. (1997). IL-1 β -converting enzyme (ICE) is present and functional in human alveolar macrophages: macrophage IL-1 β release limitation is ICE independent. *J. Immunol.* **159**: 5964-5972.

Weyand, C.M., Hickey, K.C., Hunder, G.G., and Gorozny, J.J. (1992). The HLA-DRB1 locus as a genetic component in giant cell arteritis. *J. Clin. Invest.* **90**: 2355-2361.

Weyand, C.M., Schonberger, J., Oppitz, U., Hunder, N.N., Hickey, K.C., and Gorozny, J.J. (1994). Distinct vascular lesions in giant cell arteritis share identical T cell clonotypes. *J. Exp. Med.* **179**: 951-960.

Weyand, C.M., Wagner, A.D., Bjornsson, J., and Gorozny, J.J. (1996). Correlation of the topographical arrangement and the functional pattern of tissue-infiltrating macrophages in giant cell arteritis. *J. Clin. Invest.* **98**: 1642-1649.

Wilson, K.P., Black, J.F., Thomson, J.A., Kim, E.E., Griffith, J.P., Navia, M.A., Murcko, M.A., Chambers, S.P., Aldape, R.A., Raybuck, S.A., and Livingston, D.J. (1994). Structure and mechanism of interleukin-1 β converting enzyme. *Nature* **370**: 270-275.

Wong, P., Colucci-Guyon, E., Takahashi, K., Gu, C., Babinet, C., and Coulombe, P.A. (2000). Introducing a null mutation in the mouse K6 α and K6 β genes reveals their essential structural role in the oral mucosa. *J. Cell. Biol.* **150**: 921-928.

Wood, D.D., Ihrie, E.J., Dinarello, C.A., and Cohen, P.L. (1983). Isolation of an interleukin 1-like factor from human joint effusions. *Arthritis Rheum.* **26**: 975-983.

Wooley, P.H., Luthra, H.S., Stuart, J.M., and David, C.S. (1981). Type II collagen-induced arthritis in mice. I. Major histocompatibility complex (I region) linkage and antibody correlates. *J. Exp. Med.* **154**: 688-700.

Wooley, P.H., Whalen, J.D., Chapman, D.L., Berger, A.E., Richard, K.A., Aspar, D.G., and Staite, N.D. (1993). The effect of an interleukin-1 receptor antagonist protein on type II collagen-induced arthritis and antigen-induced arthritis in mice. *Arthritis Rheum.* **36**: 1305-1314.

Wooley, P.H., Whalen, J.D., Chapman, D.L., Berger, A.E., Richard, K.A., Aspar, D.G., and Staite, N.D. (1993). The effect of an interleukin-1 receptor antagonist protein on type II collagen-induced arthritis and antigen-induced arthritis in mice. *Arthritis Rheum.* **36**: 1305-1314.

Wordsworth, B.P., Lanchbury, J.S.S., Sakkas, L.I., Welsh, K.I., Panayi, G.S., and Bell, J.I. (1989). HLA-DR4 subtype frequencies in rheumatoid arthritis indicate that *DRB1* is the major susceptibility locus within the HLA class II region. *Proc. Natl. Acad. Sci. USA* **86**: 10049-10053.

Woronicz, J.D., Gao, X., Cao, Z., Rothe, M., and Goeddel, D.V. (1997). I κ B kinase- β : NF- κ B activation and complex formation with I κ B kinase- α and NIK. *Science* **278**: 866-860.

Wright, S.D., Ramos, R.A., Tobias, P.S., Ulevitch, R.J., and Mathison, J.C. (1990). CD14, a receptor for complexes of lipopolysaccharide (LPS) and LPS binding protein. *Science* **249**: 1431-1433.

Wrone-Smith, T., and Nickoloff, B.J. (1996). Dermal injection of immunocytes induces psoriasis. *J. Clin. Invest.* **98**: 1878-1887.

Yam, L.T., Li, C.Y., and Crosby, W.H. (1971). Cytochemical identification of monocytes and granulocytes. *Am J Clin Pathol.* **55**: 283-290.

Yamada, T., Fukuda, T., Wada, A., and Itoh, Y. (1999). Monoclonal antibody-based sensitive enzyme-linked immunosorbent assay for murine serum amyloid A. *J. Immunoassay* **20**: 223-235.

Yamamoto, T., Eckes, B., Mauch, C., Hartmann, K., and Krieg, T. (2000). Monocyte chemoattractant protein-1 enhances gene expression and synthesis of matrix metalloproteinase-1 in human fibroblasts by an autocrine IL-1 α loop. *J. Immunol.* **164**: 6174-6179.

Yoo, T.J., Kim, S., Stuart, J.M., Floyd, R.A., Olson, G.A., Cremer, M.A., and Kang, A.H. (1988). Induction of arthritis in monkeys by immunisation with type II collagen. *J. Exp. Med.* **168**: 777-782.

Zandi, E., Rothwarf, D.M., Delhase, M., Hayakawa, M., and Karin, M. (1997). The I κ B kinase complex (IKK) contains two kinase subunits, IKK α and IKK β , necessary for I κ B phosphorylation and NF- κ B activation. *Cell* **91**: 243-252.

Zanelli, E., Huizinga, T.W.J., Guerne, P., Vischer, T.L., Tiercy, J., Verduyn, W., Schreuder, G.M.T., Breedveld, F.C., and de Vries, R.R.P. (1998). An extended *HLA-DQ-DR* haplotype rather than *DRB1* alone contributes to RA predisposition. *Immunogenetics* **48**: 394-401.

Zarins, C.K., Giddens, D.P., Bharadvaj, B.K., Sottiurai, V.S., Mabon, R.F., and Glagov, S. (1983). Carotid bifurcation atherosclerosis. Quantitative correlation of plaque localisation with flow velocity profiles and wall shear stress. *Circ. Res.* **53**: 502-514.

Zhang, Y., McCluskey, K., Fujii, K., and Wahl, L.M. (1998). Differential regulation of monocyte matrix metalloproteinase and TIMP-1 production by TNF- α , granulocyte-macrophage CSF, and IL-1 β through prostaglandin-dependent and -independent mechanisms. *J. Immunol.* **161**: 3071-3076.

Zheng, H., Fletcher, D., Kozak, W., Jiang, M., Hofmann, K.J., Conn, C.A., Soszynski, D., Grabiec, C., Trumbauer, M.E., Shaw, A., Kostura, M.J., Stevens, K., Rosen, H., North, R.J., Chen, H.Y., Tocci, M.J., Kluger, M.J., and Van der Ploeg, L.H.T. (1995). Resistance to fever induction and impaired acute-phase response in interleukin-1 beta-deficient mice. *Immunity*. **3**: 9-19.

Zvaifler, N.J., and Firestein, G.S. (1994). Pannus and pannocytes. Alternative models of joint destruction in rheumatoid arthritis. *Arthritis Rheum.* **37**: 783-789.

Appendix

List of suppliers

γ -[³² P] ATP	NEN
3-Aminopropyltriethoxysilane (APES)	Sigma
Acid fuchsin	BDH
Acrylamide	Sigma
Agarose	Promega
Ammonium bicarbonate	Sigma
Ammonium persulfate	Gibco
Anhydrous disodium hydrogen phosphate	BDH
<i>Apal</i>	Promega
<i>Apal</i> buffer	Promega
Autoradiograph film	Kodak
Bis-acrylamide	Gibco
Boric acid	Gibco
Bromophenol blue	Sigma
BSA	Promega
Chloroform	Fisher Scientific
CIAP	Promega
<i>Cot1</i> DNA	Gibco
Diaminoethanetetra-acetic acid (EDTA)	BDH
Eosin Y	Sigma
<i>Escherichia coli</i> LPS	Sigma
Ethanol	Gibco
Ethidium bromide	BDH
Eukitt mounting medium	Agar
Fast red violet LB base solution	Sigma
Filter paper	Whatman
Formaldehyde	BDH
Formamide	Sigma
Gill's No.1 hematoxylin	Sigma
Glycerol	Sigma
Glycogen	Gibco
Heat inactivated foetal calf serum	Gibco
<i>HindIII</i> digested λ DNA size marker	New England Biolabs
<i>HpaII</i>	Promega
Hydrogen peroxide	BDH
Isoamyl alcohol	BDH
Klenow fragment	Promega

Magnesium sulphate 7-hydrate	BDH
<i>Mbo1</i>	New England Biolabs
Microscope slides	Chance-Propper Ltd
Miller's solution	NuStain
N,N,N',N'-Tetramethylethylenediamine (TEMED)	Sigma
Naphthol AS-D chloroacetate solution	Sigma
Optimum cutting temperature (O.C.T) compound	Tissue-Tek
Oxalic acid	BDH
Paraffin oil	Sigma
Penicillin	Gibco
Phenol	Gibco
Picric acid	BDH
pNEB193 plasmid	New England Biolabs
Potassium chloride	BDH
Potassium dihydrogen phosphate	BDH
Potassium permanganate	BDH
Proteinase K	Promega
RPMI1640 medium	Sigma
Saponin	Sigma
Saran wrap	Dow
Sellotape glue	Duro-Tak, ICI
Sephadex G50	Pharmacia Biotech
Sodium acetate	Sigma
Sodium bicarbonate	Sigma
Sodium chloride	BDH
Sodium chloride	BDH
Sodium chloride	Sigma
Sodium dihydrogen orthophosphate dihydrate	BDH
Sodium dodecyl sulphate	Melford Laboratories Ltd
Sodium nitrite solution	Sigma
Sodium phosphate	Sigma
Sodium phosphate	Sigma
Spectra/Por molecular porous membrane	Spectrum Medical Industries
Streptomycin	Gibco
T4 polynucleotide kinase (PNK)	Promega
T7 Quickprime kit	Pharmacia Biotech
<i>Thermus aquaticus (Taq)</i> DNA ploymerase	Gibco
<i>Thermus aquaticus (Taq)</i> DNA ploymerase buffer	Gibco
Toluidine blue	BDH
Tris	Gibco

Trisodium citrate	Sigma
TRIZMAL 6.3 buffer concentrate	Sigma
Urea	BDH
Xylene	Genta Medical
Xylene cyanole FF	BDH
Zetaprobe GT membrane	Biorad